CHANGES IN SURFACE WATER AND SEDIMENT QUALITY AT A COMPLEX TIDAL-INFLUENCED RIVER: A CASE STUDY OF GANH HAO RIVER, MEKONG DELTA, VIETNAM

Mr. Muoi Le Van

A Dissertation Submitted in Partial Fulfillment of the Requirements for the Degree of Doctor of Philosophy in Hazardous Substance and Environmental Management
Inter-Department of Environmental Management
GRADUATE SCHOOL
Chulalongkorn University
Academic Year 2021

การเปลี่ยนแปลงคุณภาพน้ำและตะกอนในแม่น้ำที่ได้รับอิทธิพลของน้ำขึ้นน้ำลงที่มีความซับซ้อน กรณีศึกษา แม่น้ำกานห์เฮา ดินดอนสามเหลี่ยมปากแม่น้ำโขง ประเทศเวียดนาม

นายโม เล วัน

วิทยานิพนธ์นี้เป็นส่วนหนึ่งของการศึกษาตามหลักสูตรปริญญาวิทยาศาสตรดุษฎีบัณฑิต
สาขาวิชาการจัดการสารอันตรายและสิ่งแวดล้อม สหสาขาวิชาการจัดการสิ่งแวดล้อม
บัณฑิตวิทยาลัย จุฬาลงกรณ์มหาวิทยาลัย
ปีการศึกษา 2564

Thesis Title	CHANGES IN SURFACE WATER AND SEDIMENT QUALITY AT A COMPLEX TIDAL-INFLUENCED RIVER: A CASE STUDY OF GANH HAO RIVER, MEKONG DELTA, VIETNAM
By	Mr. Muoi Le Van
Field of Study	Hazardous Substance and Environmental Management
Thesis Advisor	Professor SRILERT CHOTPANTARAT, Ph.D.
Thesis Co Advisor	Associate Professor Van Pham Dang Tri, Ph.D. Associate Professor Pham Van Toan, Ph.D.

Accepted by the GRADUATE SCHOOL, Chulalongkorn University in Partial Fulfillment of the Requirement for the Doctor of Philosophy

..... Dean of the GRADUATE SCHOOL
(Associate Professor Dr. YOOTTHANA CHUPPUNNARAT)

DISSERTATION COMMITTEE

..... Chairman
(Associate Professor CHANTRA TONGCUMPOU, Ph.D.)
..... Thesis Advisor
(Professor SRILERT CHOTPANTARAT, Ph.D.)
..... Thesis Co-Advisor
(Associate Professor Van Pham Dang Tri, Ph.D.)
..... Thesis Co-Advisor
(Associate Professor Pham Van Toan, Ph.D.)
..... Examiner
(Assistant Professor PENRADEE CHANPIWAT, Ph.D.)
..... Examiner
(Doctor. SEELAWUT DAMRONGSIRi, Ph.D.)
..... External Examiner
(Doctor Somchai Chonwattana, Ph.D.)

โม เล วัน : การเปลี่ยนแปลงคุณภาพน้ำและตะกอนในแม่น้ำที่ได้รับอิทธิพลของน้ำขึ้นน้ำลงที่มีความซับซ้อน กรณีศึกษา แม่น้ำกานห์เฮา ดินดอนสามเหลี่ยมปากแม่น้ำโขง ประเทศเวียดนาม. (CHANGES IN SURFACE WATER AND SEDIMENT QUALITY AT A COMPLEX TIDAL-INFLUENCED RIVER: A CASE STUDY OF GANH HAO RIVER, MEKONG DELTA, VIETNAM) อ.ที่ปรึกษาหลัก : Prof.ศรีเลิศ โชติพันธรัตน์Ph.D., อ.ที่ปรึกษาร่วม : Assoc. Prof.วาน พาม แดง ทริPh.D,Assoc. Prof.พาม วาน โตนPh.D

การวิจัยนี้ได้ดำเนินการวิจัยด้านค่ามลพิษของน้ำผิวดินและตะกอนโดยใช้พารามิเตอร์ทางกายภาพและเคมีและปริมาณความเข้มข้นของโลหะหนัก โดยดำเนินการเก็บตัวอย่างน้ำผิวดินและตะกอนจำนวน 25 สถานที่ ในลำน้ำในวันที่ 22 มีนาคม และ 5 กันยายน 2019 โดยแม่น้ำสายหลักนี้ได้รับอิทธิพลของน้ำขึ้นน้ำลงที่ซับซ้อน (complex tidal regime) และการเพาะเลี้ยงสัตว์น้ำในคาบสมุทร Ca Mau ในสามเหลี่ยมปากแม่น้ำโขงของเวียดนาม. โดยเปรียบเทียบกับมาตรฐานคุณภาพน้ำระดับสากลและระดับประเทศ ในขณะที่คุณภาพตะกอนที่วัดได้นั้นเปรียบเทียบกับมาตรฐานของเวียดนามและดัชนีภาระมลพิษ (geo-accumulation index, contamination factor และ pollution load index) การศึกษานี้ได้ดำเนินการการวิเคราะห์องค์ประกอบหลัก (Principal component analysis) และการวิเคราะห์ความสัมพันธ์ทางสถิติแบบถดถอยโลจิสติกส์ซึ่งนำมาใช้เพื่อการอธิบายปัจจัยหลักที่มีผลต่อระดับมลพิษทางน้ำและความสัมพันธ์ของพารามิเตอร์คุณภาพน้ำและความแปรผันของคุณภาพน้ำอันเนื่องมาจากจากปัจจัยน้ำขึ้นน้ำลงตามฤดูกาล โดยผลการศึกษาจะแสดงโดยเครื่องมือระบบสารสนเทศภูมิศาสตร์ QGIS ทั้งนี้ในการศึกษาได้วิเคราะห์อุทกพลศาสตร์โดยใช้แบบจำลอง Delft 3D โดยเปรียบเทียบกับผลการศึกษาจากภาคสนาม. ความเข้มข้นของปริมาณธาตุอาหารและสารประกอบอินทรีย์สูงกว่ามาตรฐานคุณภาพน้ำผิวดิน 2-3 เท่า อย่างไรก็ตามปริมาณเข้มข้นของโลหะหนักในตะกอนลำน้ำพบว่ามีต่ำกว่ามาตรฐาน ซึ่งพบว่ามีความสอดคล้องกับระดับทั่วไปของมลพิษทางอากาศ(Background level การศึกษานี้ยังพบว่าอิทธิพลของกระแสน้ำและฤดูกาลการเปลี่ยนแปลงมีความสัมพันธ์คุณภาพน้ำอย่างมีนัยสำคัญทางสถิติ ($P<0.05$). ในการศึกษาการวิเคราะห์องค์ประกอบหลัก (PCA) พบว่ามีจำนวน 3 องค์ประกอบที่สามารถอธิบายถึงความแปรปรวน (variance) จำนวนร้อยละ 79.84 ของความแปรปรวนทั้งหมดของคุณภาพน้ำโดยองค์ประกอบดังกล่าวคือ คุณสมบัติทางเคมีกายภาพและมลพิษของสารอินทรีย์ สารแขวนลอยและสารอาหาร และปริมาณออกซิเจนละลายน้ำ DO สามารถอธิบายเป็น 53.64%, 18.43% และ 7.77% ตามลำดับ. การศึกษาครั้งนี้ได้ดำเนินการจัดทำแผนที่คุณภาพน้ำเชิงพื้นที่ (Spatiotemporal) มีมีการบ่งชี้จุดที่มีมลพิษ (hot spot) โดยพบว่าบริเวณพื้นที่การเพาะเลี้ยงกุ้งสูงมีความสัมพันธ์ทางสถิติกับระดับของคุณภาพแหล่งน้ำ โดยพบว่าการเปลี่ยนแปลงในคุณลักษณะไฮดรอลิกของแม่น้ำได้รับอิทธิพลอย่างมากจากระบอบกระแสน้ำรวมถึงการเปลี่ยนแปลงทางธรณีสัณฐานวิทยา ผลการวิจัยระบุช่องว่างจากการศึกษาก่อนหน้านี้เพื่อระบุความเสื่อมโทรมของคุณภาพน้ำผิวดินมีความสัมพันธ์กับพื้นที่การเพาะเลี้ยงกุ้ง ผลการศึกษาที่ได้นี้อาจมีประโยชน์ไม่เฉพาะกับผู้กำหนดนโยบายท้องถิ่นในการพัฒนายุทธศาสตร์การบริหารจัดการน้ำเท่านั้น แต่ยังมีประโยชน์กับแม่น้ำสายอื่นๆ ในภูมิภาคอื่นอีกด้วย

สาขาวิชา	การจัดการสารอันตรายและสิ่งแวดล้อม	ลายมือชื่อนิสิต .....
ปีการศึกษา	2564	ลายมือชื่อ อ.ที่ปรึกษาหลัก .....
		ลายมือชื่อ อ.ที่ปรึกษาร่วม .....
		ลายมือชื่อ อ.ที่ปรึกษาร่วม .....

5987845620 : MAJOR HAZARDOUS SUBSTANCE AND ENVIRONMENTAL MANAGEMENT
KEYWORD: POLLUTION INDICES, PRINCIPAL COMPONENT ANALYSIS, SURFACE WATER QUALITY, COMPLEX TIDAL REGIME, DELFT3 MODEL, GANH HAO RIVER

Muoi Le Van : CHANGES IN SURFACE WATER AND SEDIMENT QUALITY AT A COMPLEX TIDAL-INFLUENCED RIVER: A CASE STUDY OF GANH HAO RIVER, MEKONG DELTA, VIETNAM . Advisor: Prof. SRILERT CHOTPANTARAT, Ph.D. Co-advisor: Assoc. Prof. Van Pham Dang Tri, Ph.D.,Assoc. Prof. Pham Van Toan, Ph.D.

The research was carried out to determine the extent of surface water and sediment pollution using the physicochemical parameters and heavy metal concentrations. The surface water and sediment samples were obtained from 25 sites along the river on March 22 and September 5, 2019 at the main river influenced by the complex tidal regime and aquaculture practices in Ca Mau peninsular in the Vietnamese Mekong Delta. The water quality was compared with international and national standards, while the sediment quality was compared with Vietnamese standards and pollution indices (geo-accumulation index, contamination factor, and pollution load index). Principal component analysis (PCA) was employed to explain the main factors responsible for the observed levels of water pollution. The dependence of water quality parameters and variations in water quality due to tidal regimes and seasonality were also evaluated by statistical comparisons. Based on the logistic regression models, the temporal variability of selected water quality parameters was visualized using QGIS. The Delft 3D model was used to evaluate changes in hydraulic characteristics based on actual fieldwork. The concentrations of nutrients and organic compounds exceeded 2-3 times greater than the standard for surface water quality. The contents of heavy metals were below the standard for sediment quality and consistent with the background levels. The influence of the tidal regime and seasonality caused significant changes in water quality and its association with various flow regimes ($P<0.05$). Three components based on the PCA accounted for approx. 79.84% of the total variance in water quality characteristics of which the first, second, third component explained for 53.64%, 18.43%, and 7.77% of total variance related to physicochemical properties and organic matter pollution, suspended solids and nutrients, and DO consumption, respectively. Water quality maps indicated pollution hotspots, and the extensive and improved – extensive shrimp culture practices were identified in connection to the changes in water quality. Changes in the river's hydraulic characteristics were influenced remarkably by the tidal regime as well as geomorphological changes. The results of the research addressed the gaps

Field of Study:	Hazardous Substance and Environmental Management	Student's Signature .....
Academic Year:	2021	Advisor's Signature .....
		Co-advisor's Signature .....

ACKNOWLEDGEMENTS

I deeply express my gratitude and appreciation to my thesis advisor Prof. Dr. Srilert Chotpantarat and co-advisor Assoc. Prof. Dr. Van Pham Dang Tri and Assoc. Prof. Dr. Pham Van Toan for their support and guidance throughout the entire process of this research.

I would like to express my sincere thanks to all lecturers and staffs at International Postgraduate Program in Hazardous Substance and Environmental Management (IP-HSM), Chulalongkorn University for their continuous support and useful comments. I am especially thankful to the Graduate Scholarship Program for ASEAN countries and the 90th Year Chulalongkorn University Scholarship, Chulalongkorn University for the financial support throughout the study period of my Ph.D. program. Financial support from the CU Graduate School Thesis Grant is also gratefully acknowledged. In addition, I would like to express my heartfelt appreciation to the Center of Excellent on Hazardous Substance Management for funding my research.

I would also like to thank the College of Environment and Natural Resources and Research Institute for Climate Change, Can Tho University (CTU) for kindly allowing me to use the facilities. I would like to thank the members of the hydro-information office (CTU) for the kind help during the campaign fields. I am grateful to Assoc. Prof. Dr. Nguyen Thi Hong Diep, Department of Land Resources (CTU) for kindly advising me to develop the land-use map. Special thanks are given to Tech Center Quality Measurement Standards Can Tho, Can Tho City Department of Science and Technology for helping me during my sample analysis.

One of the most important things to reach the success of my study that I have never forgotten a great support in terms of spiritually and materially from every member of my great family and friends. I endlessly thank my parents and wife for being always beside and encouraging me during my study. The best Vietnamese and Thai friends have been encouraging and sharing cheerful smiles for me to overcome the challenges of studying far away from home.

Muoi Le Van

TABLE OF CONTENTS

Page

CHAPTER 1
INTRODUCTION

1.1 Background and Rationale

River and sediment contamination has been one of the most concerning environmental issues in recent decades, and it continues to pose a global threat to humans, biodiversity, and aquatic organisms [1]. The contamination of surface water poses serious environmental and health risks [2, 3]. They presented all of the sediments and surface water found over last years [4, 5]. The natural and anthropogenic activities are main causes supporting the accumulation of polluted sediments in streams and leading directly or indirectly to the increase of pollutants into the environment. The discharge of contaminants from the non-point and point sources is considered as the main source that pollutes the water and sediment [6]. All pollutants occur in surface water at dissimilar forms, although they are mostly at low dissolved contents. Upon entry into the surface water, precipitation of the contaminants happens on the bottom sediments (e.g., rivers, streams, and estuaries). The availability and mobility of the pollutants are governed by the different physicochemical processes occurred in the water and sediments [7]. The extent of the pollutants (e.g., nutrients, organic substances, and heavy metals in the surface water and sediments) have been studied and observed over years [8-17].

The Vietnamese Mekong Delta (VMD), located in the South of Vietnam, obtains around 39,400 km^2 (approx. 8.1% area of the Mekong basin) (Figure 1.1), the region has dense artificial and natural canal/river networks supply for irrigation, drainage, and water navigation. The VMD is characterized by the tropical semi-equatorial climate with an average temperature and humidity of about 27^oC and 83%, respectively. An average rainfall ranged annually between 1,600-2,000 mm, of which 90% occurred during the wet season from May to October and the dry one generally elongates from October to May. The flood season comes normally in the period between September and October [18-20]. The VMD is a major agricultural and aquaculture region in the South of Vietnam where inhabitants were around 17.3 million [21]. The land used for rice crops and other agricultural practices in the upper

Delta and aquaculture in the coastal areas was approx. 55.9% and 93%, accordingly [22, 23]. The application of various fertilizers and pesticides maintained and enlarged agricultural and aquaculture production, but this resulted in the large number of residual chemicals represented as the potential sources of pollutants to the Delta [24]. Besides, industrial activities were additional sources of pollutants degrading the environmental quality [24, 25]. Due to the influences of anthropogenic activities, the previous studies revealed that the concentration of the pollutants in surface water and sediments in the main rivers and canals has not only increased over the past decades but also exceeded the allowable standards [26-29]. Moreover, the effects of hydrodynamic and seasonal factors were also additional causes of great changes in the physicochemical properties of the surface water [30, 31].

The Ca Mau Peninsula, located in the southernmost section of the VMD, is within the seawater intrusion zone, which is influenced by both East and West Sea tidal regimes, resulting in unsuitable water quality for irrigation during the dry season. As a consequence of seawater intrusion, traditional rice production was limited to only one wet season crop, this resulted in a constraint of priority policy for agriculture led-growth since the 1990s. As a result, up until the year 2000, a series of coastal embankments and tidal sluices had been completed to prevent seawater intrusion for rice farming. When freshwater within protected zones was supplied adequately for rice production increasing in double or triple rice crops, conflicts occurred among stakeholders who used brackish and saline water for aquaculture practices. Thus, a new policy for the balanced development of aquaculture and agriculture practices, adopted in the year 2000, significantly promoted the region's economic growth [32, 33]. However, adverse consequences for the environmental impacts have not been considered adequately [34]. Over the last few decades, there has been a prompt increase in the modified landscape due to land-use and seawater intrusion management, which have resulted in remarkable effects on surface water quality in the Ca Mau Peninsular. The surface water quality at main rivers has been polluted due to urbanization, aquaculture and agriculture practices [35, 36]. In addition, the region is influenced by the complex tidal regimes of the East and West Sea, which are inundated twice daily with the various tidal amplitudes. The East Sea, characterized by a mixed semi-diurnal tidal regime with a tidal range of up to 3 m, and an average

flow of 871.9 $m^3.s^{-1}$, has daily twice neap and spring tides of different amplitudes. The tidal regimes affect widely the area from the Ganh Hao River to the Ca Mau Peninsula, the southernmost tip. The tidal range falls from 3.0 m at the Ganh Hao River to 1.0 m at the Ca Mau peninsula. While the West Sea described by a diurnal tide with a tidal range of about 0.8 m is fairly much smaller than that of the East Sea. The surface water in the rivers is either brackish or saline with an average salinity of 24.5-26.0‰, decreasing to 18.0-20.0‰ after heavy rainfall [37-40]. The previous studies [31, 41, 42] stated that the hydrodynamic and seasonal element were one of the primary causes leading to the pollutant diffusion and contributing to variability of the surface water quality in the river.

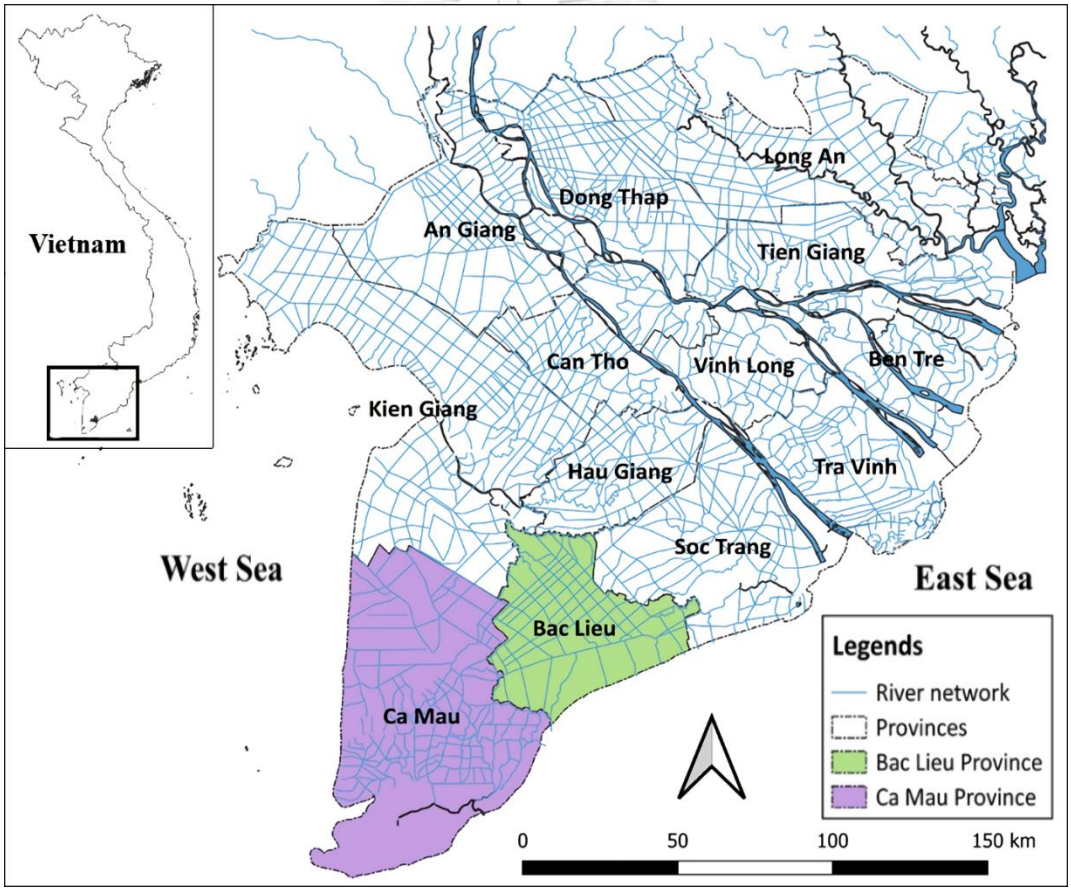

Figure 1.1 Map of the Vietnamese Mekong Delta

Together with the impact of tidal regimes, the discharge of untreated or improper treated domestic, agriculture, and aquaculture sources entering the receiving waters,

which found the most apparent consequences of water pollution in the Ganh Hao River, caused the negative effects making changes in physicochemical characteristics of surface water [43, 44]. The status of surface water and sediment quality at Ganh Hao River has been polluted considerably, the high contents of nutrients, organic substances, and metal (loid)s have been discovered at the river courses over the years. For instance, the spatial and temporal variability of arsenic (As) and cadmium (Cd) contents found in the surface water and sediment, of which the former spotted the concentrations of the As in ranges of 2.13-2.27 ($\mu g.L^{-1}$) and 0.4-23.33 ($\mu g.L^{-1}$), and 0.2-0.26 ($\mu g.L^{-1}$) and 0.39-0.4 ($\mu g.L^{-1}$) for the Cd in the dry and wet seasons, respectively. The later illustrated the contents of the As in ranges of 4.9-6.7 ($mg.kg^{-1}$) and 10.77-14.97 ($mg.kg^{-1}$), and 0.3-0.6 ($mg.Kg^{-1}$) and 0.3-0.5 ($mg.Kg^{-1}$) for the Cd in two seasons [45]. The surface water and sediment polluted with high pollution of the As contents, compared to the previous study, ranged from 15.43-78.41 ($\mu g.L^{-1}$) and 7.10-12.4 ($mg.kg^{-1}$), accordingly [46]. The surface water quality at Ganh Hao River and tributaries deteriorated by nutrients and organic substances, of which dissolved oxygen (DO), ammonium ($N\text{-}NH_4^+$), and phosphorous ($P\text{-}PO_4^{3+}$), discovered at sampling sites, varied from 3.32-7.12 mg L^{-1}, 0.195-1.577 mg L^{-1}, and 0.019-0.185 mg L^{-1}, respectively [47]. The content of nutrient and organic substance, detected at canals/rivers and Ganh Hao River belonging to Ca Mau province, was at ranges such as DO 1.37-7.95 mg L^{-1}, $N\text{-}NH_4^+$ 0-3.111 mg L^{-1}, and $P\text{-}PO_4^{3+}$ 0.008-0.963 mg L^{-1} [48]. Therefore, degradation of the surface water quality at Ganh Hao River has not only remarkably affected aquatic organisms but also inhabitants who have relied chiefly on the water resources for daily purposes [49]. However, few studies assessed entirely the variation of the surface water and sediment quality under the various drivers of influence. The previous studies just investigated either the content of pollution in the surface water or sediment at a large scale. It is difficult to assume that the water and sediment quality of tributary systems are similar to that of the key waterway. Therefore, to fill the gap in the literature, the research was conducted to evaluate the water and sediment quality at representative sites along the river by referring the national and international standards. The influence of tidal regimes and seasonality and factors for interpreting the variability on water quality were assessed and specified in the research. Changes in hydrodynamic characteristics and water

quality responding to different flow regimes were also addressed the study. The results of the study did not only assist policymakers in developing strategies of water resources management but also the scientific basic for further studies in the future.

1.2 Research objectives

The general objective of the study was to evaluate the status of surface water and sediment quality at the Ganh Hao River where has been impacted significantly by the sources of the pollutants from the aquaculture practices.

According to the general objective, three sub-objectives of the study are as follows:

1.2.1 To assess the contamination levels of surface water and sediment.

+ Comparing with the Vietnamese guidelines (2015) and the USEPA (2001) standards for quality of surface water.

+ Comparing with the Vietnamese guidelines (2017) and sediment pollution indexes as Geo – Accumulation Index (I-geo), Contamination Factor (CF), and Pollution Load Index (PLI) for quality of the bottom sediment.

1.2.2 To identify the variability of surface water quality at the study area.

+ To identify the main factors explaining the oscillation of the surface water for the possible sources of contaminants.

+ To evaluate the tidal and seasonal fluctuations of the surface water quality.

+ To create a map of water quality to visualize spatially in the surface water quality of the study river and determine hot-spot areas of contamination.

1.2.3 To simulate the hydrodynamics and evaluate changes in water quality

+ To evaluate changes in hydraulic characteristics of the river reaches.

+ To evaluate changes water quality and its association with different flow regimes

1.3 Research hypotheses

Given the objectives above, this research was conducted the following three hypotheses:

+ Concentrations of the pollutants are expected to be above national and international standards
+ Pollution of the surface water and sediment comes from aquaculture activities.
+ The tidal dynamics contribute greatly to changes in variability of the pollutants.

1.4 Research questions

In order to test three above hypotheses, the following research questions was considered:

+ How much the contents of pollutants were there in the surface water and sediment at the study area?
+ How was the temporal and spatial variability of contaminants in surface water and sediment at the study area?
+ How were changes in water quality between neap and spring tide?
+ Where are the possible sources of pollutants contributing to the study area?
+ How to know which observed sites in the study area were mostly influenced by aquaculture practices?
+ How to know the changes in hydraulic characteristics and water quality to various flow regimes?

1.5 Scope of the study

The scope of the study was as follows:

- The segment of the study river locating in the lower area of Ganh Hao River with a total length of ~ 11 km was specified by the upstream and downstream boundaries, of which the former was primarily the confluence of Kenh Xang canal belonging to Dinh Thanh commune. The latter was the confluence of the Ganh Hao-Ho Phong canal associating with An Phuc commune around 6 km from the estuary of the river. Changes in water quality of the river was specified by major effects of shrimp culture systems from the communes, where they are located in Dong Hai and Dam Doi districts belonging to Bac Lieu and Ca Mau provinces, respectively. Collection of the surface water and sediment samples was conducted in two consecutive seasons that were the dry season in March 2019 and the rainy one in September 2019.

- A total of 25 measured parameters consists of 18 water quality parameters which were temperature, electrical conductivity (EC), total dissolved solids (TDS), total suspended solids (TSS), pH, dissolved oxygen (DO), chemical oxygen demand (COD), salinity, ammonium ($N\text{-}NH_4^+$), nitrogen-nitrite ($N\text{-}NO_2^-$), nitrogen-nitrate ($N\text{-}NO_3^-$), total-nitrogen (TN), total-phosphorus (TP), phosphate-phosphorus ($P\text{-}PO_4^{3-}$), and metal(loid) (e.g., arsenic (As), coper (Cu), lead (Pb), and zinc (Zn)). For sediment quality, seven parameters were measured such as EC, pH, total organic carbon (TOC), As, Cu, Pb, and Zn.

- The surface water quality was evaluated by comparing with the Vietnamese guidelines (2015) and the US.EPA (2001). The sediment quality was compared with the Vietnamese guideline (2017) and three indices of pollution (e.g., the Geo-Accumulation Index (I-geo), the Contamination Factor Index (CF), and Pollution Load Index (PLI)). The temporal and tidal oscillation of the contaminants in the surface water was assessed by statistical comparison. The principal component analysis (PCA) was employed to specify the main factor elucidating the seasonal changes in the quality of the surface water. The map of water quality was created by the Quantum Geographic System (QGIS-3.12) to identify the hot spot-areas of pollution. Changes in hydraulic properties were simulated using the Delft 3D model. The variation in water quality and its dependence to flow regimes were evaluated by statistical analysis.

CHAPTER 2
LITERATURE REVIEW

2.1 Sources of surface water pollution

Surface water is considered the most controllable natural resources due to its utilization (e.g., alteration, navigation, storage, and reuse. These characteristics bring to water its large usage for humankind. The surface water contributes a central role in variety of fields (e.g., agriculture and aquaculture practices, hydropower production, industrial and recreational activities, transportation, etc.). The freshwater obtains approx. 0.5% (2.84x105 km^3) of the earth's surface, while rivers form a quantity of 0.1% in the land surface and waters of the earth occurring in rivers/channels gain an insignificant amount of 0.01% [50]. The rapid increase in the population and industrial activities has resulted in the great demand for water in the last few decades [51]. The productive activities, particularly agricultural practices utilizing an enormous amount of fertilizers and pesticides, have threated to human beings [52]. The degradation of water quality relating primarily to anthropogenic activities due to direct or indirect discharge of the pollutants into the surface water [53, 54].

The point and non-point sources are specified as major ones influencing the surface water quality. Of which point sources originate mainly from municipal and industrial effluents, which can control with technological measures; therefore, the effect of pollutants occur generally the areas near them. Whilst non-point ones derive from a number of various sources (e.g., runoff from aquaculture, agriculture, and urban, etc.). Due to coming from the non-identifiable sources; therefore, the pollutants being discharged into the environment do not only affect in one area but also the further distance away. The pollutants, adverse impacts of the surface water, may principally be organic and inorganic ones, of which the former comprise of insecticide and herbicide products and other kind of chemicals, bacteria, and other organic compounds, etc. the latter arrive from the application of fertilizers, industrial wastewaters, landfill, and mine drainage, etc. [55].

2.2 Sediments and sources of contaminants

The sediments are layers of solid particles in water bodies (e.g., reservoirs and rivers) formed by sedimentation process of eroded soil particles conveyed by the water flow. It is a complicated process due to variation of basin sediments, transportation and deposition. The sedimentary deposition reduces significantly the storing capacity of basins and river flow [56, 57]. The temporal sedimentation can occur at floodplains and lakes in the natural river networks, however, the trapped sediments behind dams and reduced sediment supply at the downstream area were found in the controlled rivers [58]. The sedimentation remains globally substantial threats to stream eco-networks, a study recording long-term sediments in 145 chief rivers of the world illustrated that a remarkably downward flow trend due to deposition was observed around 50% of the rivers [59].

The pollutants are introduced the receiving water through different pathways from rural and urban areas and direct sources. The erosion of soils, channel banks, the waste of dumping sites, and indirect sources due to atmospheric removals is identified as sources from the rural areas, while sources discharged by building materials and drain systems are contributed from urban areas. Eventually, the industrial and shipping activities are ascribed as direct sources of the pollutants [60]. The differences between the point and diffusive sources of the pollution demonstrated their nature due to changes in meteorological factors. The extent of contamination caused by point sources is not affected by the magnitude of the meteorological elements while the meteorological factors are associated closely with spreading the sources of the pollutants derived from diffusive sources [60].

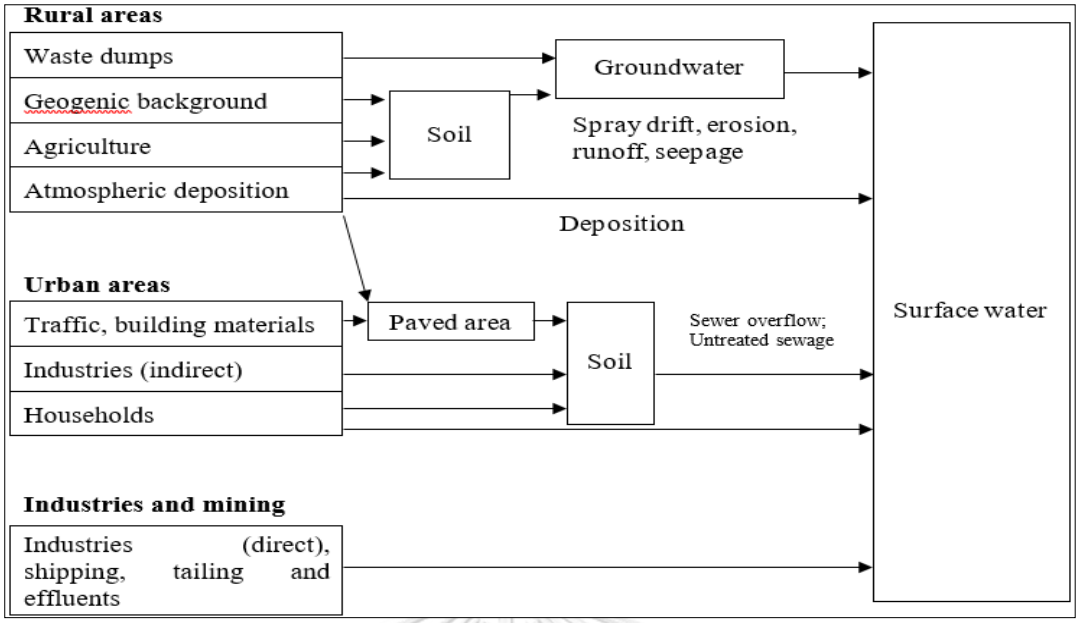

Figure 0.2 A general overview of land-use and sources of the pollutants into the coastal basin, source [60]

2.3 Parameters of water quality and sediments

2.3.1 Temperature

Temperature illustrates to the status of the water (e.g., hot or cold condition) and express in degree Celsius. Changes in water temperature would involve closely with dissolved oxygen, rate of substance diffusion, and photosynthetic reactions, etc. Thus, temperature is a crucial factor in aquatic environment due to its impacts on the properties of water chemistry. A higher temperature leads to an increase in chemical reactions, this makes more dissolved minerals in the environment. Consequently, it will increase greatly an electrical conductivity. Temperature does not only largely effect on biological processes and growth but also management of aquatic organisms in the streams and lakes. Therefore, monitoring programs the temperature should conduct regularly [60].

A higher temperature can increase the toxicity of compounds to aquatic life, the temperature therefore is a factor influecing substantially the surface water. The influences of temperature are follow as: i) more dissolved oxygen in cold water than warm one was observed; ii) high water temperature can promote greatly the

photosynthetic process of aquatic plants leading to degration of the water quality due to phenomenon of algal bloom; iii) alterations of water temperature can affect capacity of aquatic organism resistance resulting in lowering their resistance (e.g., pollutants and diseases) [61].

2.3.2 pH

The pH is an indicator showing water property in the rivers, for example, pH value of 6 to 9, less than 7, and greater than 7 indicates neutral, acidic, and base condition, respectively. The sunlight plays an major role in photosynthesis altering carbon dioxide and water into oxgyen and carbonhydrate. The pH is raised in water bodies due to the generated hydroxy ions. Moreover, a huge amount of carbon dioxide used by aquatic plants during photosynthesis process lowers the extent of carbonic acid in the water bodies, this process therefore contributes to an increase in water pH. While the water pH tends to decrease gradually at night, this is because an large amount of carbon dioxide released by aquatic organisms through respiration activities produces significantly the carbonic acid and hydro ions in the water. The aquatic organisms can be influenced substantially by high or low values of the pH. This is because some compounds become more toxic wih high pH values and affect to parts of aquatic organisms (e.g., grills, eyes, and skin of the fish). Whereas, the pollutants such as heavy metal species in soils or bottom sediments can be easily dissloved and be more mobile with low pH values. The nutrients are also an increase in ability of availability resulting in the problems of enrich basin [62, 63].

2.3.3 Salinity

The salinity of any water body is the result of an equilibrium between the environmental ionic inputs and removals. The open oceans are characterized by remarkable stability and similarity of their composition, not only in their total salinity but also for the relative proportions of the constituents within and between them [64]. Whereas the coastal areas, intermediate water column, and creeks follow to the effects of tides, freshwater inputs, evaporation, and anthropogenic pollutants [65]. This increases the salinity variability on temporal and spatial cycles. The salinity as the amount of dissolved salts may behave conservatively. However, changes in salinity may occur due to dilution or, in the case of semi-tropical areas or, evaporation [66].

Salinity is an environmental master factor for aquatic organisms such that they can be described in accordance with their salinity tolerances. Hence, a stenohaline organism has a restricted salinity tolerance in contrast to a euryhaline organism. Thus, any change to ambient salinity has the potential to affect the ability of animals to carry out vital biological processes and thus their ability to survive and thrive. Therefore, the salinity is regarded as a major element in productivity, dispersion of larval species, distribution of geography, and activity of marine organisms. This is because changes in the salinity does not only influence the structures but also boundaries of species communities. Thus, it should have a cost requested to adapt changes in the salinity that may cause the impacts on the organisms [64, 67].

2.3.4 Electrical conductivity (EC) and Total dissolved solids (TDS)

The electrical conductivity (EC) and total dissolved solids (TDS) are two parameters used regularly for evaluating changes in water quality in the coastal areas. They are utilized popularly for studies focusing on seawater intrusion, demonstrating the extent of salinity in water, the EC and TDS contents correlate closely together. The EC illustrates the water ability to conduct the charge of electrics; it is therefore dependent on the contents of dissolved ions, ionic power, and temperature. While TDS represents normally as the content of dissolved ions [68-71]. The content of TDS shows the existence of inorganic and organic substances in the water while EC measures the electrical currents [72]. The natural and anthropogenic activities are the main factors causing high content of TDS and EC in the environment (e.g., runoff, erosion, salinity intrusion, wastes of domestic and industries, and aquaculture and agricultural practices) [70, 73].

Due to effects of high TDS and EC, some standards are established to control the TDS and EC in the water. For health protection, the permissible thresholds for TDS and EC are between 500 mg L^{-1} and 1,000 mg L^{-1}, and 1,500 µS cm^{-1}, respectively [74]. The salt concentration or extent of salinity is also refered to categorize the parameters [75]. The TDS is sorted as follow: less than 1,000 mg L^{-1} (type I) , range of 1,000 to 10,000 mg L^{-1} (type II), from 10,000 to 100,000 mg L^{-1} (type III), and greater than 100,000 mg L^{-1} (type IV) indicate freshwater, brackish water, saline water, and brine water [76]. While EC is classified in to six forms as the following types: the non-

saline (type I), slight saline (type II), moderate saline (type III), high saline (type IV), very high saline (type V), brine water (type VI) follow respectively. The contents of EC consisting of less than 700 µS cm^{-1}; from 700 to 2,000 µS cm^{-1}; greater than 2,000 µS cm^{-1} and less than 10,000 µS cm^{-1}; range of 10,000 to 25,000 µS cm^{-1}; between 25,000 to 45,000 µS cm^{-1}; and greater than 45,000 µS cm^{-1} [77].

2.3.5 Total suspended solids (TSS)

Total suspended solids (TSS) is defined one of the water quality parameters indicating the amount of suspended materials in a specific identified volume of water trapped by a filter [78], it is expressed in mass (mg) or content (mg L^{-1}) of organic and inorganic substances that is found in the water bodies of rivers, lakes, and channels. Whilst suspended solids (SS) are primarily specified the fine particles having a diameter of less than 62 mm, they are commonly the cohesive forms. The pattern of bigger combined flocs occurs regularly through the transportation found in the previous studies [79]. The transportation of SS is governed by natural conditions in the rivers, their contents increase due to effects of anthropogenic turbulences. This can cause a great change in physicochemical and biological characteristics of the water column.

Physical influences caused by SS consist of preventing from the light penetration, temperature alterations, and reduction of channel and reservoir volume due to deposition process, they also involve with lowering deficiency of treatment plants and water supply and reduce the life span of constructed dams and reservoirs [80]. While chemical effects induced by SS relate to the discharge of pollutants (metal(loid)s, fertilizers, and pesticides) into the aquatic environment [81-83]. In addition, the contents of dissolved oxygen can be reduced in the water due to a large amount of organic substance in suspended solids; this can result in a critical dissolve oxygen deficiency influencing aquatic species [84]. Eventually, the biological influences due to the elevated concentration of SS on various species are primarily the decreasing in productivity, motivated growth, and biomass of algae [85].

2.3.6 Dissolved oxygen (DO) and chemical oxygen demand (COD)

Dissolved oxygen (DO), which is the dissolved gases of oxygen, plays an important role in activities of aquatic organisms, DO is introduced to the aquatic environment

through atmospheric diffusion and photosynthesis process of aquatic plants. In the water bodies, the level of DO balances persistently with the content of oxygen in the atmosphere to sustain 100% status of DO saturation. The over-growth of aquatic plants can induce the over-saturation of DO in the waters, this occurs when the process of photosynthesis is greater than the one of diffusion from the atmosphere. Normally, the DO is found at low content in waters when the amount of dissolved oxygen consumed by aquatic organisms does not have a replacing mechanism [86]. The unnecessary growth of major producers (e.g., bacteria and fungi) relates closely to high loading of nutrients, this leads to an increase in the metabolic activities of river water resulting in degradation of dissolved oxygen in the water bodies. High content of DO is provided by photosynthesis process from the aquatic plants during the day; however, the level of DO reduces gradually in the night due to organism activities. The death of producers is also one of the causes leading to a great reduction in the dissolved oxygen because decomposers (e.g., bacteria) utilize much dissolve oxygen for their activities [87].

Chemical oxygen demand (COD) (milligram per litter mg L^{-1}), which is one of the parameters determining the level of pollution by organic compounds, measures the equivalent amount of oxygen requested to chemically oxidize organic substances in water. Thus, elevated the chemical oxygen required illustrates high loading of the pollutants in the water samples. Therefore, COD is popularly used for controlling wastewater quality in treatment plants [88, 89]. The content of COD ranged from 20 mg L^{-1} O_2 or less to 200 mg.L^{-1} O_2 in the surface waters and receiving waters, respectively. The surface water is attributed to be highly contaminated by organic compounds and influence significantly to the aquatic organisms when the content of COD is over than 12 mg L^{-1} [90].

2.3.7 Nutrient elements

Nitrogenous species are one of the elements playing a crucial role for living organisms; they are a major component of proteins and genetic materials as well. The inorganic nitrogen can be altered to the forms of organic nitrogen by plants and microorganisms. The compounds of inorganic nitrogen exist in the states of oxidation (e.g., nitrite, nitrate, and ammonium) which undergo processes of biological and non-

biological transformation occurring in the nitrogen cycle in the natural environment. The processes of non-biological involvement are characterized by transfer phases (e.g., volatilization, sorption, and deposition). While the transformation of biological phases include as follow: i) inorganic forms are converted to organic ones by plants and microorganisms; ii) nitrogen gas is reduced by microorganisms to ammonia and organic nitrogen; iii) complicated heterotrophic forms from organism are transferred to another; iv) ammonia is oxidized to nitrite and nitrate; v) process of organic nitrogen ammonification generates ammonia; vi) nitrate is reduced by bacteria to nitrous oxide and molecular nitrogen. All nitrogen compounds (e.g., $N\text{-}NO_3^-$, $N\text{-}NH_4^+$, and $N\text{-}NO_2^-$) are expressed in moles per liter or $mg.L^{-1}$) [91].

The form of un-ionized ammonia occurs in equilibrium with the ammonium ion in the aquatic environment. Therefore, total ammonia is the sum of these forms. Whilst ammonia also exists in complex forms with some metal ions and is adsorbed onto suspended solids, bottom sediments, and colloidal particles. It is also exchanged between bottom sediments and water bodies. The total ammonia content, temperature, and pH influence significantly the content of ionized ammonia. In the aquatic environment, the nitrate ion exists commonly the form of combined nitrogen; it is reduced to nitrite through denitrification processes. The nitrite ion is quickly oxidized to nitrate. The igneous rocks, drainage, plants, and animal debris are principal sources providing nitrate to surface waters. Nitrate playing an important role in supplying nutrient for aquatic plants and temporal variations can be originated by decay and plant growth. Its natural contents seldom is greater than 0.1 $mg.L^{-1}$, however, its contents can be enhanced by contributing from sources (e.g., municipal and industrial wastewaters, disposal sites, and landfills). Other can contribute remarkable sources of nitrate that are the application of inorganic nitrate fertilizers. In freshwater, nitrite contents are generally very low, its concentrations ranges commonly from 0.001 $mg.L^{-1}$ to 1.0 $mg.L^{-1}$. High nitrite contents are often associated with unsatisfactory microbiological quality of water and industrial effluents. The existence of nitrate and nitrite in the waters illustrates a general status of nutrient and organic contamination. Thus, they are the most basic water quality parameters in monitoring programs, they also include in monitoring programs to assess the influences of organic or relevant industrial inputs [92, 93].

The other form of nutrients also playing a major role for living organisms and existing in the waters is phosphorus species consisting of both dissolved and particle ones. In the aquatic environment and wastewaters, the phosphorus existed typically in the species of dissolved orthophosphates, polyphosphates, and bound phosphates. Alterations among these forms happen continuously due to decomposition and synthesis of organically bound and oxidized inorganic species. The various forms of phosphate occurred the equilibrium at different pH values. The content of phosphorus is expressed as phosphorus (e.g., $mg.L^{-1}$ $P\text{-}PO_4^{3-}$). The natural activities contribute chiefly the phosphorus sources (e.g., weathering of phosphorus–bearing rocks and organic substance decomposition). While anthropogenic activities in relation to discharge of domestic wastewaters including detergents, industrial wastewaters, and fertilizer runoff resulted in high concentrations in the surface water. The phosphorus involved with organic and mineral components of sediments in the water column, therefore, it could be mobilized by bacterial community and discharged to the water bodies. In the waters, the phosphorus is easily take up by aquatic plants, thus it is hardly found in elevated contents. The seasonal factor affected significantly changes in phosphorus contents in the surface water, its concentrations varied normally from 0.005 to 0.020 $mg.L^{-1}$. Low content of 0.001 $mg.L^{-1}$ $P\text{-}PO_4^{3+}$ may be discovered in pristine water, while high concentration of 200 $mg.L^{-1}$ may be found in enclosed saline waters. The phosphorus plays a crucial form of the biological cycle in the waters; it is often comprised in basic water quality monitoring programs. It is an indicator for degradation of the water relating to eutrophic conditions [94-97].

2.3.8 pH in sediments

Sediment pH is specified as the hydronium ion activity (H_3O^+ or the H^+) in the sediment solution, it is stated as the negative logarithm (base 10) of the H^+ activity in the solution (mole per liter) [98]. Changes in pH may influence to biogeochemical processes, nutrient recycle, and carbon burial in the coastal sediments [99, 100]. pH is one of the factors affecting directly to alteration of physicochemical properties in the bottom sediments, particularly an increase of mobility and solubility of the metal speciation [101, 102]. Hydrogen ions are absorbed to surface negative charges and hold the power to exchange other cations [103]. Low pH can cause the mobility of

metal species while the mobility reduces at higher pH, although the impact of pH on the mobility of metal speciation varies greatly depending on the concentration and kind of organic substance [104, 105]. The metal dynamic is affected remarkably by pH because it governs processes of adsorption and precipitation, which are the major mechanism of the metal preservation in sediments [106].

2.3.9 Total organic carbon (TOC)

The organic substance in the sediments expressing as total organic carbon (TOC) is a major representative reservoir for the global carbon cycle, it contributes to main role in ocean chemistry [107]. The inorganic carbon precipitation of atmospheric CO_2 though the process of photosynthesis in the water bodies produces the greatest fraction of carbon entraining in the sediments. However, only a minor fraction enters the sediment as most of it is oxidized [108]. It is estimated approx. 80% of the carbon is attached in the continental margins; hence, the greatest carbon appears for the current world ocean [109]. On the global scale, reservation of organic substance (TOC) reflects the distribution form of phytoplankton biomass [108]. The presence of organic carbon in the sediments derived from the natural and anthropogenic sources, of which the former related to the plant decay, animals, and plankton, the latter was chemical pollutants, fertilizers, and organic rich wastes [110]. At a regional scale, the reservation of organic substance finding in deep-sea sediments was less than 0.5%. Its level ranges various types of sediments and is governed by the rate of organic substance production [111].

The diverse patterns such as organic and inorganic fragments and plankton cells precipitate the bottom sediments, which can be ascribed as a complex accumulation of organic and inorganic components, the sedimentary organic substances contribute greatly in aquatic organisms as a food sources in the photic zone. The high sorption of hydrophobic organic contaminants and metal species leads significantly the distribution and bioavailability of pollutants [112, 113]. Hence, benthic species and the nutritive value of organic substance in the bed sediments can cause a remarkable impact on the bioaccumulation of both metal patterns and organic contaminants. As trace elements, concentrating typically within the surface of finer-grained sediments and organic substances has a strong affinity for metal speciation [114, 115].

2.3.10 Heavy metals

Heavy metals, which are defined as metallic components, have an excessive density as they are compared with water or more than 5 g/cm^3 [116]. They including vital and non-essential metals, heavy metal species play a key role in living organisms as co-element in enzyme functions. They support significantly the activity of antioxidant enzymes such as glutathione peroxidase. Moreover, they are necessary for some enzymes like carboxypeptidase and constituent of redox enzymes consisting of cytochrome oxidase. Whilst non-essential metal speciation (e.g., cadmium, mercury, lead and titanium) are not involved by living organisms because they inhibit with the function of essential metals and enzymes as well [117].

The essential and non-essential metals may cause the toxicity when they are the supra-optimal extents of crucial metals and higher levels of non-essential metals. Besides, the living organisms would be at risk as their contents of metals increasing in the environment, there were variety of contents of bioavailable toxic and necessary metals that were required in micro-amounts by critical organs and biochemical processes. When there was excessive or deficient quantity in the diet of one or more than one of these components over time, the organism could develop an unusual condition, disease, or even die. For instance, the congestive heart failure for young children relates to the absence of Se in one's body. Inversely, an excessive amount of Se is responsible for acute vascular disturbance, chronic dermatitis, and hair loss. Therefore, it requires different threshold contents of metals in critical organs and biochemical systems of organisms. The ingestion of the available metal species is one of the ways resulting in accumulation of the heavy metals through a food chain or bioaccumulation of low concentrations occurs over the period of time [118].

The toxicity of heavy metals is dissimilar to other toxic elements, they neither are generate nor damaged by human beings. The existence of hazardous metals derives mainly from natural and anthropogenic activities [119, 120]. The anthropogenic activities contribute greatly the pollution of heavy metals into the environment, they include as follow: the industrial effluents, paper mills, application of fertilizers, and pesticides, dyes, pigment, metal cleaning, leather, and mining, etc. [121]. In addition, redistribution of hazardous metals could be found through activities (e.g., combustion

of fossil fuel, metallurgy, and waste transport) [122, 123]. Eventually, the natural sources such as the urban storm, runoff, landfill, weathering of minerals, and soil leaching contribute to releasing the heavy metals into the environment [124, 125]. It differs from herbicides, pesticides, and other toxicants, which have to undergo the process of breakdown, while the heavy metals cannot eliminated from the water column and persevere sediments [126, 127].

The heavy metals (e.g., As, Cu, Zn, and Pb), which would be evaluated in this study, are the class 01 impurity heavy ones [128]. Elevated contents of these metals varied seasonally and spatially and tended gradually to increase over time [129, 130]. They also occurred generally in the natural environment and bio-accumulate possibly in the human, organisms. Thus, they cause the most remarkable toxic to humans and animals [131]. The routes (e.g., oral, dermal, and inhalation) are main pathways that the heavy metals enter into the body. They can go across the body through the bloodstream and accumulate to the target organs. Due to toxicity's heavy metals, the chronic exposure to metalloids can lead to serious effects at relatively low extents. Consequently, they are concerned increasingly in the developed world due to increasingly demanding for a better environment and reduction of pollutants influencing to people [132-134].

a. Arsenic (As)

Arsenic (As) is a popular element in the nature and found widely in waters, soils, rocks, and organisms. More than 200 different minerals as inorganic compounds with lead, gold, and other metalloids are associated with the existence of As. It presents generally at elevated contents in igneous and sedimentary rocks [135]. The inorganic As is defined as combination of As with oxygen, chlorine, and sulfur, while As combining with carbon and hydrogen is specified as organic As. As compounds do not have smell and taste and white or colorless powders [136]. The major sources releasing As into the environment are associated with the natural and anthropogenic activities. The presence of As in groundwater and surface water involves with process of erosion and weathering of rocks in the nature [137]. In addition, anthropogenic activities at mining sites distribute significantly the contents of As into soils, surface water and the deposit down sediments [138].

It is estimated that millions of people are exposed chronically to As in the worldwide, mainly in countries, where the groundwater and surface water are contaminated with high extents of As. The ingestion, inhalation, dermal contact, and parenteral routes are the chief pathways occurring As exposure [139]. As is a class 1 human carcinogenic heavy metal with enough evidence from human epidemiological data [131, 140]. Three pathways of exposure are through oral, dermal, and inhalation. Although dermal exposure to As can enter a small amount into the body compared with oral and inhalation routes, basically As can accumulate and affect to any organs depending on the lifestyles, demographic factors, frequency, and duration of exposure [137, 141]. As contents differing from remote areas and cities vary from 1 to 3 ng m^{-3}, and from 20 to 10 ng m^{-3}, respectively. Generally, contents of As in water are less than 10 µg L^{-1}, but its contents are high in soil fluctuating in ranges of 1 to 40 mg Kg^{-1} [142].

Contamination with high contents of As is one of the causes resulting in the effects of severe health. Many studies have indicated a great correlation between As exposure and an increase of risks (e.g., carcinogenic and systemic effects of health). The organ systems (e.g., nervous, renal, dermatologic, and respiratory systems) are influenced significantly by As exposure. In many areas of As pollution, the considerably higher standardized mortality rates for cancers (e.g., kidney, skin, and liver) are also shown by many researchers. The extent of serious health effects involves with the chemical type of As, time, and dose-dependent, as well [143, 144].

The dangerous inorganic patterns of As are methylated by bacteria, algae, fungi through the biotransformation of As to offer mono-methylarsonic (MMA) and dimethylarsinic (DMA) acids. In the process of biotransformation, these inorganic As patterns (iAs) are conveyed enzymatically to methylated arsenicals that are the end process of metabolites and the biomarker of chronic As exposure.

iAs (V) $\rightarrow$ iAs (III) $\rightarrow$ MMA (V) $\rightarrow$ MMA (III) $\rightarrow$ DMA (V)

A process of detoxification is called bio-methylation, the end products are methylated by inorganic As (e.g., MMA (V) and DMA (V)), which are emitted through urine (bio-indication of chronic As exposure). Nevertheless, MMA (III) is not removed and presents inside the cells as intermediate products. While mono-methylarsonic acid

MMA (III) is found as toxicity in comparison with other arsenicals, having potential for arsenic-induced carcinogenesis [145].

2.3.10.1 Lead (Pb)

Lead (Pb), a soft, blue-gray element, is found naturally in combination with others in the crust of the earth. It has been existed in the form of both organic and inorganic compounds, which have no nutrient benefits for the human body. Pb is released into the surrounding environment through natural sources (e.g., soil erosion and atmospheric deposition). Natural deposits commonly happen together with heavy species. The anthropogenic activities have discharged a great source of Pb into the environment (e.g., mining, burning, fossil fuels, and lead-polluted products) [137, 146]. The mean level of Pb in surface soil was 32 mg Kg^{-1} with a range of 10 to 67 mg Kg^{-1}, whilst the elevated contents of Pb found at the gold mine tailings was 80 mg Kg^{-1} [147, 148].

Pb, which is the most unsafe heavy species, can enter into the human body through routes (e.g., oral, the dermal, and inhalation). The effects of Pb to organs and systems of the human body depend on the duration and magnitude of exposure [132]. The absorption rate of Pb through drinking water on adults and children is 35 to 50% and greater than 50%, respectively. The Pb absorption is influenced by factors such as age and physiology. The highest percentage of Pb is absorbed into the kidney, followed by the liver and the other soft tissues (e.g., the heart and brain) [149]. The nervous system is the most susceptible target of the Pb, the early impacts of Pb exposure on the central nervous system are associated with the symptoms (e.g., headache, poor attention spam, and loss of memory). Moreover, a plant containing high extent of Pb holds on the production of reactive oxygen patterns leading to lipid membrane damage that finally causes impairment of chlorophyll and photosynthetic processes. Eventually, the entire growth of the plant is suppressed [150].

Pb metal becomes to toxicity in living cells by the following ionic mechanism and oxidative stress. Of which oxidative stress in living cells is generated by the imbalance between the production of free radicals and the generation of antioxidants to detoxify the reactive intermediates. The occurrence of heavy species on a cell and the balance between ROS production and the later defense offered by antioxidants.

The antioxidants show the protection of the cells from free radicals as H_2O_2 under the impacts of Pb, but the extent of the ROS increases and the level of antioxidants reduces. Once glutathione persists both reduced (GSH) and oxidized (GSSG) forms, the reduced pattern of glutathione offers its reducing equivalents (H^++e^-) from its thiol groups of cysteine to ROS making them stably. In the existence of enzyme glutathione peroxidase, the reduced glutathione certainly combines with another molecular of glutathione after giving the electron and generates glutathione disulfide (GSSG) [149, 151]. The reduced (GSH) of glutathione elucidates for 90 per cent of the total glutathione content and the oxidized pattern (GSSG) explains for 10 per cent under typical conditions. On the other hand, the concentration of GSSD outdoes the content of GSH under the status of oxidative stress. Additionally, the lipid peroxidation considers as another biomarker of oxidative stress, since the electron from lipid molecules demonstrating inside the cell membrane is collected by the free radical, which eventually leads to lipid peroxidation. ROS may lead to structural harm (e.g., cells, proteins, nucleic acid, membranes, and lipids) causing a stressed case at the extent of cellular [152]. The ionic mechanism of Pb toxicity happens principally due to the capacity of Pb metal ions replacing other bivalent cations (e.g., Ca^{2+}, Mg^{2+}, and Fe^{2+}) and monovalent cations such as Na^+, which ultimately disturbs the biological metabolism of the cells. Moreover, this mechanism causes significantly in alterations of various biological processes. Pb can exchange calcium even in pico-molar concentration affecting on protein kinase C, which controls neutral excitation and memory storage [149].

2.3.10.2 Copper (Cu)

The atmospheric deposition, geologic input, roadways, and pressure-treated lumber are possible sources releasing Cu into the environment. The atmospheric statement and stream water involve with burning of Cu-holding coal and weathering of Cu-comprising bedrock. Cu can be deposited on the roads by transport activities such as burning of gasoline, diesel, and tire wear. In addition, the runoff due to rainfall can wash out the Cu from the surfaces directly into the surrounding environment [153, 154]. The natural concentration of Cu in soil, atmosphere and water follows 50 ppm, ranges of 5 to 20 ng m^{-3}, and from 40 to 10 ng L^{-1}, respectively.

The potential sources of Cu originate from the air (e.g., dust, volcanoes, forest fires), while Cu is absorbed to the organic substances in the aquatic environment. The anthropogenic sources comprise of Cu water pipes, drinking water, mineral supplements, and fungicides including Cu [155]. Cu is an alteration metal having the capacity of moderate solubility. However, it binds freely to sediments and organic substances [156]. Because of high nuclear charge, small size, and high ionization potential, Cu has low reactivity. The pattern of cuprous ion (Cu+) can be dissolved to produce Cu (II) and Cu (0). The cupric ions (Cu++) is the most chief oxidation state of Cu, and it universally occurs in the aquatic environment [157]

The exposure to Cu via environmental or occupational pathways often include exposure other metals such as As, Fe, Hg, and chemicals (e.g., polychlorinated biphenyl and pesticides consisting of Cu [158]. Cu uptake depends on food choices, dietary customs, and environmental factors. An amount of 1-5 mg Cu containing in the most diets prevents a deficiency. Therefore, it is recommended that dietary intakes of Cu base on the amount of 0.9 mg d-1 for adults both male and female from 19 to 70 years old [159]. It is around 6 to 13% of the mean daily intake of Cu via drinking water. The maximum extent of Cu has been set at 1.3 ppm (US.EPA, 2013). It is quite difficult to determine the upper intake extent of Cu consumption due to health impacts of both Cu deficiency and excess. Thus, it suggests that it is considerably important to re-evaluate and develop the scientific basis for an acceptable upper intake level of Cu and Cu deficiency as well [160].

Copper (Cu) is explored a number of cells and tissues with the highest concentrations in the liver and brain [161]. Most organisms gain a combination of controlled import and enhanced export mechanisms protecting against metal-induced toxicity. The mechanisms adjusted the status of metals via metal-combing proteins at the levels of transcription and enzyme. The existence of chaperones controls Cu homeostasis certifying Cu is offered to vital proteins without leading to severe effect of cellular, whilst tissue damages and diseases are associated with disruption in the homeostasis of Cu [162]. The reactive oxygen species (ROS)-induced oxidative damage, one of the toxic mechanisms, contributes a major role in Cu toxicity. Overbalance Cu can lead to per-oxidative to membrane lipids via the reaction of lipid

radicals and oxygen to generate peroxy radicals [163]. High content of Cu illustrates oxidative damage consisting of reduced extents of hepatic GSG, rose levels of mitochondrial lipid peroxidation products. Moreover, it decreases the activity of cytochrome oxidase and degrades liver mitochondrial respiration. The Cu deficiency associates to the inactivation of major metabolic enzymes, whilst over-accumulation of Cu involving with Wilson's disease derives Cu reduced oxygen radical-mediated damages [164]

d. Zinc (Zn)

Zinc (Zn), which is omnipresent in the environment, occurs in the crust of the earth at mean concentration of approx. 70 mg kg^{-1}. It is not found freely, the form of +2 oxidation happens mainly in the nature as various minerals (e.g., zinc sulfide, zinc carbonate, and zinc oxide). It is Fifty-five minerals containing Zn. The metal smelters and mining activities as anthropogenic sources release Zn into the environment. The production and use of minerals consisting of Zn lead to its release via various waste effluents [165]. Zn can be found in natural streams in different chemical patterns (e.g., hydrated ions, metal-inorganic and organic complexes. The hydrolyzing process of hydrated zinc cations forms the zinc hydroxide, while zinc sulfide may be favorable in anaerobic environment. Zn accumulates in aquatic organism and bio-content factors indicating from 1,000 to 2,000 for freshwater and marine fish [166].

Zn enters into the human body via three main pathways comprising of inhalation, dermal, and ingestion. The effects and uptake of Zn to specific parts of the body depend on the type of exposure. The inhalation of Zn including smoke is called the metal fume fever derived from the uptake of Zn oxide. The acute syndrome relating to industrial diseases chiefly occurs via inhalation of fumes with a particle size of <1 μm, the symptoms of alterable syndrome begin a few hours after acute exposure (e.g., fever, muscle, soreness, fatigue). The respiratory indicators go with an increase in bronchiolar leukocytes. It is suggested that the allowable exposure limit of Zn oxide is 5 mg Kg^{-1} in workplace air during an 8-hour workday, 40-hour workweek to ensure the occupational safety and health. The pH of the skin does greatly the effects of Zn entering the human body via dermal absorption [167]. Previous studies indicated that it was around 25% Zn oxide path (2.9 mg cm^{-2}) was placed on human skin for 48

hours, dermal irritation did not occur, while the dermal impacts of various Zn patterns illustrated obviously the strongest irritation [137].

The Zn consumption via oral absorption as supplemental Zn has involved increasingly with health consequence in the human body. It causes hematological effects; reduces in cholesterol extents [168, 169]. Elevated levels of Zn can lead to a capacity of the carrier-mediated path of zinc absorption. It is proved that intake of Zn excess may cause a lack of Cu. Severe Cu deficiency surveyed by individuals ingested highly doses of Zn for over one year. More subtle signs of impaired Cu status are demonstrated visibly at lower Zn doses. Small amount of Zn up taken is vital for survival. Therefore, it is recommended the permissible dietary for Zn is 11 mg day^{-1} and 8 mg day^{-1} for men and women, respectively. For infants and children are requested (2-3 mg day^{-1}) and (5-9 mg day^{-1}), accordingly. Overall, intake of such a quantity is improbable, an amount of 225-400 mg could cause emetic symptom [159].

2.4 Hydrodynamic model

In recent years, numerical models, which have not only increased but also improved remarkably, focus on the studies of the water quality and pollutant diffusion in surface water as well. Over the last decades, studies relating to the fate and transport of hazardous materials have been intensely conducted in aquatic systems. Nowadays, many numerical models are used to simulate hydrodynamics and water quality, of which the most common numerical models are as follow: the Streeter-Phelps models in 1925, which consists of versions (e.g., S-P model, Thomas BOD-DO model, O'Connor BOD-DO model, and Dobbins-Camp BOD-DO model), concentrates on oxygen balance and one-order decay of BOD. They are chiefly one-dimensional steady-state models. The QUAL models in 1970, including the patterns of QUAL I, QUAL II, QUAL 2E, QUAL 2E UNCAS, and QUAL 2K, are suitable for dendritic river and non-point source pollution. They are one-dimensional steady state or dynamic models. The WASP models in 1983, which comprise of WASP1-7 models, suit for water quality simulation (e.g., river, lakes estuaries, coastal areas, and reservoirs). They associate with one - (1D), two - (2D), or three-dimensional (3D) models. The QUASAR model is applied for dissolved oxygen simulation in larger

rivers; it is a one-dimensional dynamic model consisting of PC QUA SAR, HERMES and QUESTOR modes. The MIKE models comprising of MIKE11, MIKE 21, and MIKE 31 are employed for hydrodynamic and water quality simulation such as rivers, estuaries, and tidal wetlands. They include one-(1D), two-(2D), or three-dimensional (3D) modes. The BASINS models in 1996 consisting of BASINS 1, BASINS 2, BASINS 3, and BASINS 4 are used for multi-purpose in the environmental system; they combine point and non-point sources. The models suit to water quality analysis at basin scale. Finally, the EFDC model in 1997 used for effective water quality simulation (e.g., rivers, lakes, estuaries, and wetlands), comprises one-(1D), two-(2D), or three-dimensional (3D) models [170].

The Delft 3D model developed by Deltares is the multi-dimensional (2D or 3D) simulation program. The model can be applied for the various areas: i) tide-influenced flows, wind, and density gradients; and wave-caused currents; ii) propagation of short waves spreads directionally; iii) advection and dispersion of discharges; iv) calculation of online morpho-dynamic (e.g., local erosion, short time and long scales); v) transport of sediments; vi) water quality phenomena (e.g., the project of heavy metal contents, relations between organic and inorganic suspended sediments, and the water and bottom phase as well; vii) tracking particles such as oil spill; viii) changes in dynamic 2D-morphology (time-fluctuating) [171].

In this research, the hydrodynamic module, which are integrated in the Delft3D model, are used to simulate changes in hydrodynamics at Ganh Hao River. The hydrodynamic module, Delft3D-FLOW, is a multi-dimensional simulation program that computes unsteady flows as well as transport phenomena deriving from tide and meteorology forcing on curvilinear and boundary-suitable grids as well. The hydrodynamic module is associated with the full Navier-Stokes equations with the applied shallow water approximation. The equations are with a procedure of unconditionally stable solution. The hydrodynamic model can employ for several areas, for examples, seawater intrusion, freshwater river effluents, thermal stratification (e.g., lakes and seas), transport of sediments and dissolved substances, storm surges, effects in combination with tide and wind, river flows, reservoir deposition and degradation the bottom dams, and weirs.

The coordinate system is principally Cartesian-x, y coordinate systems, orthogonal curved coordinates (ξ,η), and spherical coordinate systems (λ,ϕ).

Where: ξ=λ; η=ϕ; ξξ=RG cosϕ; ηη= RG; R-earth radius; ϕ-geographical latitude.

The system of vertical coordinate (σ) is specified as follows:

$$\sigma = \frac{z-\xi}{d+\xi} = \frac{z-\xi}{H}$$

Where: z: the vertical co-ordinate in physical space; ζ: the free surface elevation above the reference plane (at z= 0); d: the depth below the reference plane; H: the total water depth, given by (H=d+ζ). At the bottom σ=-1; the free surface σ=0.

Continuity equation: the depth-averaged continuity equation is originated by a combination the continuity equation for incompressible fluids (∇*vector (u)= 0) over the total depth, included the kinematic boundary conditions at the water surface and bed levels, and is offered by: (1)

$$\frac{\partial \zeta}{\partial t} + \frac{1}{\sqrt{G_{\xi\xi}}\sqrt{G_{\eta\eta}}} \frac{\partial ((d+\zeta)U\sqrt{G_{\xi\xi}})}{\partial \xi} + \frac{1}{\sqrt{G_{\eta\eta}}\sqrt{G_{\xi\xi}}} \frac{\partial ((d+\zeta)V\sqrt{G_{\xi\xi}})}{\partial \eta} = Q$$

With *U* and *V*, the depth averaged velocities

$$U = \frac{1}{d+\zeta}\int_d^{\zeta} u\, dz = \int_{-1}^{0} u\, d\sigma$$

$$V = \frac{1}{d+\zeta}\int_d^{\zeta} v\, dz = \int_{-1}^{0} v\, d\sigma$$

In addition, Q represents as the contributions per unit area because of the discharge or withdrawal of water, precipitation and evaporation:

$$Q = \int_{-1}^{0}(qin - qout)d\sigma + P - E \quad (4)$$

Where: q_{in} and q_{out} are the local sources and sinks of water per unit of volume (1/s), accordingly; P and E are the non-local source of the precipitation and non-local sink due to evaporation, respectively.

Momentum equations in horizontal direction are the momentum equations in ξ and η direction as follow:

$$\frac{\partial \mathrm{u}}{\partial \mathrm{t}} + \frac{u}{\sqrt{G_{\xi\xi}}}\frac{\partial \mathrm{u}}{\partial \xi} + \frac{v}{\sqrt{G_{\eta\eta}}}\frac{\partial \mathrm{u}}{\partial \eta} + \frac{\omega}{d+\zeta}\frac{\partial \mathrm{u}}{\partial \sigma} + \frac{uv}{\sqrt{G_{\eta\eta}}\sqrt{G_{\xi\xi}}}\frac{\partial\sqrt{G_{\xi\xi}}}{\partial \eta} - \frac{v^2}{\sqrt{G_{\xi\xi}}\sqrt{G_{\eta\eta}}}\frac{\partial\sqrt{G_{\eta\eta}}}{\partial \xi} - f_v$$

$$= -\frac{1}{\rho_0\sqrt{G_{\xi\xi}}}P_\xi + F_\xi + \frac{1}{(d+\zeta)^2}\frac{\partial}{\partial\sigma}(v_v\frac{\partial \mathrm{u}}{\partial\sigma}) + M_\xi \quad (5)$$

$$\frac{\partial \mathrm{v}}{\partial \mathrm{t}} + \frac{u}{\sqrt{G_{\xi\xi}}}\frac{\partial \mathrm{v}}{\partial \xi} + \frac{v}{\sqrt{G_{\eta\eta}}}\frac{\partial \mathrm{v}}{\partial \eta} + \frac{\omega}{d+\zeta}\frac{\partial \mathrm{v}}{\partial \sigma} + \frac{uv}{\sqrt{G_{\eta\eta}}\sqrt{G_{\xi\xi}}}\frac{\partial\sqrt{G_{\xi\xi}}}{\partial \eta} - \frac{u^2}{\sqrt{G_{\xi\xi}}\sqrt{G_{\eta\eta}}}\frac{\partial\sqrt{G_{\xi\xi}}}{\partial \eta} + f_u$$

$$= -\frac{1}{\rho_0\sqrt{G_{\eta\eta}}}P_\eta + F_\eta + \frac{1}{(d+\zeta)^2}\frac{\partial}{\partial\sigma}(v_v\frac{\partial \mathrm{v}}{\partial\sigma}) + M_\eta \quad (6)$$

Where: $\frac{\partial \mathrm{u}}{\partial \mathrm{t}}$: equation (5) is alteration of velocity in u direction over time.

$\frac{\partial \mathrm{v}}{\partial \mathrm{t}}$: equation (6) is variation of velocity in v direction over time.

2.5 Related studies

In the Vietnamese Mekong Delta (VMD), the south of Vietnam, studies focusing on pollution of the surface water and sediment have been carried out over the last decades. The results of these studies found that pollutants (e.g., nutrients, organic substances, and metalloids) have contaminated surface water and sediment considerably. Concentrations of pollutants have not only varied significantly by time and space but also illustrated the temporal increase of pollutants in the previous studies.

The contents of metal species in both dissolved phase and suspended matter during the different conditions of hydrological regime were normally explored within the range detected for the unpolluted environment. The average dissolved phase contents (n M) of heavy metals (e.g., Cd, Cu, Ni, and Pb) in the river from March to October ranged in 0.03 and 0.09, 14 and 15, 7.8 and 8.4, 0.51 and 0.50, respectively. Overall, the measured concentrations of two seasons illustrated no significant difference.

Between the particulates and dissolved phase were not noticeable exchange due to changing in the dissolved phase metal levels in surface water with the salinity gradient. Whilst, the average contents of metal species (e.g., As, Co, Cr, Ni, Pb, and Al in the suspended matter (*A*g/g) surveyed in March to October at the river end-associate) varied between 24 and 11, 17 and 9, 49 and 29, 32 and 18, 42 and 19, 113 000 and 67 000, accordingly. The average contents of trace metals in March were twice higher than that in October, this was due to the effect of smaller particles supplying during the dry season. The concentration of core components (e.g., carbon total, carbon organic, Si, Al, Ca, K, Fe, Mg, and Ti) and trace metals (e.g., Pb, Zn, Cu, Ni, Mn, Cr, Cd, and Hg) in external sediments illustrated similarly values during the seasons and showed any major changes in depth [25].

The findings illustrated the contamination of trace metals (e.g., Hg, Cd, Pb, As, Cu, Zn) in the river sediment in the estuaries of the VMD increased generally in the order of Hg < Cd < Pb < As < Cu < Zn. Particularly, the average contents (mg Kg-1) of Hg, Cd, Pb, As, Cu, and Zn were 0.1, 1.1, 3.8, 5.9, 33.4, and 96.6, respectively. It was found that the great interaction between the river flow and seawater at downstream and estuaries resulted in the deposition of particles comprising of metalloids, which derived from the inland. Therefore, most metal species increased progressively towards the sea. Additionally, elevated contents of heavy metals found in the small tributaries where they follow into the course of the main rivers, this illustrated that the existence of the metalloids in the sediments did not only originated from natural sources but also anthropogenic ones. In general, the contents of detected metals in the research were slightly less than the Vietnamese guidelines referred for assessing the extent of adverse impacts to aquatic ecosystems), except for Pb. By compared with the norms of several countries in the world, the findings in the observed areas were at high levels [26].

The quality of surface water at main rivers/canals in the Ca Mau Peninsular was assessed with parameters of temperature, pH, EC, TDS, DO, P-PO43-, and NH4+. The results indicated that temperature, pH, EC, TDS, P-PO43- met the allowable standards, which were suitable for aquatic organisms. However, the contents of NH4+ exceeded a double of the allowable norm with an average value of 0.638 mg L-1.

Similarly, DO also was lower than the permissible limitation with an average content of 4.8 mg L-1. This illustrated that degradation of surface water quality was associated with the nutrient and organic substances. The findings showing agricultural practices were the major factor resulting in the impairment of water quality [47]

The levels of heavy metal contamination (e.g., As, Cu, Pb, Zn, and Cd) were evaluated in sediment and surface water at the canals, rivers, estuaries, swamp, and mangrove forests in consecutive two seasons in Ca Mau province. The findings indicated that the contents of As increased gradually from inland to estuaries with elevated values found at Ganh Hao estuary. The measured contents of As in surface water fluctuated from 0.4 to 23.3 µg L-1 and exceeded Vietnamese guidelines at sampling sites. The levels of Cd in sediment and surface water were measured in ranges of 0.027 to 0.093 mg Kg-1 and 0.023 to 0.06 mg Kg-1; 0.38 to 2.63 µg L-1 and 0.18 to 0.28 µg L-1 in the wet and dry season, respectively. Overall, the contamination of As tended to increase gradually from the inland to the estuaries. Additionally, it is found that As had a positive correlation with EC and pH. Changes in the seasonal factor influenced significantly the variability of trace metals. The sediment was polluted slightly by metal species (e.g., As, Zn, and Cu), which exceeded the allowable standard for aquatic organisms [45].

The Vietnam River System and Plains model (VRSAP model) was used to manage water resources in the Ca Mau peninsular, which has been improved with new options. The study aimed to simulate the hydraulic and water quality as a basis of avoiding the conflicts in water use among agriculture and aquaculture practices in the coastal zones. The results enabled to specify the best measures for constructing schedule, which would take the elevated return on investment; this was because model measures could illustrate the impacts of sluice operation on water level and salinity yearly as well. In addition, the schedules of sluice operation by using the model solved the conflicts the demand for water used for rice cultivation and shrimp culture in eastern and western part of the Ca Mau peninsular, respectively [172].

[31] conducted in variability analysis and relation among climate, hydrology and water quality in the downstream of the Mekong River. The study based on the monitoring data (e.g., climate, hydrology, and water quality) collected from 1985 to

2004. Overall, the water quality was good or very good for water quality parameters (e.g., DO, pH, EC, NO_3^-, PO_4^{3-} and TP). The seasonal element did not only influence on the climatic and hydrologic factor but also water quality parameters. The flow and precipitation could be used for projecting changes in the climatic and hydrological variables, and water quality, which were performed using ARIMA models. The results showed that three variables (e.g., TSS, alkalinity, and EC) were bio-chemically conventional parameters, whilst the predicting results of model regarding to other parameters were consistent with shorter period in comparison the former parameters.

The assessment of surface water deterioration was associated with the As pollution at different ecological zones including freshwater, brackish water, saline water in the VMD. The results indicated that the average contents of As differed remarkably from various ecological zones. Particularly, low levels of As found in freshwater with contents in ranges of 0.26 to 8.63 µg L^{-1}, higher contents were around 0.30 to 15.39 µg L^{-1} in brackish water, and highest contents were around 24.47 to 78.41 µg L-1 in saline area. The findings showed that As concentrations increased progressively from inland to estuaries and from the upstream to the lower part of Tien and Hau River. The content of As in saline areas was about 4 times higher than the allowable standard for coastal water quality at Bac Lieu and Ca Mau province. The contents of As in saline areas, which had significant difference from that in brackish and freshwater areas, had the average contents of 49.47 µg L^{-1}, 8.51 µg L^{-1}, and 1.48 µg L^{-1}, respectively. Additionally, it is found that As contents had a positive correlation with pH, EC, and SS in saline areas, and EC and SS in brackish areas [130].

The findings revealed that pollution of surface water in the VMD causing considerably risks to human, animal and ecosystem health due to intensive utilization for drinking, irrigation, and domestic purpose. The research was implemented from November 2011 to July 2012 at 32 observed locations demonstrating in the fresh, brackish and saline environment. The findings illustrated that pH (max. 8.6), turbidity (max. 461 FTU), highest contents of N-NH_4^+ (14.7 mg L^{-1}), metalloids (e.g., As (44.1 µg L^{-1}), Ba (157.5 µg L^{-1}), Cr (84.7 µg L^{-1}), Hg (45.5 µg L^{-1}), Mn (1,659.7 µg L^{-1}), Al (14.5 mg L^{-1}), and Fe (17.0 mg L^{-1})) in canals exceeded the allowable limitation for drinking and domestic use. Urbanization, metal species leaching from soils,

aquaculture practices, and tidal cycles elucidated 85% of the variation of water quality through the PCA (principal component analysis) analysis. Moreover, water quality maps denoted hotspot areas of pollution apparently with selected pollutants relating to land-use [29].

The degradation of water quality at main rivers in Ca Mau province was investigated through the parameters such as DO, COD, BOD_5, $N\text{-}NH_4^+$, and $P\text{-}PO_4^{3-}$. The measurements showed that DO was lower than the allowable standard for surface water quality with the content of 4.66 mg L^{-1}. Similarly, $N\text{-}NH_4^+$ and $P\text{-}PO_4^{3-}$ exceeding the permissible limitation had the values of 3.111 mg L^{-1} and 0.963 mg L^{-1}, respectively. However, COD and BOD_5 still satisfied the permissible standard. The results of WQI indicated that the status of surface water quality was polluted moderately; the agricultural activities and domestic wastewater were specified as the possible sources of contaminants leading to impairment of water quality in this province [173].

The water quality in mainstream and tributaries of the Hau River surveyed at observed 36 sites has been degraded in the rainy season (June 2013 and September 2013) and the dry season (December 2013 and May 2014). The measurements illustrated the temperature and pH were suitable for aquatic organisms. The higher level of TSS in the rainy season than the dry one was discovered one at most sampling locations while DO contents varied from 1.76-7.96 mg L^{-1}, with a mean of 4.9±1.4 mg L^{-1}. In addition, the concentrations of nutrients and organic substances in the dry season were higher than that in the wet one. Particularly, the measured average values of $N\text{-}NO_3^-$, TN, $P\text{-}PO_4^{3-}$, TP, and COD were 0.11±0.07 mg L^{-1}, 1.17±0.6 mg L^{-1}, 0.1±0.07 mg L^{-1}, 0.29±0.25 mg L^{-1}, and 14.3±6.3 mg L^{-1}, respectively. A great variability of water quality parameters was found in the study area shown by PCA analysis. The content of suspended solids reaches a peak in the rainy season, while nutrient and organic substance contents had the highest values in the dry season. In general, water quality on the Hau River was relatively eutrophic, especially in the areas affected by agricultural practices [174].

The developed hydrodynamic model using the MIKE 11 model and the application of the developed model projected salinity intrusion under the different scenarios of seal

level rise until 2030. The main objective of the research was to suggest mitigated and adaptive solutions of salinity tolerance for maintainable agricultural practices in the Ca Mau peninsula respect with proposed scenarios. The findings revealed that the seawater intruding into inland, particularly the Hau River coastal areas, was less than 10 km, however, the salinity would be reduced in inside area of the Peninsular depending on the different salinity levels. The complicated variation of seawater intrusion would lead to a strong influence on the agricultural practices. Therefore, the proper measures mitigating and adapting the sea level rise due to effects of climate change should focus on land-use planning; the selective plants can tolerate to different salinity limitations; solutions of less water irrigation utilized advanced techniques; infrastructure used for seawater prevention was necessary in this area [37].

The simulation and computation the water level as well as water quality were carried out through four variables (e.g., DO, NH_4^+, NO_3^-, and BOD_5). A 1D model coupling with 2D one employed for evaluating changes in water quality during the dry and wet season of the year 2016 was associated with the coastal estuaries. The calibrated and validated hydrodynamic model illustrated high degree of agreement respect with the phase and amplitude of water level at observed stations with mean absolute error (MAE), root mean square error (RMSE), and per cent bias varied from 0.05 to 0.37 m, 0.12 to 0.64, and -8.9 to 3.2 %, respectively. The findings of water quality model demonstrated that the selected parameters such as DO and BOD_5 in the dry and rainy season exceeded the Vietnamese guidelines established for the surface and coastal water quality as well as water quality for domestic water purposes [44].

A multivariate statistical method was used to conduct in analysis of surface water quality based fifty one sample sites at main rivers in Ca Mau peninsular in the wet and dry seasons in 2020. The results of the research revealed that the surface water was polluted with organic matters, suspended solids, nutrients, and microorganisms. DO, TSS, BOD_5 and pH were specified to contributed up to 76.91 to seasonal variability of water quality based on DA model. The water quality was classified from bad to heavy pollution. Three main components (PC1-PC3) were the principal sources influencing on water quality, explaining 85.54% of total variation on water quality. The sources of contamination could derive from anthropogenic activities (e.g., domestic wastewater,

waste from agriculture, fisheries, industry, landfills) and natural sources (e.g., hydrological regimes, rainwater overflow, and riverbank erosion) [175].

CHAPTER 3
RESEARCH METHODOLOGY

3.1 Study location

Ganh Hao River with a total length of about 55 km runs through Bac Lieu and Ca Mau provinces in VMD (Figure 0.3). It starts from Ca Mau City and flows southward, then confluence in Ca Mau City, Dam Doi, and Cai Nuoc districts. This river then changes eastward and courses to the East Sea [176]. The research area, a common boundary of Dong Hai and Dam Doi districts in Bac Lieu and Ca Mau provinces, is located in lower part of the Ganh Hao River with a total length of approx.11 km, which was specified by the upstream and downstream boundaries. The upstream boundary is primarily the confluence of Xang canal in Dinh Thanh commune, the downstream boundary is the confluence of Ganh Hao-Ho Phong canal in An Phuc commune around 6 km from the estuary of Ganh Hao River (Figure 0.3). The predominant land use in the study area has been mostly aquaculture activities focusing mainly on intensive, semi-intensive, extensive, and advanced-extensive shrimp culture. Particularly, the Dong Hai district has a natural area of 57,008.74 ha of which shrimp culture obtained for 39,387.5 ha. The district consists of 11 administrative units at the level of commune, of which Dinh Thanh, An Trach, and An Phuc communes accounted for 14,140.47 ha of a total natural district's area with 11,095.12 ha used for shrimp farms [177, 178]. Whilst the Dam Doi district, which has the same types of shrimp culture as Dong Hai district, comprised 42,821.2 ha out of a total natural district's area of 78.204,04 ha utilized for the shrimp farming. Six out of 15 communes, namely Tan Trung, Ta An Khuong, Ta An Khuong Dong, Ta An Khuong Nam, Tan Duc, and Tan Thuan districts, had a total natural area of 30,858.96 ha

including 23144.89 ha used for aquaculture practices [179, 180].

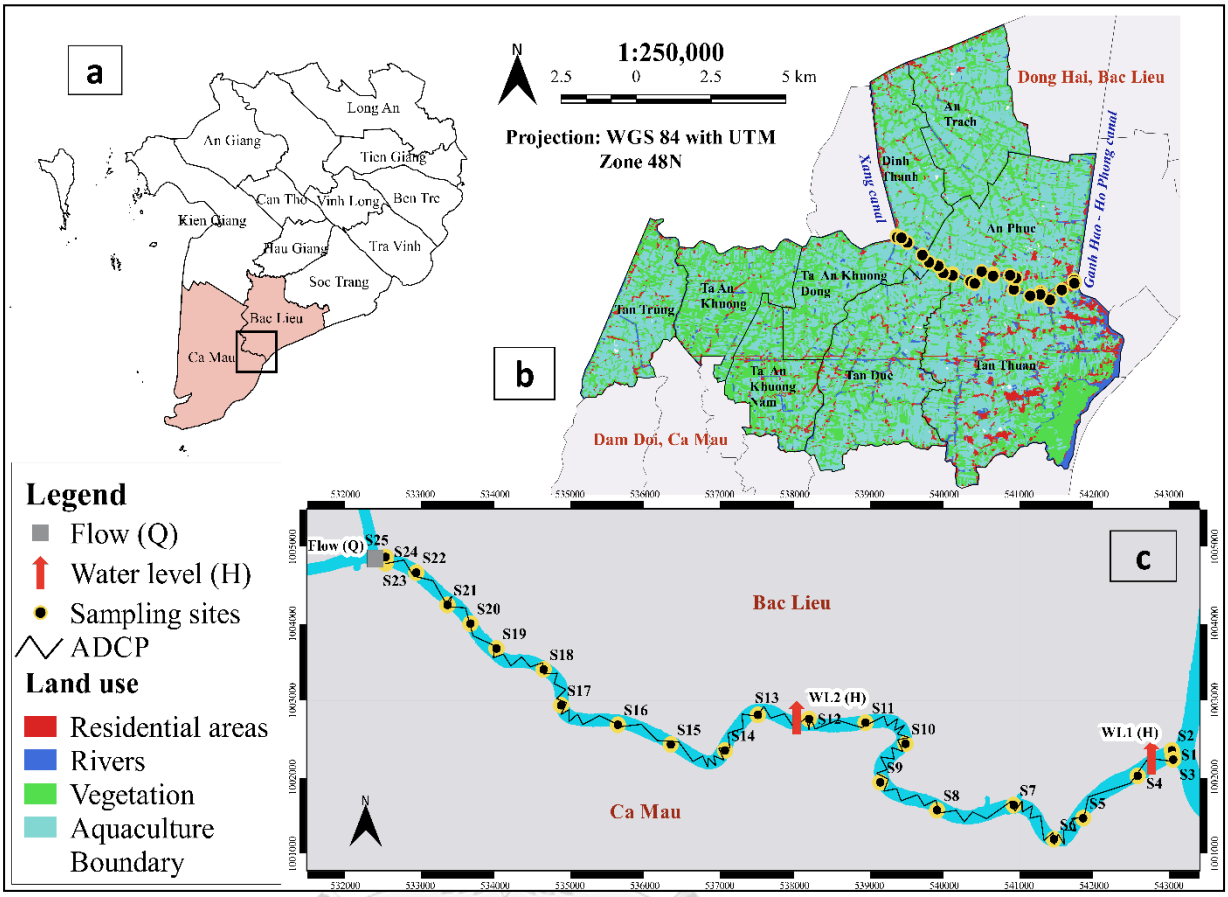

Figure 0.3 The study area catchment (a); the segment of study river where it was mainly impacted by aquaculture practices (b); and sampling sites and hydrological measurements were marked in figure (b) that was shown in figure (c)

The shrimp was stocked at different times of a year consisting of two crops per year for various types of culture. Specifically, the first and second crops in Dong Hai district started in January 2019 and May 2019 for types of intensive and semi-intensive culture, respectively, while the extensive and improved extensive culture was only one crop per year commencing since November 2018 [178]. Two crops per year for the intensive, semi-intensive, extensive, and improved extensive types of shrimp farming were also practiced in the Dam Doi district beginning in January 2019 and November 2019, accordingly [178]. The extensive and improved extensive shrimp culture systems are known for having a low shrimp density and relying mainly on natural feeds; however, a limited amount of organic fertilizers is occasionally added to ponds. While a greater input of fertilizers and supplemental feeds is added to

the intensive and advanced intensive shrimp culture systems that are reared with a high density of shrimp [181]. (Cassou et al., 2017). The water exchange from shrimp ponds differed from among types of culture. The extensive and improved extensive ponds, the cycle of water supply and discharge, was specified twice a month with an average of 4 days through direct interviews with the local community. While types of intensive and semi-intensive culture exchange the water every ten days during the stage of shrimp stock [182]. Pollutants from anthropogenic activities in the upstream region and along the river reaches have been reported to have insignificant effects on the river's lower reaches [183]. As a result, changes in water quality were understood to be mainly associated with aquaculture activities, which contributed the most to the receiving waters.

3.2 Water and sediment sample collection

3.2.1 Sampling sites

Sampling was conducted in the spring and neap tide in the dry (22/03/2019) and the wet (05/09/2019) seasons at 25 observed sites by a distance of 0.5 km for each site, except for the first sites (S1 to S3) and the last (S23 to 25), obtaining representative sites for the study area (Figure 0.3). These were specified using satellite images and interviews with local authorities. Consequently, sites were certified in situ by investigating the actual land use and discovering potential disturbing factors (e.g., presence of shrimp farms or land use mixtures). All the observed sites selected based on characteristics of impact sources and status of land use. Additionally, coordinates of sampling sites were recorded by a global positioning system (GPS) as illustrated in Table 0.1.

Table 0.1 The possible sources of pollutants contributed to the receiving water

Observed sites	Coordinates	Description/sources

	E (UTM)	N (UTM)	
S1	543054	1002295	Shrimp farms; tributary
S2	543043	1002353	Shrimp farms
S3	543061	1002232	Shrimp farms
S4	542586	1002019	Shrimp farms; erosion
S5	541858	1001469	Shrimp farms; tributary
S6	541465.6	1001195	Shrimp farms; erosion
S7	540930.5	1001639	Shrimp farms
S8	539906.9	1001573	Shrimp farms; erosion
S9	539148.1	1001936	Shrimp farms
S10	539483.9	1002438	Shrimp farms; erosion; ferry station
S11	538950.3	1002713	Landslides, shrimp farms
S12	538196	1002762	Shrimp farms; the large tributaries
S13	537512	1002815	Shrimp farms
S14	537072.5	1002352	shrimp farms
S15	536349.6	1002431	The large tributaries; ferry station
S16	535641.7	1002686	Landslides, shrimp farms
S17	534883.8	1002940	Construction material yards; tributary
S18	534650.6	1003407	Ferry station; tributary; shrimp farms
S19	534020	1003679	Multi-waste sources from shrimp farms
S20	533673.3	1004004	Shrimp farms; tributary
S21	533366	1004247	Multi-waste sources from shrimp farms
S22	532948.9	1004668	Shrimp farms
S23	532539	1004788	Shrimp farms; tributaries
S24	532538	1004827	Shrimp farms; erosion; tributaries
S25	532539	1004871	shrimp farms; tributaries

3.2.2 Surface water samples

Collection of water samples, which was performed on the boat along the river starting at down to up boundary of the river reach, avoided closely to riverbanks because stagnant phenomenon could lead to various water quality (e.g., direct inhabitant's discharges close to the riverbanks). Samples, analyzed for nutrient and organic

pollution, were collected approx.10-30 cm below the surface to prevent intrusion of floating debris and held in the opposite direction to the water flow. Bottles were closed underwater to stop air intrusion. For measuring heavy metals, the collected samples by using Vandorn equipment were at different three depths of each sampling site. Samples were contained in high-density polyethylene (HDPE) bottles (1 L) (Figure 0.4). The pre-labeled sample bottles were washed with 10% HNO_3 acid to avoid any contamination from metal and non-metal ions and rinsed repeatedly with distilled water [184]. Before sampling, the sample bottles were rinsed three times with river water. For the measurement of heavy metal content, 65% HNO_3 acid was added to each sample immediately to bring pH below 2 to prevent metal absorption into the walls of the bottle. Directly after sampling, the bottles were stored in ice until they were transported to the laboratory [185].

Figure 0.4 Surface water collection and in-situ measurement on the field

3.2.3 Sediment samples

Sediment samples, which were conducted at the same sampling sites as the water samples, were collected by the Peterson grab from the sediment surface at the depth of around 10 cm [186]. The total weight of each about 2-3 kilogram sample was

contained in plastic bags made from polyethylene to avoid exposure to light; the symbol was prescribed and brought to the laboratory. Before sampling, the polyethylene bags were washed with a 10% HNO_3 acid solution and rinsed with distilled water [187]. Samples, which were dried at room temperature and then crushed up and through a sieve with a mesh of 0.5 mm, remained the dry weight of about 0.5-1 kilograms [188] (Figure 0.4).

Figure 0.5 Collection and process of sediment samples

3.3 Hydrological and bathymetric data

All field data used as inputs for the hydrodynamic model development were measured on a cruise in the wet season (5-6 September 2019). The water level at the downstream boundary (WL1) and middle location (WL2) was measured manually for 36 hours (one-hour intervals) (Figure 0.3 and Figure 0.6). The water discharge, flow velocity, and bathymetric measurement was measured using two Acoustic Doppler Current Profiler (Rio Grande ADCP-a 600 kHz configured for 0.25m bin size, USA) mounted to the boats. The first ADCP, which was used for water discharge measurement at the upstream boundary's traverse section, operated repeatedly for 36 hours (one-hour intervals) (Figure 0.3 and Figure 0.6). The second ADCP was set up for the velocity profile and bathymetric measurement on the zigzag trajectory at the same time as the water sample collection (Figure 0.3 and Figure 0.6)

Figure 0.6 Data collection on the field: (a) water sample collection, velocity and bathymetric measurements, (b) water discharge measurement at the upstream, and (c) water level measurement at downstream of the river.

3.4 Analytical procedures

A total of 25 surface water and sediment quality parameters was measured in this research. Surface water samples are analyzed for 18 water quality parameters including temperature, electricity conductivity (EC), total dissolved solids (TDS),

total suspended solids (TSS), pH, dissolved oxygen (DO), chemical oxygen demand (COD), salinity, nutrients (e.g., nitrogen-ammonium ($N\text{-}NH_4^+$), nitrogen-nitrite ($N\text{-}NO_2^-$), nitrogen-nitrate ($N\text{-}NO_3^-$), total-nitrogen (TN) and phosphate-phosphorus ($P\text{-}PO_4^{3-}$), total-phosphorus (TP)), metal(loid)s (e.g., arsenic (As), copper (Cu), lead (Pb), and Zinc (Zn)). The seven sediment quality parameters were detected for electrical conductivity (EC), pH, total organic carbon (TOC), arsenic (As), copper (Cu), lead (Pb), and Zinc (Zn).

3.4.1 Analysis of surface water samples

The temperature, EC, DO, pH. TDS, and salinity were measured in situ by using a HandyLab 680 FK instrument (SI Analytics GmbH, Germany).

For nutrients, all samples were stored from 2 to 4^0C until analyzed, and pre-treated by syringe filters (0.45 μm, Minisart Sartorius, Goettingen, Germany) and measured within twenty-four hours of sampling. $N\text{-}NO_3^-$, $N\text{-}NO_2^-$, $N\text{-}NH_4^+$, TN, $P\text{-}PO_4^{3-}$, TP, COD were detected by the following methods:

- $N\text{-}NH_4^+$: spectrometric method (ISO 7150-1: 1984)

Spectrometric measurement was conducted at 655 nm of the blue compound created by reaction of ammonium with salicylate and hypochlorite ions in the presence of sodium nitrosopentacyanoferrate (lll). Hypochlorite ions were generated in-situ by the alkaline hydrolysis of N, AI'-dichloro-1, 3, 5-triazine-2, 4, 6 (1 H, 3H, 5H)-trione, and sodium salt (sodium dichloroisocyanurate). The reaction between the chloramine and sodium salicylate occurred at pH of 12.6 in the existence of sodium nitroprusside. The presence of chloramines in the sample were quantitatively specified. Sodium citrate was coupled with the reagent to cover interference from cations, particularly calcium and magnesium. The method was applied for a range of 0.003 to 1 mg L^{-1}.

- $N\text{-}NO_2^-$: colorimetric method (SMEWW 4500-NO_2^- B: 2012)

Nitrite was measured through the creation of a reddish purple azo dye that was produced at pH level of 2.0 to 2.5 by combining diazotized sulfanilamide *N*-(1-naphthyl)-ethylenediamine dihydrochlori. The spectrophotometric measurements could be applied for a range of 0.01 to 1 mg L^{-1} ($N\text{-}NO_2^-$) if a light path and green

color of 5 cm were utilized. The color system follows Beer's law up to 0.18 mg N L^{-1} with a-1cm light path at 543 nm.

- N-NO_3^-: colorimetric method (SMEWW 4500-NO_3^- B: 2012)

The method was applied for only screening samples containing low concentration of organic substances. The curve calibration of nitrate conforms the Beer's law up to 11 mg L^{-1}. Of which methods (e.g., titanous chloride(G), hydrazine reduction (H), and automated cadmium reduction (F)) was the following ranges of 0.01 to 10 mg L^{-1} N-NO_3^-, 0.01 to 10 mg L^{-1} N-NO_3^-, and 0.5 to 10 mg L^{-1} N-NO_3^-. Water samples, which were consisted of high contents of organic matters, were diluted into the range of the selected method.

- Total-nitrogen (TN): TCVN 6638:2000 (ISO 10048:1991) method

Nitrogen patterns were eliminated by using Devarda's alloy to ammonium. The nitrogen was altered to ammonium sulfate in the existence of concentrated sulfuric acid comprising of high content of potassium sulfate. The aim of this step was to increase the boiling point of the mixture with the existence of the copper. The ammonia was eliminated out of the solution by providing alkali, and then the mixture was distilled in boric acid solution. The quantity of ammonium was measured by spectrophotometer at 655 nm. The method could determined the content of substance in range of 1 to 200 mg L^{-1}.

- P-PO_4^{3-}: colorimetric method (SMEWW 4500-P E: 2012)

Firstly, phosphate was changed to the phosphorus pattern of interest to dissolved orthophosphate; the second was colorimetric measurement of dissolved orthophosphate. The different phosphorus patterns were specified analytically; however, analytical differences had to be chose so that they could be utilized for explanatory purposes. This was because phosphorus could occur in coupling with organic substances, a digestion measurement determining a total phosphorus could oxidize organic substance to discharge phosphorus as orthophosphate. Consequently, the method using nitric acid-sulfuric acid was required for most water samples. After digesting the samples, the ascorbic acid method (E), which was performed to measured phosphate, followed the applicable range of 0.01 to 6 mg L^{-1}.

- Total-phosphorus (TP): colorimetric method (SMEWW 4500-P E&B: 2012)

The measurement was the same as method of 4500-P E: 2012 for the digestion. Nevertheless, the acid-hydrolysable phosphorus concentration of the samples was specified operatively as the difference between reactive phosphorus that was detected in the untreated samples and phosphate was found after slight acid hydrolysis. Normally, it comprised of patterns of condensed phosphates (e.g., pyro-, tripoly-), and higher-molecular-weight species. Moreover, some water samples contained organic phosphate species, which were hydrolyzed to orthophosphate under the test conditions. Commonly, patterns of polyphosphates did not react to reactive phosphorus tests; however, they could be hydrolyzed to orthophosphate by boiling with acid. After hydrolysis process, reactive phosphorus, which was measured by a colorimetric method, varied from 0.01 to 6 mg L^{-1}.

- TSS: SMEWW 2540 D: 2012 method

The well-mixed samples were filtered through a weighed standard glass-fiber. The residues were held on the filter, which was dried to a constant weight at 103 to 105°C. The increase in weight of the filter represented the total suspended solids. If the suspended substances choked the filter and extended filtration, the increased diameter of the filter or reduced the sample volume was requested. To obtain an estimation of total suspended solids, it required to compute the difference between total dissolved solids and total solids. The lowest limitation of detection (LOD) is 2 mg L^{-1}.

- COD: SMEWW 5220 C: 2012 method

The principle of the method was most organic substances oxidized by a boiling mixture of chromic and sulfuric acids. The samples were refluxed in strong acid solution with a known excess of potassium dichromate ($K_2Cr_2O_7$). After digestion, the titration process was conducted in the residual unreduced $K_2Cr_2O_7$ with ferrous ammonium sulfate solution to measure the amount of consumed $K_2Cr_2O_7$ and then oxidized substances were computed in terms of oxygen equivalent. The ratios of reagent weights, volumes, and strengths constant were retained when sample volumes over than 50 mL were utilized. A less reflux time of standard 2 hours was performed

if the same results have yielded in a shorter period. The results, which were further enhanced by reacting a maximum amount of dichromate, provided some residual dichromate remains. The applicable range of the method was from 5 to 50 mg L^{-1}.

- Heavy metals in surface water: US.EPA method 200.7 ICP-OES

The first of all, the acidified sample of around 50ml was taken at a rate of 5ml of concentrated HNO_3 acid solution in a 1l sample solution that put into a 100ml glass beaker. The glass beaker, which then was added 2ml of HNO_3 acid solution (1:1) and 1ml of HCl acid solution (1:1), was covered with a watch glass to avoid the contamination. The mixture was put on an electric hotplate at a temperature that was not exceeded 85^0C until the remaining volume of sample was about 20ml (do not boil). The mixture then was taken down to cool at a room temperature and transferred the acidified solution into a 50ml volumetric flask with distilled water to the mark. The solution, which was filtered by filter paper with pore diameters of 0.4-0.45µm, was quantified by using the ICP-OES (Inductively Coupled Plasma Emission Spectrometry). The calibration blank and standard were conducted similarly at the same time. The concentrations of heavy metals were measured by the following formula:

$$C(mg\ L^{-1}) = (C_1 - C_2) * f$$

C: content of metal in water samples (mg L^{-1})

C_1: metal content in the water sample measured (mg L^{-1})

C_2: metal content measured from sample not containing analyte (distilled water) (mg L^{-1})

f: dilution factor (if diluted).

3.4.2 Analysis of sediment samples

pH and EC in sediment samples were measured in situ by using HI 99121-HANNA instrument (Soil pH Test Kit, USA) and HI 8633-HANNA instrument (Multi-Range Conductivity Meters, USA), respectively.

TOC content was measured by using an amount of 0.5g sediment sample was added into a triangular flask, which was then put 10 ml of $K_2Cr_2O_7$ and 20 ml of

concentrated H_2SO_4. The mixture was slightly shaken to mix well between the sample and chemicals within 20-30 minutes. The well mixed solution would be added 100 ml of distilled water and 10 m of H_3PO_4. Finally, the solution was titrated with 1N $FeSO_4$ after adding 1 ml of the color indicator. The procedures were conducted in the same steps without the sample of sediment for the blank samples [189]. The measurement of TOC was determined by the following formula:

$C(\%) = [(Vo-V)*N*0.003*100*1.33]/W$

V_o(ml): volume of $FeSO_4$ was used to titrate the sample of blank

V(ml): volume of $FeSO_4$ was used to titrate the sample of sediment

W(g): weight of sample

N: ferrous sulfate ($FeSO_4$).

- Heavy metals in sediment: US.EPA method 3051A ICP-OES

A sediment sample of 0.3g weight was put into a container connecting with a controlled pressure reduction mechanism. The pressure reducing digestion flask was added a volume of 10±1ml concentrated HNO_3 acid solution or 9±0.1ml concentrated HNO_3 acid. Then these reactors, which were closed according to the manufacturer's instructions, were put properly into a microwave system and connect the appropriate temperature and pressure sensors. The temperature of microwave was increased to 175 ± 5^0C for about 15±0.25 minutes. The temperature was then lowered to 80^0C for 25 minutes. The microwave oven was cooled down to a room temperature and removed the decompression sample vessels from the microwave systems. To check the weight of the sample can be carried out before and after the process to assess the tightness. If the difference in weight of the sample exceeded 1%, the sample was considered to be lost. The obtained solution was transferred to a 20ml volumetric flask and quantify with distilled water to filter it. Finally, the solution was analyzed for the content of heavy metals on ICP-OES. The process was conducted in the same way with the blank samples. The concentration of metals would be measured as follow:

$C_m(mg\ Kg^{-1}) = [(C_1 – C_2)*V*10^3*f]/m$

C_m: content of metals in sediment samples (mg Kg^{-1})

C_1: content of metals in measured sediment sample (µg L^{-1})

C_2: content of metals in blank sample (µg L^{1-})

V: volume of the volumetric flask (ml)

m: weight of the sample (g)

f: dilution factor (if diluted)

10^3: transfer from gram to kilogram.

3.4.3 Quality assurance (QA) and quality control (QC) in the laboratory

QC procedure was done by using the standard samples (CRMs-Certified Reference Materials) for all parameters. The CRM sample was analyzed seven times (the procedure was the same as real samples). The results of CRM were calculated mean values and standard deviation (SD), then the graph for QC control was created by using mean values and SD. QA was done by checking the analyzed results. If the results are in a range of -2 SD to +2SD, the analysis procedures were reliable and high accuracy.

3.5 Assessment of surface water and sediment quality

3.5.1 Surface water quality

The levels of surface water pollution were assessed by comparing with i) the Vietnamese guidelines (QCVN 08-MT:2015/BTNMT) [190] and ii) the US. EPA [191] for surface water quality.

3.5.2 Sediment quality assessment

The levels of sediment contamination were assessed by comparing with i) the Vietnamese guidelines (QCVN 43:2017/BTNMT) [192] and ii) three contamination indices including Geo-Accumulation Index (I_{geo}), Contamination factor (CF) and Pollution Load Index (PLI).

- *Geo-Accumulation Index (I_{geo})*

I_{geo} was utilized to measure and assess the metal contamination of the bottom sediment [193]. The previous study of [194] illustrated that I_{geo} was calculated the following formula:

$$I_{geo} = \log (C_n/1.5xB_n)$$

C_n is the measured concentration of the metal (n) and B_n is the geochemical background of the metal (n). Factor 1.5 is used for possible variations of the background data due to lithological variations [195]. I_{geo} values were classified into seven grades or classes: $I_{geo} \leq 0$ (grade 0), unpolluted; $0< I_{geo} \leq 1$ (grade 1), slightly polluted; $1 < I_{geo} \leq 2$ (grade 2), moderately polluted; $2< I_{geo} \leq 3$ (grade 3), moderately severely polluted; $3< I_{geo} \leq 4$ (grade 4), severely polluted; $4< I_{geo} \leq 5$ (grade 5), severely extremely polluted; $I_{geo} > 5$ (grade 6), extremely polluted [196].

- *Contamination Factor (CF)*

CF was used to evaluate the pollution content of the sediment with respect to heavy metals [197]. The CF was determined by the following formula [198].

$$\mathrm{CF} = \frac{\text{Measured metal concentration}}{\text{Background concentration of the same metal}}$$

The CF has provided four grade ratings of the sediment based on CF values: 0<CF<1 (grade 1), low CF; 1<CF<3 (grade 2), moderate CF; 3<CF<6 (grade 3), considerable CF; CF≥6 (grade 4), very high CF.

- *Pollution Load Index (PLI)*

The PLI was performed to find out the mutual pollution effects at different observed sites and the overall toxicity status of each observed site [199]. The PLI was determined as the n^{th} root of the multiplications of the contents (CF metals) by the following formula [200]: $_n$

$$\mathrm{PLI} = \sqrt[n]{\mathrm{CF1\ x\ CF2\ x\ CF3\ x\ \dots\ x\ CFn}}$$

The PLI value of zero indicates excellence, a value of one shows the presence of only baseline levels of pollutants and values above one illustrating the progressive deterioration of the observed sites and estuarine quality [200]. In this study, the world

mean contents of heavy metals were referred as the following values: Cu (45 μg g^{-1}), As (13 μg g^{-1}), Pb (20 μg g^{-1}), and Zn (95 μg g^{-1}) [201].

3.6 The seasonal variability of water quality parameter

3.6.1 Seasonal variability

The dataset of the 25 sampling sites, consisting of measured water quality parameters in the dry (22/3/2019) and wet (5/9/2019) seasons, was utilized to assess seasonal differences in water quality. The water quality in two seasons was statistically compared (significance of 5%) with the non-parametric Mann-Whitney U test since the normal distribution of the dataset checked by the Shapiro-Wilk test was not met. The variations of water quality were visualized by box diagrams for the 14 representative parameters due to not discovering the existence of heavy metal contents at most of the investigated sites.

3.6.2 The effect of tidal regimes

The Mann-Whitney U test (significance of 5%) was performed to observe the influence of tides among water quality parameters because the normal distribution of the dataset checked by the Shapiro-Wilk test was not met. For this analysis, the seasonal dataset of 25 sampling sites was divided into two groups, one of them represented at the spring tide and another was at the neap one. The variation of water quality parameters were visualized by box diagrams for the 14 selected parameters.

3.6.3 Identification of pollutant sources

In this research, to identify the impact of each water quality parameter on water quality and reduce the computation load, PCA was utilized to analyze the original monitoring data. The objective of PCA was to extract the key information representative of the characteristics of the water environment from a large amount of data and characterize it as a new dataset of independent variables of the principal component (Abdi and Williams [202], 2010). PCA reduces the dimensionality of a multivariate data set to a small number of independent principal components. Each principal component contains all the variable information, thus reducing the missing of information [203]. In PCA, the Kaiser

criterion drops the components, for which the eigenvalues are less than 1. Greater than 1 eigenvalue suggests that the corresponding component interprets more variance than a single variable. Therefore, the component in question can be used for reducing the number of variables. In contrast, components with eigenvalues less than 1 would not be useful for reducing the dimensionality of the data. The eigenvalue threshold is zero, since the eigenvalues, obtained from the adjusted correlation (or covariance) matrix can be negative. The reason for this is that the adjusted matrices do not have full rank – the common variance is less than the total. The negative eigenvalues cannot be safely interpreted as partitions of the common variance. Therefore, factor analysis focuses only on the common variance, only factors with corresponding positive eigenvalues are selected for rotation [204]. For this analysis, the initial dataset of 25 sampling sites, comprising mean contents for all parameters, was reduced to satisfy the criteria for the test (Bartlett test of sphericity, Kaiser-Meyer-Olkin). First, the parameters of As, Cu, Pb, and Zn were removed due to the low variabilities and almost not detected among the observed sites. Second, $N\text{-}NH_4^+$ was distributed at two components, resulting significantly in reducing convergence of other components and it was therefore excluded from the dataset as well. The reduced dataset (e.g., temperature, EC, TDS, TSS, pH, COD, salinity, $N\text{-}NO_2^-$, $N\text{-}NO_3^-$, TN, $P\text{-}PO_4^{3-}$, and TP) was further rotated by a Varimax with Kaiser normalization to indicate the loadings in the explaining components. Loadings of selected water quality parameters in three components with eigenvalues of > 1. The dataset comprises a reduced number of parameters to meet the criteria of the analysis.

3.7 Surface water quality maps

The effects of various land-use systems used for shrimp culture were further evaluated by the logistic regression model to identify which types of shrimp culture systems (e.g., intensive, advanced-intensive, or extensive and improved extensive shrimp farms) were responsible mainly for the degradation of water quality at Ganh Hao River. The logistic regression model works the same as linear regression one, with a binomial response variable. The advantage of the model can utilize continuous explanatory variables and it is easier to address more than two explanatory variability simultaneously. It is essential when the interest is the effect of different explanatory

variables on the response variable. If multiple explanatory variables are considered independently [205]. The contents of pollutants, which were detected seasonally at twenty-five observed sites, were utilized for this analysis. The land-use systems, particularly areas utilized for a kind of different shrimp farms, were specified by a digital map (satellite image solution) coupling with data (e.g., areas and the status of land-use) collected from Dong Hai and Dam Doi people's committee as shown in Table 0.2.

Table 0.2 Types of land-use were available in Dong Hai and Dam Doi Districts

Districts	Admin-Units (Communes)	Natural area (1)	Kinds of land-use (ha)		
			Intensive & advanced intensive (2)	Extensive & Improved-extensive (3)	Non-agriculture (4)
Dam Doi	Tan Trung	3311.41	83.24	2544.32	683.85
	Ta An Khuong	3773.79	64.3	2929.5	779.99
	Ta An Khuong Dong	3633.54	88.25	2841.57	703.72
	Ta An Khuong Nam	3001	222	2308	471
	Tan Duc	6304.71	210.53	4919.18	1175
	Tan Thuan	10834.51	103.73	6342	4388.784
Dong Hai	Dinh Thanh	3162.7	8.89	2024.48	1129.33
	An Trach	5210.77	63	4204.55	943.22
	An Phuc	5767	9.2	4785	972.8

Table 0.2 including six communes belonging to Dam Doi District and three located in Dong Hai District, did not show the differences among areas used for extensive and improved-extensive shrimp culture systems. However, the rate calculated by dividing the areas utilized for shrimp culture systems with the natural areas illustrated a significant difference as presented in Table 0.3.

Table 0.3 The rates computed for types of land-use

Districts	Admin-Units	Kinds of land-use (ha)

	(communes)	Intensive & advanced intensive (2)	Extensive & Improved-extensive (3)
Dam Doi	Tan Trung	0.025	**0.768**
	Ta An Khuong	0.017	**0.776**
	Ta An Khuong Đong	0.024	**0.782**
	Ta An Khuong Nam	0.074	**0.769**
	Tan Duc	0.033	**0.780**
	Tan Thuan	0.010	0.58
Dong Hai	Dinh Thanh	0.003	0.64
	An Trach	0.012	**0.807**
	An Phuc	0.002	**0.823**

Table 0.3 showed that the rates of the land-use system (extensive and improved-extensive) consisted clearly of two groups and did not meet the normal distribution (Shapiro test's sig=0.012<0.05). Therefore, these rates would be divided by two groups of zero and one, of which zero was communes having the rates (<0.7), and one included the communes with the rates (>0.7). To identify the mean difference between the two groups, the Mann-Whitney test (sig=0.05) was performed as shown in Table 0.4.

Table 0.4 The difference between the two groups

Test statistics	Variables (Land-use)
Mann-Whitney U	0
Wilcoxon W	3
Z	-2.095
Asymp. Sig. (2-tailed)	0.036
Exact Sig. [2*(1-tailed Sig.)]	**.044**

The result revealed a significant difference (sig=0.044<0.05) (Table 3.4) on rates of extensive and improved-extensive between the two groups of the communes. Based on the rates, the distribution of the observed sites and communes was presented in Figure 0.7.

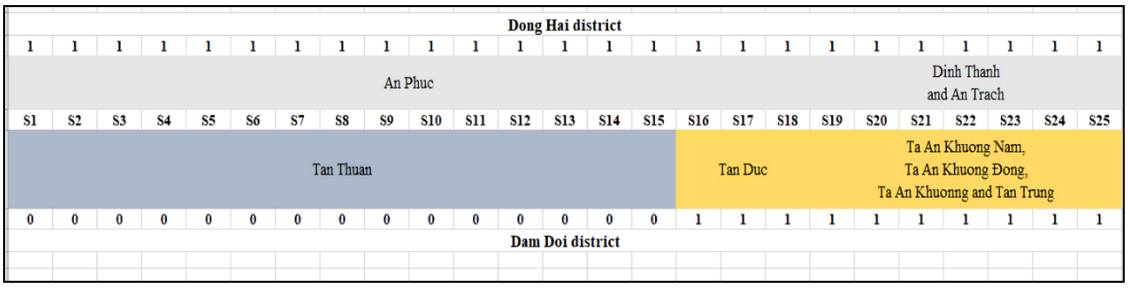

Figure 0.7 the observed sites associating with communes distributed along with the river

It was obvious that the difference in land-use was insignificantly among communes in Dong Hai district, whereas it was shown apparently in the Dam Doi district. This was because the total area of extensive and improved-extensive shrimp farms in Dam Doi district was greater than that in Dong Hai district. Due to the insignificant difference in land-use; therefore, it was supposed that the discharge of the pollutants into the receiving water was evenly along the river reach. Consequently, the logistic regression model was performed to evaluate the correlation between the land-use systems and the release of the pollutants in the Dam Doi district. Using the logistic regression method coupled with the multi-collinear reduction to find the highly classifiable variables (parameters) of two groups of land-use and remove unnecessary variables. The results of the analysis were denoted in Table 0.5.

Table 0.5 Summary of variables in logistic regression models

Model results	Variables	Percentage correct (%)	Sig.
Dry	EC, TSS, TP, N-NO_2^-	93.3	0.00
Wet	pH, EC, N-NO_2^-, TP	93.3	0.00

Dry: the content of each water quality parameter among different sites in the dry season

Wet: the content of each water quality parameter among different sites in the wet season

Table 0.5 indicated that the results analyzed by the logistic regression model showed a highly classifiable percentage (percentage correct of 93.3%) in both seasons.

Moreover, the results of the model analysis indicated the observed sites consisting of 18, 19, 20, 21, 22, 24, 25 and 17, 18, 20, 21, 22, 23, 24, 25 in the dry and rainy seasons (Table 0.6) accordingly were associated with land-use (extensive and improved-extensive shrimp culture) due to having a high probability of classification.

Table 0.6 The analysis results of the logistic regression model

Observed sites	Dry season				Wet season			
	*Rep	*Y	*P_ estimates	Y_ estimates	Rep	Y	P_ estimates	Y_ estimates
1	1	0	0.64632	1	1	0	0.00002	0
1	2	0	0.00739	0	2	0	0.00007	0
1	3	0	0.19277	0	3	0	0.00082	0
2	1	0	0.00003	0	1	0	0.00015	0
2	2	0	0.00000	0	2	0	0.00089	0
2	3	0	0.00000	0	3	0	0.00012	0
3	1	0	0.12559	0	1	0	0.00011	0
3	2	0	0.01810	0	2	0	0.00057	0
3	3	0	0.00190	0	3	0	0.00583	0
4	1	0	0.00041	0	1	0	0.00225	0
4	2	0	0.00002	0	2	0	0.00006	0
4	3	0	0.00500	0	3	0	0.00722	0
5	1	0	0.00356	0	1	0	0.00000	0
5	2	0	0.02530	0	2	0	0.00000	0
5	3	0	0.00661	0	3	0	0.00000	0
6	1	0	0.00001	0	1	0	0.00004	0
6	2	0	0.00000	0	2	0	0.00052	0
6	3	0	0.00002	0	3	0	0.00278	0
7	1	0	0.00047	0	1	0	0.00001	0
7	2	0	0.00000	0	2	0	0.00015	0
7	3	0	0.00001	0	3	0	0.02431	0
8	1	0	0.12398	0	1	0	0.00000	0

Observed sites	Dry season				Wet season			
	*Rep	*Y	*P_ estimates	Y_ estimates	Rep	Y	P_ estimates	Y_ estimates
8	2	0	0.00826	0	2	0	0.00000	0
8	3	0	0.05395	0	3	0	0.00000	0
9	1	0	0.00001	0	1	0	0.00000	0
9	2	0	0.00000	0	2	0	0.00000	0
9	3	0	0.00000	0	3	0	0.00000	0
10	1	0	0.00015	0	1	0	0.00022	0
10	2	0	0.00003	0	2	0	0.00456	0
10	3	0	0.00033	0	3	0	0.01488	0
11	1	0	0.00052	0	1	0	0.00012	0
11	2	0	0.00146	0	2	0	0.00044	0
11	3	0	0.00002	0	3	0	0.00341	0
12	1	0	0.02419	0	1	0	0.02241	0
12	2	0	0.08065	0	2	0	0.21924	0
12	3	0	0.34076	0	3	0	0.52961	1
13	1	0	0.06094	0	1	0	0.00254	0
13	2	0	0.08658	0	2	0	0.03617	0
13	3	0	0.67732	1	3	0	0.17856	0
14	1	0	0.33920	0	1	0	0.00036	0
14	2	0	0.00721	0	2	0	0.00077	0
14	3	0	0.02286	0	3	0	0.01099	0
15	1	0	0.28033	0	1	0	0.13993	0
15	2	0	0.14616	0	2	0	0.60036	1
15	3	0	0.01674	0	3	0	0.92650	1
16	1	1	0.93274	1	1	1	0.47034	0
16	2	1	0.01533	0	2	1	0.89030	1
16	3	1	0.77276	1	3	1	0.97761	1
17	1	1	0.97673	1	**1**	**1**	**0.96859**	**1**
17	2	1	0.44170	0	**2**	**1**	**0.99654**	**1**

Observed sites	Dry season				Wet season			
	*Rep	*Y	*P_ estimates	Y_ estimates	Rep	Y	P_ estimates	Y_ estimates
17	3	1	0.57105	1	**3**	**1**	**0.99922**	**1**
18	**1**	**1**	**0.99975**	**1**	**1**	**1**	**0.99958**	**1**
18	**2**	**1**	**0.99996**	**1**	**2**	**1**	**0.99995**	**1**
18	**3**	**1**	**0.99999**	**1**	**3**	**1**	**0.99994**	**1**
19	**1**	**1**	**0.99959**	**1**	1	1	0.19510	0
19	**2**	**1**	**0.99581**	**1**	2	1	0.56098	1
19	**3**	**1**	**0.99131**	**1**	3	1	0.92954	1
20	**1**	**1**	**0.99709**	**1**	**1**	**1**	**0.88414**	**1**
20	**2**	**1**	**0.87534**	**1**	**2**	**1**	**0.97881**	**1**
20	**3**	**1**	**0.99091**	**1**	**3**	**1**	**0.99754**	**1**
21	**1**	**1**	**0.99989**	**1**	**1**	**1**	**0.84373**	**1**
21	**2**	**1**	**0.92400**	**1**	**2**	**1**	**0.97423**	**1**
21	**3**	**1**	**0.99994**	**1**	**3**	**1**	**0.99678**	**1**
22	**1**	**1**	**0.94174**	**1**	**1**	**1**	**0.97282**	**1**
22	**2**	**1**	**0.99080**	**1**	**2**	**1**	**0.99746**	**1**
22	**3**	**1**	**0.98568**	**1**	**3**	**1**	**0.99966**	**1**
23	1	1	0.89103	1	**1**	**1**	**0.98350**	**1**
23	2	1	0.93200	1	**2**	**1**	**0.99780**	**1**
23	3	1	0.49714	0	**3**	**1**	**0.99625**	**1**
24	**1**	**1**	**0.99471**	**1**	**1**	**1**	**0.90794**	**1**
24	**2**	**1**	**0.99855**	**1**	**2**	**1**	**0.98432**	**1**
24	**3**	**1**	**0.98549**	**1**	**3**	**1**	**0.99843**	**1**
25	**1**	**1**	**0.99995**	**1**	**1**	**1**	**0.93797**	**1**
25	**2**	**1**	**0.99444**	**1**	**2**	**1**	**0.84063**	**1**
25	**3**	**1**	**0.99945**	**1**	**3**	**1**	**0.98328**	**1**

*Rep: number of measurement at each observed site

*Y: observed sites associate with land-use (0: low rate of extensive and improved-extensive; 1: high rate of extensive and improved-extensive).

*P_estimates: estimation probability

*Y_estimates: when estimation probability (>=0.5) showed that the observed site was polluted highly (1) and the estimation probability (<0.5) illustrated inversely (0)

While the rates, which were calculated for land-use systems (Table 3.3), showed small values for types of land-use systems utilized for intensive and advanced-intensive shrimp farms. Therefore, based on geographical location, Dong Hai district would be divided into two groups of land-use (An Phuc; and Dinh Thanh and An Trach) and Dam Doi district included three groups (Tan Thuan; Tan Duc; and Ta An Khuong, Ta An Khuong Nam, Ta An Khuong Dong, and Tan Trung) as illustrated in Table 0.7. To assess the mean difference in the content of pollutants among groups of land-use, the Kruskal-Wallis test (sig=0.05) was performed as shown in Table 0.7 and Table 0.8, and the confidence intervals for mean were illustrated in Table 0.9 and Table 0.10.

Table 0.7 Significant differences among parameters for groups of land-use in the dry season

Groups of land-use	Parameters	Sig.
Dong Hai	EC	0.000
	TDS	0.001
	Salinity	0.000
	TN	0.000
	$N\text{-}NH_4^+$	0.000
Dam Doi	EC	0.000
	TDS	0.001
	Salinity	0.000
	TN	0.000
	TP	0.046
	DO	0.000
	$N\text{-}NH_4^+$	0.000

Table 0.8 Significant differences among parameters for groups of land-use in the wet season

Groups of land-use	Parameters	Sig.

Dong Hai	Temperature	0.000
	pH	0.001
	TSS	0.000
	$N\text{-}NO_2^-$	0.000
	$N\text{-}NH_4^+$	0.017
	TP	0.000
Dam Doi	Temperature	0.000
	pH	0.001
	EC	0.000
	TDS	0.000
	TSS	0.001
	Salinity	0.000
	$N\text{-}NO_2^-$	0.000
	$N\text{-}NH_4^+$	0.001
	$P\text{-}PO_4^{3-}$	0.008
	TP	0.000
	COD	0.013

Table 0.9 Confidence intervals for mean on each group (parameters in the dry season)

Parameters	Dong Hai		Dam Doi		
	Group 1	Group 2	Group 1	Group 2	Group 3
Temperature (^oC)	(30.9, 31.08)	(30.9, 31.2)	(30.8, 31.1)	(30.9, 31.2)	(30.9, 31.2)
Salinity (‰)	(21.79, 22.02)	(22.2, 22.5)	(21.7,22)	(22.1, 21.9)	(548.3, 637.1)
TSS ($mg.L^{-1}$)	(420, 552)	(592, 548)	(375.1, 526.1)	(638.0,693.8)	(139.33, 266)
$N\text{-}NO_2^-$ ($mg.L^{-1}$)	(0.014, 0.019)	(0.013, 0.018)	(0.013, 0.019)	(0.012, 0.018)	(0.013, 0.017)
$N\text{-}NH_4^+$ ($mg.L^{-1}$)	(0.069, 0.099)	(0.019, 0.036)	(0.07, 0.11)	(0.05, 0.09)	(0.02,0.012)

Table 0.10 Confidence intervals for mean on each group (parameters in the wet season)

Parameters	Dong Hai		Dam Doi		
	Group 1	Group 2	Group 1	Group 2	Group 3
Temperature (^oC)	(29.51,30.14)	(29.05,29.2)	(29.6,30.34)	(28.98,29.2)	(29.05,29,23)
Salinity (‰)	(6.44,7.81)	(5.86,6.27)	(6.94,8.31)	(4.7,5.07)	(5.86,6.27)
TSS ($mg.L^{-1}$)	(529, 1011)	(139, 266)	(574, 1141)	(286.88,377.12)	(139.33, 266)
$N\text{-}NO_2^-$ ($mg.L^{-1}$)	(0.051,0.062)	(0.068,0.078)	(0.046,0.055	(0.081,0.094)	(0.067,0.078)
$N\text{-}NH_4^+$ ($mg.L^{-1}$)	(0.17,0.22)	(0.11,0.12)	(0.15,0.21)	(0.21,0.28)	(0.11,0.12)

Table 0.7 and Table 0.8 indicated that the selected parameters differed among the groups that occurred mostly in the wet season, the pollutants like $N\text{-}NO_2^-$ and $N\text{-}NH_4^+$ came about in most cases. Two districts showed a higher mean content of pollutants in the wet season than that in the dry one (Table 3.9 and Table 3.10); however, the differences in the confidence intervals for mean in both districts. Particularly, higher confidence intervals of salinity, TSS, and $N\text{-}NH_4^+$ in group 1 than those in group 2 were found in Dong Hai district in the wet season while $N\text{-}NO_2^-$ showed a higher confidence interval in group 2 than that in group 1 (Table 0.10). In the Dam Doi district, higher confidence intervals of salinity and TSS in group 1 than group 2 and 3 were illustrated in the wet season, whilst the highest confidence intervals of $N\text{-}NO_2^-$ and $N\text{-}NH_4^+$ were group 2 in comparison with other groups. It was obvious that water quality parameters did not only differ among groups of land-use but also vary in each group. Consequently, discharge of pollutants caused by intensive and advanced-intensive shrimp culture did not show clearly the pollution respect with water quality parameters at different groups. This was because the area utilized for extensive and improved-extensive shrimp farms in each commune was greater than that used for intensive and advanced-intensive shrimp culture. Therefore, the effects of extensive

and improved-extensive shrimp culture were determined as a major factor influencing changes in water quality at Ganh Hao River.

The maps of water quality, which were produced by using the Inverse Distance Weighted (IDW) method integrated with the QGIS software, showed intuitively seasonal changes in water quality for the selected parameter. IDW is based on estimating interpolation by which unknown values were calculated by a linear couple of values at identified points [206]. It assumes that each input point has a local impact reducing with distance and the surfaces were generated by establishing an adjacent search of points and weighting them by a power function [207].

3.8 Assessment of hydraulic characteristics, changes in water quality and its association with various flow regimes

3.8.1 Hydrodynamic model

The Delft 3D model was performed to simulate changes in hydrodynamics of the river reach. All data used for inputs of the model were measured on a cruise in the wet season (5-6/9/2019). A hydrodynamic model was developed based on a series of water levels and water discharge values, of which water levels were measured manually at the downstream of the river, and water discharge values were measured by an Acoustic Doppler Current Profiler (ADCP) upstream of the river reaches. The hydrodynamic model is based on Navier-Stoke's shallow water equations for an incompressible fluid in 2D and 3D integrated into Delft3D-FLOW, which is fully non-linear and physic-based. Modeling is carried out on a curvilinear, unstructured grid in 2D while the vertical grid includes layers divided by σ-planes, which follow the bottom topography. The layers are constant over the computational domain [208].

- Computational grid

RGFGRID (Delft3D tool) is used to create orthogonal curvilinear grids in 2D model. A curvilinear grid allows a high resolution of the grid near the area of interest and a low resolution outside the area. Therefore, it reduces not only the total number of cells but also and the computational time. In addition, it is used to check the orthogonality, smoothness, and ratio of the mesh. The model's grid is created by many cells which

are different quadrilaterals combined to form a grid system with its coordinates (M Direction and N Direction). A grid of different quadrangular components was created for a studied segment of the river, which has a resolution of 27x1800 distributed along with the grid domain with a total number of 48,600 cells (Figure 0.8). In 3D simulation, the vertical grid comprised of layers divided by σ-planes, which follow the bottom geomorphology and the free surface. The number of layers is constant over the computational domain. In this research, the 3D model was developed simply by adding σ-layers to the 2D model. Based on the depth of the river (average depth of 2 m), the developed 3D model included four vertical layers that did not pose difficulties in simulation (Figure 0.8d) [209].

- Bathymetric interpolation

QUICKIN (Delft 3D tool) was used to combine and create bathymetries by assigning data of sample points to the cells. The Inverse Distance Weighting method (IDW) was performed to interpolate the geomorphology of the river. The IDW interpolator is a relatively popular technique as few parameters are required from the operator. The IDW carries out the assumption that a value of an attribute at an unmeasured area is a weighted average of known data points within a local neighborhood surrounding the unmeasured one [210]. However, the original IDW method was not used due to manipulating circular search neighborhoods. Therefore, the Rectilinear Inverse Distance Weighting (RIDW) method was applied by using a rectangular box in the flow direction found in the samples [211]. Geomorphology of the river reach was interpolated as shown in Figure 0.8.

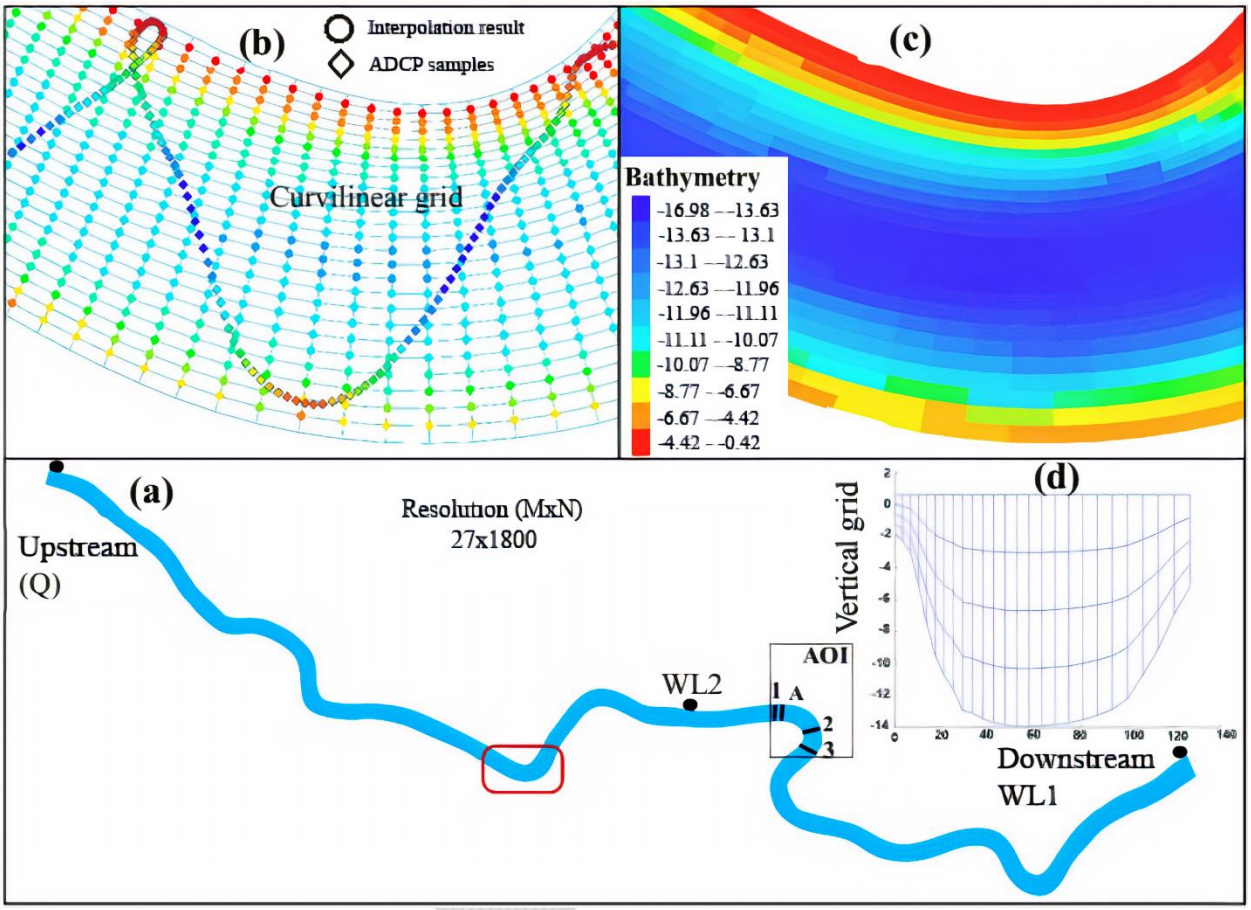

Figure 0.8 Study area: (a) the entire modeled reach. Water level (WL1, 2), water discharge (Q) measurement stations, and cross-sections (A, 1, 2, and 3), as well as downstream and upstream boundaries, are marked in the figure. A cross-section is marked by a red box in the figure where it represents a curvilinear grid (b) and interpolated geomorphology (c). An area of interest (AOI) is marked by a black box where it is interested in exploring changes in velocities. (d) A vertical grid is created by the sigma coordinate system

- Boundary condition

Two boundary conditions included water discharge and water level values measured on a cruise (5-6 September 2019) as input data for hydrodynamic model's development. The landward boundary condition was forced by hourly time series of water discharge measured at the upstream part of the river reaches. The downstream boundary was forced by tidal levels at hourly intervals, covering within 36 hours as shown in Figure 0.9.

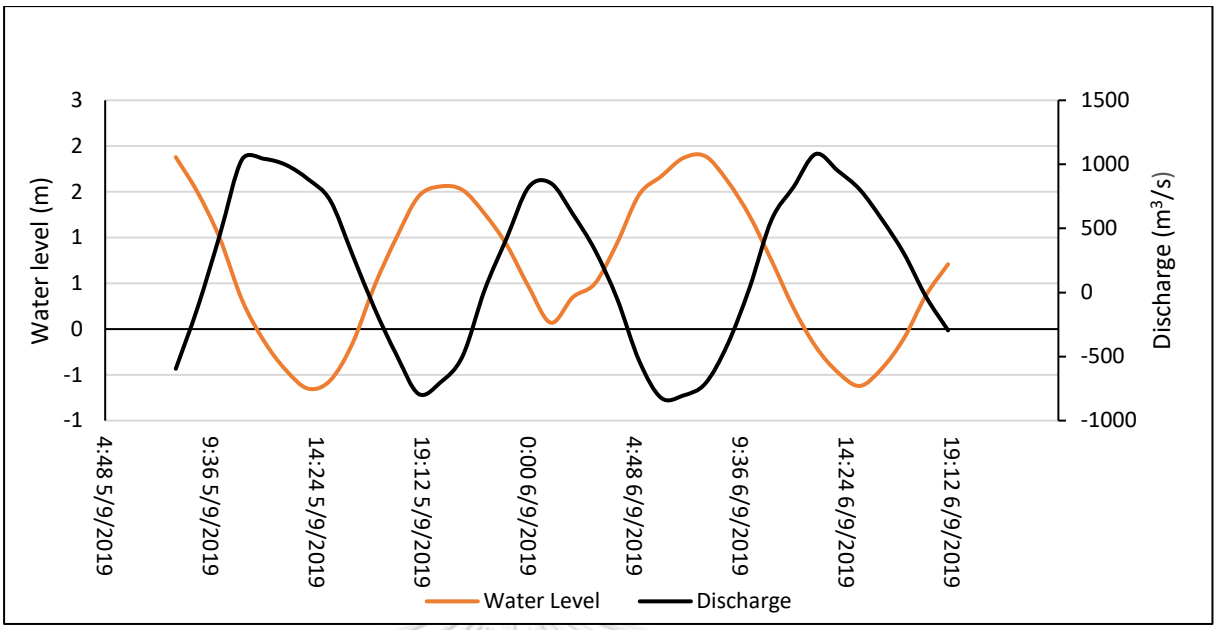

Figure 0.9 A series of measured water discharge and water level values at upstream and downstream of the river.

- Initial condition and physical parameters

All data used as inputs for the hydrodynamic model included water level's initial conditions and physical parameters, of which the first one was set to 2 meters and the second was presented in Table 0.11. The selected parameters are based on many trials running the model

Table 0.11 Input data selected for model set up.

Parameters	Type	Range	Selected values	Unit
Gravity	Constant	9.5 - 12	9.81	m/s^2
Water Density	Constant	900 -1500	1000	kg/m^3
Manning coefficient *n*	Specify	0 - 0.04	0.022	$m^{-1/3}/s$
Horizontal eddy viscosity	Specify	0 - 100	2	m^2/s
Vertical eddy viscosity	Specify	0 - 100	0	m^2/s

- Time frame

The time frame applied for the model setup was illustrated in Table 0.12. A time step of 15 seconds was chosen for the model run. The selected time step based on the size

of the grid cells and calculated time to ensure spatial distribution of courant numbers for all the grid cells was not underestimated during the simulation process. Processes entering the input data into the Delft 3D-Flow model were illustrated in the attached Appendices.

Table 0.12 The time frame selected for model setup

Time frame	*Date and time (hh:mm:ss dd/mm/yyyy)*
Reference date	05/09/2019
Simulation start time	8:00:00 05/09/2019
Simulation stop time	19:00:00 06/09/2019
Time step	00:00:15
Storing interval time	00:30:00

- Calibration and validation model

The process of calibrating a hydrodynamic model under the steady-state condition relates to manipulation of the model inputs that agree closely the outputs based on the field observations [208]. Calibration was performed by adjusting the 2D model's hydraulic roughness, coupling with user-dependent parameters, running for 36 hours (with boundary conditions of water discharge and water level). The first parameters were calibrated to obtain a good agreement between simulated and measured results. The 3D model was calibrated by adjusting the horizontal eddy viscosity, combining with the parameters defined by the 2D model. The 2D and 3D model was tested respectively against the water level (WL2) and ADCP-based flow velocity measurements at the cross-section (A). The suitable roughness and horizontal eddy viscosity values, which maintain the model stability, were 0.022 $m^{-1/3}/s$ and 2 m^2/s, respectively. To assess the model accuracy after calibration, the model validation performance was quantified and reported as coefficient of determination (R^2), Root Mean Square Error (RMSE) for 2D model and Mean Absolute Error (MAE) for the 3D model. The RMSE, R^2 and MAE was performed as follows:

- Root Mean Square Error (RMSE)

RMSE was calculated based on simulated and measured values of water level after the model was calibrated to obtain a good agreement between simulated and observed

results. Table 0.13 showed measured and simulated water levels at the observation site (WL2).

Table 0.13 Simulated water levels (WL_{Si}) and observed water levels (WL_{Ob}) at the observation site (WL2)

Date and time	WL_{Si}	WL_{Ob}
5/9/2019 8:00	2	1.9065
5/9/2019 8:30	1.429913	1.7865
5/9/2019 9:00	1.752274	1.5975
5/9/2019 9:30	1.382553	1.3855
5/9/2019 10:00	0.95538	1.1515
5/9/2019 10:30	0.996028	0.8445
5/9/2019 11:00	0.586835	0.4765
5/9/2019 11:30	0.302166	0.2755
5/9/2019 12:00	0.156761	0.0465
5/9/2019 12:30	-0.00726	-0.2335
5/9/2019 13:00	-0.16682	-0.3935
5/9/2019 13:30	-0.31085	-0.6035
5/9/2019 14:00	-0.4403	-0.7835
5/9/2019 14:30	-0.49782	-0.9635
5/9/2019 15:00	-0.46004	-0.9435
5/9/2019 15:30	-0.39895	-0.8035
5/9/2019 16:00	-0.21599	-0.5235
5/9/2019 16:30	0.076985	-0.1835
5/9/2019 17:00	0.433162	0.1765
5/9/2019 17:30	0.683233	0.5565
5/9/2019 18:00	0.897063	0.8825
5/9/2019 18:30	1.16143	1.1265
5/9/2019 19:00	1.351631	1.3655
5/9/2019 19:30	1.513921	1.4345
5/9/2019 20:00	1.528749	1.5165

Date and time	WL_{Si}	WL_{Ob}
5/9/2019 20:30	1.504682	1.5525
5/9/2019 21:00	1.428642	1.5105
5/9/2019 21:30	1.405168	
5/9/2019 22:00	1.364476	
5/9/2019 22:30	1.134243	
5/9/2019 23:00	0.992759	
5/9/2019 23:30	0.848472	
6/9/2019 0:00	0.612726	
6/9/2019 0:30	0.413932	
6/9/2019 1:00	0.244893	
6/9/2019 1:30	0.207006	
6/9/2019 2:00	0.374692	
6/9/2019 2:30	0.449067	
6/9/2019 3:00	0.449024	
6/9/2019 3:30	0.630202	
6/9/2019 4:00	0.941608	
6/9/2019 4:30	1.096988	
6/9/2019 5:00	1.361901	
6/9/2019 5:30	1.590902	
6/9/2019 6:00	1.521138	
6/9/2019 6:30	1.722833	1.5915
6/9/2019 7:00	1.885115	1.7765
6/9/2019 7:30	1.815631	1.8215
6/9/2019 8:00	1.880588	1.8245
6/9/2019 8:30	1.8354	1.7545
6/9/2019 9:00	1.595847	1.6545
6/9/2019 9:30	1.536019	1.5265
6/9/2019 10:00	1.321356	1.3555
6/9/2019 10:30	1.050954	1.1515
6/9/2019 11:00	0.90451	0.9385

Date and time	WL_{Si}	WL_{Ob}
6/9/2019 11:30	0.62174	0.6565
6/9/2019 12:00	0.395986	0.5465
6/9/2019 12:30	0.251476	0.2565
6/9/2019 13:00	0.120681	0.0365
6/9/2019 13:30	-0.04897	-0.2235
6/9/2019 14:00	-0.22594	-0.4535
6/9/2019 14:30	-0.34744	-0.6335
6/9/2019 15:00	-0.44928	-0.7435
6/9/2019 15:30	-0.47916	-0.8335
6/9/2019 16:00	-0.38915	-0.7535
6/9/2019 16:30	-0.27494	-0.6035
6/9/2019 17:00	-0.12309	-0.4435
6/9/2019 17:30	0.067737	-0.2635
6/9/2019 18:00	0.334403	-0.0835
6/9/2019 18:30	0.533368	0.4065
6/9/2019 19:00	0.630186	0.6565

- Root Mean Square Error (RMSE) formula

$$RMSE = \sqrt{\frac{\sum_{i=1}^{N}(WLSi_i - WLOb_i)}{N\ (Samples)}} = 0.22$$

- Coefficient of determination (R^2)

$$R^2 = 1 - \frac{\sum_{i=1}^{N}[Q_{obs,i} - Q_{sim,i}]^2}{\sum_{i=1}^{N}[Q_{obs,i} - \bar{Q}_{obs}]^2} = 0.98$$

Where: $Q_{obs,i}$, $Q_{sim,i}$: Simulated and measured data; and, $\bar{Q}_{obs}$: Mean measured data.

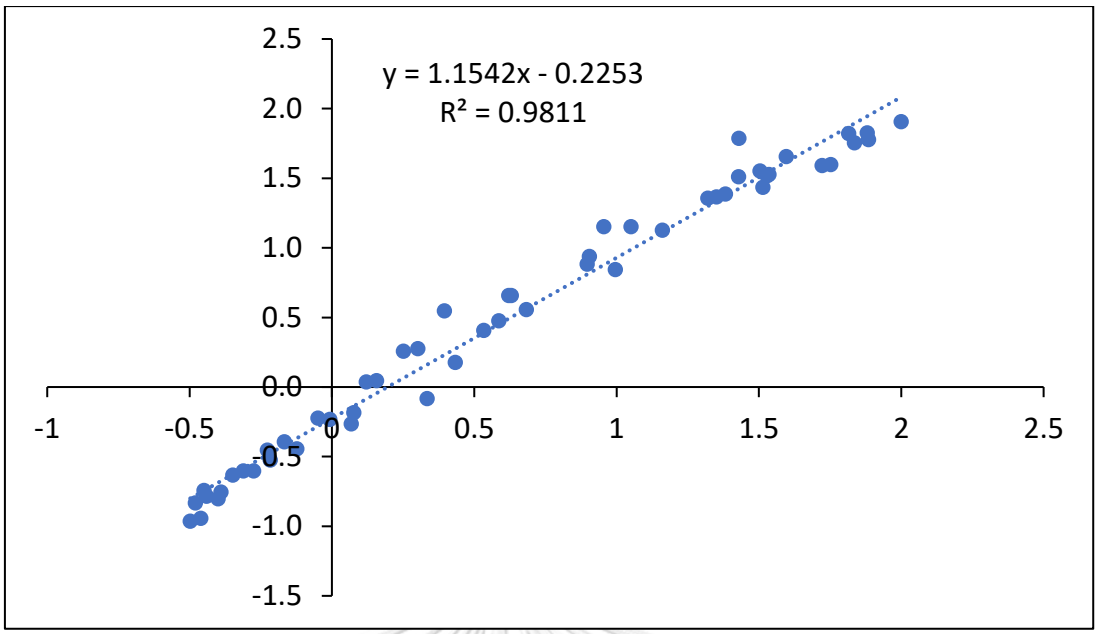

Figure 0.10 Correlation coefficient between simulated and measured values

- Mean Absolute Error (MAE)

MAE values, which were calculated for different layers responding to horizontal eddy viscosity (HEV=2, 4, 5, and 6 $m^2.s^{-1}$), followed the formula:

$$MAE = d_{Simulation} - d_{ADCP} \quad (1)$$

Where d was determined using the following a function:

$$ax^3 + bx^2 + cx + d = f(x) \quad (2)$$

a, b, c, and d: constants

This equation is established based on the simulated velocity points and the ADCP based velocities, representing the velocity distributions in different layers. The graphs showed velocity distribution at different layers as shown in result and discussion. Table 3.14 demonstrated the constant determination based on the function (2) for different HEVs and layers. Table 3.15 showed MAE values for various HEVs at different layers.

Table 0.14 Constants determined by using the function (2) for various simulation's scenarios

Simulations	a	b	c	d	Layer
HEV = 2	0.000001	-0.000198	0.014	**0.83**	1
	0.000001	-0.000209	0.015	**0.81**	2
	0.000001	-0.000214	0.015	**0.78**	3
	0.000000	-0.000139	0.009	**0.71**	4
HEV = 4	0.000001	-0.000159	0.011	**0.86**	1
	0.000000	-0.000151	0.011	**0.84**	2
	0.000000	-0.000082	0.007	**0.83**	3
	0.000000	-0.000099	0.005	**0.74**	4
HEV = 5	0.000000	-0.000123	0.008	**0.89**	1
	0.000000	-0.000118	0.008	**0.87**	2
	0.000000	-0.000086	0.006	**0.85**	3
	0.000000	-0.000072	0.003	**0.77**	4
HEV = 6	0.000000	-0.000113	0.007	**0.89**	1
	0.000000	-0.000108	0.007	**0.87**	2
	0.000000	-0.000085	0.006	**0.85**	3
	0.000000	-0.000065	0.003	**0.77**	4
d_{ADCP}	0.000000	-0.000161	0.015	**0.92**	1
	0.000001	-0.000382	0.030	**0.65**	2

Simulations	a	b	c	d	Layer
	0.000	0.000	-0.003	**1.31**	3
	0.000	0.000	0.000	**0.78**	4

Table 0.15 MAE (Mean Absolute Error) calculated for different horizontal eddy viscosities (HEVs) at the various layers

Simulations	Layers	MAE
HEV=2	1	0.09
	2	0.16
	3	**0.25**
	4	0.13
HEV=4	1	0.07
	2	0.19
	3	**0.31**
	4	0.07
HEV=5	1	0.04
	2	0.22
	3	**0.33**
	4	0.06
HEV=6	1	0.04
	2	0.22
	3	**0.34**
	4	0.05

3.8.2 Changes in water quality and its association with different flow regimes

Low, medium, and high flow regimes, which respond respectively to incoming, gentle/unchanged, and outgoing tides, were used to explore the spatiotemporal variabilities of both flow and water quality. The tidal states such as incoming, gentle/unchanged, and outgoing tides responding to low, medium and high flow regimes were classified based on the fieldwork. The analyzed results of water quality parameters at sampling sites responding to different tidal states were used to assess variabilities of water quality. The magnitude of water discharge corresponding to three tidal states at the observed sites was extracted from the results of the developed hydrodynamic model. Dataset of both flow and water quality parameters at the observed sites, which were set into three groups, met a normal distribution for the only flow dataset (determined by Kolmogorov-Smirnov test at the significant level of 5%). Therefore, the Duncan test (significant level of 5%) was used to examine the significant differences among the mean of the flows. While the significant differences among medians of water quality parameters were compared using the Kruskal-Wallis test (significant level of 5%). The dependence of water quality on various flow regimes was calculated using the Spearman test. All statistical analyses were performed using SPSS 20.0 software.

3.9 Framework of methodology

Figure 0.11 showed the methods and contents conducted in the research.

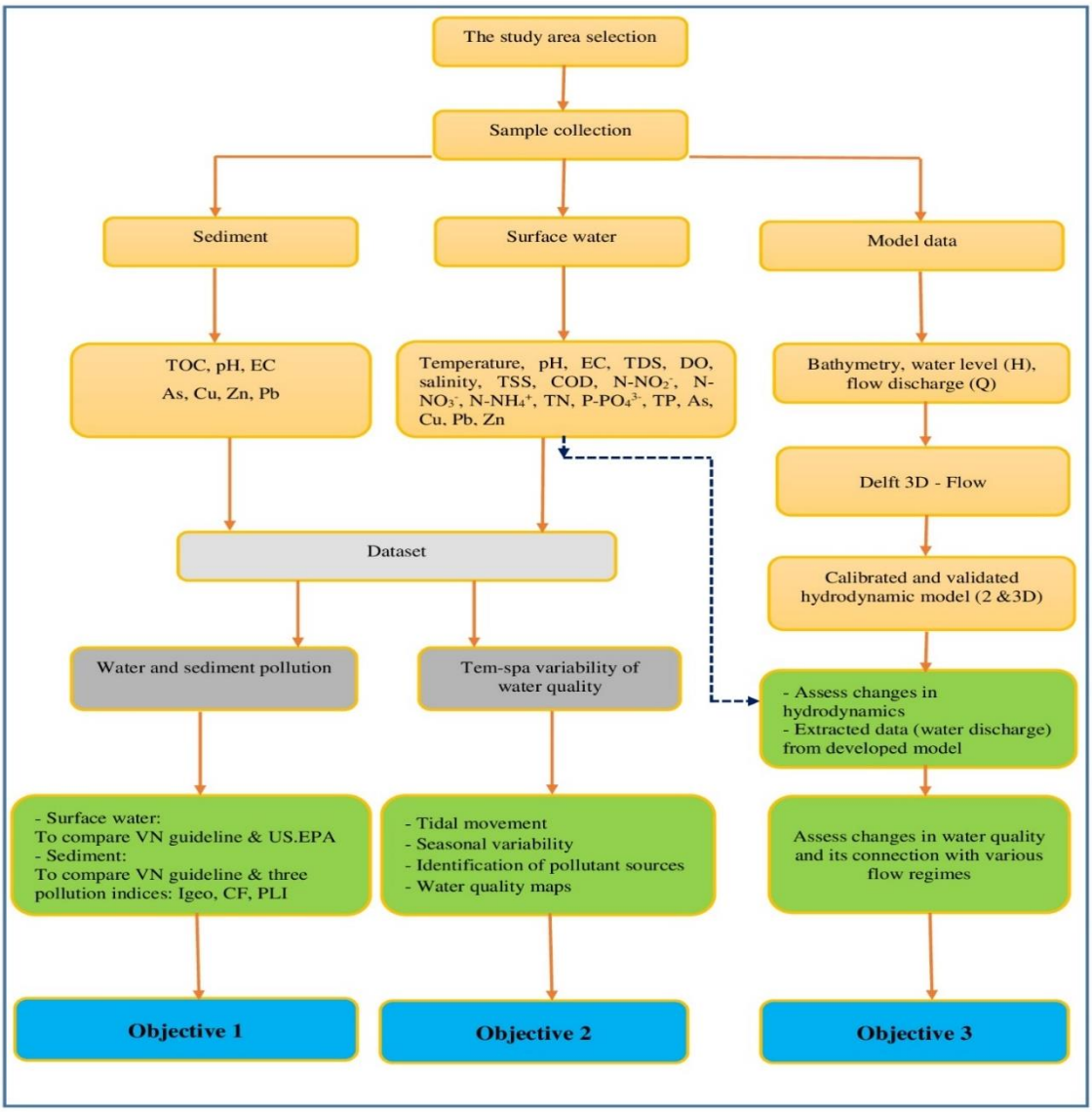

Figure 0.11 Methods and contents were conducted in the research.

CHAPTER 4
RESULTS AND DISSCUSTION
SPATIOTEMPORAL VARIABILITIES OF WAER AND SEDIMENT QUALITY

4.1 Spatial variations of the water and sediment quality

4.1.1 Surface water quality

a. Temperature

The spatial fluctuations of water quality parameters measured seasonally during the spring and neap tide at 25 observed sites. The findings indicated that physicochemical and biological elements were chiefly responsible for the water quality variations of the river reach while metal(loids) were hardly detected at most of the observed sites. Figure 0.12 showed that the temperature varied from 30.3 to 31.52^{o}C with the mean value of 31.01±0.34^{o}C and from 28.73 to 34.10^{o}C with the mean value of 29.64±1.05^{o}C in the dry and wet seasons, respectively. The variabilities of the temperature among sampling sites in two seasons were not substantial, this was due to the strong effects of the tidal cycle resulting in the spatially small increase of the temperature and the sampling sites occurred during similar weather conditions [212]. In addition, the tropical estuaries are a more steady temperature than the temperate ones [213]. In general, the variations of the temperature in the seasons were completely suitable for the aquatic ecosystems [214].

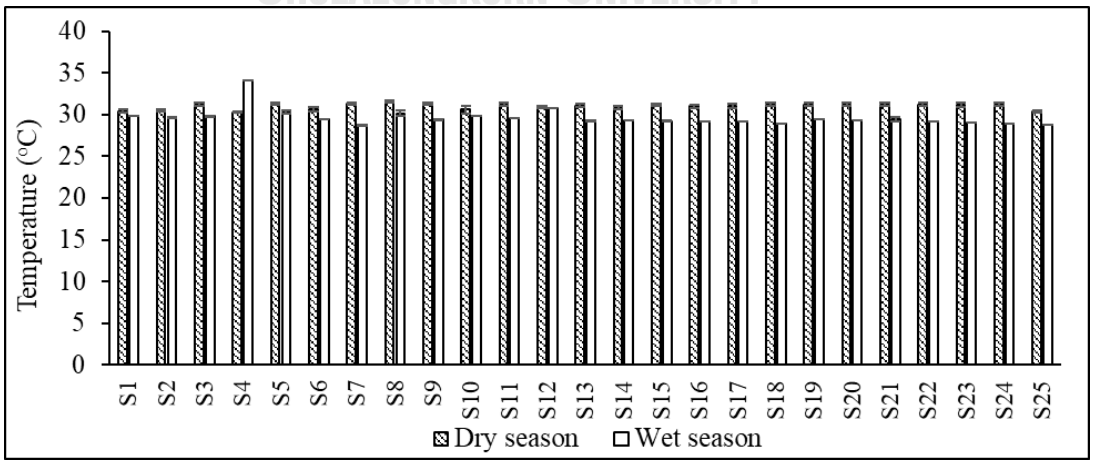

Figure 0.12 The spatial variabilities of water temperature in both seasons

b. pH

pH values, showing slightly spatial oscillation the same as the temperature, ranged from 7.67 to 7.77 with the mean value of 7.72±0.03 and from 6.90 to 7.33 with the mean value of 7.15±0.13 in the dry and wet seasons, accordingly (Figure 0.13). The study of [215] reported that two factors influencing primarily on changes in pH were the temperature and salinity, of which the former triggered relatively small effects, and the latter impacted substantially the dissimilar equilibrium constants, and few constituents of sea salt were included in the acid-base reactions of seawater. This could explain that the minor vacillations of pH resulted from intruding seawater with slight alkaline (7.5-8.4) [213] due to the impacts of the semi-diurnal regime of the East Sea; therefore, the sampling sites received correspondingly the seawater twice daily. Besides, the same weather conditions occurring during the field sampling led to slight variations of pH because of trivial alterations of the temperature among sampling sites in the seasons. Otherwise, the direct discharge of untreated wastewater from the shrimp farming into the surface water also was one of the causes resulting in changes in pH values because pond bottoms concentrate largely nutrients and organic substances residues during the rearing of aquatic organisms, acidifying the water [216]. However, the fewer effects caused by shrimp cultures into the surface water were observed during the field campaign occurring along banks of the river, it could therefore explain that all sampling sites recorded the extensively unchanged values of the pH. The spatial oscillations of the pH in the seasons were not exceeding the allowable standard for water quality.

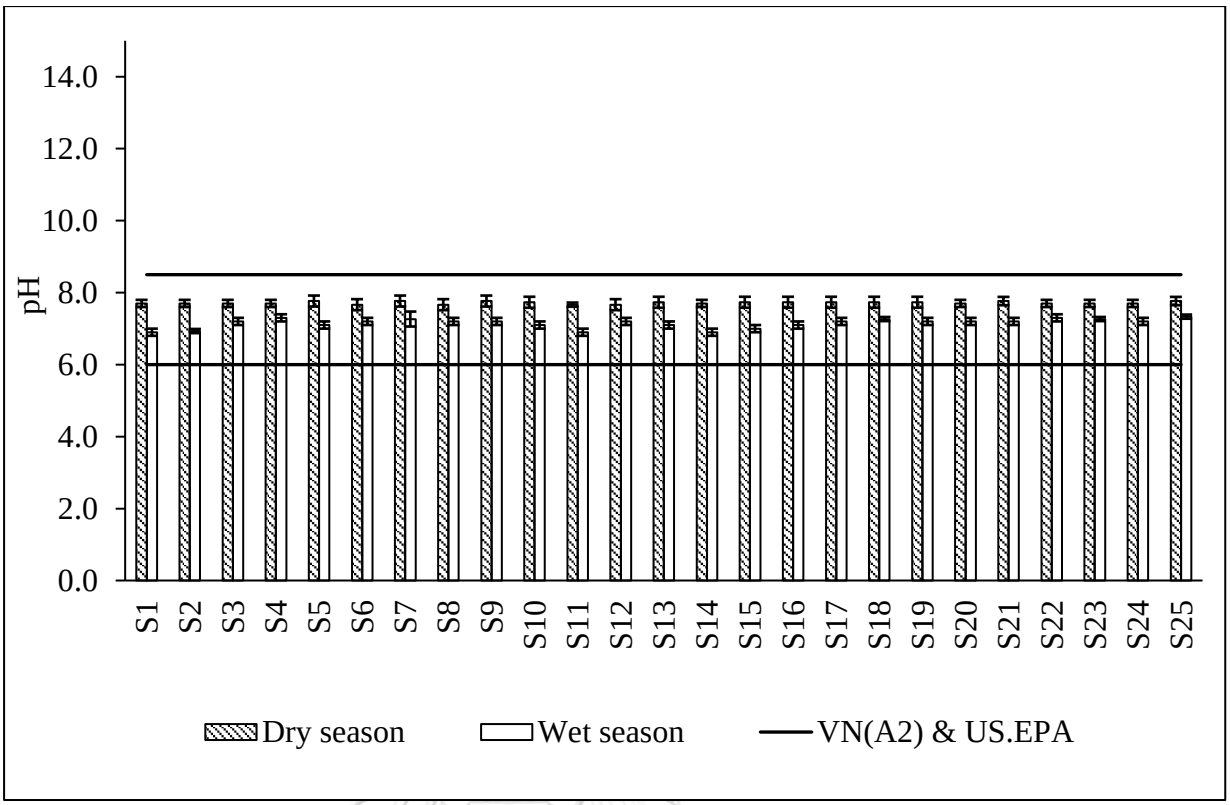

Figure 0.13 The spatial variabilities of water pH in both seasons

c. Electrical conductivity (EC)

High EC level was observed in all the sampling sites of the river. Its values varied marginally between 34.1 and 35.63 mS $cm^{-1,}$ with the mean EC value of 34.78±0.47 mS cm^{-1} in the dry season while the rainy season showed the mean value of 12±3.33 mS cm^{-1} and oscillated considerably in range of 8.30 to 21.37 mS cm^{-1} (Figure 0.14). The EC illustrated an increase in the spring tide moving upstream in the wet season; it is due to seawater from the East Sea containing a substantial amount of dissolved salt supplying the river reach. The previous study of [217] found that the agricultural activities would involve in the increase of the EC level. Consequently, the highest EC at sampling site S4 (EC=21.37 mS cm^{-1}) lying downstream of the river reaches, especially near the Ganh Hao-Ho Phong tributary and Tan Thuan commune where land use utilized for the shrimp culture obtained the biggest areas compared to other ones, would be related to aquaculture activities. Otherwise, the highest temperature, measured at S4 (34.1^{0}C) in comparison to other sites, would link to an expansion of the EC level; it is due to an increase in temperature causing an increase in the number

of ions in solution [218]. The spatial variation of EC values in the seasons met the water quality for marine aquatic life due to EC values being less than 50 mS cm^{-1} [219].

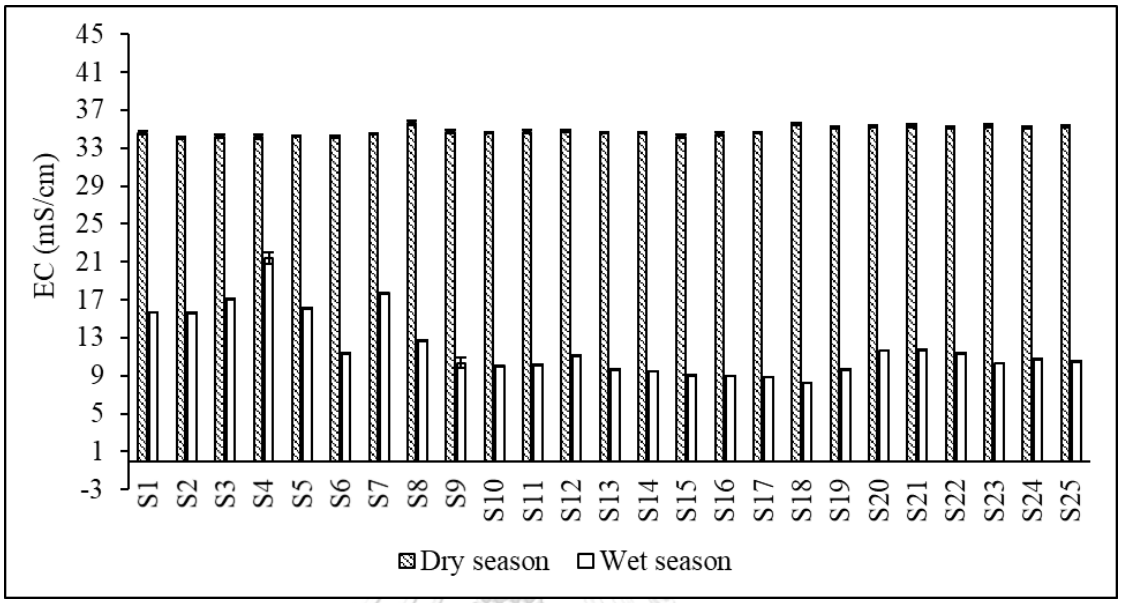

Figure 0.14 The spatial variabilities of water EC in both seasons

d. Total dissolved solids (TDS)

TDS varied spatially from 28.3 to 35.67 mg L^{-1}, with the detected mean value of 34.11±1.99 mg L^{-1} in the dry season while the measured mean value of TDS 11.98±3.31 mg L^{-1}, with a range of 8.30 to 21.10 mg L^{-1} in the wet season (Figure 0.15). The high EC values demonstrating in the seasons were involved in temperature, salinity oscillations, and aquaculture related-activities as well [219]. Of all of these effects, increased temperature of the water, influencing remarkably conductivity and causing ions to move in solution more quickly, results in high content of TDS. Thus, the EC and TDS correlated closely with each other [68, 220], it is therefore evident that the variation of TDS values showed the same trend as that of EC values in the wet season. The recorded TDS values among sampling sites, lowering substantially the normal range of seawater (TDS=35,000 mg L^{-1}), were suitable for aquatic organisms [219, 221]

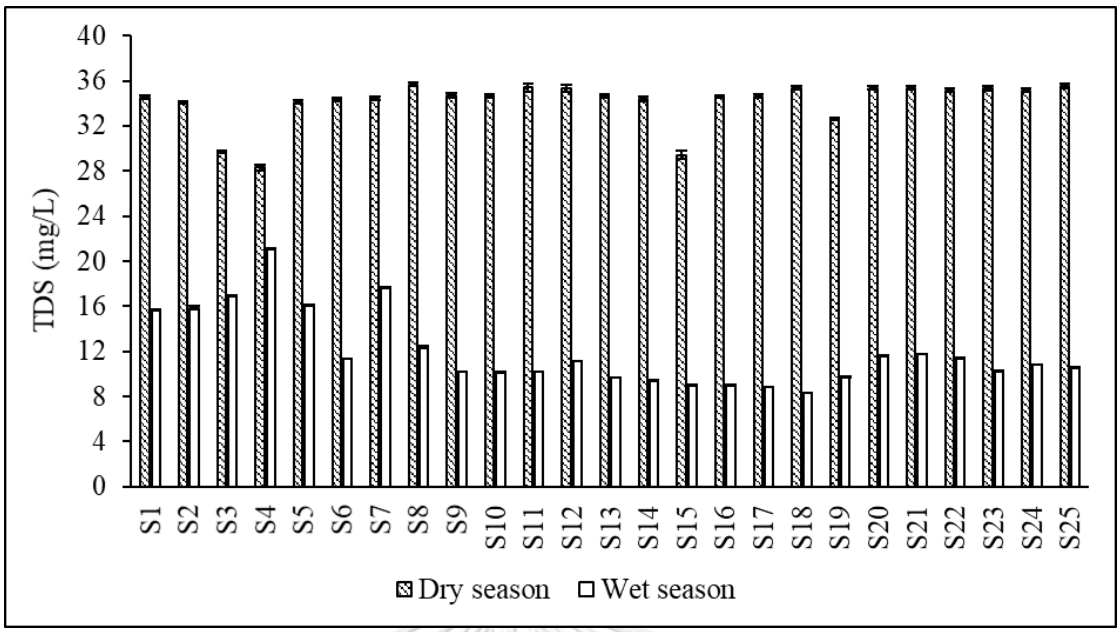

Figure 0.15 The spatial variabilities of TDS concentration in both seasons

e. *Salinity*

Figure 0.16 showed that measured salinity ranged from 21.23 to 22.67‰, with the mean value of 22.03±0.4‰ and varied from 4.70 to 12.83‰, with that of 6.88±2.06‰ in the dry and wet season, accordingly. The minor fluctuations of the salinity showing among sites were in the dry season, while the significant ones illustrated in the wet one. It could elucidate the tidal cycles and location within the estuary were responsible for changes in the salinity. It is therefore clear that the dry and wet seasons demonstrating similar oscillations in distributing the salinity, which was respectively found at highest values at S8 (22.67‰) and S4 (12.83‰) lying in the downstream, declined progressively at the upper reaches of the estuary. The observed results agreed with the study of [222] reporting that, higher values of the salinity occurred near the estuary and lower ones were upstream of the river reaches. The spatial alterations of the logged salinity in both seasons were not harmful to aquatic organisms as well as the excess of an allowable standard [223].

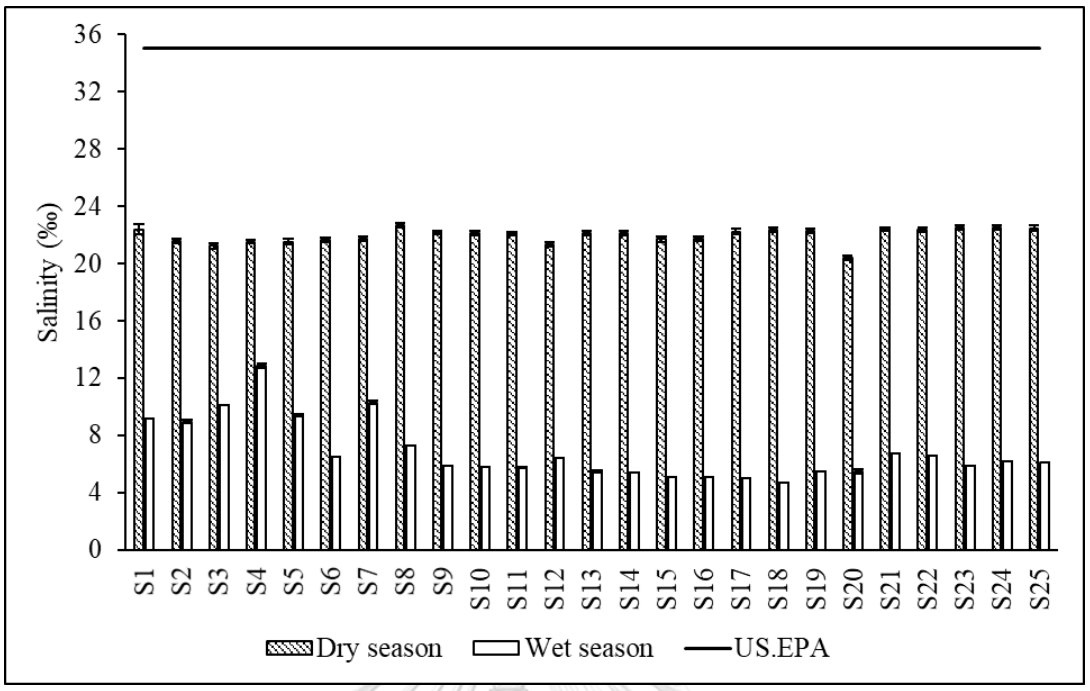

Figure 0.16 The spatial variabilities of TDS concentration in both seasons

f. Total suspended solids (TSS)

Concentration of TSS, which showing spatially the highest levels at all sites, ranked from 100 to 730.67 mg L^{-1}, with the mean value of 516.21±220.34 mg L^{-1}, and from 87.33 to 3,642.33 mg L^{-1}, with that of 611.52±804.66 mg L^{-1} in the dry and wet seasons, correspondingly (Figure 0.17). Higher TSS levels at sampling sites of S1 to S5 and S13 to S25 than S5 to S12 were observed in the dry season, of all of these sites, the sampling site obtained the most elevated value (S1=731 mg L^{-1}), compared to other sites. Whereas higher values in order of S9 (3,642.33 mg L^{-1} and S8 (2,188.33 mg L^{-1}) than those in the rest of other sites were recorded in the wet season. High concentrations of TSS, given the spatial variations of all the sites, were mostly explored near the downstream of the river reaches; this could explain that the sampling sites locating adjacent to the lower area of the reaches would link to aquaculture released-sources and the effect of tidal regime. The discharges of aquaculture consisting of numerous pollutants played a chief role in distributing the possible sources of TSS to the surface water [224]. Additionally, an extreme current flow impacted by semi-diurnal regimes prevented the normal transport upstream of suspended solids due to confronting the current flow front moving downstream of the

reaches, resulting in accumulating high concentrations of TSS at the lower area. The finding showed relatively the same as the study of [225] reported that contents of TSS tended to increase from upstream to downstream, related to the source of pollutants as well as effects of tidal cycles to transport upstream of suspended sediments [226]. All sampling sites in both seasons being logged with contents of TSS exceeded approximately twice to three greater than the permissible level for the water quality [190].

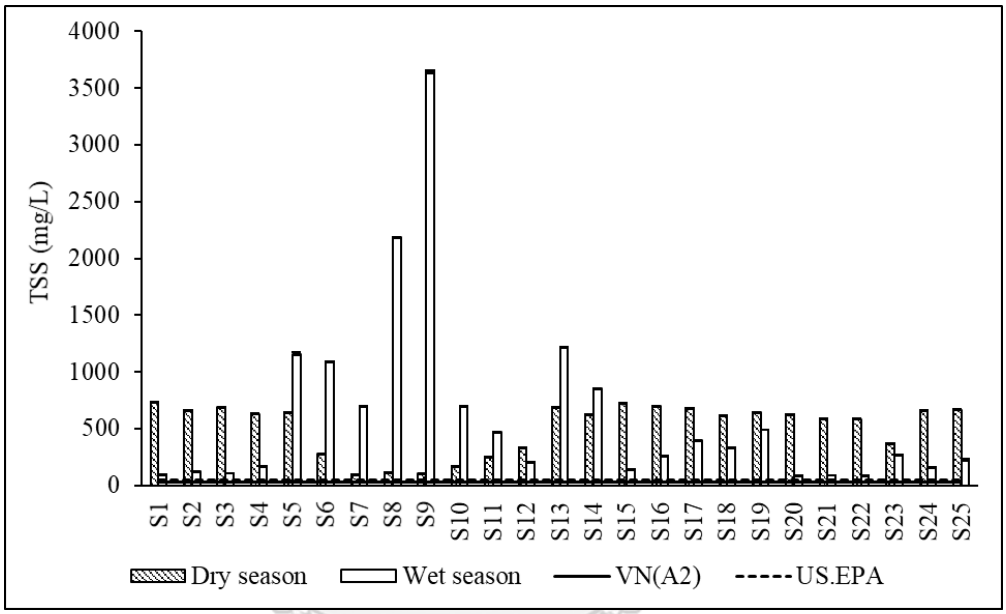

Figure 0.17 The spatial variabilities of TSS concentration in both the seasons

g. Chemical oxygen demand (COD)

Figure 0.18 illustrated that the spatial concentrations of measured COD varied widely at different sites in both the seasons. The mean value of COD among sites was 36.04±6.05 mg L^{-1} and fluctuated broadly from 26.67 to 49.00 mg L^{-1} in the dry season, while the contents of COD fluctuating from 12.80 to 36.27 mg L^{-1}, with the mean value of 22.19±6.19 mg L^{-1} were found in the wet season. High concentrations of measured COD were discovered spatially at all sites, except for S16 (12.8 mg L^{-1}) in the wet season, which were related to the wastewater discharged from aquaculture practices popularly occurring along the river reaches. In addition, the phase of tidal cycle, particularly semi-diurnal regimes, caused in high buildup of contaminants surrounding released sources leading to elevated concentrations of COD. [227] stated

that the solute pollutants would be discharged into the river/estuary at lower part of tides and be backed up the ones at spring tide so that the one would be deposited in the surrounding areas. Given the lower stage of the tidal regimes, the pollutants would also tend to have a longer retention time, which may probably result in a higher accumulation in contents. The COD values were substantially greater than the permissible standard, indicating the water quality was greatly polluted by organic substances.

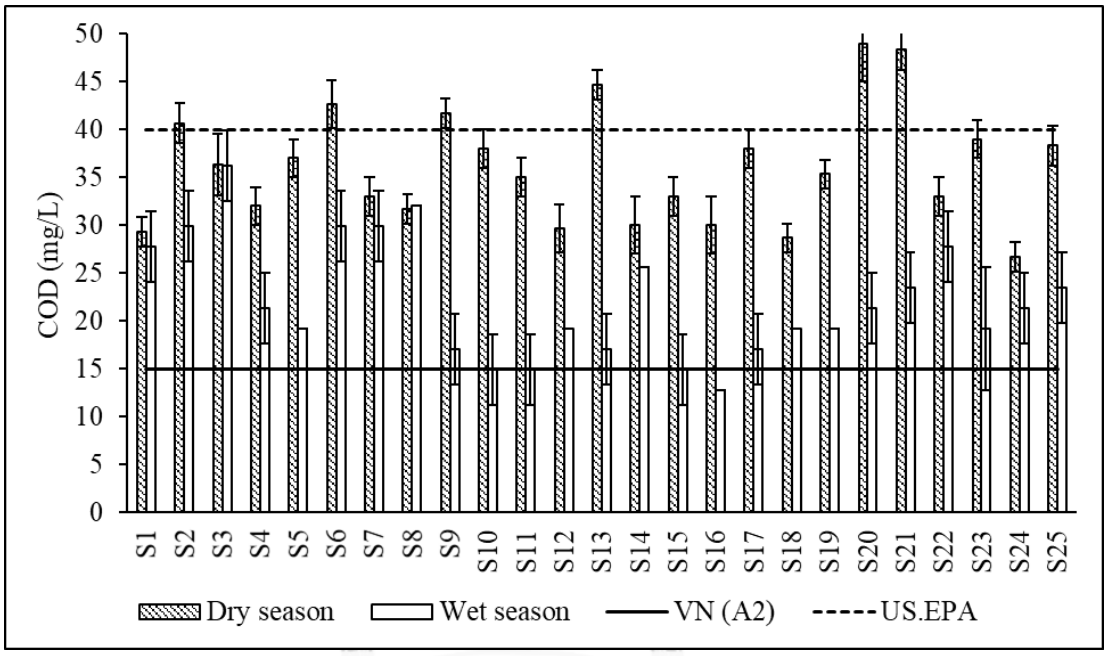

Figure 0.18 The spatial variabilities of COD concentration in both seasons

h. Dissolved oxygen (DO)

The mean concentration of DO at various sites was 5.88±0.91 mg L^{-1}, with a range of 4.09 to 7.09 mg L^{-1} in the dry, whereas a relatively wide variation from 2.79 to 6.99 mg L^{-1}, with the mean value of 5.68±1.21 mgL^{-1} was recorded in the wet season (Figure 0.19). The gradual decrease of DO showed evidently at sampling sites from S14 to S18, with lowest value at S18 (4.09 mg L^{-1}) and the one illustrating at different sites, principally S9, S11, S15, S19, S21, S25, had the lowest content at S9 (2.79 mg L^{-1}), compared to other sites in dry and wet season, respectively. The low concentrations of DO finding at noticed sites could involve in sources of wastewater discharged from aquaculture activities and temperature as well. DO contents varied spatially and reduced with an increase of the temperature in the watercourse [228,

229]; however, the influence of the temperature changes in DO levels was considered negligibly in the sense that the oscillation of the temperature was not widely at various sites in both the seasons. Hence, the pollutants containing high nutrients and organic substances were responsible for small DO contents, as documented by [217], this was explained that activities of microorganisms consuming a large amount of oxygen for decomposing the contaminants would drop possibly the DO levels in the river water. Couple with this could closely relate to the high presence of the salinity, causing to impairment of DO contents, the study of [230] revealed that high salinity would decline the capacity of holding dissolved oxygen in the water. In general, the mean value of DO was not much greater than the allowable norms; however, lower values comparing to the permissible standards were detected spatially at different sites in the seasons.

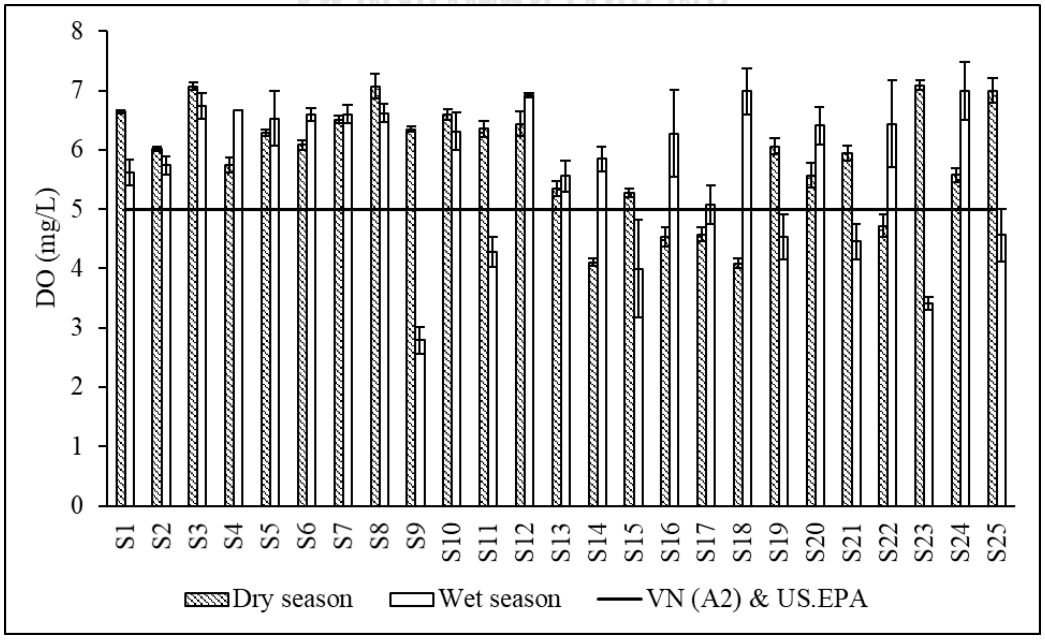

Figure 0.19 The spatial variabilities of DO concentration in both seasons

i. Nitrogen-nitrite (N-NO_2^-)

Nitrogen-nitrite (N-NO_2^-) values ranging spatially between 0.01 and 0.04 mg L^{-1} had the mean content of 0.02±0.01 mgL^{-1} and from 0.02 to 0.09 mgL^{-1}, with the mean content of 0.06±0.02 mgL^{-1} in the dry and wet seasons, accordingly (Figure 0.20). The gradual increase of N-NO_2^- starting at S1 reached the elevated value of 0.04 mg L^{-1} (S4) and then dropped progressively to the upper part of the river course in the dry season. However, the contents of N-NO_2^- rising gradually from the downstream to the upper part of the river reaches in the wet season got the highest value of 0.09 mg L^{-1} (S18). Concentration of N-NO_2^- in natural water is typically in a small range and lower value was apparently found in the seawater [41, 231]. It is therefore obvious that high levels of N-NO_2^- at observed sites would link to land use in which wastewater sources released by aquaculture practices containing high content of nutrients. As reported by [232], nitrogen waste produced by the shrimp culture system made deterioration of water quality due to excess of the assimilating capacity of receiving waters. The finding illustrated the mean content of N-NO_2^- in the wet season exceeding the allowable standards compared to the dry one still lowering norms the [190, 191]; however, some of the observed sites in both the seasons revealing the levels of N-NO_2^- were beyond the standards.

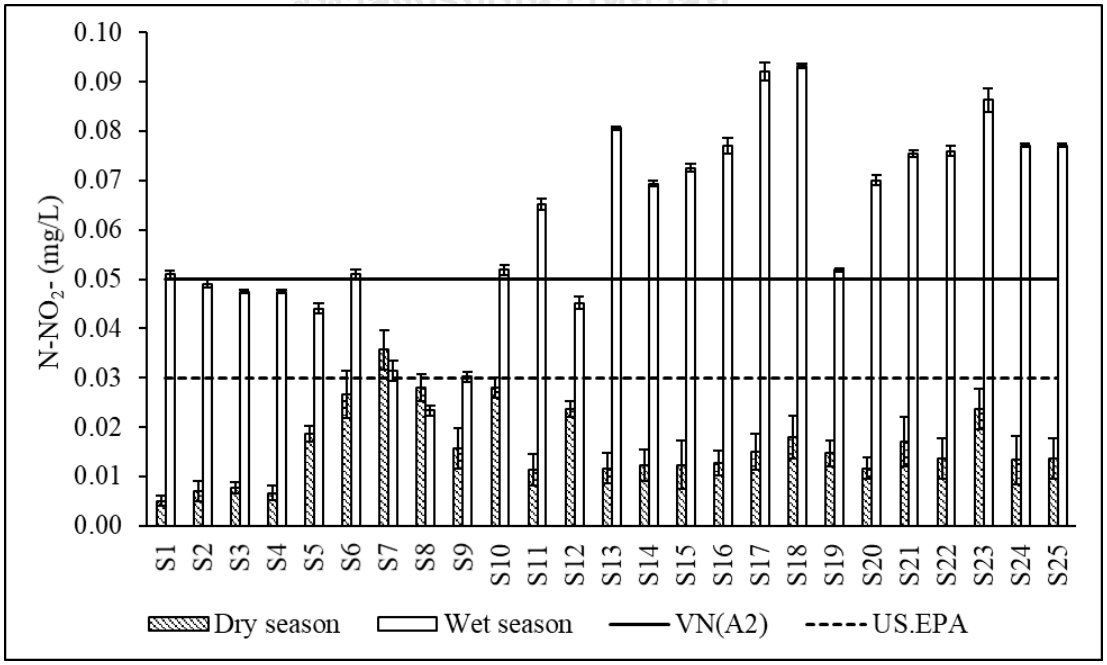

Figure 0.20 The spatial variabilities of $N\text{-}NO_2^-$ concentration in both seasons

j. Nitrogen nitrate ($N\text{-}NO_3^-$)

Nitrogen-nitrate ($N\text{-}NO_3^-$) concentrations, which sunk significantly in comparison with the acceptable norms [190], oscillated respectively between 0.12 and 0.21 mg L^{-1}, with the mean value of 0.16±0.02 mgL^{-1} in the dry season and from 0.70 to 1.99 mg L^{-1}, with that of 1.19±0.26 mgL^{-1} in the wet one (Figure 0.21). The concentrations of $N\text{-}NO_3^-$ demonstrated small fluctuations at observed sites in the dry season, the progressive increase of $N\text{-}NO_3^-$ starting at downstream (S1) reached the highest value of 1.99 mg L^{-1} (S8) where the lowest $N\text{-}NO_2^-$ value existed in the wet season. The rapid augment of $N\text{-}NO_3^-$ here suggested that there was a mixture of $N\text{-}NO_3^-$ pollution sources, which was also impacted by nitrification processes [233]. The concentrations of $N\text{-}NO_3^-$ varied slightly and declined gradually from observed sites S9 to S20, however, these augmented progressively again within S21 to S25. This could explain that washing out pollutants with high nutrients by aquaculture practices was associated with changes in $N\text{-}NO_3^-$ [224]. Additionally, a high spatial alteration of $N\text{-}NO_3^-$ concentrations occurred in some watercourses owing to the catchment features [234]. The results illustrated that $N\text{-}NO_3^-$ pollution in the river reaches had distinct differences among the observed sites.

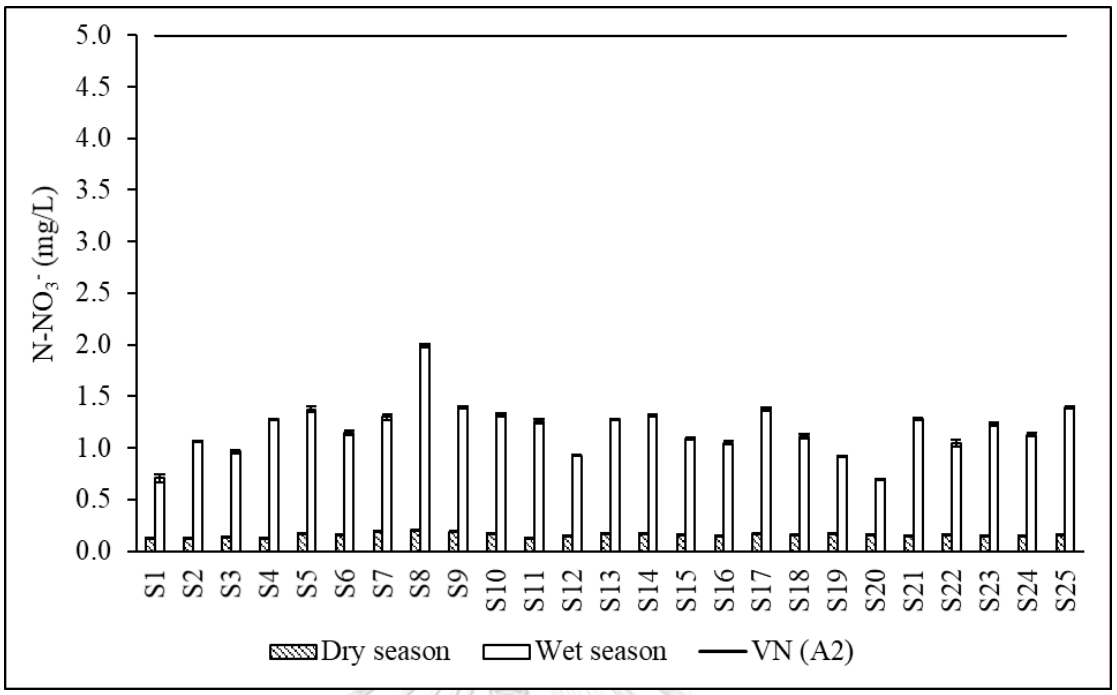

Figure 0.21 The spatial variabilities of $N\text{-}NO_3^-$ concentration in both seasons

k. Nitrogen ammonium ($N\text{-}NH_4^+$)

The concentrations of $N\text{-}NH_4^+$ in both seasons lowered greatly in comparison with the allowable standard [190] (except for the observed site S3) in the wet season. They varied respectively between 0.01 and 0.28 mg L^{-1}, with the mean concentration of 0.07±0.05 mg L^{-1} in the dry season and 0.06 to 0.44 mg L^{-1}, with that of 0.17±0.09 mg L^{-1} in the wet one (Figure 0.22). Both seasons showed spatially a various variation of $N\text{-}NH_4^+$contents. The concentrations enlarged progressively from the S1 to S6 (the highest value of 0.28 mgL^{-1}) at the downstream and then fell gradually within S7 to S25 at the upper part of the river reaches in the dry season. Whilst an unsteady fluctuation, particularly high values of $N\text{-}NH_4^+$ at observed sites as S2, S3, S8, S10, S14, S17, and S18 compared to other sites, occurred along with the river courses in the rest of the season. It was due to the impacts of wastewater sources induced by the aquaculture practices, containing excretion and decomposition of aquatic organisms and differing also the number of pollutant outputs at the influenced sites, were responsible for high $N\text{-}NH_4^+$ concentrations [235, 236]. In overall, the results illustrated relatively high contents in the seasons, but still met the allowable standard for water quality. This could be due to the effects of water pH (>7.0) found at most of

the sampling sites. The previous study [237] reported that the existence form of NH_4^+ depended greatly on pH values, which would promote the species of NH_4^+ in the acidic water environment (pH < 7.0).

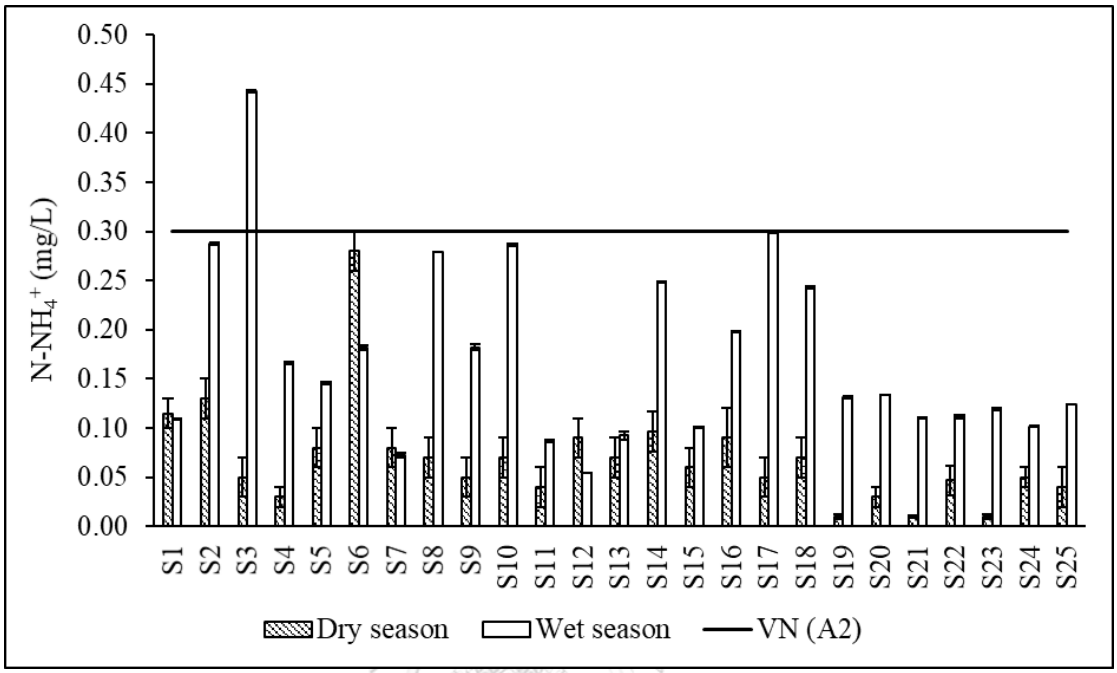

Figure 0.22 The spatial variabilities of N-NH_4^+ concentration in both seasons

l. Total nitrogen (TN)

TN concentration fluctuated broadly in a range of 0.84 to 4.76 mg L^{-1}, with the mean concentration of 2.43±0.87 mg L^{-1} in the dry season and varied from 1.40 to 5.32 mg L^{-1}, with that of 3.12±1.2 mgL^{-1} in the wet one. Higher contents of TN at S11, S20, and S25 than other observed sites occurred along with the study river in dry season, while high TN values were detected at the sampling sites (S8, S9, S14, S18, S19, and S24), comparing to other sites in wet seasons (Figure 0.23). The apparent lack of trends along the river reach indicated that high contents of TN, which were found at the observed sites both the seasons, would not relate to nitrogen sources contributing to the study area from the upstream of the Ganh Hao River, but was rather linked to effluents released by aquaculture practices occurring along the river. In addition, high spatial changes in TN concentrations came out among the sampling sites, which could associate with the catchment attributes [234]. The results illustrated that the mean content of TN both seasons was over the established norms for water quality [238].

The previous study of [239] reported that contents of TN ranging from 0.1 to 0.75 mg L^{-1} could lead to plankton blooms in coastal waters; it is therefore evident that water quality was polluted substantially by TN loads.

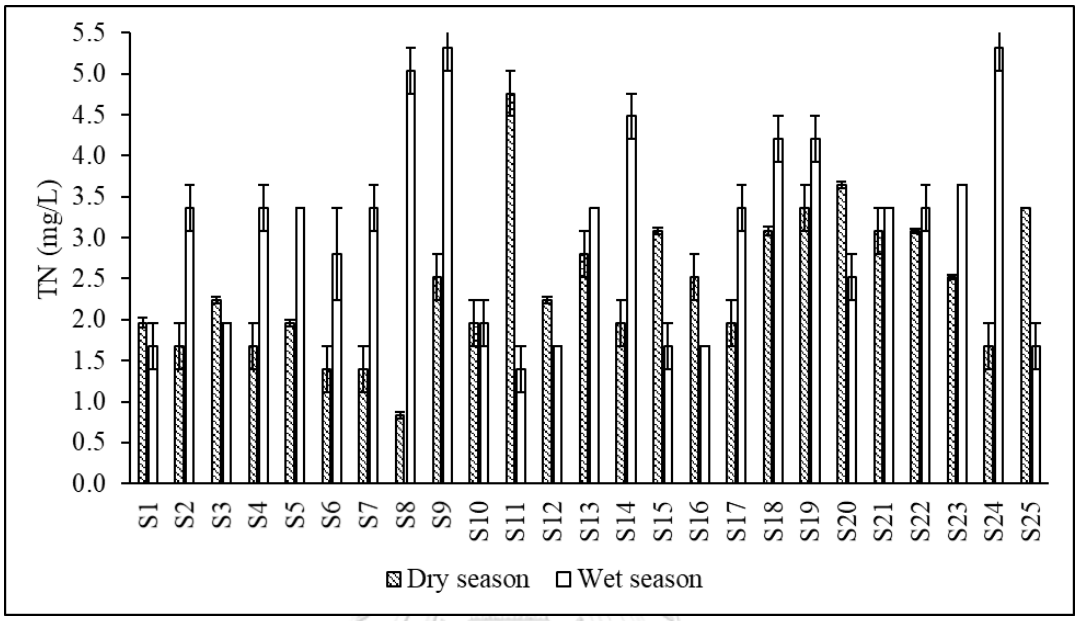

Figure 0.23 The spatial variabilities of TN concentration in both seasons

m. Phosphate phosphorus ($P\text{-}PO_4^{3-}$)

Phosphate phosphorus ($P\text{-}PO_4^{3-}$) concentrations, which were significant lower than established standards [190, 191], varied respectively from 0.02 to 0.08 mg L^{-1}, with the mean value of 0.04±0.01 m gL^{-1} and 0.01 to 0.20 mg L^{-1}, with that of 0.04±0.04 mg L^{-1} in the dry and wet seasons (Figure 0.24). Except for the observed site (S16) has a high value of $P\text{-}PO_4^{3-}$ (0.20 mg L^{-1}) in the wet season, the distinct sites presented pretty much the low spatial contents of $P\text{-}PO_4^{3-}$ and oscillated negligibly in the seasons. The presence of $P\text{-}PO_4^{3-}$ could associate with wastewater sources discharged into the surface water containing residual chemicals, which were used at different stages of aquatic animal feed and health management in aquaculture activities [240]. The results illustrated that the contents of $P\text{-}PO_4^{3-}$ were greatly smaller than these of nitrogen species, demonstrating both the seasons, it was due to the fact that $P\text{-}PO_4^{3-}$ could be absorbed by a high amount of suspended solids. As stated by [241], $P\text{-}PO_4^{3-}$ content, its soluble state in the surface water, was affected by suspended solids

through adsorption; therefore, the less available in concentration was in the aquatic environment.

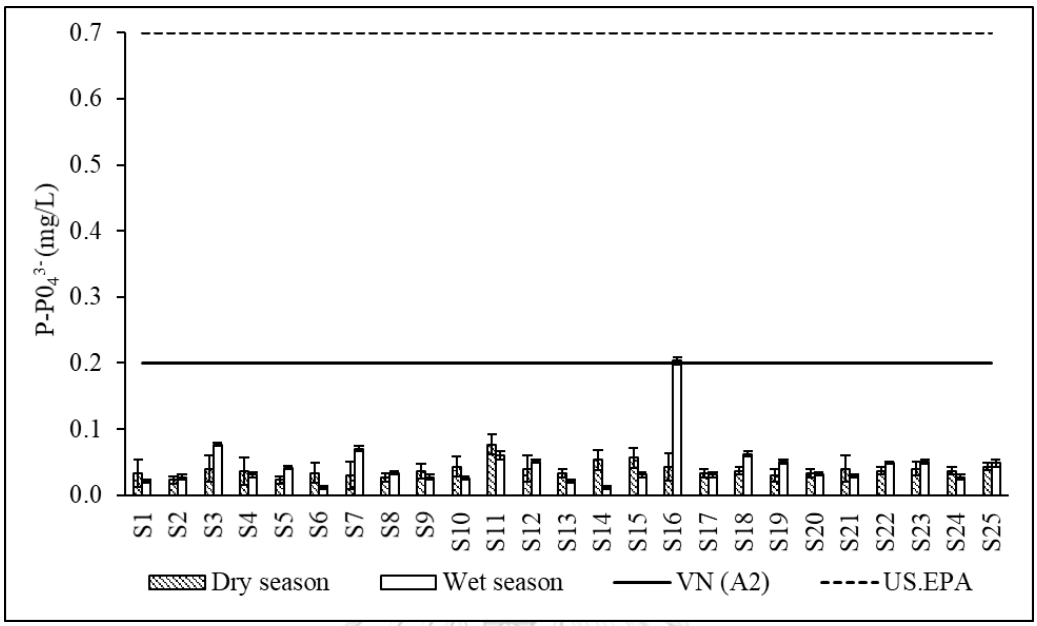

Figure 0.24 The spatial variabilities of P-PO_4^{3-} concentration in both seasons

n. Total phosphorus (TP)

Total phosphorus (TP) concentrations had accordingly the mean value of 0.38±0.1 mg L^{-1}, with a range of 0.14 to 0.53 mg L^{-1} and that of 0.57±0.63 mg L^{-1}, with a variation of 0.01 to 2.97 mg L^{-1} in the dry and wet seasons (Figure 0.25). The spatial contents of TP fluctuated slightly at different sites in the dry season, while these augmented gradually from S1 to the highest value of 2.97 mg L^{-1} (S16) and drop progressively to S25 in the rest of season. A direct linking to wastewater source containing high phosphorous content at sampling stage would accelerate the value of TP at S16 comparing to other sites; however, the fluctuations may be transitory because the magnitude of distinct sources of phosphorus oscillated remarkably throughout the catchment [242]. The previos study of Cavalcante [243] reported that phosphorus in suspended solids chiefly existed in absorbed forms, leading to the low concentrations in the surface water, however, the results showed that relatively elevated TP loads were explored among the sampling sites. It was illustrated that deterioration of water quality caused by phosphorus contents would be of 0.001 to 0.1 mg L^{-1}, resulting in plankton blooms in the coastal waters [244]. It is therefore evident that the water

quality polluted by nutrients, particularly phosphorus concentrations, occurred along the studied segment at the period of the survey field.

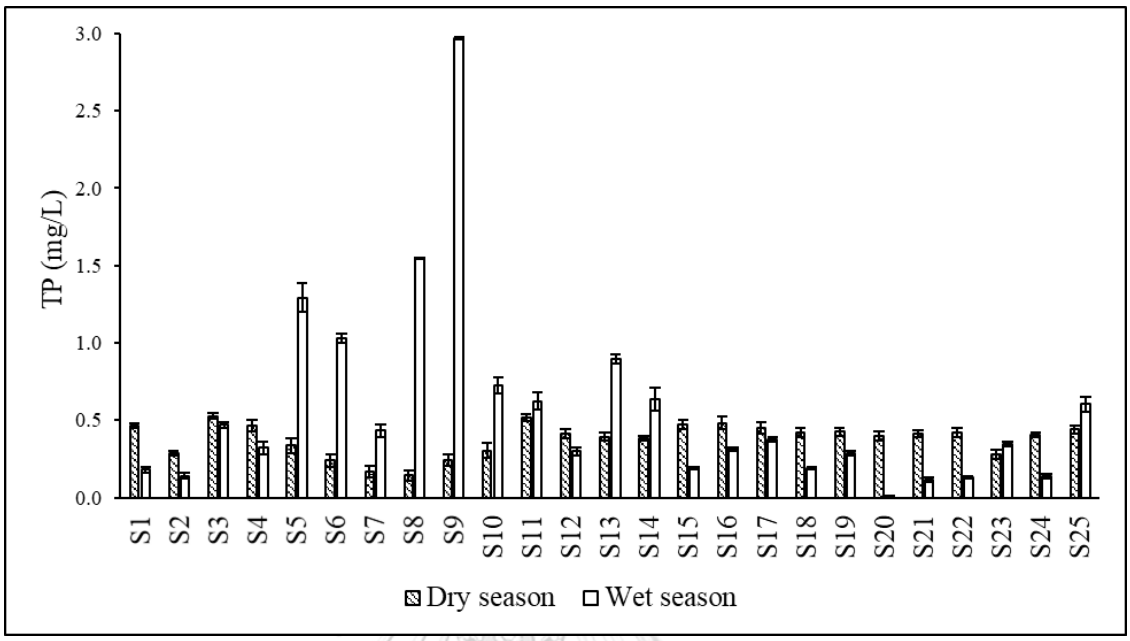

Figure 0.25 The spatial variabilities of TP concentration in both seasons

o. Heavy metal(oid)s

Table 0.17 indicated that concentrations of As, Cu, Pb, and Zn were hardly discovered at most of the sampling sites; however, the few observed sites were detected substantially the low concentrations and lowered greatly the established norms [190, 191]. In particular, the As contents were not detected in all the sampling sites in the dry season while they ranged slightly from N.D. to 0.01 mg L^{-1} in the wet season. The concentrations of Cu illustrated spatially the same range of N.D. to 0.01 mg L^{-1} both the seasons. The Pb contents did not detect all the observed sites in the dry season, but varied marginally from ND to 0.04 mg L^{-1}, the mean value of 0.01±0.01 mg L^{-1} in the wet season. Ultimately, the contents of Zn differed from ND to 0.05 mg L^{-1}, with the mean value of 0.0±0.01 mg L^{-1} and ND to 0.08 mg L^{-1}, with that of 0.01±0.02 mg L^{-1} in the dry and wet seasons, respectively. The studied segment has been influenced intensively by aquaculture practices for which high loadings of heavy metals including in the effluents could introduce possibly into the surface water [245, 246]. Nevertheless, the results indicated that the least contents of metal(oid)s or even not detected could associate with physicochemical processes

occurring popularly in the aquatic environment, which could lessen remarkably the presence of heavy metal(oid)s. The principal process governing the distribution of the different soluble forms of metals were dilution, dispersion, sedimentation, and absorption and physicochemical properties of the water (e.g., pH, temperature, and dissolved ions) as well [106]; thus, it could explain that the minor loadings of metals would relate to the high existence of TSS contents. In addition, the studied river lying inland is away approx. 6 km from the estuary of Ganh Hao River. Consequently, the interplay of river flow and seawater under the impact of the tidal cycles produced a rotational circulation enlarging water and sediment residence times within the estuary, which usually led to the deposition of particulate metals within the estuary [247]. This has been confirmed by several studies in coastal regions [41, 46, 247].

Table 0.16. Spatial variation of metal concentrations among sampling sites in two seasons.

Parameters	Seasons	Min	Max	Mean±SD[a]	LOD (mg L^{-1})b	VN(A_2)[c]	US.EPA[d]
As (mg L^{-1})	Dry	ND	ND	ND	0.005	0.02	0.05
	Wet	ND	0.01	0.0±0			
Cu (mg L^{-1})	Dry	ND	0.01	0.0±0	0.03	0.2	0.1
	Wet	ND	0.01	0.0±0			
Pb (mg L^{-1})	Dry	ND	ND	ND	0.002	0.02	0.05
	Wet	ND	0.04	0.01±0.01			
Zn (mg L^{-1})	Dry	ND	0.05	0.0±0.01	0.06	1.0	5
	Wet	ND	0.08	0.01±0.02			

Number of samples for statistical analysis (n=25 for heavy metals in the dry and wet seasons)

ND: not detected;

[a] Standard deviation

LOD: Limit Of Detection

[c] Vietnamese water quality standard refers to the water supply but must apply properly treating technologies and other purposes require lower water quality.

[d] US.EPA allowable limit for surface water quality

4.1.2 Sediment quality

a. pH

The recorded mean of pH values having a value of 5.95±0.21 fluctuated variously from 5.63 to 6.37 and 6.16±0.12, with a range of 5.91 to 6.42 at the observed sites in the dry and wet seasons, respectively (Figure 0.26). The results indicated that the lack of apparent trends and substantial variabilities of the pH among the sampling sites were found evidently in the dry and wet seasons, the measurements demonstrated slightly a lower the pH value than those in the surface water. This could be due to fact that decomposition of deposited organic substances deriving from the aquaculture practices resulted in low pH values in the sediment. The previous studies [248, 249] reported that the low values of pH in the sediment could associate with the presence of humic acid formed from decaying organic substances and deposits of acid sulfate soils. Generally, sediment pH, showing slightly acidic property in comparison with the common range observed for marine and estuarine sediment, was found in the studied segment [250].

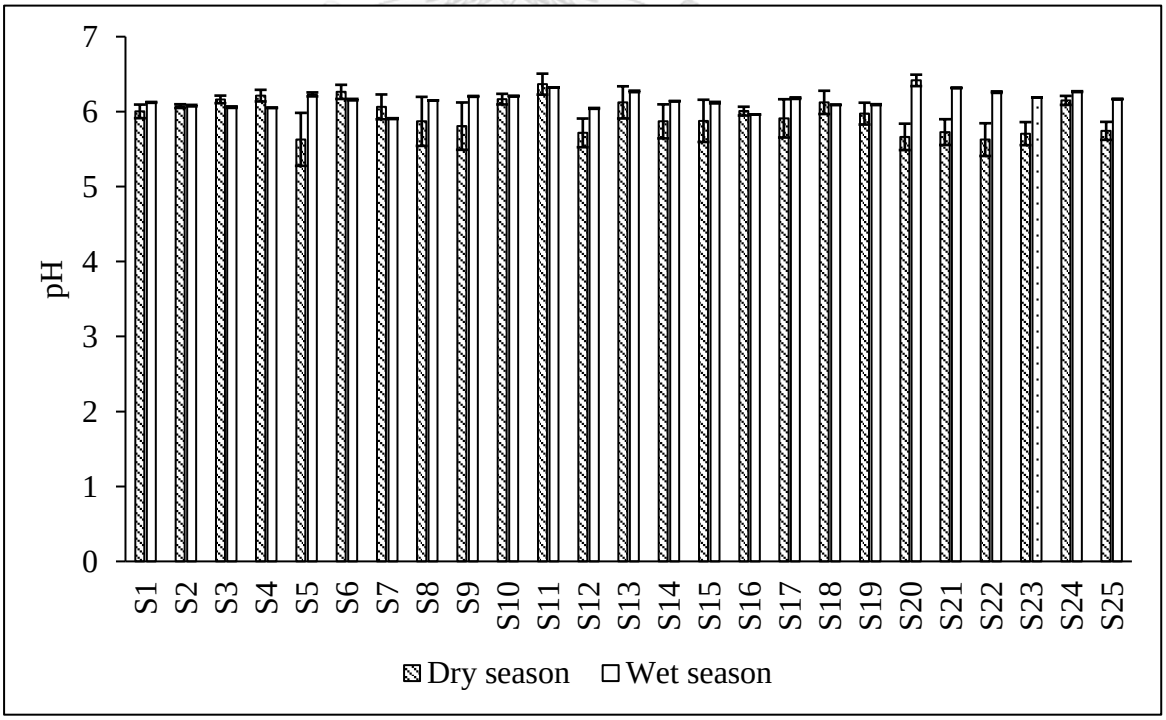

Figure 0.26 The spatial variabilities of sediment pH values in both seasons

b. Electrical conductivity (EC)

Figure 0.27 showed that EC values differed greatly from 76.13 to 191.87 mS cm^{-1}, with the mean value of 137.76±29.71 mS cm^{-1} in the dry season while the mean of EC value was 92.42±26.52 mS cm^{-1}, with a range of 39.37 to 142.53 mS cm^{-1} in the rest of the season. Higher values of EC at S2, S13, S17, and S22 than the other sampling sites were recorded in the dry season; however, variability without apparent trend occurred from the lower to the upper part of the river reach. Whilst, the highest values in the wet season detecting at S5, S6, S10, and S12 compared to the other observed sites and showed the same variation as the dry season. The finding illustrating high EC contents both the seasons would associate with seawater under greatly impacted by tidal cycles of the East Sea. The previous study of [251] stated that a strong positive correlation between cation and capacity of exchange cation was remarkably affected by the seawater, leading to high EC found in the sediment. In situ measurement was also one of the factors resulting in elevated EC in the sediment. The study of [252] indicated that high EC contents were measured directly in reduced sediments because the direct conductivity measurement consisted of the ionic contribution and electron conductivity and prevented the conductivity due to the air-oxidation processes.

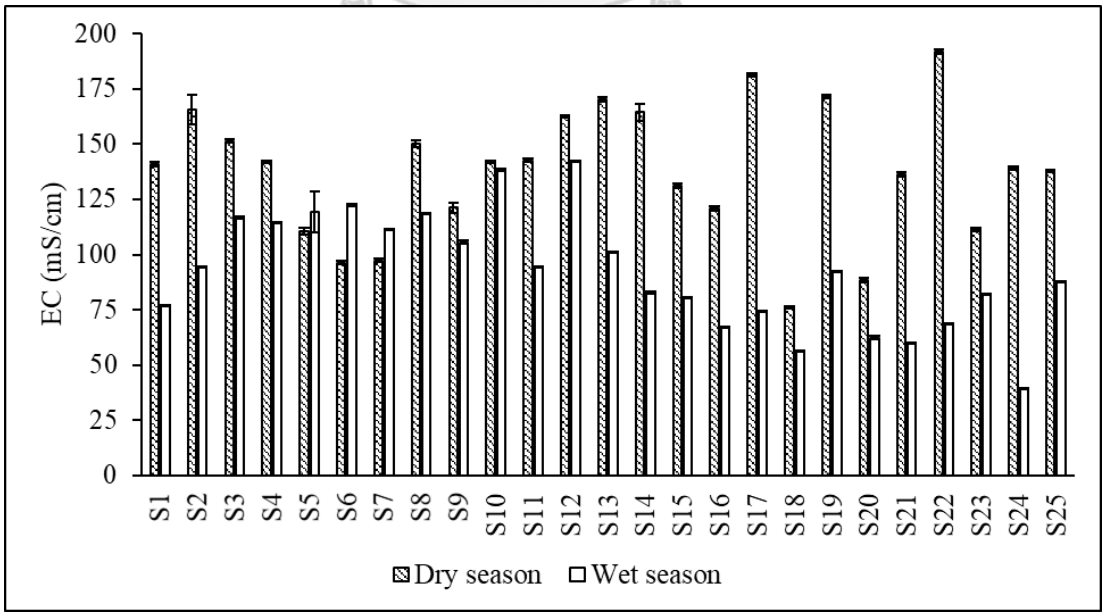

Figure 0.27 The spatial variabilities of sediment EC values in both seasons

c. Total organic carbon (TOC)

The TOC values among the observed sites fluctuated moderately from 1.03 to 3.32%, with the mean value of 1.98±0.65% and from 1.92 to 4.75%, with that of 3.2±0.83% in the dry and wet seasons, accordingly (Figure 0.28). Theo TOC indicated an inexplicit trend of variation in the dry season starting from the down to upstream of the river segment. The highest content obtained at observed sites (S7, S15, and S22) in comparison with the other ones. The measurements were found at different sites in the wet season showing the same trend as the dry season. A high content of TOC was found in the wet season compared with the dry one. The receiving waters at the river reach have been substantially influenced a numerous amount of aquaculture derived-inputs, which were considered to be one of the sources causing a high buildup of organic matter loads in the sediments. Nevertheless, the minor contents of TOC measured illustrated spatially at different sites in both seasons, this could derive from strong effects of the hydrodynamics and sedimentary components. The previous studies [253, 254] interpreted that sediment dispersion depended remarkably on the tidal flow; therefore, high TOC contents were beneficial to the burial in the sediment with the weak hydrodynamic environment. Additionally, sediment texture in the course contained primarily clay-silt, fine sand, silty-green, and many shells [255]. The study of [254] noticed that coarse-grained sediments (silty sand and sand) had the lowest organic substance concentrations. Overall, the oscillation of TOC contents was consistent with the normal range of 1.2 to 5.2% found in marine sediments [256].

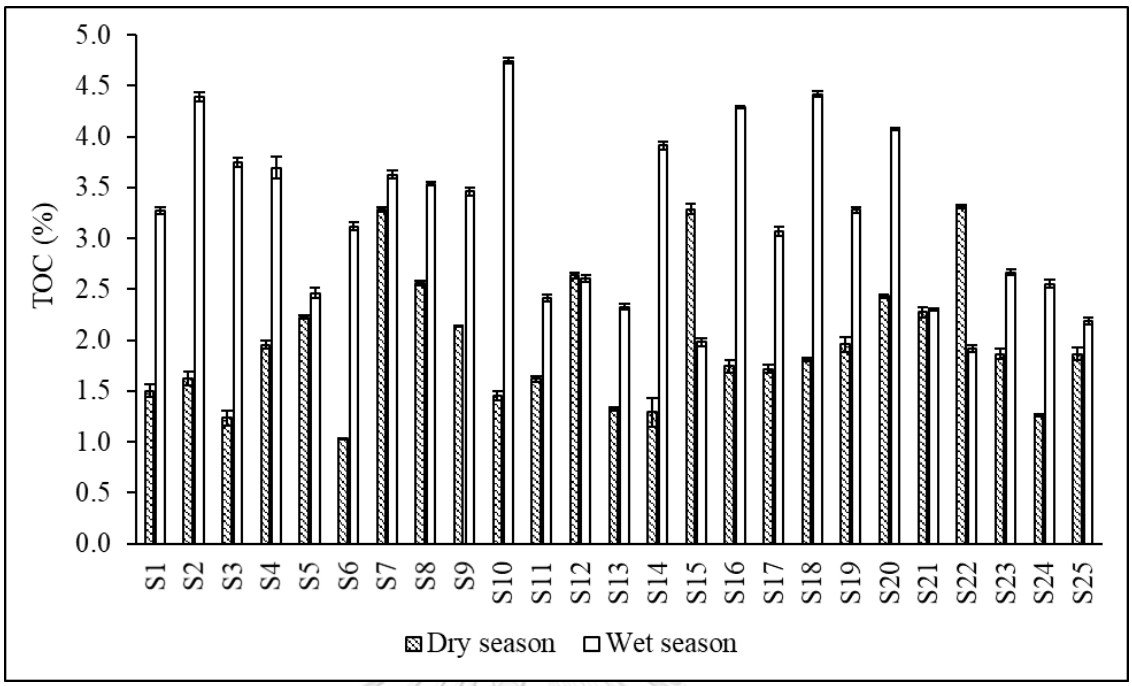

Figure 0.28 The spatial variabilities of TOC values in both seasons

d. Heavy metal(oid)s

The concentrations of As, Cu, Pb, and Zn varied widely among the observed sites. Specifically, the As content averaged 9.24±2.94 mg kg^{-1}, with a range of 5.35 to 15.2 mg kg^{-1} at different sites and 5.84±1.59 mg kg^{-1}, with a fluctuation of 2.22 to 8.49 mg kg^{-1} in the dry and wet seasons, respectively (Figure 0.29a). The highest values of As finding at S7, S8, S11, S12, S19, and S22 as well as S1, S11, and S14 compared respectively to the others in the dry and wet seasons, which showed spatially the vague trend of variation with a start of lower to upper part of the river reach. The Cu contents ranged from 8.72 to 16.28 mg kg^{-1}, with the mean of 12.76±1.82 mg kg^{-1}. The observed sites (S2, S12, and S16) had much more the Cu loads than the others did in the dry season. While a relatively wide range of Cu contents from 7.43 to 22.92 mg kg^{-1}, with the mean of 18.21±3.84 mg kg^{-1} were detected in the wet season (Figure 0.29b). Among the observed sites illustrated greater the values of Cu at S1, S2, S20, S24, and S25 than the other sites. Similar to As, the spatial trend of fluctuation in Cu contents was inexplicit seasonally at the sampling sites along the river reach. The spatial Pb contents differing slightly from 8.84 to 13.22 mg kg^{-1} averaged 11.04±1.19 mg kg^{-1} at various sites, showing the highest values at S8 and S22 in comparison to

the other relatively steady changes of the sites in the dry season. Whilst a significant fluctuation of Pb contents among the sampling sites ranged from 4.58 to 17.09 mg kg^{-1}, with the mean value of 12.21±2.73 mg kg^{-1} in the wet season (Figure 0.29c). The finding indicated the Pb loads, exploring at S1, S2, S3 was top of among the observed sites, demonstrated also the uncertain changes in space. The Zn contents departing from 35.21 to 45.58 mg kg^{-1} had the mean of 39.48±2.9 mg kg^{-1}, the values of Zn among the observed sites denoted a narrow alteration in dry season, except for the highest value (S14=45.58 mg kg^{-1}). Whereas the Zn loads, altering widely from 21.59 to 61.13 (mg.kg^{-1}), with the mean value of 48.64±9.42 mg kg^{-1} obtained a higher value at S4 and S23 than the others did (Figure 0.29d). Both the seasons figured out spatially the contents of Zn with an unspecific trend of variability from the down to upstream of the course.

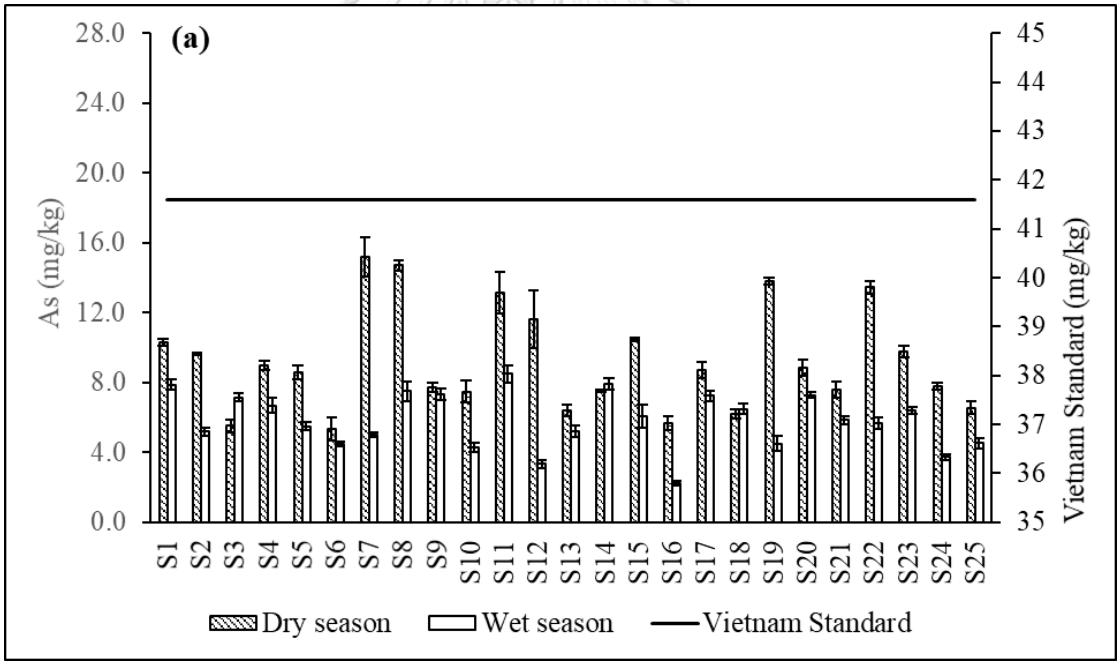

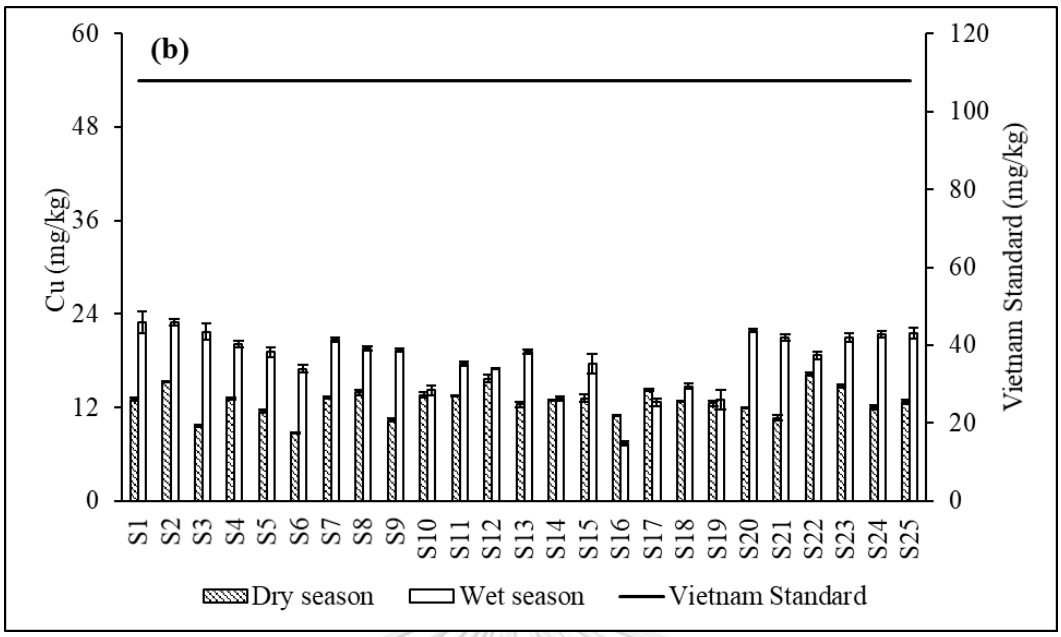
(b)
Cu (mg/kg)
Vietnam Standard (mg/kg)
60
48
36
24
12
0
120
100
80
60
40
20
0
S1 S2 S3 S4 S5 S6 S7 S8 S9 S10 S11 S12 S13 S14 S15 S16 S17 S18 S19 S20 S21 S22 S23 S24 S25
Dry season
Wet season
Vietnam Standard

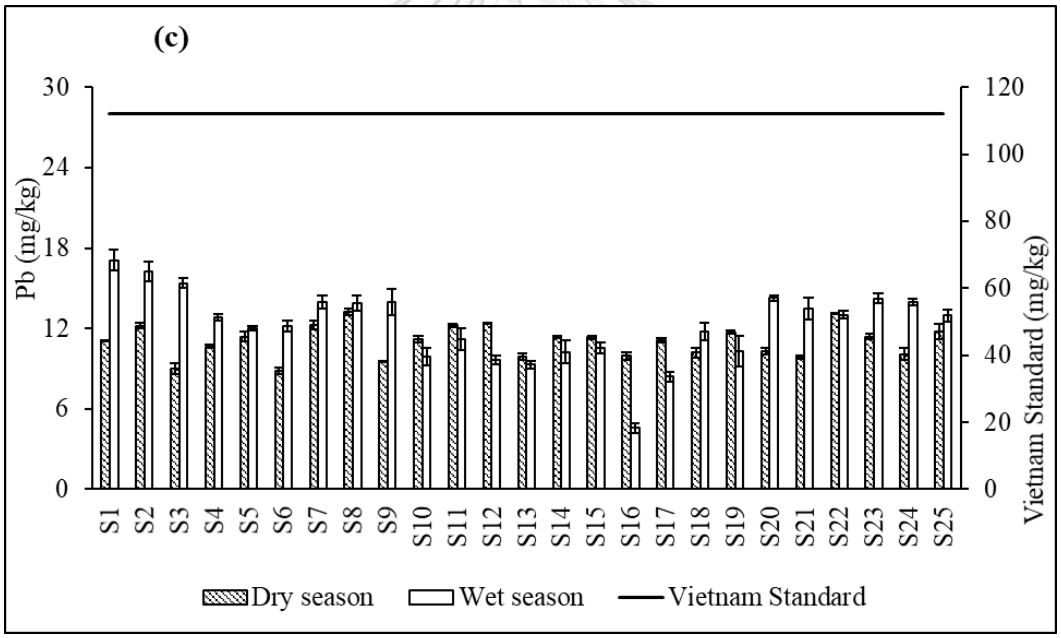
(c)
Pb (mg/kg)
Vietnam Standard (mg/kg)
30
24
18
12
6
0
120
100
80
60
40
20
0
S1 S2 S3 S4 S5 S6 S7 S8 S9 S10 S11 S12 S13 S14 S15 S16 S17 S18 S19 S20 S21 S22 S23 S24 S25
Dry season
Wet season
Vietnam Standard

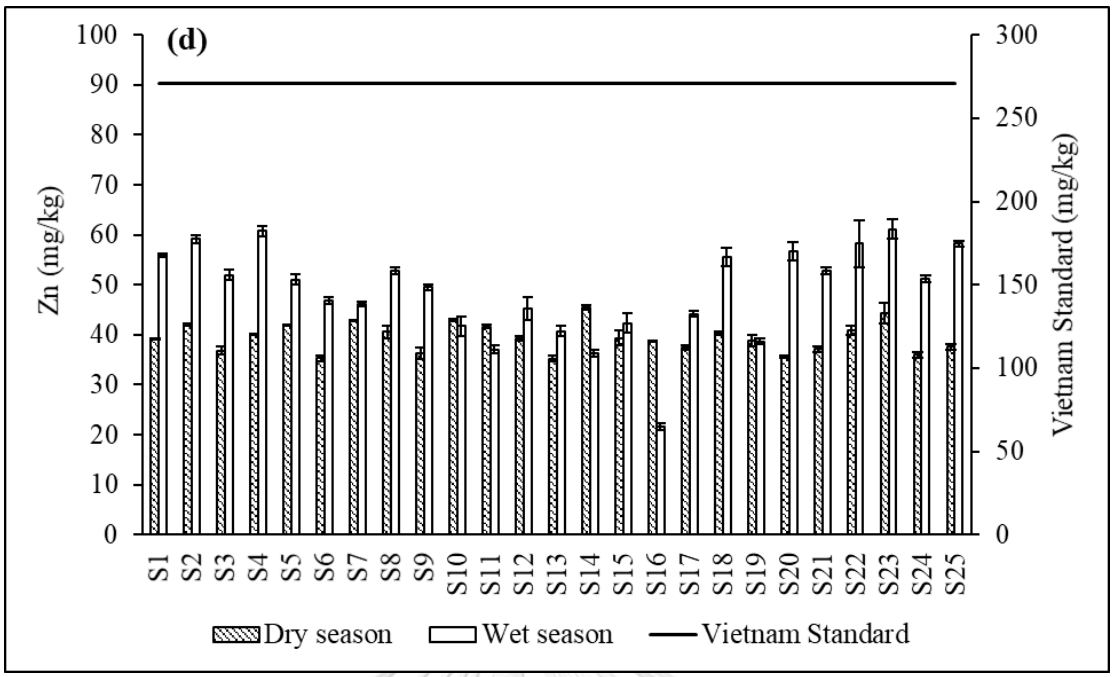

Figure 0.29 The spatial variabilities of heavy metal contents in both seasons: a (As), b (Cu), c (Pb), and d (Zn).

The results elucidated that the seasonal concentrations of heavy metals found in the sediment were much lower than those established standard for sediment quality [192]. The low contents of metal(loids) in the sediments at the studied river could associate with several factors, of which relative lowering of pH and TOC contents, elevated salinity, and intense hydrodynamics would be a core prerequisite causing the minor contents in the bottom sediment. Concerning the pH found seasonally the observed sites with a slight acidic property, which could drive the release of metals into the water column. The previous studies [257, 258] reported that the release of metals in sediments hardly occurred with a pH range of 7.0 to 9.0; however, metal ions would be liberated with pH less than 6.0. This was because the coined ions (H^+) would be involved in the competition with absorbed metal ions in the particles, which drove desorption of the metals [259, 260]. The sinks of organic matter, also portraying a central role in attaching the metal ions with particles, caused immensely accumulation of metal species in the bottom sediments [261, 262]. Nevertheless, the seasonal contents of TOC measured at the various sites denoted the relatively low percentage; therefore, it was associated with reduction of metal speciation concentrations in the sediment. It was obvious that an increase of heavy contents binding to organic species

in the sediment had directly proportional with an elevated content of organic substances. This was due to having a potent affinity for organic matters and high mobility of metals, which were linked with the low concentrations of organic substances [263-265].

High salinity and electrical conductivity measured were considered as the core elements resulting in desorption of metal speciation, the total adsorption concentration of heavy metals would reduce with the increasing salinity and electrical conductivity due to stimulating mobility and competing among heavy metals and other cations [265-267]. In addition, the elevated salinity could promote a vibration of high acidity due to substitution of involved protons on the negatively charged clay colloids surface in the bottom sediments by salt cations. The salts replace reduced acidic metal cations (e.g., Al^{3+} and Fe^{2+}) with later oxidation and hydrolysis inducing acidification, influencing positively the desorption of sediment absorbed-metal species [268, 269]. A close relationship was found in the exchangeable mechanism of metal species between the sediments and water column. The metal speciation released by sedimentary dynamics was absorbed by the organic substances in the water and then settles to the bottom sediments [270-272]. However, the minor total contents of heavy metals or even not detecting at most of the observed sites was illustrated in both seasons; thus, the complex hydrodynamics, especially irregular semi-diurnal regimes at the studied river, was responsible for significant changes in metal contents. The metal species discharging from the sediment were attributed to involving absorbing particles in the water, heading a seaward direction, and accumulated high loads at the estuaries and tidal mudflats. The previous studies [273, 274] discovered that the distribution of metal loads increased progressively from inland towards the estuaries in the sediments because the mixture of polluted sediment bearing-river flow and seawater occurred greatly deposition of the pollutants at the estuaries. The findings showed that As concentrations in the dry season was greater than the ones in the wet season. While the concentrations of heavy metals (e.g., Cu. Zn, and Pb) in the wet seasons were greater than the ones in the dry seasons. Low concentration of As in the wet season could be explained by the effect of pH and presence of phosphate, leading to As release to water environment. The previous study of [275] stated that As release underwent pronounced kinetic effects, which were strongly affected by pH and

phosphate. As release from the sediments may be associated with solid phase dissolution processes under both acid and alkaline pH.

c. Sediment pollution indices

Table 0.18 indicated that the calculated PLI values of metals ranged spatially from 0.34 to 0.57, with the mean of 0.46±0.06 and 0.20 to 0.62, with that of 0.48±0.09 in the dry and wet seasons, accordingly. The results confirmed that the sediment of the studied river was not polluted by the heavy metals due to PLI less than 1 [200]. Higher PLI indicated the central contribution of metals causing the sediment contamination, relating to anthropogenic sources [276, 277]; therefore, the existence of metals in the sediment might be associated with other sources (e.g., natural sources).

Table 0.19 demonstrated that the values of CF for all metals denoted a seasonally low degree of contamination (CF <1). However, CF values of As at the observed sites (e.g., S7, S8, S11, S19, and S22) had a moderate degree of pollution (1≤ CF < 3) with the respective values of 1.17, 1.13, 1.01, 1.06, and 1.03 in the dry season [197]. Generally, the CF for all heavy metals in the dry and wet seasons was the descending order of As > Pb > Zn > Cu and Pb > Zn > As > Cu, correspondingly. Eventually,

Table 0.19 indicated the I-geo values were negative for As, Cu, Pb, and Zn, indicating a noncontaminated status of the sediment and background levels of these metals. The I-geo values in the dry season were raked as Cu < Zn < Pb < As, while those in the wet season were ranked as Cu < As < Zn < Pb.

Table 0.17 Pollution Load Index (PLI) calculated for all metals in each observed sites

Observed sites	Seasons	PLI
S1	Dry	0.48
	Wet	0.63
S2	Dry	0.51
	Wet	0.57
S3	Dry	0.36
	Wet	0.58
S4	Dry	0.46
	Wet	0.55
S5	Dry	0.45
	Wet	0.49
S6	Dry	0.34
	Wet	0.44
S7	Dry	0.56
	Wet	0.49
S8	Dry	0.56
	Wet	0.56
S9	Dry	0.40
	Wet	0.55
S10	Dry	0.46
	Wet	0.39
S11	Dry	0.53
	Wet	0.49
S12	Dry	0.53
	Wet	0.39
S13	Dry	0.40
	Wet	0.43
S14	Dry	0.46
	Wet	0.43
S15	Dry	0.48

Observed sites	Seasons	PLI
S16	Wet	0.45
	Dry	0.38
S17	Wet	0.20
	Dry	0.46
S18	Wet	0.42
	Dry	0.41
S19	Wet	0.49
	Dry	0.52
S20	Wet	0.38
	Dry	0.43
S21	Wet	0.58
	Dry	0.40
S22	Wet	0.53
	Dry	0.57
S23	Wet	0.52
	Dry	0.51
S24	Wet	0.57
	Dry	0.42
S25	Wet	0.48
	Dry	0.43
Min	Wet	0.51
	Dry	0.34
Max	Wet	0.20
	Dry	0.57
Mean ± SD	Wet	0.63
	Dry	**0.46±0.06**
	Wet	**0.48±0.09**

Table 0.18 Contamination factor (CF) calculated for each metal

Observed sites	Seasons	As	Cu	Pb	Zn
S1	Dry	0.79	0.29	0.55	0.41
	Wet	0.61	0.51	0.85	0.59
S2	Dry	0.74	0.34	0.61	0.44
	Wet	0.40	0.51	0.81	0.62
S3	Dry	0.42	0.21	0.45	0.39
	Wet	0.55	0.48	0.77	0.55
S4	Dry	0.69	0.29	0.53	0.42
	Wet	0.51	0.45	0.64	0.64
S5	Dry	0.66	0.26	0.57	0.44
	Wet	0.42	0.42	0.60	0.54
S6	Dry	0.41	0.19	0.44	0.37
	Wet	0.35	0.38	0.61	0.49
S7	Dry	1.17	0.29	0.61	0.45
	Wet	0.38	0.46	0.70	0.49
S8	Dry	1.13	0.31	0.66	0.43
	Wet	0.58	0.43	0.69	0.56
S9	Dry	0.59	0.23	0.48	0.38
	Wet	0.56	0.43	0.70	0.52
S10	Dry	0.58	0.30	0.56	0.45
	Wet	0.33	0.32	0.49	0.44
S11	Dry	1.01	0.30	0.61	0.44
	Wet	0.65	0.39	0.56	0.39
S12	Dry	0.89	0.35	0.62	0.41
	Wet	0.26	0.38	0.48	0.48
S13	Dry	0.49	0.28	0.49	0.37
	Wet	0.40	0.43	0.46	0.43
S14	Dry	0.58	0.29	0.57	0.48
	Wet	0.61	0.29	0.51	0.38
S15	Dry	0.81	0.29	0.57	0.41

Observed sites	Seasons	As	Cu	Pb	Zn
S16	Wet	0.47	0.39	0.53	0.45
	Dry	0.44	0.24	0.50	0.41
S17	Wet	0.17	0.17	0.23	0.23
	Dry	0.67	0.32	0.56	0.39
S18	Wet	0.56	0.28	0.42	0.46
	Dry	0.48	0.28	0.51	0.42
S19	Wet	0.50	0.33	0.59	0.59
	Dry	1.06	0.28	0.59	0.41
S20	Wet	0.35	0.29	0.51	0.41
	Dry	0.68	0.26	0.51	0.38
S21	Wet	0.56	0.49	0.71	0.60
	Dry	0.58	0.24	0.49	0.39
S22	Wet	0.45	0.47	0.67	0.56
	Dry	1.03	0.36	0.65	0.43
S23	Wet	0.44	0.42	0.65	0.61
	Dry	0.75	0.33	0.57	0.47
S24	Wet	0.49	0.47	0.71	0.64
	Dry	0.60	0.27	0.50	0.38
S25	Wet	0.29	0.47	0.70	0.54
	Dry	0.50	0.28	0.59	0.40
Min	Wet	0.35	0.48	0.65	0.61
	Dry	0.41	0.19	0.44	0.37
Max	Wet	0.17	0.17	0.23	0.23
	Dry	1.17	0.36	0.66	0.48
	Wet	0.65	0.51	0.85	0.64
Mean ± SD	**Dry**	**0.71±0.23**	**0.28±0.04**	**0.55±0.06**	**0.42±0.03**
	Wet	**0.45±0.12**	**0.40±0.09**	**0.61±0.14**	**0.51±0.1**

Table 0.19 Geo-accumulation index (Igeo) calculated for each element

Observed sites	Seasons	As	Cu	Pb	Zn
S1	Dry	-0.92	-2.37	-1.44	-1.86
	Wet	-1.31	-1.56	-0.81	-1.35
S2	Dry	-1.02	-2.13	-1.30	-1.76
	Wet	-1.91	-1.56	-0.88	-1.27
S3	Dry	-1.82	-2.81	-1.73	-1.95
	Wet	-1.45	-1.64	-0.96	-1.46
S4	Dry	-1.12	-2.36	-1.50	-1.83
	Wet	-1.55	-1.75	-1.23	-1.23
S5	Dry	-1.18	-2.55	-1.40	-1.76
	Wet	-1.83	-1.82	-1.32	-1.48
S6	Dry	-1.87	-2.95	-1.76	-2.01
	Wet	-2.12	-1.99	-1.30	-1.60
S7	Dry	-0.36	-2.35	-1.29	-1.73
	Wet	-1.97	-1.71	-1.10	-1.63
S8	Dry	-0.41	-2.28	-1.18	-1.81
	Wet	-1.38	-1.79	-1.11	-1.43
S9	Dry	-1.33	-2.71	-1.65	-1.97
	Wet	-1.41	-1.80	-1.10	-1.52
S10	Dry	-1.38	-2.31	-1.42	-1.73
	Wet	-2.18	-2.25	-1.60	-1.77
S11	Dry	-0.57	-2.32	-1.30	-1.77
	Wet	-1.20	-1.94	-1.42	-1.94
S12	Dry	-0.75	-2.10	-1.28	-1.86
	Wet	-2.54	-1.99	-1.64	-1.65
S13	Dry	-1.61	-2.45	-1.60	-2.02
	Wet	-1.90	-1.81	-1.69	-1.81
S14	Dry	-1.37	-2.38	-1.40	-1.64
	Wet	-1.30	-2.36	-1.55	-1.97
S15	Dry	-0.90	-2.36	-1.40	-1.86

Observed sites	Seasons	As	Cu	Pb	Zn
S16	Wet	-1.69	-1.94	-1.51	-1.75
	Dry	-1.79	-2.62	-1.59	-1.88
S17	Wet	-3.13	-3.18	-2.71	-2.72
	Dry	-1.16	-2.24	-1.43	-1.93
S18	Wet	-1.43	-2.42	-1.84	-1.69
	Dry	-1.66	-2.40	-1.56	-1.82
S19	Wet	-1.59	-2.20	-1.35	-1.36
	Dry	-0.50	-2.43	-1.36	-1.87
S20	Wet	-2.12	-2.37	-1.54	-1.88
	Dry	-1.14	-2.50	-1.55	-2.00
S21	Wet	-1.42	-1.63	-1.07	-1.33
	Dry	-1.36	-2.66	-1.60	-1.94
S22	Wet	-1.74	-1.69	-1.15	-1.43
	Dry	-0.54	-2.05	-1.20	-1.80
S23	Wet	-1.78	-1.85	-1.20	-1.29
	Dry	-1.00	-2.19	-1.40	-1.68
S24	Wet	-1.60	-1.69	-1.07	-1.22
	Dry	-1.32	-2.49	-1.57	-1.98
S25	Wet	-2.39	-1.66	-1.11	-1.48
	Dry	-1.58	-2.40	-1.35	-1.92
Min	Wet	-2.10	-1.65	-1.21	-1.29
	Dry	-1.87	-2.95	-1.76	-2.02
Max	Wet	-3.13	-3.18	-2.71	-2.72
	Dry	-0.36	-2.05	-1.18	-1.64
Mean ± SD	Wet	-1.20	-1.56	-0.81	-1.22
	Dry	**-1.15±0.45**	**-2.42±0.21**	**-1.45±0.16**	**-1.86±0.11**
	Wet	**-1.8±0.45**	**-1.93±0.37**	**-1.34±0.39**	**-1.58±0.33**

4.2 Tidal and seasonal variabilities of water quality

4.2.1 Tidal movement

Surface water along the Ganh Hao River is strongly affected by irregular semi-diurnal tides from the East and West seas. These cause the water level to change and influence the spatial variabilities of water quality due to fluctuations in the dilution of pollutants. Figure 0.30 showed that high EC levels were observed during the ebbing tide (neap tide) after seawater intruded, whereas low EC values were observed during incoming tide (spring tide) before saltwater intruded. Similar results were found for temperature, pH, TDS, salinity, DO, and COD, but not for the TSS concentration, which was higher during the spring tide than during the neap tide.

A statistically significant difference was found between the neap and spring tides with respect to temperature, TDS, DO, COD, and salinity ($P < 0.05$), while nonsignificant differences were found for pH, EC, and TSS ($P > 0.05$). Hence, the changes in temperature, TDS, DO, COD, and salinity could be explained by the variation in the tidal regime, while the changes in pH, EC, and TSS values were probably associated with other factors. The impacts of ebbing and spring tides also resulted in various changes in the N and P concentrations; $N–NO_2^-$ and $N–NH_4^+$ concentrations were statistically higher during the ebb tide than during the spring tide ($P < 0.05$). Higher $N–NO_3^-$, TN, $P–PO_4^{3-}$, and TP concentrations occurred during the spring tide than during the neap tide, although only the TN and $P–PO_4^{3-}$ concentrations were statistically higher ($P < 0.05$). The previous study of [278] also reported that the effect of tides caused significant alterations in nutrient patterns. The authors found that riverine inputs of pollutants during the ebb tide resulted in high nutrient concentrations, while lower nutrient concentrations during the spring tide were associated with river water–seawater mixing. Our findings are also consistent with those of other studies that observed differences in pollutant concentrations between high and low tides [279, 280].

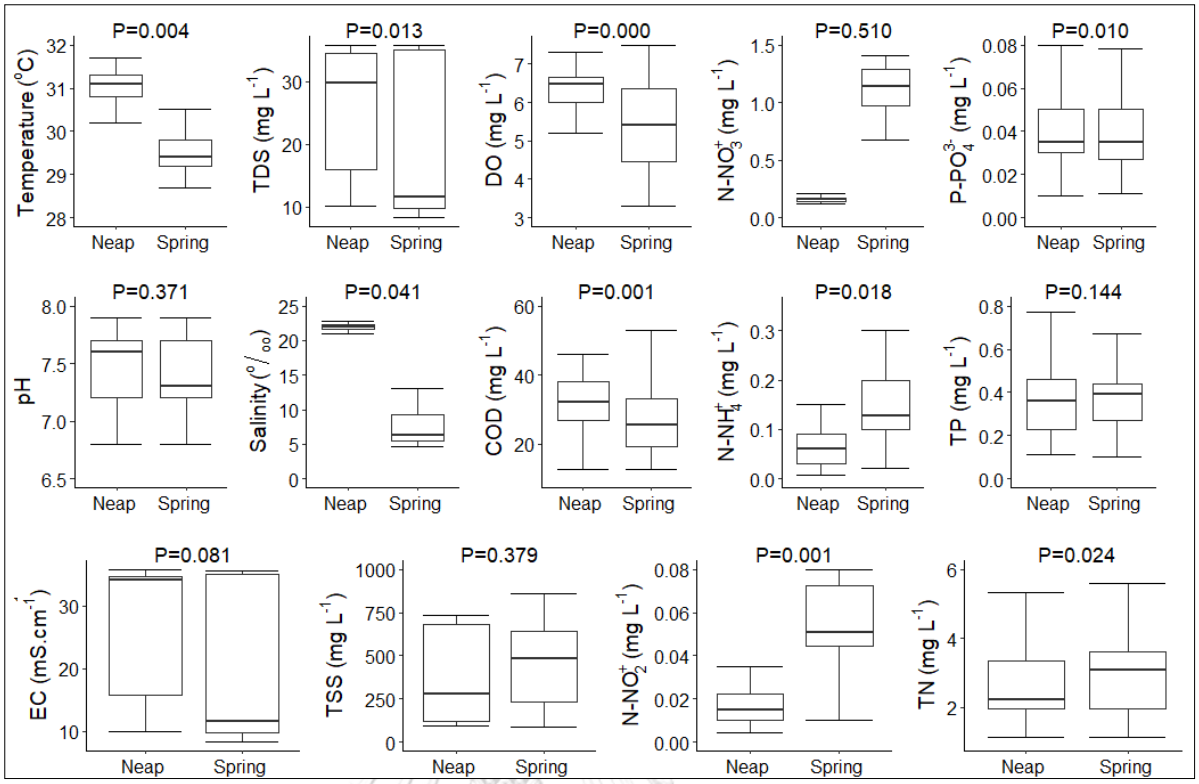

Figure 0.30 Differences in water quality parameters between the neap and spring tide

4.2.2 Seasonal variabilities

Figure 0.31 indicated the seasonal variabilities of water quality for representative elements (e.g., physicochemical and biological parameters). The higher physical parameters (e.g., temperature, pH, EC, TDS, salinity, and TSS) being measured in the dry season than the wet one exhibited a statistically significant difference between two seasons ($P<0.05$), except for TSS ($P>0.05$). The study of [275] revealed that solar radiation governed primarily the temperature in the estuaries also received greatly the heat by supplying from the tidal flow of the sea. Moreover, the highest solar radiation was usually found for the dry season, comparing to the wet one in the VMD [281]. Consequently, it could explain the increase in temperature in the dry season was greater than the wet one. A slightly lowering in pH level detected in the wet season could be the consequence of higher run-off rates associating with acid soils in the early wet season and the decomposition of nutrient residues and organic substances discharged by aquaculture practices. EC, TDS, and salinity showed similar patterns that substantially high levels in the dry season were discovered in comparison with

the wet one. Elevated TDS extent was due to the effects of dissolved salts and agricultural run-off [219]; therefore, impacts of seawater and aquaculture practices coupling with less dilution coined by the rainfall would lead to a high level of TDS in the dry season in comparison with the rainy one. Among TDS, EC, salinity presented a strong correlation indicating the level of salinity; thus, one of them expanded would result in an extension of other ones [282, 283]. This could interpret a higher level of EC and salinity in the dry season than the rainy one would involve further saline intrusion into the inland in the dry season occurred usually in the VMD [284, 285].

TSS displayed a greater median of content in the dry season than the wet one. This was because of the effect of low water level in the dry season [286] coupled with consistently strong flow velocities, generating a continuous disturbance and erosion of soils and sediments. In fact, the river flow data was measured in different seasons and the average water discharge in the rainy season (571.84 m^3/s) is lower than that in the dry season (842.09 m^3/s). Overall, TSS ($P>0.05$) indicated the variability of TSS contents was regardless of the seasons. DO level, denoting a minor oscillation in the median of content, disclosed a statistically insignificant difference between the seasons ($P>0.05$), whereas a greater median of COD content in the dry season than the rainy one differed from statistical significance ($P<0.05$). The elevated extent of COD in the dry season may ascribe to the decrease of the water column, coupling with accumulated organic and inorganic matters in ponds released by aquaculture activities along the course. A similar pattern was observed by the study of [287] revealed the effects of dilution in the wet season combining with lower river flow in dry one would visualize high loadings of COD in the dry season. Whilst a strong dilution due to the effluent of tidal flow and rainfall events would lead to less concentration of COD in the wet season. Inversely, the previous studies of [41, 287] logged the highest concentrations for COD during the dry season.

All the nitrogenous compounds (e.g., $N\text{-}NO_2^-$, $N\text{-}NO_3^-$, $N\text{-}NH_4^+$, and TN) showed much more concentrations in the wet season than the dry one, with a significant difference between the seasons ($P<0.05$). Application of various chemicals and residual feeds in the ponds discharged by overland runoff from aquaculture areas along the river reach was responsible for elevated content of nutrients found in the

wet season. Nonetheless, the finding obtained the higher content of $P\text{-}PO_4^{3-}$ and TP in the dry season than the rainy one testified slightly an oscillation of concentrations in the dry and rainy seasons. In the aquatic environment, TSS affected greatly the phosphorus species through adsorption [288]; however, the elevated $P\text{-}PO_4^{3-}$, TP, and TSS contents were visible proportionally during the dry season. The statistical result showed respectively an insignificant difference of $P\text{-}PO_4^{3-}$ and TP between the seasons ($P>0.05$), indicating that temporal variability of them was not dependent on the seasons.

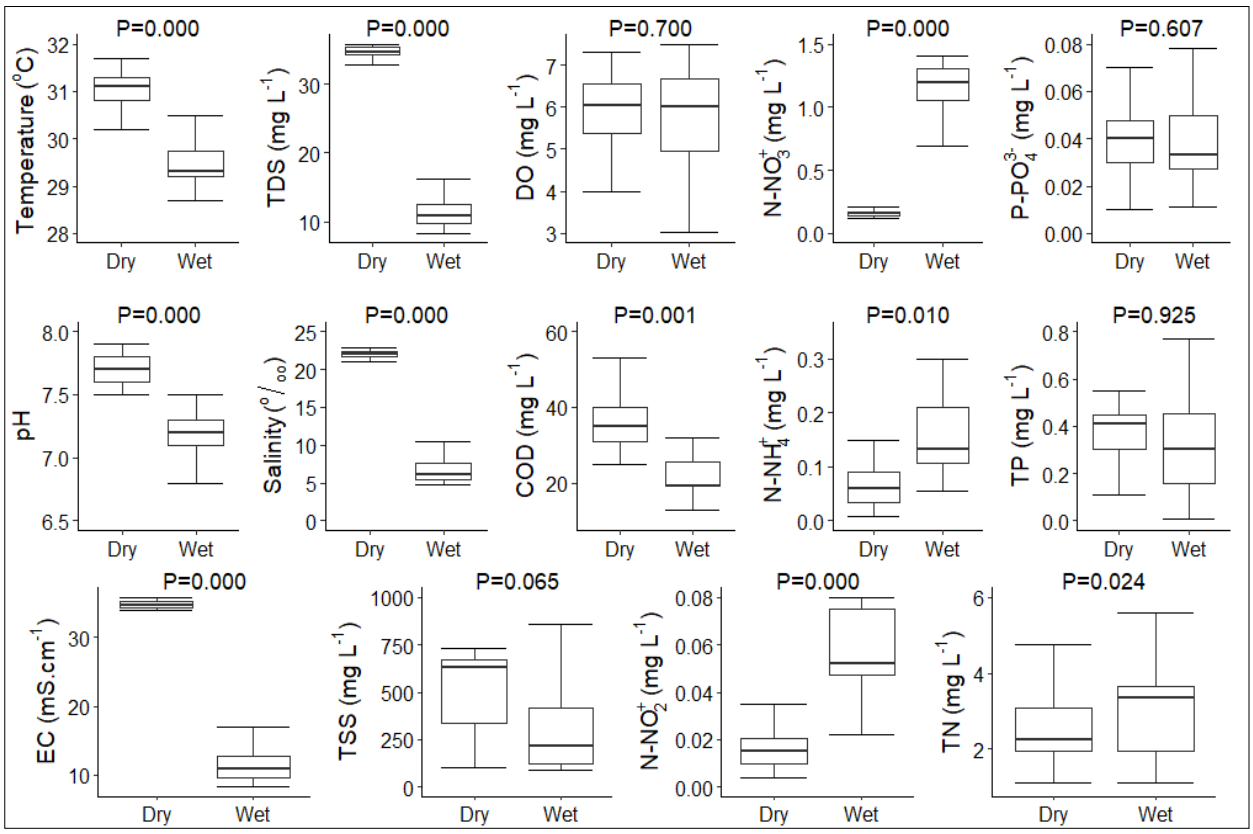

Figure 0.31 Variabilities of the water quality parameters between the dry and wet seasons

4.2.3 Identification of pollutant sources

Figure 0.32 shows that three components with eigenvalues of > 1 were extracted based on the PCA, which accounted for approximately 79.84% of the total variance of the water quality deterioration with respect to the selected parameters.

The first component explained 53.64% of the total variance and had positive high loadings for temperature, pH, EC, TDS, salinity, and COD, but negative loadings for $N–NO_2^-$ and $N–NO_3^-$. This component was explained as pollution related to physicochemical properties and organic matter. Elevated loading for EC, TDS, salinity, and COD were primarily influenced by the tidal cycle and untreated wastewater discharges from shrimp culture activities. Both TDS and EC are indicators of salinity and seawater intrusion in coastal areas, the high existence of them also regarded to the high temperature due to promoting dissolved ions [69, 289] . In addition, TDS includes inorganic salts and minor quantities of organic substances in water; thus, aquaculture practices could not be ignored as a contributor to the TDS content in the study area [224, 290]. High pH levels could be due to seawater intrusion moving inland between the dry and wet seasons. The previous studies of [291, 292] found that generally low pH values in coastal regions were due to the influence of chemicals applied during farm operations as well as the formation of organic acids through the decomposition of organic compounds. Hence, the high pH levels in the present study may have originated from high salinity, while untreated wastewater discharges from shrimp farms could explain the elevated COD content. Pollution sources derived from culture systems include solid waste comprising uneaten feed and fecal droppings, and dissolved waste associated with food metabolism or decomposition products. Solid waste material can contribute to an increased TSS content and increased N species [293]. The previous study of [294] reported that the discharge of accumulated solid waste associated with bacterial activity was the main cause of an increased COD content of the water column. Negative high loadings for $N–NO_2^-$ and $N–NO_3^-$ in both seasons could be related to the high salinity levels. A low content and narrow variation of N compounds in coastal regions were due to elevated salinity levels [231].

The second component expounding 18.43% of the total variance included positively high loadings of TSS and TP and moderate loading of TN. The suspended solid and nutrient sources related-deterioration was considered for this component. The elevated level of TSS is likely related to culture systems and tidal currents. The study of [295] reported that a large number of solid wastes generated by aquaculture activities augmented loadings of total suspended and dissolved solids. Besides, strong flow

currents on the coast would disturb the settled particles, leading to an increase of TSS [296]. The existence of TP and TN was involved greatly with coined residues from aquaculture practices releasing into the surface water. Nitrogen and phosphorus products are not only representative of nutrient pollution but also the major components of protein found in a variety of aquatic organism foods. Therefore, the elevated protein feeds consist of high amounts of nitrogen and phosphorus [297]. It has been estimated that approximately 20%–30% of the nitrogen and phosphorus added to feeds is released to the nearby environment [298].

The third component represented pollution corresponding to DO consumption. This component accounted for 7.77% of the total variance, and consisted of a positive loading for DO and small negative loading for $P–PO_4^{3-}$. Low DO concentration in receiving water bodies can be associated with effluent discharges with a high content of organic matter, which consumes a significant amount of oxygen through decomposition processes [239]. Moreover, the decreased level of DO was most likely due to relatively remaining high temperature between the seasons [299]. The small negative loading for $P–PO_4^{3-}$ suggests a slight effect of phosphorus on the surface water of the river because of its prompt absorption by aquatic plants or suspended substances [300].

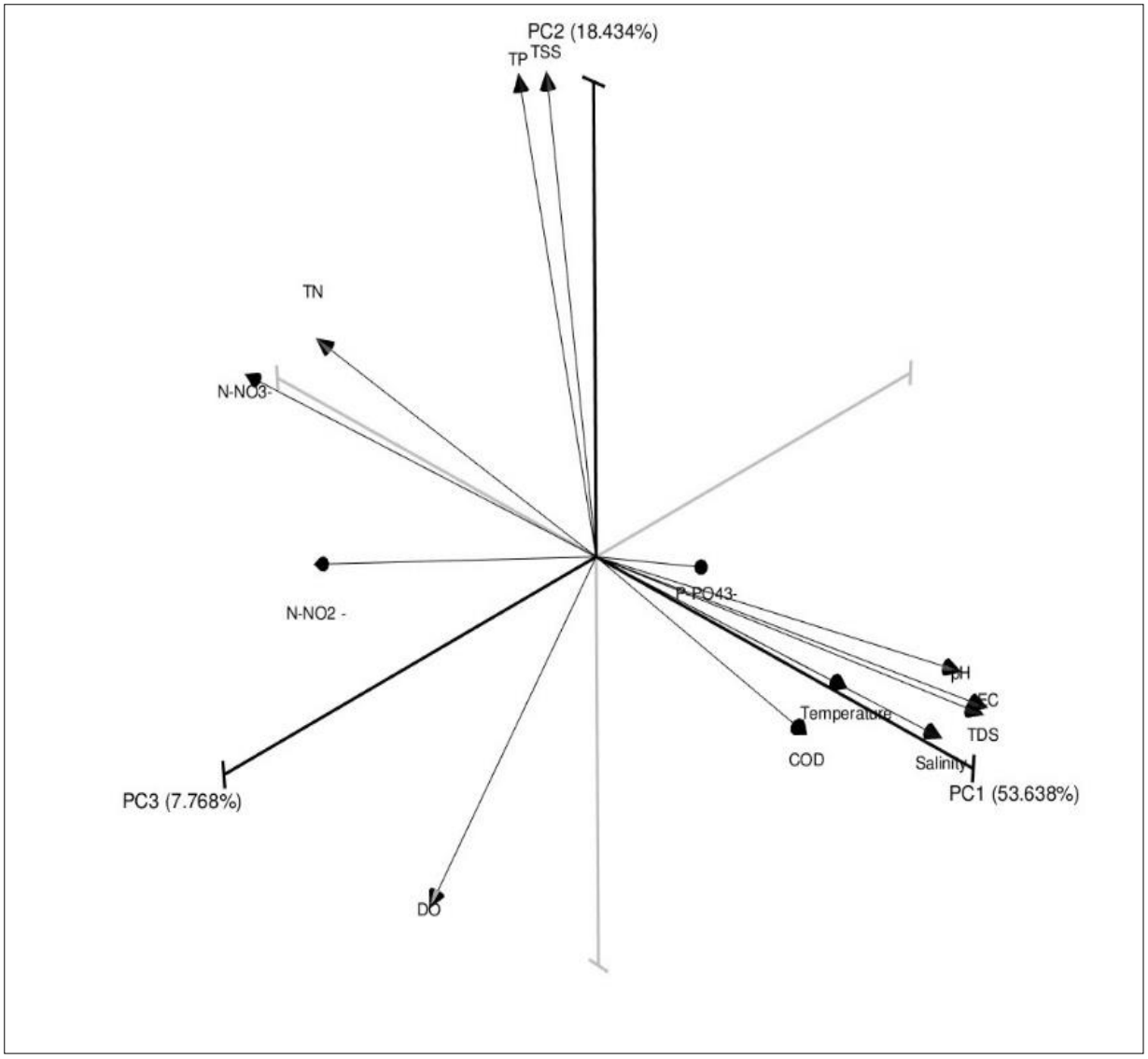

Figure 0.32 Loadings of selected water quality parameters in three principal components with eigenvalues of > 1. The dataset comprises a reduced number of parameters to meet the criteria of the analysis.

4.3 Water quality map

The land use for extensive and improved extensive shrimp cultivation systems was found to be mostly connected to the temporal change in water quality. Based on this relationship, logistic regression models were developed to specify the variables (selected quality parameters) exhibiting a temporally high rate of classification (percentage correct) with land use. The regression models of the water quality patterns were utilized to generate water quality maps with a high probability of

classification. The maps were based on the seasonal mean concentrations of pollutants, as determined from the water samples for both seasons.

Figure 0.33 indicated that the water quality parameters were associated with the land use type mainly that of extensive and improved extensive shrimp culture systems along the river. The elevated TP concentrations were visualized mainly at the middle and lower parts of the river in the dry season while the highest TP concentrations were visible at the upper and lower parts of the river in the wet season. $N–NO_2^-$ concentrations were high in areas far away from the upstream parts of the river in the wet season but they were found high concentrations at the upper and lower areas of river reach in the dry season. Lower TP concentrations during the dry season compared with the wet season were associated with elevated TSS contents because of the potential absorption of available P to suspended solids. The presence of $N–NO_2^-$ related to land use in both seasons could be explained by the low DO concentration of surface water due to the input of nutrients and organic pollutants from shrimp culture activities. As an intermediate product in the N cycle, $N–NO_2^-$ was found at relatively low concentrations, and the available form of $N–NO_2^-$ was involved in the influence of DO on the nitrification process in the water column [301, 302].

The EC values differed between the two seasons, and reduced gradually from the upstream areas to the downstream parts of the river in the wet season compared with the dry season; however, the spatial differences in the EC values were relatively small over the entire area. The higher EC values could be explained by the direct impact of aquaculture practices along with the tidal cycle of the East Sea [303]. In addition, pH was also found to relate to land use, and could be explained by the impacts of effluent discharges from shrimp farms and runoff from (acidic) soils in the wet season. The previous study of [304] found that higher pollutant concentrations were discharged by intensive shrimp culture in comparison to extensive and improved extensive shrimp culture practices in interlaced shrimp farms. However, our logistic model analysis suggested that extensive and improved extensive shrimp farms were very relevant to the reduced surface water quality of the river. This was because a larger area of land is used for extensive and improved extensive shrimp culture systems in comparison to that used for intensive and advanced intensive shrimp farms. This coupled with the

fertilizers and chemicals used for preparing the ponds and supplemental feeds during stocking stages were specified as the main contributors to the water quality deterioration [305, 306]. All the maps showed a relatively low diffusion of pollutants among the investigated sites, partly because the sampling was carried out near the peak of the tide, leading to a reduced transport of contaminants.

Overall, the findings of this study are helpful for policymakers to identify pollution hotspots and develop strategies for water resource management. Additionally, the water quality maps are useful for environmental practitioners because they are simpler to understand than data tables and statistical model analyses.

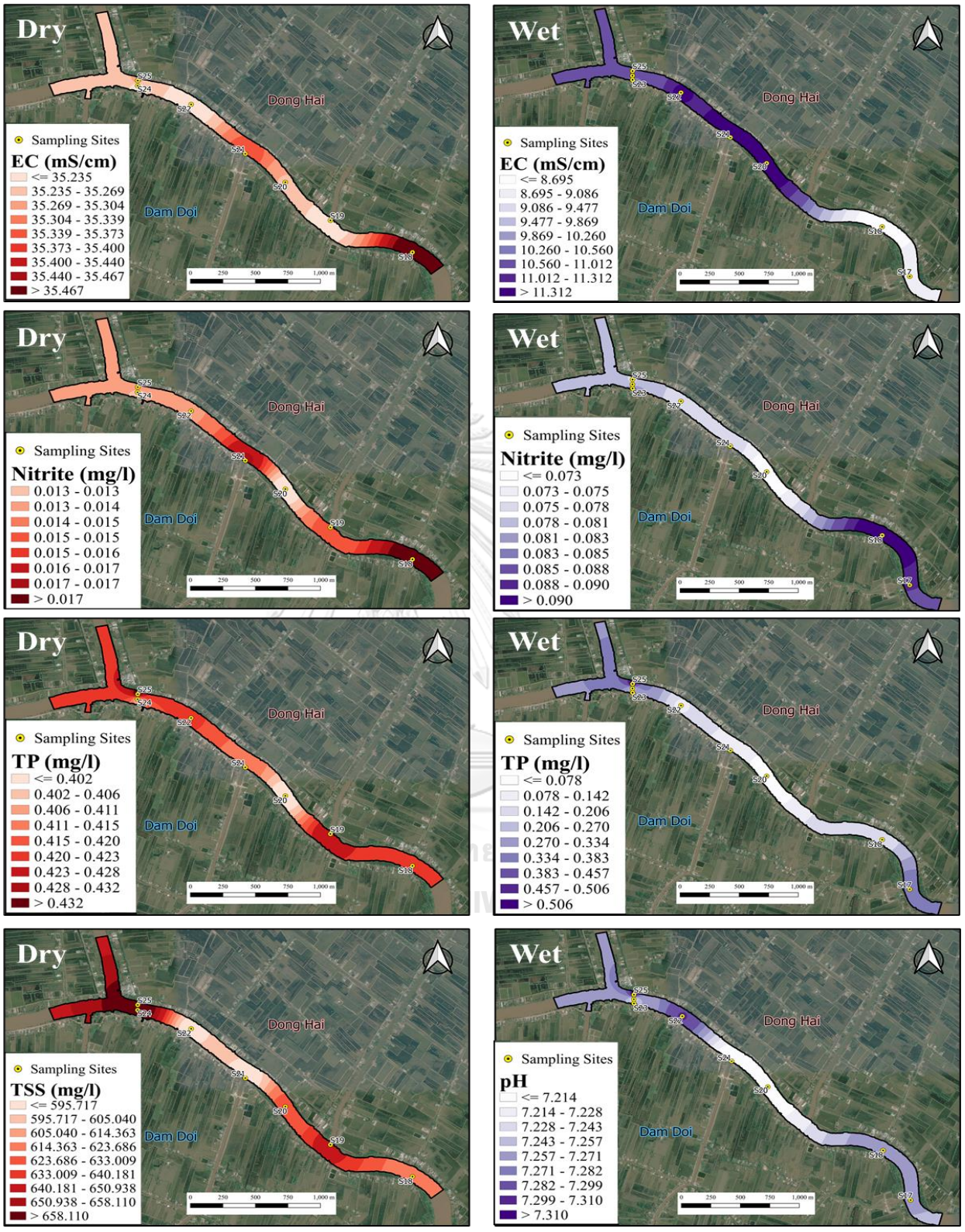

Figure 0.33 Spatial distribution of water quality parameters in the dry (Orange) and wet (Purple) seasons

CHAPTER 5
RESULTS AND DISSCUSTION
CHANGES IN HYDRAULIC CHARACTERISTICS AND SURFACE WATER QUALITY FOR DIFFERNENT FLOW REGIMES

5.1.1 Hydrodynamic model performance

The 2D model was calibrated with the most suitable Manning roughness coefficient (n=0.022 $m^{-1/3}s$) based on a range of values (n=0.02-0.05 $m^{-1/3}s$) applying for natural rivers, coastal and riverine areas in the plain [307]. The result indicated that the simulated water levels agreed with the measured ones in terms of phase and amplitude (Fig 5.1). The tidal phase was quite well re-produced and the tidal peak tended to decrease gradually at the high tidal period. Even though water levels were not monitored from 9 p.m. (5/9/2019) to 5 a.m (6/9/2019) due to bad weather conditions during the wet season, there was a high level of agreement between measured and simulated water levels at the tidal peaks. However, the observed water levels varied and were lower than modeled ones, which showed clearly at 1 pm to 4 pm (5/9/2019), a similar trend was explored on 6/9/2019. Overall, the calibrated model demonstrated a good agreement between simulated and measured water levels. The *n* value used for the model calibration was within the selected range of values confirmed by the previous studies in the coastal areas, VMD [44, 308]. In addition, the validated model with an RMSE and R^2 value was 0.22 and 0.98, respectively. Thus, the calibrated and validated model showed high reliability and accuracy [309].

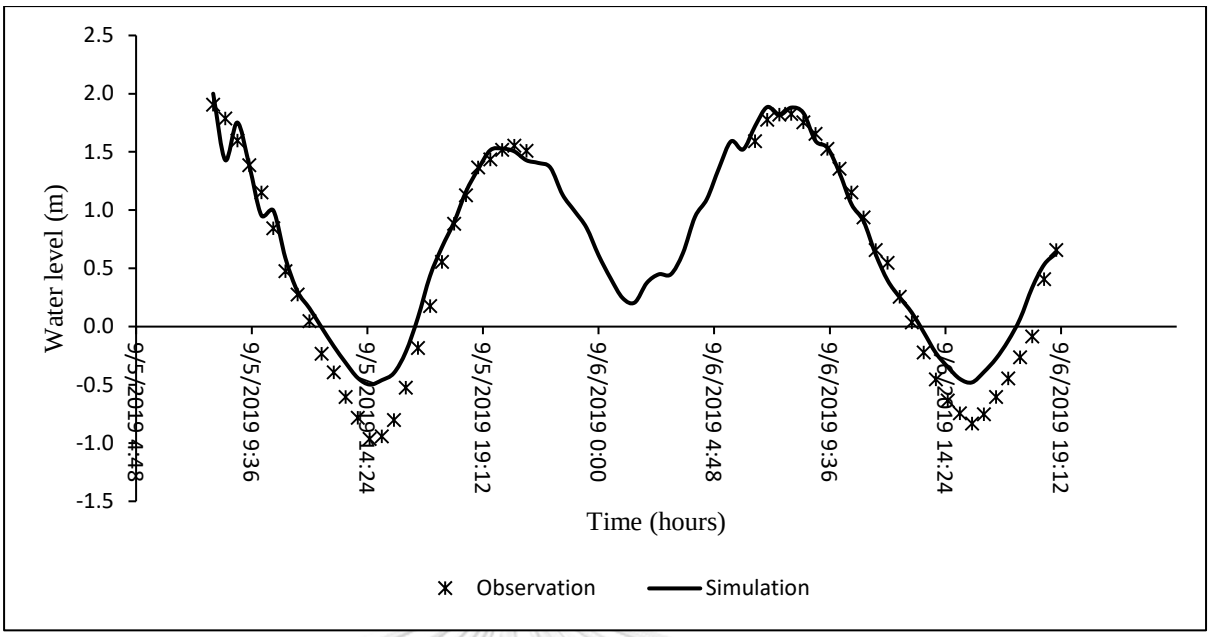

Figure 0.34 Modeled and measured water level at the observation site (WL2)

The 3D model was developed using the defined roughness coefficient as well as user-dependent parameters in the 2D model. The model was calibrated with the most suitable horizontal eddy viscosity (HEV=2 $m^2.s^{-1}$) based on a range of values (0-10 $m^2.s^{-1}$) [208]. Figure 5.2 demonstrated that the flow velocities were distributed unevenly at the cross-section A where it was found high velocities on the right bank (Figure 5.2a and 5.2b marked by a black circle) near the meander bend entrance of the river reach. Changes in geomorphology along the meander bends could explain the distribution of increased flow velocities. The flow pattern entering the bend was dependent on the river's morphology and differed from the areas. Because of the point bar, the high velocity was near the convex bank at the bend entrance, gradually going towards the concave bank (Kasvi et al., 2017)). In addition, the simulated and measured velocities showed a similar pattern (Figure 5.2a and 5.2b); nevertheless, the depth-averaged velocities simulated were lower than ADCP-based velocities. The previous study of [310] stated that depth-averaged velocities differed by 5-14 percent from ADCP-based data, demonstrating the 3D hydrodynamic model's ability to simulate vertical flows. The measured near-surface velocities, however, were different and higher than the simulated velocities, which could be due to tidal flow disturbance. As a result, high velocities were detected at dark red depth cells (Fg.34b), resulting in higher ADCP-based velocities than simulated measurements. (Mueller [311] et al.,

2007) confirmed that the turbulent fluctuations could bias measured velocities near the ADCP. Aside from the fact that the model predicted lower velocities than the ADCP data, the differences between simulated and measured velocity magnitudes were mostly random [310]. The contingent differences from the field-based flow may suggest numerous causes relating to spatial variation of flow velocities and measuring uncertainty (e.g., Doppler noise, flow heterogeneity among measurement beams) [312].

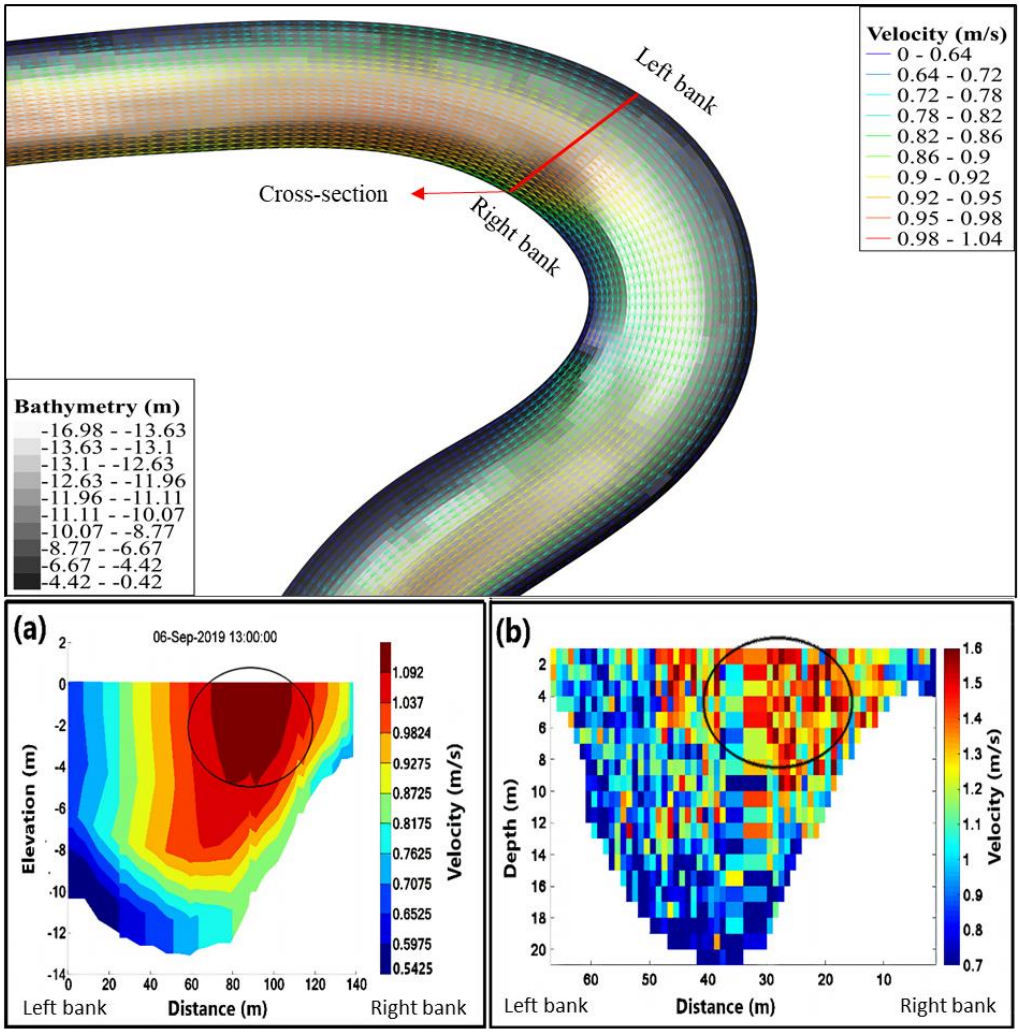

Figure 0.35 Modeled velocity (a) and ADCP-based velocity measurement (b) at the cross-section (A). Note that the black circle was marked in the figure where the highest velocities were measured at the neap tide.

Figure 5.3 demonstrated that the results of different HEV values explained in model calibration. Changes in velocity distributions at diverse layers would be associated

with various values of HEVs (Figure. 5.3 a, b, c, and d). Variations in velocity amplitudes were induced by a rise in HEV values greater than 2 $m^{2-}.s^{-1}$, presenting in typically straight lines with HEV values of 4 and 5 $m^{2-}.s^{-1}$ at the third and bottom layer (Figure. 5.3 c, d). As a result, an amount of velocity error could increase in model calibration because the 3D calibration approach was more sensitive to small changes in HEV [313]. Therefore, in comparison to various HEV values at different layers, the HEV=2 $m^2.s^{-1}$ revealed the most suitable velocity distributions.

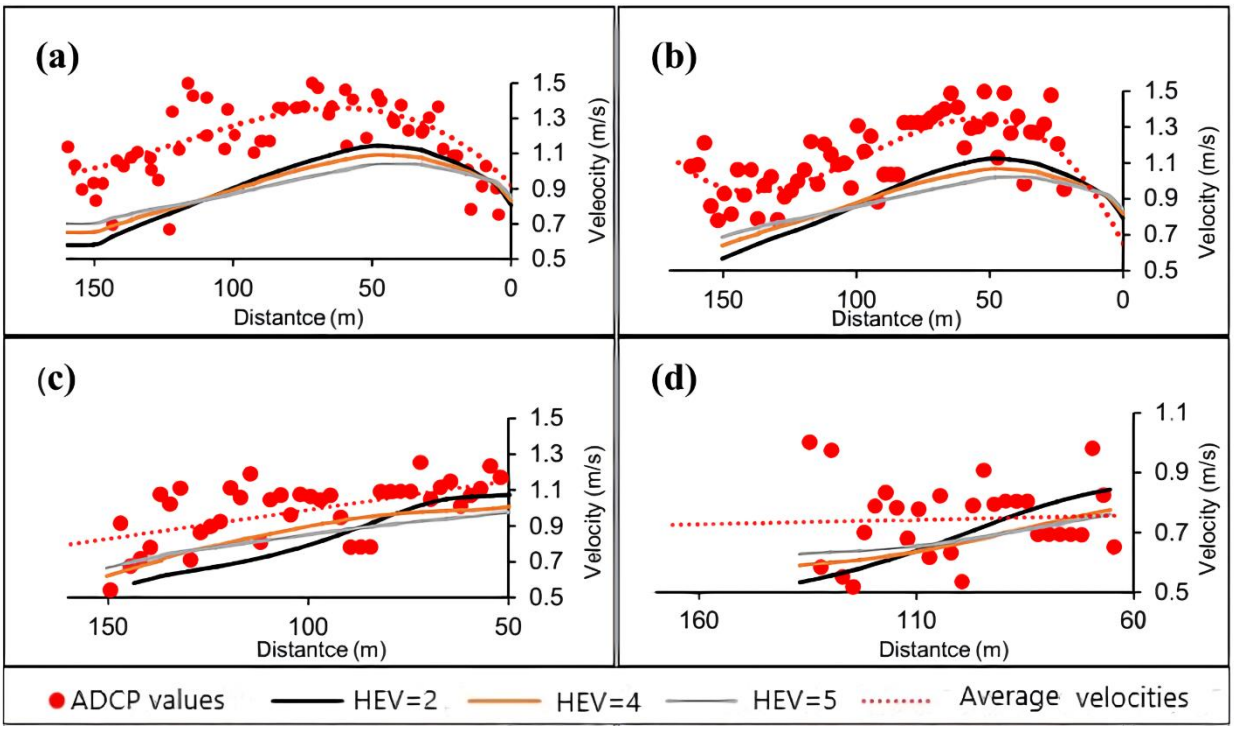

Figure 0.36 (Color) velocity error distributions for analyzing horizontal eddy viscosities (HEVs) at various layers: (a), (b), (c), and (d) shows the velocity's distributions at the surface, second, third, and bottom layers, respectively

Table 5.1 further revealed that the model accuracy was determined by the model mean errors, which demonstrated a good degree of conformity in terms of MAE with HEV values of 2 $m^2.s^{-1}$ at various layers. The overarching changes in HEV values caused insignificant variability of MAE at the layers (e.g., 1, 2, and 4); however, the MAE value tended to rise gradually with the increase of HEV values greater than 2 $m^2.s^{-1}$ in the third layer. The study of [314] stated that lower MAE values approaching zero showed a good agreement between the measured and simulated values. As a result,

the model accuracy for the HEV value of 2 $m^2.s^{-1}$, which had the smallest amount of velocity error, was confirmed consistently. However, a higher value of MAE was found in layer 3 compared to other layers, this could be due to ADCP's limitations caused by the effects of temperature, salinity, and high suspended sediment loads. Due to the effects of the suspended sediments, backscattered acoustic energy and bottom tracking were reduced, resulting in inaccurate water depth and invalid vessel velocity measurements. In addition, the measurement of the vertical velocity patterns and the depths was related to changes in sound speed, depending greatly on the temperature and salinity for specifying the speed of sound for vessel-mounted ADCP [315].

Table 0.20 MAE (Mean Absolute Error) calculated for different horizontal eddy viscosities (HEVs) at the various layers

Simulations	Layers	MAE
HEV=2	1	0.09
	2	0.16
	3	**0.25**
	4	0.13
HEV=4	1	0.07
	2	0.19
	3	**0.31**
	4	0.07
HEV=5	1	0.04
	2	0.22
	3	**0.33**
	4	0.06
HEV=6	1	0.04
	2	0.22
	3	**0.34**
	4	0.05

5.1.2 Changes in hydraulic characteristics

Figure 5.4 indicated the distribution of velocity magnitudes, directions, and the geomorphological changes in the area of interest (AOI), with high velocities at the bend entrance, concave, and inflection bank during the neap tide (Figure 5.4a). This could be due to high flow powers and low water levels preventing the flow from straightening its way across the point bar, resulting in the outward flow. Other processes were influenced by the outward velocity over the top of the point bar. The net cross-stream discharge contributed to the maximum average velocity passing the outer bank quickly [316]. High velocities caused by the outward flow at the outer bank were enforced a downward flow along the bank that extended as an inward flow and an upward flow at the convex bank [317]. This mechanism was referred to as secondary circulation. Moreover, the geomorphological alterations influenced the distribution of flow velocities at various locations. The velocity exhibited the same oscillation phase at different times, as shown in Figure. 5.5 a and c; however, the higher magnitude and distribution were focused on the higher inner bank than on the outer bank. In contrast to the inner bank, the velocity distribution was towards the outer bank, resulting in increased velocity (Figure 5.5b). In general, when the degree of reverbed rose, the current velocity distribution at cross-sections 1, 2, and 3 increased correspondingly. The study of [317] discovered a negative association between topographical change and stream power and velocity, implying that more erosion had occurred in those areas. Furthermore, velocities were highest at mid tide (12 p.m.) when compared to velocity at high tide (9 a.m.) and low tide (3 p.m.) (Figure 5.5). The current velocities at low and high tide were lower than flow velocities throughout the intertidal period, and were close to zero during the unchanging tide [318]. Changes in hydrodynamic characteristics, on the other hand, resulted in spatial geomorphological alterations of the river reach as a result of deposition or erosion, which arose closer to the outer bank than the inner bank (Figure 5.4). This could indicate that the meander migration drove the outer bank erosion, that the inner and outer bank processes were in balance, and that the outer bank was eroded while the point bar developed laterally [319].

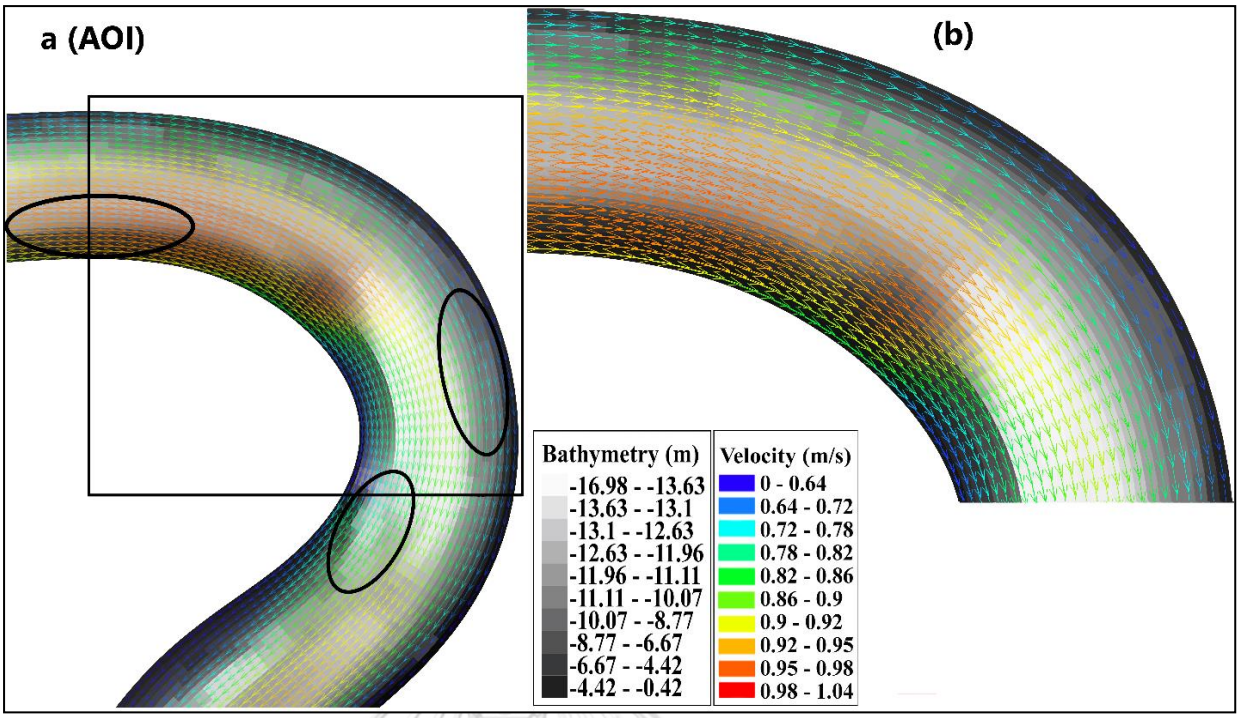

Figure 0.37 (a) the overall spatial distribution of high horizontal velocity (oval boxes), and the bed level changes at an area of interest (AOI); (b) the interesting location (black box) where it shows the measured velocity magnitude at the concave bank (left) and inflection bank (right), and the geomorphological changes at the neap tide on 6 September 2019

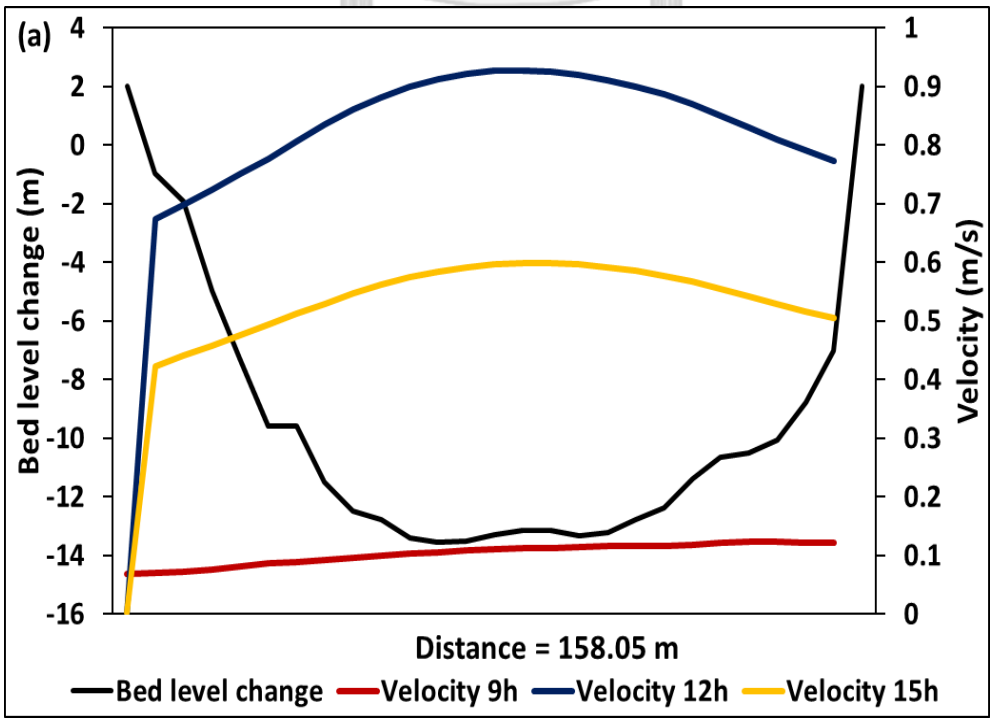

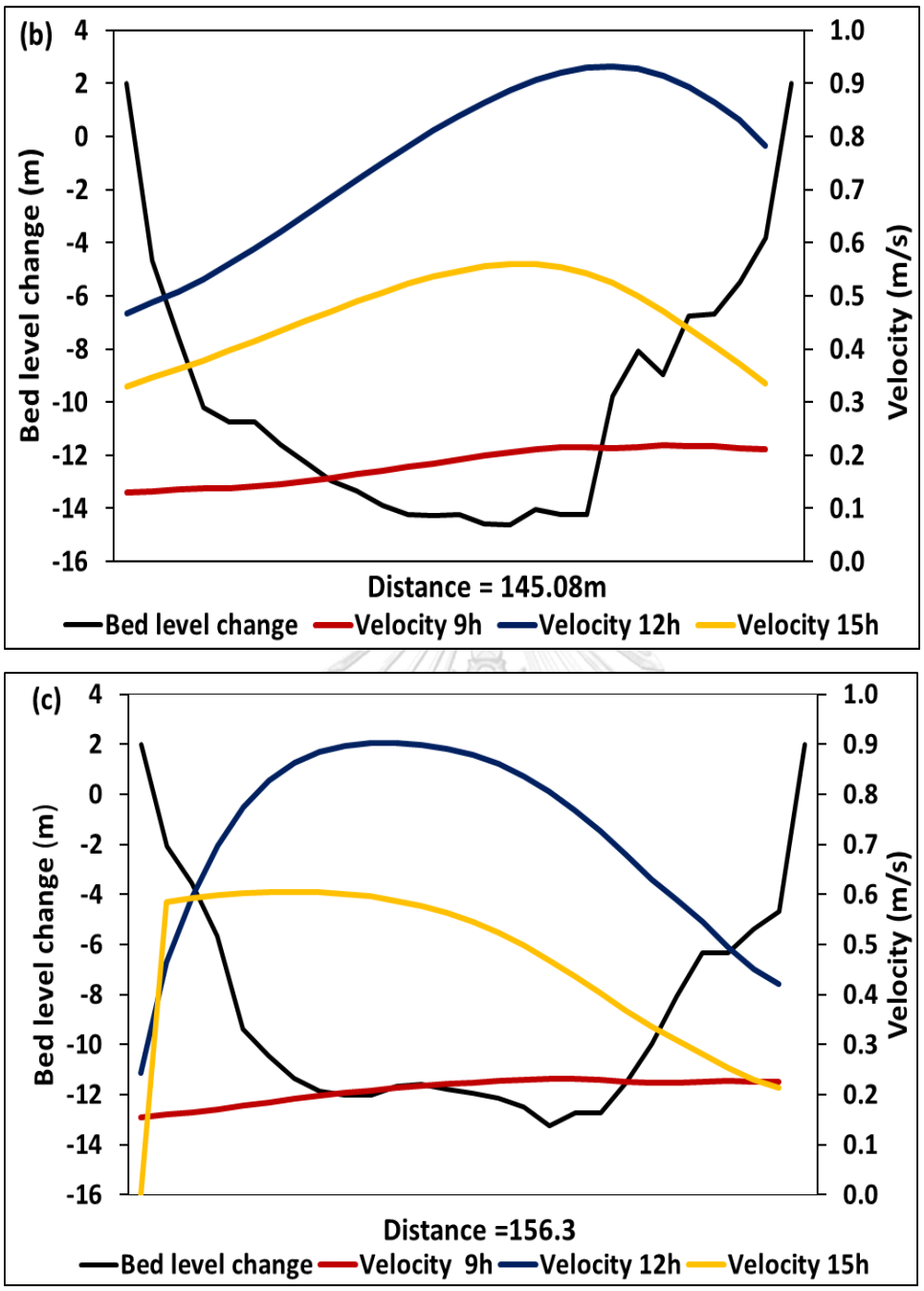

Figure 0.38 The distribution of velocity and bed level at different cross-sections: (a), (b), and (c) show respectively cross-sections 1, 2, and 3 at 9 a.m, 12 p.m, and 3 p.m on 6 September 2019

5.1.3 Spatiotemporal variability of different flow regimes

A statistically significant variability of flow was found at low and high regimes, which responded to incoming and outgoing tides, respectively (Figure. 5.6).

The most variation of flow occurred at the downstream and upstream of the river reaches. In general, the river's lowest flow occurred during the stage of the incoming tide at the upstream area, whereas medium and peak flow were observed at gentle/unchanged and outgoing tide at midstream and downstream river reach. The average flows at the downstream, midstream and the upstream area responding to high, medium, and low flow regimes were 951±336, 714±231, and 475±249 m^3/s, respectively. Effects of hydrological and topographical factors could explain changes in the average flows at distinct flow regimes, confirmed by previous studies [320, 321].

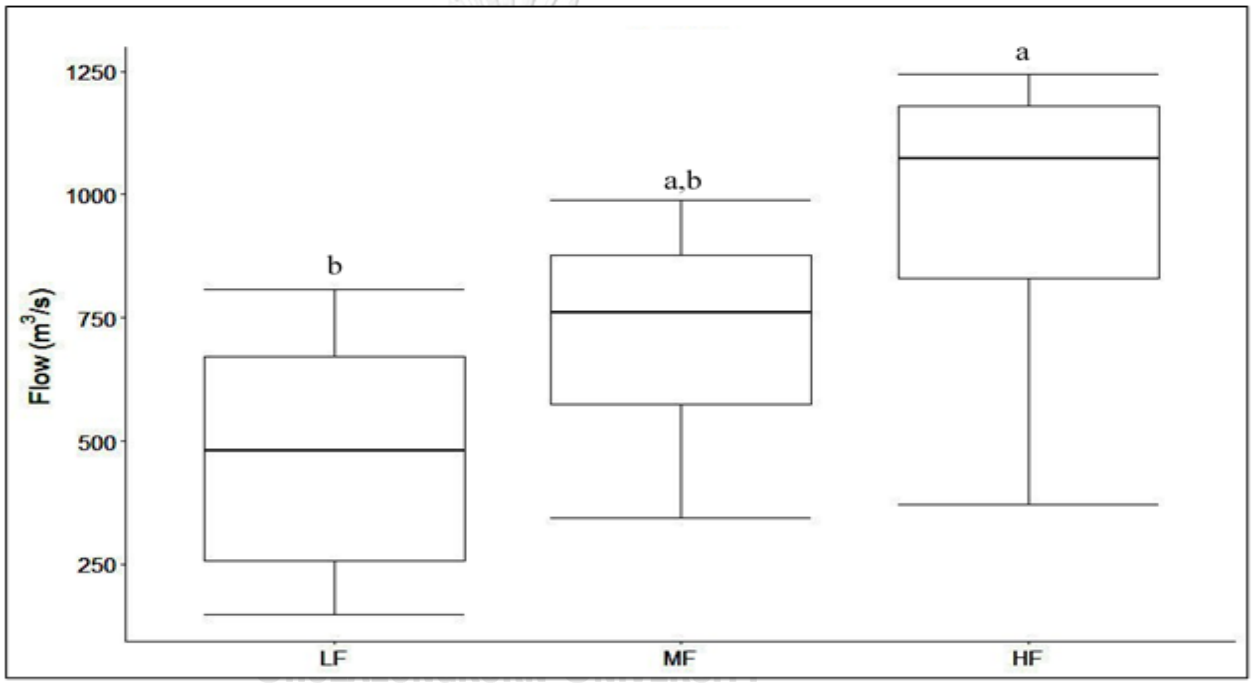

Figure 0.39 Differences in flow regimes including low flow (LF-based on nine observed sites at incoming tide), medium flow (MF- based on seven observed sites at gentle/unchanged tide), high flow (HF- based on nine observed sites at outgoing tide). Note the same letters marked in the figure show statistically insignificant differences among flow regimes ($p<0.05$)

5.1.4 Spatiotemporal water quality variations for various flow regimes.

Similar to water discharge, the selected water quality parameters were detected statistically significant variabilities in all flow regimes, except for DO, N-NO_3^-, and P-PO_4^{3-} (Figure 5.7). The flow regimes caused a significant impact on the

variation of physical parameters. The temperature and pH responded inconsistently to the different flow regimes, whereas EC, salinity, and TDS increased with the magnitude of flows (except for TSS). The highest pH, which was found in response to the low flow during the incoming tide, could be due to the seawater effect [213]. High concentrations (e.g., EC, salinity, and TDS) were observed at high flow (outgoing tide) compared with other flows, this could be explained by the effect of the tidal regime and landward discharges during the outgoing tide. The dissolved solids caused by aquaculture discharges along the reaches coupling with seawater intrusion led to the increase in their concentrations [224, 322]. TSS concentrations were likely high due to a strong flow velocity combined with pollution sources in the coastal area impacted by the tidal regime and anthropogenic activities. However, the TSS value peaked at a medium flow corresponding to a gentle/unchanged tide, which could restrain the transport of suspended solids, resulting in an elevated level of TSS. DO and COD representing organic pollution in water bodies responded differently to flow regimes. The independent DO from the flows might be influenced by other factors [323], implying that the river water has been polluted during the investigation. While flow regimes caused a remarkable variation of COD concentrations that was detected the highest level at high flow occurring at the lower part of the river reach. The elevated COD could be due to accumulated organic and inorganic substances discharged by aquaculture activities along the river, coupled with the impact of the tidal regime at high flow.

The influences of various flow regimes also led to different variations in patterns of nitrogen and phosphorus. Species of nitrogen (e.g., $N\text{-}NO_2^-$, TN, and $N\text{-}NH_4^+$) fluctuated significantly to flow regimes, except for $N\text{-}NO_3^-$ varying without the effect of flows. The variability of $N\text{-}NO_2^-$ and TN showed the same trend with flow regimes, which were observed at the highest concentrations at low flow, whereas the elevated concentration was detected at high flow for $N\text{-}NH_4^+$. A high existence of TN was possibly associated with a reduction in dilution process through the low flow (incoming tide), which could increase greatly TN concentration, as reported by [324]. In addition, elevated TN value could not only relate to flows but also its existing patterns as TN measures the various constituents of nitrogen in terms of dissolved and particulate forms [325]. Therefore, high $N\text{-}NO_2^-$ concentration was explored at the

same state of flow, as an example. Elevated N-NO_2^- was likely due to depletion of DO concentration coming out during the low flow. [231] reported that nitrite was an intermediate in nitrification and denitrification processes, which could have the adverse influences of increasing nitrite and nitrate levels, decreasing significantly DO concentration. Presence of N–NH_4^+ depends greatly on pH value (pH < 7.0) in aquatic environment [326]; however, pH value measured during high flow demonstrated an alkaline property (pH > 7.0). Thus, high N–NH_4^+ concentration could be explained by the impacts of nutrient discharges containing high patterns of nitrogen derived from aquaculture activities [327, 328]. The flow regimes caused a large change in TP concentration, whereas P-PO_4^{-3} responded to statistically nonsignificant flows. Phosphorus was greatly influenced by suspended solids through adsorption, resulting in low phosphorus concentration in the aquatic environment [288]. However, elevated TP value was measured in the same flow regime as TSS, where the tidal regime was identified to be gentle/unchanged. This suggested that TP concentration was caused by opportunities for retention time, leading to deposition of phosphorus originating from aquaculture practices [329].

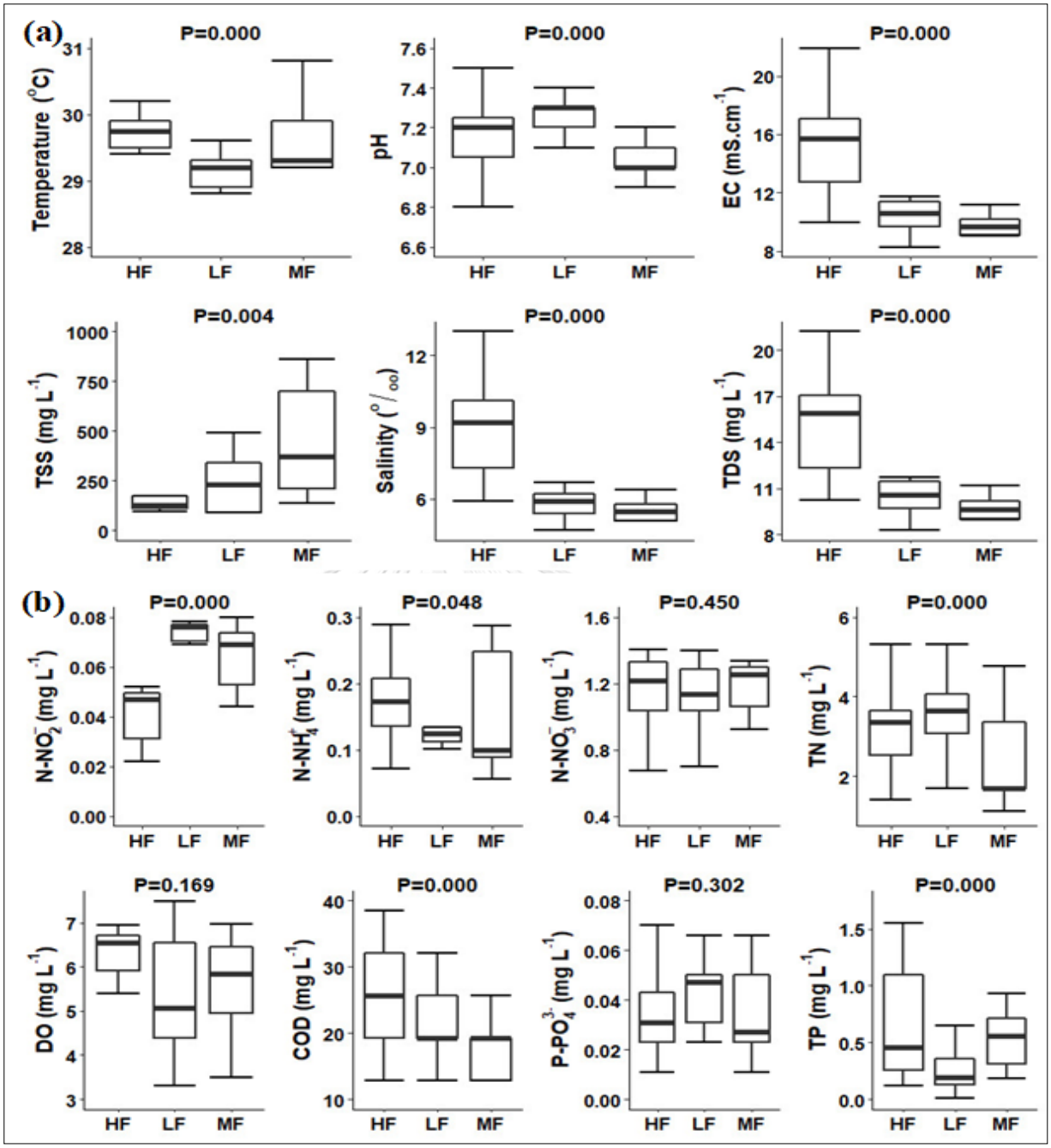

Figure 0.40 Differences in water quality including (a) the physical and (b) biological parameters among the flow regimes for low flow (LF-based on nine observed sites at incoming tide), medium flow (MF-based on seven observed sites at gentle/unchanged tide), and high flow (HF-based on nine observed sites at outgoing tide). Note the statistically significant differences of water quality parameters among flow regimes ($p<0.05$)

5.1.5 Dependence of water quality on different flow regimes

As illustrated in Table 0.21, several water quality parameters depending consistently on various flow regimes were found in temperature and $N\text{-}NO_2^-$; however, the degree of dependency varied among flows. The temperature had a significantly negative and positive correlation with the low and medium flow regime, respectively, whereas a significantly positive and negative correlation was found for $N\text{-}NO_2^-$. Other parameters were dependent on the flow regimes in diverse ways. The parameters (e.g., EC, TDS, salinity, and TP) were significantly positively correlated with the medium flow, whereas the parameters (e.g., pH, $N\text{-}NO_3^-$, COD, and DO) showed a significantly positive correlation with the high flow. Water quality parameters' dependencies and degrees of dependability varied inconsistently across flow regimes, showing that water quality was influenced not only by flow regimes but also by physicochemical processes in the aquatic environment.

Among measured water quality parameters, patterns of nitrogen such as $N\text{-}NO_2^-$ concentration was dependent variously on two flows, showing a reducing concentration with an increase with the flow. While $N\text{-}NO_3^-$ depended primarily on the high flow. This suggested that the concentration of nitrogen species was not only impacted by the flow regimes but also their behavior [323, 325] Similarly, the dependency of temperature varied distinctly on the flows, which increased with a reduction in flow. The previous study of [330] reported that the low flow would provide warm and clear conditions in the natural river systems. TP and TSS were likely associated with suspended solids, which were found respectively their dependency on the medium/high flow compared with the low flow. Elevated TSS and TP on these flows could be mainly caused by the nonpoint source pollutants and pollutant resuspension from suspended sediments [331, 332]. Dissolved pollutants (e.g., EC, TDS, and salinity) were dependent greatly on the medium flow, which was the result of seawater intrusion combined with landward loadings from nonpoint source pollution. With an increase in flow, DO and COD increased appropriately in the high flow. Under the tidal effect, high flow coupled with turbulence supports a large potential for dissolved oxygen in the watercourse [331]. High COD concentration at high flow was ascribed to a high level of organic substances

discharged primarily by aquaculture practice along the reach. The previous study of [333] revealed a significantly positive correlation between COD and suspended organic matter-containing sediments, as well as an increased COD value at high flow due to high suspended sediment concentration. Similarly, the pH value was discovered to be dependent on the high flow, which was likely to organic acid dilution derived mainly from shrimp farming, the high pH of released water from eutrophic reservoirs into waterbodies would increase owing to the dilution process at high flow [334].

Table 0.21 Spearman correlation coefficients between water quality parameters and various flow regimes

Parameters	Flow regimes		
	LF (27*)	MF (21*)	HF (27*)
Temperature	**-0.855**	**0.790**	0.315
pH	0.359	0.058	**0.549**
EC	-0.133	**0.852**	0.315
TDS	-0.133	**0.860**	0.332
TSS	-0.128	0.283	**0.464**
Salinity	0.078	**0.869**	0.316
$N\text{-}NO_2^-$	**0.538**	**-0.674**	-0.237
$N\text{-}NO_3^-$	0.291	0.413	**0.518**
$N\text{-}NH_4^+$	-0.236	-0.103	-0.318
TN	0.103	-0.096	0.283
$P\text{-}PO_4^{3-}$	0.357	-0.136	0.149
TP	0.150	**0.508**	0.324
COD	0.159	0.045	**0.383**
DO	0.274	0.140	**0.522**

LF: low flow regime at incoming tide; MF: medium flow regime at gentle/unchanged tide; HF: high flow regime at the outgoing tide. Significant correlation coefficients are boldface and sample sizes are in parentheses

* Number of samples used for statistical analysis

CHAPTER 6
CONCLUSIONS AND SUGGESTIONS

6.1 Conclusions

The findings showed that the surface water quality of the Ganh Hao River was generally poor during the study period, particularly with respect to parameters representing nutrient and organic pollution, which exceeded the guidelines for surface water quality. However, heavy metal concentrations were very low or undetected in water samples from most sites. The metal concentrations of sediment samples were much lower than the Vietnamese guidelines for sediment quality. Moreover, the pollution indices (I-geo, CF, and PLI) indicated that the sediment in the study area was consistent with the background concentrations of As, Cu, Pb, and Zn.

The tidal regime had a considerable influence on the variation in values of physicochemical parameters, with significant differences between the ebb and spring tides for all parameters excluding pH, EC, TSS, $N–NO_3^-$, and TP. There were also significant differences in the pollutant concentrations between the dry and wet seasons (except for TSS and TP). The PCA explained that nutrients and organic substances were primarily responsible for the deterioration of the surface water quality in the study area. The logistic regression model analysis identified the extensive and improved extensive shrimp systems as the main source of pollutants influencing the degradation of river water in both seasons. Based on the water quality maps, pollution hotspots could be identified to recommend water extraction areas to meet the daily water requirements of the population.

The 2D model was calibrated with the most suitable Manning roughness coefficient (n=0,022 $m^{-1/3}s$) which showed a good agreement between the simulated and measured in terms of phase and amplitude. The validated model with an RMSE and R^2 value was 0.22 and 0.98, showing high reliability and accuracy. The 3D model was developed using the defined roughness coefficient as well as user-dependent parameters in the 2D model. The model was calibrated with the most suitable horizontal eddy viscosity (HEV=2 $m^2.s^{-1}$). The simulated and measured velocities showed a similar pattern; the depth-averaged velocities differed by 5-14 percent from

ADCP-based data, demonstrating the 3D hydrodynamic model's ability to simulate vertical flows. The model accuracy was determined by the model mean errors, which demonstrated a good degree of conformity in terms of MAE with HEV values of 2 $m^2.s^{-1}$ at various layers. Based on the hydrodynamic model, the result indicated that changes in the river hydraulic characteristics were influenced remarkably by the tidal regime as well as geomorphological. These changes also had an impact on the water quality, resulting in significant differences in water quality. The investigated water quality parameters not only had different responses but also were dependent on the flow regimes, confirming that flow was one of the primary causes of spatiotemporal variability in water quality. The diverse responses of the water quality parameters to flow regimes were due to the discharges of aquaculture practices and the governing processes under the tidal drivers.

6.2 Suggestions

Because of the intensive direct use of surface water and pollution of the Ganh Hao River, water management strategies should be set for different areas of the river to monitor water quality during various periods. Further studies should be performed sampling in the river and in the shrimp ponds of different types of aquaculture practices in order to comprehensively assess the status of local surface water quality. Water quality management should not only focus on pollution sources but also pay much attention to various flow regimes. As a result, different strategies and guidelines should be considered in order to manage water resources more effectively. Moreover, the application of technical solutions (e.g., numerical models and automatic monitoring systems) should be executed in the studied area to control and manage water resources in the context of climate changes and land-use changes. Despite the fact that the data were conducted over a short period of time, the results of this study were helpful for developing policies to better managing water resources and might have likely widespread implications for other rivers beyond the geographical regions.

Although the study effectively addressed the existing environmental problems in the study area. However, the research was conducted a short period in the dry and wet seasons. Therefore, insufficient data series on water quality parameters simulate water quality fluctuations as well as scenarios related to sea level rise and changes in land-use.

REFERENCES

[1] Bashir, I., Lone, F.A., Bhat, R.A., Mir, S.A., Dar, Z.A., and Dar, S.A. Concerns and Threats of Contamination on Aquatic Ecosystems. in Hakeem, K.R., Bhat, R.A., and Qadri, H. (eds.),Bioremediation and Biotechnology: Sustainable Approaches to Pollution Degradation, pp. 1-26. https://doi.org/10.1007/978-3-030-35691-0_1. Cham: Springer International Publishing, 2020.

[2] Hassaan, M.A. and Rayis, E.O.A. Calculations and solutions for heavy metals pollution load from Umum and Qalaa drains to Lake Mariut, Egypt. Indian Journal of Geo Marine Sciences 47(07) (2018): 1460-1467. http://nopr.niscair.res.in/bitstream/123456789/44604/1/IJMS%2047%287%29%201460-1467.pdf.

[3] Liang, Y., Yi, X., Dang, Z., Wang, Q., Luo, H., and Tang, J. Heavy metal contamination and health risk assessment in the vicinity of a tailing pond in Guangdong, China. International journal of environmental research and public health 14(12) (2017): 1557. https://doi.org/10.3390/ijerph14121557.

[4] Mohammadi , R.M., Sobhan, A.S., Karimi, H., and Sorooshnia, R. Natural and anthropogenic source of heavy metals pollution in the soil samples of an industrial complex a case study. Iranian Journal of Toxicology 9(29) (2015): 1336-1341. http://ijt.arakmu.ac.ir/article-1-337-en.pdf.

[5] Kuriata, P.A., Szymczyk, S., Skwierawski, A., Glińska, L.K., and Cymes, I. Heavy metal contamination in the surface layer of bottom sediments in a flow-through lake: a case study of lake symsar in northern poland. Water 8(8) (2016): 358. https://doi.org/10.3390/w8080358.

[6] Kanu, I. and Achi, O. Industrial effluents and their impact on water quality of receiving rivers in Nigeria. Journal of applied technology in environmental sanitation 1(1) (2011): 75-86. https://www.researchgate.net/publication/287104597.

[7] Prokop, Z., Vangheluwe, M., Van Sprang, P., Janssen, C., and Holoubek, I. Mobility and toxicity of metals in sandy sediments deposited on land. Ecotoxicology and Environmental Safety 56(2) (2003): 326-326. https://doi.org/10.1016/S0147-6513(02)00022-2.

[8] Saifullah, S., Ismail, S., Khan, S., and Saleem, M. Land use—iron pollution in mangrove habitat of Karachi, Indus Delta. Earth Interactions 8(17) (2004): 1-9. https://doi.org/10.1175/1087-3562(2004)8<1:LUPIMH>2.0.CO;2.

[9] Singh, V.K., Singh, K.P., and Mohan, D. Status of heavy metals in water and bed sediments of river Gomti–A tributary of the Ganga river, India. Environmental monitoring and assessment 105(1-3) (2005): 43-67. https://doi.org/10.1007/s10661-005-2816-9.

[10] Duquesne, S., Newton, L.C., Giusti, L., Marriott, S.B., Stärk, H.J., and Bird, D.J. Evidence for declining levels of heavy-metals in the Severn Estuary and Bristol Channel, UK and their spatial distribution in sediments. Environmental Pollution 143(2) (2006): 187-196. https://doi.org/10.1016/j.envpol.2005.12.002.

[11] Kar, D., Sur, P., Mandai, S., Saha, T., and Kole, R. Assessment of heavy metal pollution in surface water. International Journal of Environmental Science and Technology 5(1) (2008): 119-124. https://doi.org/10.1007/BF03326004.

[12] Whitmore, T.J., Riedinger-Whitmore, M.A., Smoak, J.M., Kolasa, K.V.,

Goddard, E.A., and Bindler, R. Arsenic contamination of lake sediments in Florida: evidence of herbicide mobility from watershed soils. Journal of Paleolimnology 40(3) (2008): 869-884. https://doi.org/10.1007/s10933-008-9204-8.

[13] Vuković, Ž., Radenković, M., Stanković, S.J., and Vuković, D. Distribution and accumulation of heavy metals in the water and sediments of the River Sava. Journal of the Serbian Chemical Society 76(5) (2011): 795-803. https://doi.org/10.2298/JSC100420067V.

[14] Modoi, O.C., Roba, C., Török, Z., and Ozunu, A. Environmental risks due to heavy metal pollution of water resuted from mining wastes in NW Romania. Environmental Engineering & Management Journal (EEMJ) 13(9) (2014): 2325-2336. https://doi.org/10.30638/eemj.2014.260.

[15] Akaahan, T., Olabanji, F., and Azua, E. Studies on contamination of surface waters of river Benue with trace elements at Makurdi, Benue State, Nigeria. Journal of Environmental Chemistry and Ecotoxicology 7(5) (2015): 49-55. https://doi.org/10.5897/JECE. 2015. 0358.

[16] Salah, E.A.M., Al-Hiti, I.K., and Alessawi, K.A. Assessment of heavy metals pollution In Euphrates River Water, Amiriyah Fallujah, Iraq. Assessment 5(15) (2015): 1009-1023. https://doi.org/10.4236/jwarp.2012.412117.

[17] Ignatavičius, G., Valskys, V., Bulskaya, I., Paliulis, D., Zigmontienė, A., and Satkūnas, J. Heavy metal contamination in surface runoff sediments of the urban area of Vilnius, Lithuania. Estonian journal of earth sciences (2017): 13-20. https://doi.org/10.3176/earth.2017.04.

[18] White, I. Water management in the Mekong Delta: changes, conflicts and opportunities. Unesco Paris, 2002.

[19] Mak, S., Pheng, S., Khuon, K., Sin, C., Tes, S., Chea, T., Vang, R., and Sou, V. Profile of the Sub-Area Stung Treng (SA-6C). Phnom Penh: Cambodia National Mekong Committee (2011).

[20] MRC. Transboundary water resources management issues in the Mekong Delta of Cambodia and Viet Nam. Vientiane, Lao PDR: Mekong River Commission. 2017. 32.

[21] GSO. Completed resuts of the 2019 Vietnam population and housing sensus. (2019).

[22] Le, T.N., Bregt, A.K., van Halsema, G.E., Hellegers, P.J., and Nguyen, L.-D. Interplay between land-use dynamics and changes in hydrological regime in the Vietnamese Mekong Delta. Land Use Policy 73 (2018): 269-280. https://doi.org/10.1016/j.landusepol.2018.01.030.

[23] GSO. Report on labor force survey, Quarter 4, 2017. General Statistics Office. https://www.gso.gov.vn/default_en.aspx?tabid=515&idmid=5&ItemID=18833 (accessed 11 June 2019). (2018).

[24] Toan, P.V., Sebesvari, Z., Bläsing, M., Rosendahl, I., and Renaud, F.G. Pesticide management and their residues in sediments and surface and drinking water in the Mekong Delta, Vietnam. Science of the Total Environment 452 (2013): 28-39. https://doi.org/10.1016/j.scitotenv.2013.02.026.

[25] Cenci, R. and Martin, J.-M. Concentration and fate of trace metals in Mekong River Delta. Science of the total Environment 332(1-3) (2004): 167-182. https://doi.org/10.1016/j.scitotenv.2004.01.018.

[26] Tien, D.M., Nhuan, T. M., Son, V. T., Ben, D. C., Thanh, P. H., Son, N. N., and Ngoc, N. T. M. Distribution of Arsenic in water and coastal sediments of Hau river. Status of arsenic pollution in Vietnam. Vietnam Union of Science and Technology Associations. . (2005).

[27] Ky, V.N. Arsenic Contamination at Hau river in the Mekong Delta. Journal of Science and Technology Development. Journal of Science and Technology Development 12 (05) (2009): 102 - 103.

[28] Nhe, T.T. Survey on content of As, Cd, Zn in surface and shallow water of Long Xuyen quadrangle, An Giang province. Master thesis, Can Tho University, 2006.

[29] Wilbers, Becker, M., Sebesvari, Z., and Renaud, F.G. Spatial and temporal variability of surface water pollution in the Mekong Delta, Vietnam. Science of the Total Environment 485 (2014): 653-665. https://doi.org/10.1016/j.scitotenv.2014.03.049.

[30] Prathumratana, L., Sthiannopkao, S., and Kim, K.W. The relationship of climatic and hydrological parameters to surface water quality in the lower Mekong River. Environment international 34(6) (2008): 860-866. https://doi.org/10.1016/j.envint.2007.10.011.

[31] Hanh, P.T.M., Anh, N.V., Sthiannopkao, S., and Kim, K.-W. Analysis of variation and relation of climate, hydrology and water quality in the lower Mekong River. Water science and technology 62(7) (2010): 1587-1594. https://doi.org/10.2166/wst.2010.449.

[32] Hoanh, Tuong, T., Gallop, K., Gowing, J., Kam, S.P., Khiem, N., and Phong, N. Livelihood impacts of water policy changes: evidence from a coastal area of the Mekong River Delta. Water Policy 5(5-6) (2003): 475-488. https://doi.org/10.2166/wp.2003.0030.

[33] Brennan, D., Clayton, H., and Be, T.T. Economic characteristics of extensive shrimp farms in the Mekong delta. Aquaculture Economics & Management 4(3-4) (2000): 127-139. https://doi.org/10.1080/13657300009380265.

[34] Hori, H. The Mekong: environment and development. United Nations University Press, 2000.

[35] Fanslow, G., Tuong, T., Hoanh, C.T., Phong, N., An, L., and Hien, N. Land-use and salinity management effects on water quality in Ca Mau Peninsula, Vietnam. (2005).

[36] Chea, R., Grenouillet, G., and Lek, S. Evidence of water quality degradation in lower Mekong Basin revealed by self-organizing map. PLOS ONE 11(1) (2016): 1-19. https://doi.org/10.1371/journal.pone.0145527. .

[37] Nhung, T.T., Le Vo, P., Van Nghi, V., and Bang, H.Q. Salt intrusion adaptation measures for sustainable agricultural development under climate change effects: A case of Ca Mau Peninsula, Vietnam. Climate Risk Management 23 (2019): 88-100. https://doi.org/10.1016/j.crm.2018.12.002.

[38] Hak, D., Nadaoka, K., Bernado, L.P., Le Phu, V., Quan, N.H., Toan, T.Q., Trung, N.H., Van Ni, D., and Van, P.D.T. Spatio-temporal variations of sea level around the Mekong Delta: their causes and consequences on the coastal environment. Hydrological Research Letters 10(2) (2016): 60-66. https://doi.org/10.3178/hrl.10.60.

[39] Albers, T., San, D., and Schmitt, K. Shoreline Management Guidelines: Coastal

Protection in the Lower Mekong Delta. GIZ. Eschborn, Germany (2013).
[40] Albers, T. and Stolzenwald, J. Coastal engineering consultancy in Ca Mau province. Deutsche Gesellschaft für Internationale Zusammenarbeit (GIZ) GmbH (2015).
[41] Wilbers, G.J., Becker, M., Sebesvari, Z., and Renaud, F.G. Spatial and temporal variability of surface water pollution in the Mekong Delta, Vietnam. Science of the Total Environment 485 (2014): 653-665. https://doi.org/10.1016/j.scitotenv.2014.03.049.
[42] Toriman, M., Hashim, N., Hassan, A.J., Mokhtar, M., Juahir, H., Gasim, M., and Abdullah, P. Study on the impact of tidal effects on water quality modelling of Juru River, Malaysia. Asian Journal of Scientific Research 4(2) (2011): 129-138. https://doi.org/10.3923/ajsr.2011.129.138.
[43] Dinh, Q.T. Vietnam-Mekong Delta Integrated Climate Resilience and Sustainable Livelihoods (MD-ICRSL) Project: Infrastructure to prevent coastal erosion, supply fresh
water and for production of shrimp - forest model to improve livelihoods and adapting to climate change in the coastal area of Ca Mau province. 2019, The World Bank. 327. http://documents1.worldbank.org/curated/ru/660481568009638284/pdf/Environmental-and-Social-Impact-Assessment-for-Ca-Mau-Province.pdf.
[44] Tri, D.Q., Linh, N.T.M., Thai, T.H., and Kandasamy, J. Application of 1D–2D coupled modeling in water quality assessment: A case study in Ca Mau Peninsula, Vietnam. Physics and Chemistry of the Earth, Parts A/B/C 113 (2019): 83-99. https://doi.org/10.1016/j.pce.2018.10.004.
[45] Tho, N.V. Pollutions of As, Cd in sediment, soil and water in coastal areas, Camau
province. Scientific Journal of Can Tho University 12 (2007): 15-24.
[46] Nga, B.T., Muoi, L. V. Assessment the levels of arsenic pollution in surface water and sediment in fresh water, brackish and saline region in Mekong Delta. A project report. 2010, Ministry of Education and Training, Vietnam.
[47] Toan, Chheng, P., and Eric, B. Research on fluctuation of water quality parameters and occurrence of shrimp and fish nature species in Baclieu province. Journal of Can Tho University 8 (2007): 139-148.
[48] Long, V.D., Tien, H.L., and Quy, V.D. Assessment of surface water in Ca Mau province. Journal of Agricultrue and Rural Development (2015): 124-130.
[49] Chi, N., Dao, P., and Kyncl, M. Water supply status in rural areas of the Mekong Delta and development measures. GeoScience Engineering 64 (2018): 35-41. https://doi.org/10.2478/gse-2018-0005.
[50] Wetzel, R.G. Limnology: lake and river ecosystems, third ed. Elsevier, 2001.
[51] Ramakrishnaiah, C., Sadashivaiah, C., and Ranganna, G. Assessment of water quality index for the groundwater in Tumkur Taluk, Karnataka State, India. Journal of Chemistry 6(2) (2009): 523-530. https://doi.org/10.1155/2009/757424.
[52] Okeke, C. and Igboanua, A. Characteristics and quality assessment of surface water and groundwater recourses of Akwa Town, Southeast, Nigeria. J. Niger Assoc. Hydrol. Geol 14 (2003): 71-77.
[53] Mian, I.A., Begum, S., Riaz, M., Ridealgh, M., McClean, C.J., and Cresser, M.S.

Spatial and temporal trends in nitrate concentrations in the River Derwent, North Yorkshire, and its need for NVZ status. Science of the Total Environment 408(4) (2010): 702-712. https://doi.org/10.1016/j.scitotenv.2009.11.020.

[54] Xiaolong, W., Jingyi, H., Ligang, X., and Qi, Z. Spatial and seasonal variations of the contamination within water body of the Grand Canal, China. Environmental Pollution 158(5) (2010): 1513-1520. https://doi.org/10.1016/j.envpol.2009.12.018.

[55] Gupta, A. Water pollution - sources, effects and control. Pointer Publishers Jaipur. https://www.researchgate.net/publication/321289637. (2016).

[56] Eroğlu, H., Çakır, G., Sivrikaya, F., and Akay, A.E. Using high resolution images and elevation data in classifying erosion risks of bare soil areas in the Hatila Valley Natural Protected Area, Turkey. Stochastic environmental research and risk assessment 24(5) (2010): 699-704. https://doi.org/10.1007/s00477-009-0356-5.

[57] Ezugwu, C. Sediment deposition in Nigeria Reservoirs: Impacts and control measures. Innovative Systems Design and Engineering 4 (2013): 54-62. https://www.iiste.org/Journals/index.php/ISDE/article/view/9680.

[58] Brils, J. Contaminated Sediments in European River Basins. SedNet. https://sednet.org/wp-content/uploads/2016/03/Sednet_booklet_final_2.pdf., 2004.

[59] Walling, D. and Fang, D. Recent trends in the suspended sediment loads of the world's rivers. Global and planetary change 39(1-2) (2003): 111-126. https://doi.org/10.1016/S0921-8181(03)00020-1.

[60] Vink, R. and Behrendt, H. Present and future quality of sediments Iin the Rhine catchment area–heavy metals. SedNet. www.SedNet.org., 2001.

[61] Kale, V.S. Consequence of temperature, pH, turbidity and dissolved oxygen water quality parameters. International Advanced Research Journal in Science, Engineering and Technology 3(8) (2016): 186-190. https://iarjset.com/upload/2016/august-16/IARJSET%2034.pdf.

[62] Abowei, J. Salinity, dissolved oxygen, pH and surface water temperature conditions in Nkoro River, Niger Delta, Nigeria. Advance journal of food science and technology 2(1) (2010): 36-40.

[63] Zheng, L. and Paul, M.J. Effects of eutrophication on stream ecosystems. Tetratech Inc (2009): 1-42. https://www.lexissecuritiesmosaic.com/gateway/FedReg/literature_review_Eutrophication_20effects_20on_20streams.pdf.

[64] Smyth, K., Mazik, K., and Elliott, M. Behavioural effects of hypersaline exposure on the lobster Homarus gammarus (L) and the crab Cancer pagurus (L). Journal of experimental marine biology and ecology 457 (2014): 208-214. https://doi.org/10.1016/j.jembe.2014.04.016.

[65] Wolanski, E. and Elliott, M. Estuarine ecohydrology: an introduction. second ed ed.: Elsevier, 2015.

[66] Potter, I.C., Chuwen, B.M., Hoeksema, S.D., and Elliott, M. The concept of an estuary: a definition that incorporates systems which can become closed to the ocean and hypersaline. Estuarine, Coastal and Shelf Science 87(3) (2010): 497-500. https://doi.org/10.1016/j.ecss.2010.01.021.

[67] Spivak, E.D. and Cuesta, J.A. The effect of salinity on larval development of

Uca tangeri (Eydoux, 1835)(Brachyura: Ocypodidae) and new findings of the zoeal morphology. Scientia Marina 73(2) (2009): 297-305. https://doi.org/10.3989/scimar.2009.73n2297.

[68] Daniels, W., Zipper, C., Orndorff, Z., Skousen, J., Barton, C., McDonald, L., and Beck, M. Predicting total dissolved solids release from central Appalachian coal mine spoils. . Environmental pollution 216 (2016): 371-379. https://doi.org/10.1016/j.envpol.2016.05.044. .

[69] Han, D., Kohfahl, C., Song, X., Xiao, G., and Yang, J. Geochemical and isotopic evidence for palaeo-seawater intrusion into the south coast aquifer of Laizhou Bay, China. Applied Geochemistry 26(5) (2011): 863-883. https://doi.org/10.1016/j.apgeochem.2011.02.007.

[70] Marandi, A., Polikarpus, M., and Jõeleht, A. A new approach for describing the relationship between electrical conductivity and major anion concentration in natural waters. Applied geochemistry 38 (2013): 103-109. https://doi.org/10.1016/j.apgeochem.2013.09.003.

[71] Patil, P., Sawant, D., and Deshmukh, R. Physico-chemical parameters for testing of water: A review. International Journal of Environmental Sciences 3(3) (2012): 1194.

[72] Sawyer, C.N. and Parkin, G.F. Chemistry for environmental engineering and science - 5th ed. fifth ed ed.: McGraw-Hill., 2003.

[73] Appelo, C. and Postma, D. Geochemistry, groundwater and pollution,. Amsterdam, the Netherlands. Geochemistry, groundwater and pollution,. 2nd ed. Amsterdam, the Netherlands. (2005): -.

[74] WHO. Guidelines for drinking-water quality. Geneva: World Health Organization. 2015.

[75] Nthunya, L.N., Maifadi, S., Mamba, B.B., Verliefde, A.R., and Mhlanga, S.D. Spectroscopic determination of water salinity in brackish surface water in Nandoni Dam, at Vhembe District, Limpopo Province, South Africa. Water 10(8) (2018): 990.

[76] Todd, D.K. and Mays, L.W. Groundwater hydrology edition. third ed ed.: Welly Inte, 2005.

[77] Kelly, W., Panno, S., and Hackley, K. The sources, distribution, and trends of chloride in waters of Illinois. Bulletin (Illinois State Water Survey) no. 74 (2012).

[78] Yusoph, M., Diate, K., Baulo, A., Herbito, J., Capangpangan, N., Salik, M., Trillo, G., Galarita, G.M., Guinar, N., Sihagan, A., and Bayubay, S. Total suspended solids (TSS) filtration apparatus. https://www.researchgate.net/publication/325270148. 2018.

[79] Droppo, I.G. Rethinking what constitutes suspended sediment. Hydrological processes 15(9) (2001): 1551-1564. https://doi.org/10.1002/hyp.228.

[80] Verstraeten, G. and Poesen, J. Estimating trap efficiency of small reservoirs and ponds: methods and implications for the assessment of sediment yield. Progress in Physical Geography 24(2) (2000): 219-251. https://doi.org/10.1177/030913330002400204.

[81] Haygarth, P.M., Bilotta, G.S., Bol, R., Brazier, R., Butler, P.J., Freer, J., Gimbert, L.J., Granger, S.J., Krueger, T., and Naden, P. Processes affecting transfer of sediment and colloids, with associated phosphorus, from intensively

farmed grasslands: an overvie of key issues. Hydrol. Processs 20 (2006): 4407–4413. https://doi.org/10.1002/hyp.6598.

[82] Haygarth, P.M. and Jarvis, S.C. Agriculture, hydrology, and water quality. CABI Pub. New York, USA., 2002.

[83] Kronvang, B., Laubel, A., Larsen, S.E., and Friberg, N. Pesticides and heavy metals in Danish streambed sediment. Hydrobiologia 494(1-3) (2003): 93-101.

[84] Schöne, B.R., Huang, X., Jantschke, A., Mertz-Kraus, R., and Zettler, M.L. High-resolution reconstruction of dissolved oxygen levels in the Baltic Sea with bivalves–a multi-species comparison (Arctica islandica, Astarte borealis, Astarte elliptica). Frontiers in Marine Science (2022): 442.

[85] Birkett, C., Tollner, E.W., and Gattie, D.K. Total suspended solids and flow regime effects on periphyton development in a laboratory channel. Transactions of the ASABE 50(3) (2007): 1095-1104. https://doi.org/10.13031/2013.23118.

[86] Gorde, S. and Jadhav, M. Assessment of water quality parameters: a review. Journal of Engineering Research and Applications 3(6) (2013): 2029-2035. http://www.ijera.com/papers/Vol3_issue6/LV3620292035.pdf.

[87] Zheng and Paul. Effects of eutrophication on stream ecosystems. Tetratech Inc.(n-steps. tetratech-ffx. com/PDF&otherFiles/literature_review/Eutrophication% 20effects% 20on% 20streams. pdf) (2009).

[88] Alam, T. Estimation of chemical oxygen demand in wastewater using UV-VIS Spectroscopy. Applied Sciences: School of Mechatronic Systems Engineering, 2015.

[89] Chapman, P.J., Kay, P.M.G., and Pitts, C.S. Surface water quality. y. In: Holden, J, (ed.). in Water Resources: an integrated approach, pp. 99-142: Routledge, 2013.

[90] Chen, X., Hu, Y., Xie, Z., and Wang, H. Chapter 3 - Materials and Design of Photocatalytic Membranes. in Basile, A., Mozia, S., and Molinari, R. (eds.),Current Trends and Future Developments on (Bio-) Membranes, pp. 71-96: Elsevier, 2018.

[91] Rajta, A., Bhatia, R., Setia, H., and Pathania, P. Role of heterotrophic aerobic denitrifying bacteria in nitrate removal from wastewater. Journal of Applied Microbiology 128(5) (2020): 1261-1278.

[92] Davies, O., Abolude, D., and Ugwumba, A. Phytoplankton of the lower reaches of Okpoka creek, PortHarcout, Nigeria. J. Fish. Int 3(3) (2008): 70-77. https://medwelljournals.com/abstract/?doi=jfish.2008.83.90.

[93] Jagessar, R. and Sooknundun, L. Determination of nitrate anion in waste water from nine selected areas of coastal Guyana via a spectrophotometric method. IJRRAS 7(2) (2011): 203-212. https://www.arpapress.com/Volumes/Vol7Issue2/IJRRAS_7_2_15.pdf.

[94] Adesuyi, A., Nnodu, V., Njoku, K., and Jolaoso, A. Nitrate and phosphate pollution in surface water of Nwaja Creek, Port Harcourt, Niger Delta, Nigeria. International Journal of Geology, Agriculture and Environmental Sciences 3(5) (2015): 14-20.

[95] Aloe, A.K., Bouraoui, F., Grizzetti, B., Bidoglio, G., and Pistocchi, A. Managing nitrogen and phosphorus loads to water bodies: characterisation and solutions. in *JRC-Ispra, 14*. 2014. 89. https://doi.org/10.2788/14322.

[96] Johnston, A. and Dawson, C. Phosphorus in agriculture and in relation to water quality. Agricultural Industries Confederation Peterborough, United Kingdom., 2005.
[97] Mateo-Sagasta, J., Zadeh, S.M., Turral, H., and Burke, J. Water pollution from agriculture: A global review. Executive summary. Rome, Italy: FAO Colombo, Sri Lanka: International Water Management., 2017.
[98] Jones Jr, J.B. Laboratory guide for conducting soil tests and plant analysis. CRC press. Boca Raton London, New York Washington, D.C., 2001.
[99] Soetaert, K., Hofmann, A.F., Middelburg, J.J., Meysman, F.J., and Greenwood, J. Reprint of the effect of biogeochemical processes on pH. Marine Chemistry 106(1-2) (2007): 380-401. https://doi.org/10.1016/j.marchem.2007.06.008.
[100] Taylor, P., Lichtschlag, A., Toberman, M., Sayer, M.D., Reynolds, A., Sato, T., and Stahl, H. Impact and recovery of pH in marine sediments subject to a temporary carbon dioxide leak. International Journal of Greenhouse Gas Control 38 (2015): 93-101. https://doi.org/10.1016/j.ijggc.2014.09.006.
[101] Aigberua, A. Effects of Spatial, temporal and pH changes on fractionated heavy metals in sediments of the Middleton River, Bayelsa State, Nigeria. MOJ Toxicol 4(6) (2018): 424-430. https://doi.org/10.15406/mojt.2018.04.00140.
[102] Zhang, Y., Zhang, H., Zhang, Z., Liu, C., Sun, C., Zhang, W., and Marhaba, T. pH effect on heavy metal release from a polluted sediment. Journal of Chemistry 2018 (2018).
[103] Alloway, B.J. Sources of heavy metals and metalloids in soils. in Heavy metals in soils, pp. 11-50: Springer, 2013.
[104] Bodar, C.W., Pronk, M.E., and Sijm, D.T. The European Union risk assessment on zinc and zinc compounds: the process and the facts. Integrated Environmental Assessment and Management: An International Journal 1(4) (2005): 301-319. https://doi.org/10.1002/ieam.5630010401.
[105] Vamerali, T., Bandiera, M., and Mosca, G. Field crops for phytoremediation of metal-contaminated land. A review. Environmental Chemistry Letters 8(1) (2010): 1-17. https://doi.org/10.1007/s10311-009-0268-0.
[106] Namieśnik, J. and Rabajczyk, A. The speciation and physico-chemical forms of metals in surface waters and sediments. Chemical Speciation & Bioavailability 22(1) (2010): 1-24. https://doi.org/10.3184/095422910X12632119406391.
[107] Weston, N.B. and Joye, S.B. Temperature-driven decoupling of key phases of organic matter degradation in marine sediments. Proceedings of the National Academy of Sciences 102(47) (2005): 17036-17040.
[108] Seiter, K., Hensen, C., Schröter, J., and Zabel, M. Organic carbon content in surface sediments-defining regional provinces. Deep Sea Research Part I: Oceanographic Research Papers 51(12) (2004): 2001-2026. https://doi.org/10.1016/j.dsr.2004.06.014.
[109] Muller-Karger, F.E., Varela, R., Thunell, R., Luerssen, R., Hu, C., and Walsh, J.J. The importance of continental margins in the global carbon cycle. Geophysical Research Letters 32(1) (2005).
[110] Avramidis, P., Nikolaou, K., and Bekiari, V. Total organic carbon and total nitrogen in sediments and soils: A Comparison of the wet oxidation – titration method with the combustion-infrared method. Agriculture and Agricultural Science Procedia 4 (2015): 425 – 430.

https://doi.org/10.1016/j.aaspro.2015.03.048.
[111] Alkhatib, M., Schubert, C.J., del Giorgio, P.A., Gelinas, Y., and Lehmann, M.F. Organic matter reactivity indicators in sediments of the St. Lawrence Estuary. Estuarine, Coastal and Shelf Science 102-103 (2012): 36-47.
[112] Fränzle, S., Markert, B., and Wünschmann, S. Dynamics of trace metals in organisms and ecosystems: prediction of metal bioconcentration in different organisms and estimation of exposure risks. Environmental pollution 150(1) (2007): 23-33. https://doi.org/10.1016/j.envpol.2007.02.006.
[113] Li, Hall, K., Y, Y., Mattu, G., McCallum, D., and Chen, M. Mobility and bioavailability of trace metals in the water-sediment system of the highly urbanized brunette watershed. Water, air, and soil pollution 197(1-4) (2009): 249-266. https://doi.org/10.1007/s11270-008-9808-7.
[114] Frías-Espericueta, M., Osuna-López, J., Voltolina, D., Correa-González, E., Armenta-Monje, M., López-López, G., and Izaguirre-Fierro, G. Metals in shrimp farm sediments, Sinaloa, Northwest Mexico. Bulletin of Environmental Contamination and Toxicology 77(6) (2006): 912-917. https://doi.org/10.1007/s00128-006-1228-z.
[115] Thorsson, M.H., Hedman, J.E., Bradshaw, C., Gunnarsson, J.S., and Gilek, M. Effects of settling organic matter on the bioaccumulation of cadmium and BDE-99 by Baltic Sea benthic invertebrates. Marine environmental research 65(3) (2008): 264-281. https://doi.org/10.1016/j.marenvres.2007.11.004.
[116] Emsley, J. Nature's building blocks: an AZ guide to the elements. Oxford University Press, 2011.
[117] Voet, D., Voet, J.G., and Pratt, C.W. Fundamentals of biochemistry: life at the molecular level. fifth ed ed.: John Wiley and Sons, 2016.
[118] Merian, E., Anke, M., Ihnat, M., and Stoeppler, M. Elements and their compounds in the environment: occurrence, analysis and biological relevance. second ed ed.: Wiley-VCH Verlag GmbH & Co. KGaA, 2004.
[119] Masindi, V. and Muedi, K.L. Environmental contamination by heavy metals. in Heavy metals: IntechOpen, 2018.
[120] McGowen, S., Basta, N., and Brown, G. Use of diammonium phosphate to reduce heavy metal solubility and transport in smelter-contaminated soil. Journal of Environmental Quality 30(2) (2001): 493-500. https://doi.org/10.2134/jeq2001.302493x.
[121] Gautam, P.K., Gautam, R., Banerjee, S., Chattopadhyaya, M., and Pandey, J. Heavy metals in the environment: Fate, transport, toxicity and remediation technologies, pp. 101-130. Nava Science Publishers, Inc. . in, 2016.
[122] Rajaganapathy, V., Xavier, F., Sreekumar, D., and Mandal, P. Heavy metal contamination in soil, water and fodder and their presence in livestock and products: a review. Journal of Environmental Science and Technology 4(3) (2011): 234-249. https://doi.org/10.3923/jest.2011.234.249.
[123] Weissmannová, H.D. and Pavlovský, J. Indices of soil contamination by heavy metals–methodology of calculation for pollution assessment (minireview). Environmental monitoring and assessment 189(12) (2017): 1-25. https://doi.org/10.1007/s10661-017-6340-5.
[124] Dauda, M. and Odoh, R. Heavy metals assessment of soil in the vicinity of fuel filling station in some selected local government areas of Benue State, Nigeria.

Pelagia research library, Der chemica sinica 3 (2012): 1329-1336. https://www.researchgate.net/publication/327861148.

[125] Wuana, R.A. and Okieimen, F.E. Heavy metals in contaminated soils: a review of sources, chemistry, risks and best available strategies for remediation. Isrn Ecology 2011 (2011): 1-21. https://doi.org/10.5402/2011/402647.

[126] Adriano, D.C. in Arsenic trace elements in terrestrial environments, pp. 219-261: Springer, 2001.

[127] Adriano, D.C., Wenzel, W., Vangronsveld, J., and Bolan, N. Role of assisted natural remediation in environmental cleanup. Geoderma 122(2-4) (2004): 121-142. https://doi.org/10.1016/j.geoderma.2004.01.003.

[128] Jignesh, S., Vineeta, K., Abhay, S., and Vilasrao, K. Analytical methods for estimation of metals. Int. J. Res. Pharm. Chem 2(1) (2012): 146-163. http://www.ijrpc.com/files/v2i1%20(23).pdf.

[129] Tho, N.V. The concentration of heavy metal (As, Zn, Cu, Cd and Pb) at coastal areas in Ngoc Hien District, Ca Mau province. Master thesis, Can Tho University, 2007.

[130] Nga and Nu, P.V. Arsenic pollution in suface water in the Vietnamse Mekong Delta. Scientific Journal of Can Tho University (2011): 183-192.

[131] WHO. Health risks of heavy metals from long-range transboundary air pollution. World Health Organization. 2007, Copenhagen: WHO Regional Office for Europe.

[132] Castro-González, M. and Méndez-Armenta, M. Heavy metals: Implications associated to fish consumption. Environmental toxicology and pharmacology 26(3) (2008): 263-271. https://doi.org/10.1016/j.etap.2008.06.001.

[133] Figueroa Benavides, E. Are more restrictive food cadmium standards justifiable health safety measures or opportunistic barriers to trade? An answer from economics and public health. 389(1) (2008): 1-9. https://doi.org/10.1016/j.scitotenv.2007.08.015.

[134] Morais, S., Costa, F., and Pereira, M. Heavy metals and human health. in Chapters, in: Jacques Oosthuizen (ed.), Environmental health-emerging issues and practice,: IntechOpen., 2012.

[135] Chappell, W.R., Abernathy, C.O., and Calderon, R.L. Arsenic exposure and health effects IV. Elsevier., 2001.

[136] Chou, C.-H. and Harper, C. Toxicological profile for arsenic, pp. 396. The Centers for Disease Control and Prevention (CDC). http://dx.doi.org/10.15620/cdc:1148. 2007.

[137] Lansdown, A.B. The carcinogenicity of metals: human risk through occupational and environmental exposure, first ed. Royal Society of Chemistry, 2013.

[138] Harmanescu, M., Alda, L.M., Bordean, D.M., Gogoasa, I., and Gergen, I. Heavy metals health risk assessment for population via consumption of vegetables grown in old mining area; a case study: Banat County, Romania. Chemistry Central Journal 5(1) (2011): 1-10. https://doi.org/10.1186/1752-153X-5-64.

[139] Tchounwou, Patlolla, A., and Centeno, J. CarcinogenY ic and systemic health effects associated with arsenic expoY sure2a critical review. Toxicol. Pathol 31 (2003): 575-88.

[140] Tseng, C.-H. Blackfoot disease and arsenic: a never-ending story. Journal of Environmental Science and Health 23(1) (2005): 55-74. :

https://doi.org/10.1081/GNC-200051860.

[141] Steinmaus, C., Carrigan, K., Kalman, D., Atallah, R., Yuan, Y., and Smith, A.H. Dietary intake and arsenic methylation in a US population. Environmental health perspectives 113(9) (2005): 1153-1159. https://doi.org/10.1289/ehp.7907.

[142] Tchounwou, Centeno, J.A., and Patlolla, A.K. Arsenic toxicity, mutagenesis, and carcinogenesis–a health risk assessment and management approach. Molecular and cellular biochemistry 255(1-2) (2004): 47-55. https://doi.org/10.1023/B:MCBI.0000007260.32981.b9.

[143] Sutton, D., Tchounwou, P., Ninashvili, N., and Shen, E. Mercury induces cytotoxicity and transcriptionally activates stress genes in human liver carcinoma (HepG2) cells. International Journal of Molecular Sciences 3(9) (2002): 965-984. https://doi.org/10.3390/i3090965.

[144] Yedjou, C., Moore, P., and Tchounwou, P. Dose-and time-dependent response of human leukemia (HL-60) cells to arsenic trioxide treatment. International journal of environmental research and public health 3(2) (2006): 136-140. https://doi.org/10.3390/ijerph2006030017.

[145] Singh and Kalamdhad, A.S. Effects of heavy metals on soil, plants, human health and aquatic life. International journal of Research in Chemistry and Environment 1(2) (2011): 15-21. https://www.researchgate.net/publication/265849316.

[146] UNEP. Lead Pollution and Poisoning Crisis Environmental Emergency Response Mission Zamfara State, Nigeria September/October. UNEP/OCHA Environment Unit., 2010.

[147] Abdul, W.S. and Marikar, F. The environmental impact of gold mines: pollution by heavy metals. Open Engineering 2(2) (2012): 304-313. https://doi.org/10.2478/s13531-011-0052-3.

[148] Kabata-Pendias, A. Trace elements in soils and plants. CRC Press, Boca Raton London, New York Washington, D.C. 2000.

[149] Flora, G., Gupta, D., and Tiwari, A. Toxicity of lead: a review with recent updates. Interdisciplinary toxicology 5(2) (2012): 47-58. https://doi.org/10.2478/v10102-012-0009-2 .

[150] Ullah, N., Ahmad, W., Malik, Z., Zia, M., and Zhou, W. Enhancing the lead phytostabilization in wetland plant Juncus effusus L. through somaclonal manipulation and EDTA enrichment. Arabian Journal of Chemistry 10 (2014): S3310-S3317. https://doi.org/10.1016/j.arabjc.2014.01.009.

[151] Wadhwa, N., Mathew, B.B., Jatawa, S., and Tiwari, A. Lipid peroxidation: mechanism, models and significance. Int J Curr Sci 3 (2012): 29-38. https://www.researchgate.net/publication/262176367.

[152] Murphy, M.M., Lawson, J.A., Mathew, S.J., Hutcheson, D.A., and Kardon, G. Satellite cells, connective tissue fibroblasts and their interactions are crucial for muscle regeneration. Development 138(17) (2011): 3625-3637. https://doi.org/10.1242/dev.064162.

[153] Nirel, P. and Pasquini, F. Differentiation of copper pollution origin: agricultural and urban sources. NOVATECH (2010): 1-7. http://hdl.handle.net/2042/35666.

[154] Tchounwou, P.B., Yedjou, C.G., Patlolla, A.K., and Sutton, D.J. Heavy metal toxicity and the environment. in Molecular, clinical and environmental toxicology, pp. 133-164: Springer, 2012.

[155] Panagos, P., Ballabio, C., Lugato, E., Jones, A., Borrelli, P., Scarpa, S., Orgiazzi, A., and Montanarella, L. Potential Sources of Anthropogenic Copper Inputs to European Agricultural Soils. Sustainability 10(7) (2018): 2380.
[156] US.EPA. Guidance on the use of models and other analyses for demonstrating attainment of air quality goals for ozone, PM2. 5, and regional haze. US Environmental Protection Agency, O.o.A.Q.P.a.S., Editor. 2007.
[157] Andersen, C.W., Borfecchia, E., Bremholm, M., Jørgensen, M.R.V., Vennestrøm, P.N.R., Lamberti, C., Lundegaard, L.F., and Iversen, B.B. Redox-Driven Migration of Copper Ions in the Cu-CHA Zeolite as Shown by the In Situ PXRD/XANES Technique. Angewandte Chemie International Edition 56(35) (2017): 10367-10372.
[158] Pohl, P., Stecka, H., Greda, K., and Jamroz, P. Bioaccessibility of Ca, Cu, Fe, Mg, Mn and Zn from commercial bee honeys. Food Chemistry 134(1) (2012): 392-396. https://doi.org/10.1016/j.foodchem.2012.02.065.
[159] Trumbo, P., Yates, A.A., Schlicker, S., and Poos, M. Dietary reference intakes: vitamin A, vitamin K, arsenic, boron, chromium, copper, iodine, iron, manganese, molybdenum, nickel, silicon, vanadium, and zinc. National Academies Press., 2001.
[160] De Romaña, D.L., Olivares, M., Uauy, R., and Araya, M. Risks and benefits of copper in light of new insights of copper homeostasis. Journal of Trace Elements in Medicine and Biology 25(1) (2011): 3-13. https://doi.org/10.1016/j.jtemb.2010.11.004.
[161] Gaetke, L.M., Chow-Johnson, H.S., and Chow, C.K. Copper: toxicological relevance and mechanisms. Archives of Toxicology 88(11) (2014): 1929-1938.
[162] Bleackley, M.R. and MacGillivray, R.T. Transition metal homeostasis: from yeast to human disease. Biometals 24(5) (2011): 785-809.
[163] Haidari, M., Javadi, E., Kadkhodaee, M., and Sanati, A. Enhanced susceptibility to oxidation and diminished vitamin E content of LDL from patients with stable coronary artery disease. Clinical chemistry 47(7) (2001): 1234-1240. https://doi.org/10.1093/clinchem/47.7.1234.
[164] Song, M., Zhou, Z., Chen, T., Zhang, J., and McClain, C.J. Copper deficiency exacerbates bile duct ligation-induced liver injury and fibrosis in rats. Journal of Pharmacology and Experimental Therapeutics 339(1) (2011): 298-306. https://doi.org/10.1124/jpet.111.184325.
[165] Simon-Hettich, B., Wibbertmann, A., Wagner, Tomaska, and Malcolm. Environmental health criteria 221 ZINC. 2001, World Health Organization Geneva, 2001.
[166] EPA, U. Methodology for deriving ambient water quality criteria for the protection of human health. 2000, Office of Water Washington, DC.
[167] Roney, N. Toxicological profile for zinc. Agency for toxic substances and disease registry. https://www.atsdr.cdc.gov/toxprofiles/tp60.pdf., 2005.
[168] US.EPA. Toxicological review of zinc and compounds, EPA/635/R-05/002. Washington, D.U.E.P.A.h.c.e.g.n.i.i.d.d.t.t.p., Editor. 2005. 6.
[169] Plum, L.M., Rink, L., and Haase, H. The essential toxin: impact of zinc on human health. International journal of environmental research and public health 7(4) (2010): 1342-1365. https://doi.org/10.3390/ijerph7041342.
[170] Wang, Q., Lu, X., Jia, P., Qi, C., and Ding, F. A review of surface water quality

models. The Scientific World Journal 2013 (2013): 1-8. https://doi.org/10.1155/2013/231768.

[171] Deltares. 3D/2D modelling suite for integral water solutions, pp. 48. Deltares: Delft, The Netherlands., 2014.

[172] Hoanh, C., Ngo Dang, P., Gowing, J., Tuong, T.P., Ngoc, N., and Hien, N. Hydraulic and water quality modeling: A tool for managing land use conflicts in inland coastal zones. Water Policy 11(S1) (2009): 106–120. https://doi.org/10.2166/wp.2009.107.

[173] Long, T.Q. Assessment of surface water quality in Ca Mau provine. Journal of Agricultrue and Rural Development 3-4 (2015): 124-130.

[174] Lien, N.T.K. and Huy, Q.H. the characteristics of water quality in mainstream and tributaries
of the Hau River. Scientific Journal of Can Tho University 43 (2016): 68-79.

[175] Giao, N.T. Analysis of Surface Water Quality using Multivariate Statistical Approaches: A case study in Ca Mau Peninsula, Vietnam. Pollution 8(2) (2022): 463-477.

[176] Viet, T.V. and Sakuramoto. Population dynamics of Metapenaeus ensis (Decapoda: Penaeidae) in a coastal region of the Mekong Delta, Vietnam. Asian fisheries science 25(1) (2012): 1-14. https://doi.org/10.33997/j.afs.2012.25.1.001.

[177] DHPC. General introduction about Dong Hai District in Bac Lieu province. http://donghai.baclieu.gov.vn/pages/gioi-thieu-chung.aspx (accessed 17 August 2020). [Online]. 2020.

[178] DHPC. Implementation results in 2019 and plan for 2020 on agricultural and rural development in the district. 2019: Dong Hai People's Committee. 8.

[179] DDPC. The results were implemented in productive development in 2019 and solutions and tasks will be deployed in 2020. 2019: Dam Do People's Committee. 10.

[180] DDPC. General introduction on geographical location in Dam Doi district, Ca Mau province. http://damdoi.camau.gov.vn/wps/portal/?1dmy&page=trangchitiet&urile=wcm%3apath%3a/huyendamdoilibrary/siteofdamdoi/noidungtrang/gioithieu/gioithieuchung/vitridialy (accessed 18 August 2020). [Online]. 2020.

[181] Cassou, E., Tran, D.N., Nguyen, T.H., Dinh, T.X., Nguyen, C.V., Cao, B.T., Jaffee, S., and Ru, J. An overview of agricultural pollution in Vietnam: The aquaculture sector. 2017, The World Bank. 48.

[182] Anh, P.T., Kroeze, C., Bush, S.R., and Mol, A.P. Water pollution by Pangasius production in the Mekong Delta, Vietnam: causes and options for control. Aquaculture Research 42(1) (2010): 108-128. https://doi.org/10.1111/j.1365-2109.2010.02578.x.

[183] DOWRM. An alarm of organic pollution on rivers and canals of Ca Mau-Department of Water Resources Management. http://dwrm.gov.vn/index.php?language=vi&nv=news&op=Hoat-dong-cua-dia-phuong/Bao-dong-o-nhiem-huu-co-tren-song-rach-Ca-Mau-6156 (accessed 23 Semptember, 2019). [Online]. 2017.

[184] Tareq, S.M., Rahaman, M., Rikta, S., Islam, S.N., and Sultana, M.S. Seasonal variations in water quality of the Ganges and Brahmaputra River, Bangladesh.

Jahangirnagar University Environmental Bulletin 2 (2013): 71-82. https://doi.org/10.3329/jueb.v2i0.16332.

[185] APHA. Standard methods for the examination of water and wastewater. American Public Health Association, Washington DC, 1999.

[186] Hassan, M., Rahman, M.A.T., Saha, B., and Kamal, A.K.I. Status of heavy metals in water and sediment of the Meghna River, Bangladesh. American Journal of Environmental Sciences 11(6) (2015): 427. https://doi.org/10.3844/ajessp.2015.427.439.

[187] Manoj, K., Kumar, B., and Padhy, P.K. Characterisation of metals in water and sediments of subarnarekha river along the Projects' Sites in lower Basin, India. Universal Journal of Environmental Research and Technology 2(5) (2012): 402-410. http://www.environmentaljournal.org/2-5/ujert-2-5-5.pdf. .

[188] Jumbe, A.S. and Nandini, N. Heavy metals analysis and sediment quality values in urban lakes. American Journal of Environmental Sciences 5(6) (2009): 678. https://doi.org/10.3844/ajessp.2009.678.687.

[189] Nelson, D.W. and Sommers, L.E. Total carbon, organic carbon, and organic matter. Methods of soil analysis: Part 3 Chemical methods 5 (1996): 961-1010. https://doi.org/10.2136/sssabookser5.3.c34.

[190] MONRE. National technical regulation on surface water quality. Ministry of Natural Resources and Environment. 2015.

[191] US.EPA. Parameters of Water Quality: Interpretations and Standards. 2001, Environmental Protection Agency. https://www.epa.ie/pubs/advice/water/quality/Water_Quality.pdf.

[192] MONRE. National Technical Regulation on Sediment Quality. Ministry of Natural Resources and Environment. 2017.

[193] Yaqin, J., Yinchang, F., Jianhui, W., Tan, Z., Zhipeng, B., and Chiqing, D. Using geoaccumulation index to study source profiles of soil dust in China. Journal of Environmental Sciences 20(5) (2008): 571-578. https://doi.org/10.1016/S1001-0742(08)62096-3.

[194] Muller, G. Index of geoaccumulation in sediments of the Rhine River. Geojournal 2 (1969): 108-118.

[195] Abrahim, G. and Parker, R. Assessment of heavy metal enrichment factors and the degree of contamination in marine sediments from Tamaki Estuary, Auckland, New Zealand. Environmental monitoring and assessment 136(1-3) (2008): 227-238. https://doi.org/10.1007/s10661-007-9678-2.

[196] Muller, G. Heavy metal loads of the sediments of Neckar River and its affluent. Chemical Journal 105 (1981): 157-164.

[197] Varol, M. Assessment of heavy metal contamination in sediments of the Tigris River (Turkey) using pollution indices and multivariate statistical techniques. Journal of Hazardous Materials 195 (2011): 355-364. https://doi.org/10.1016/j.jhazmat.2011.08.051.

[198] Hakanson, L. An ecological risk index for aquatic pollution control. A sedimentological approach. Water research 14(8) (1980): 975-1001.https://doi.org/10.1016/0043-1354(80)90143-8.

[199] El-Sammak, A. and Aboul-Kassim, T. Metal pollution in the sediments of Alexandria region, Southeastern Mediterranean, Egypt. Bulletin of environmental contamination and toxicology 63(2) (1999): 263-270.

https://doi.org/10.1007/s001289900975.

[200] Tomlinson, D., Wilson, J., Harris, C., and Jeffrey, D. Problems in the assessment of heavy-metal levels in estuaries and the formation of a pollution index. Helgoländer meeresuntersuchungen 33(1) (1980): 566–57. https://doi.org/10.1007/BF02414780.

[201] Turekian, K.K. and Wedepohl, K.H. Distribution of the elements in some major units of the earth's crust. Geological Society of America Bulletin 72(2) (1961): 175-192. https://doi.org/10.1130/0016-7606(1961)72[175:DOTEIS]2.0.CO;2.

[202] Abdi, H. and Williams, L.J. Principal component analysis. WIREs Computational Statistics 2(4) (2010): 433-459.

[203] Yang, W., Zhao, Y., Wang, D., Wu, H., Lin, A., and He, L. Using principal components analysis and IDW interpolation to determine spatial and temporal changes of surface water quality of Xin'anjiang river in Huangshan, China. International journal of environmental research and public health 17(8) (2020): 2942.

[204] Sheytanova, T. A Monte Carlo study comparing three methods for determining the number of principal components and factors. 2015.

[205] Sperandei, S. Understanding logistic regression analysis. Biochemia medica 24 (2014): 12-8.

[206] Ahmed, H., Siddique, M., Iqbal, M., and Hussain, F. Comparative study of interpolation methods for mapping soil pH in the apple orchards of Murree, Pakistan. Soil and Environment 36 (2017): 70-76. https://doi.org/10.25252/SE/17/41154.

[207] Balakrishnan, P., Saleem, A., and Mallikarjun, N. Groundwater quality mapping using geographic information system (GIS): A case study of Gulbarga City, Karnataka, India. African Journal of Environmental Science and Technology 5(12) (2011): 1069-1084. https://doi.org/ 10.5897/AJEST11.134.

[208] Deltares. Delft3D-flow user's manual: simulation of multi-dimensional hydrodynamic flows and transport phenomena, including sediments, pp. 710. Deltares, Delft, The Netherlands., 2014.

[209] Platzek, F.W., Stelling, G.S., Jankowski, J.A., and Pietrzak, J.D. Accurate vertical profiles of turbulent flow in z-layer models. Water Resources Research 50(3) (2014): 2191-2211.

[210] Hessl, A., Miller, J., Kernan, J., Keenum, D., and McKenzie, D. Mapping paleo-fire boundaries from binary point data: comparing interpolation methods. The Professional Geographer 59(1) (2007): 87-104. https://doi.org/10.1111/j.1467-9272.2007.00593.x.

[211] Andes, L.C. and Cox, A.L. Rectilinear inverse distance weighting methodology for bathymetric cross-section interpolation along the Mississippi River. Journal of Hydrologic Engineering 22(7) (2017): 04017014. https://doi.org/10.1061/(ASCE)HE.1943-5584.0001514.

[212] Andutta, F.P., de Miranda, L.B., Schettini, C.A.F., Siegle, E., da Silva, M.P., Izumi, V.M., and Chagas, F.M. Temporal variations of temperature, salinity and circulation in the Peruípe river estuary (nova Viçosa, BA). Continental Shelf Research 70 (2013): 36-45. https://doi.org/10.1016/j.csr.2013.03.013.

[213] Fatema, K., Omar, W., and Isa, M. Effects of tidal events on the water quality in the Merbok estuary, Kedah, Malaysia. Journal of Environmental Science and

Natural Resources 8(2) (2015): 15-19. https://doi.org/10.3329/jesnr.v8i2.26858.
[214] Dallas, H. Water temperature and riverine ecosystems: An overview of knowledge and approaches for assessing biotic responses, with special reference to South Africa. Water Sa 34(3) (2008): 393-404. https://doi.org/10.4314/wsa.v34i3.180634.
[215] Hinga, K.R. Effects of pH on coastal marine phytoplankton. Marine Ecology Progress Series 238 (2002): 281-300. https://doi.org/10.3354/meps238281.
[216] Lemonnier, H., Bernard, E., Boglio, E., Goarant, C., and Cochard, J.-C. Influence of sediment characteristics on shrimp physiology: pH as principal effect. Aquaculture 240(1-4) (2004): 297-312. https://doi.org/10.1016/j.aquaculture.2004.07.001.
[217] Barakat, A., El Baghdadi, M., Rais, J., Aghezzaf, B., and Slassi, M. Assessment of spatial and seasonal water quality variation of Oum Er Rbia River (Morocco) using multivariate statistical techniques. International soil and water conservation research 4(4) (2016): 284-292.
[218] Barron, J.J. and Ashton, C. The effect of temperature on conductivity measurement. TSP 7(3) (2005): 1-5.
[219] Korey, C. Water quality field guide. the United States of America: PASCO scientific
10101 Foothills Blvd, 2010.
[220] Rusydi, A.F. Correlation between conductivity and total dissolved solid in various type of water: A review. in IOP Conference Series: Earth and Environmental Science. https://doi.org/10.1088/1755-1315/118/1/012019., p. 012019: IOP Publishing, 2018.
[221] Weber-Scannell, P.K. and Duffy, L.K. Effects of total dissolved solids on aquatic organism: a review of literature and recommendation for salmonid species. in American Journal of Environmental Sciences: Citeseer, 2007.
[222] Geawhari, M.A., Huff, L., Mhammdi, N., Trakadas, A., and Ammar, A. Spatial-temporal distribution of salinity and temperature in the Oued Loukkos estuary, Morocco: using vertical salinity gradient for estuary classification. SpringerPlus 3(1) (2014): 1-9.
[223] Velasco, J., Gutiérrez-Cánovas, C., Botella-Cruz, M., Sánchez-Fernández, D., Arribas, P., Carbonell, J.A., Millán, A., and Pallarés, S. Effects of salinity changes on aquatic organisms in a multiple stressor context. Philosophical Transactions of the Royal Society B 374(1764) (2019): 20180011.
[224] Dauda, A.B., Ajadi, A., Tola-Fabunmi, A.S., and Akinwole, A.O. Waste production in aquaculture: Sources, components and managements in different culture systems. Aquaculture and Fisheries 4(3) (2019): 81-88. https://doi.org/10.1016/j.aaf.2018.10.002.
[225] Augustijn, D. and Fares, A. Temporal and spatial variations in total suspended and dissolved solids in the upper part of Manoa Stream, Hawaii. Journal of sustainable watershed science and management 1(1) (2011): 1-9. https://doi.org/10.5147/jswsm.v1i1.128.
[226] Jiang, X., Lu, B., and He, Y. Response of the turbidity maximum zone to fluctuations in sediment discharge from river to estuary in the Changjiang Estuary (China). Estuarine, Coastal and Shelf Science 131 (2013): 24-30.
[227] Uncles, R.J. Physical Properties and Processes in the Bristol Channel and Severn

Estuary. Marine pollution bulletin 61 (2010): 5-20.
[228] Kumari, M., Tripathi, S., Pathak, V., and Tripathi, B. Chemometric characterization of river water quality. Environmental monitoring and assessment 185(4) (2013): 3081-3092.
[229] Connolly, N., Crossland, M., and Pearson, R. Effect of low dissolved oxygen on survival, emergence, and drift of tropical stream macroinvertebrates. Journal of the North American Benthological Society 23(2) (2004): 251-270.
[230] Deacutis, C.F. Dissolved oxygen. Encyclopedia of estuaries edited by Michael J. Kennish/Encyclopedia of Earth Science Series/Springer Science and Business Media Dordrecht 2016. in, pp. 202. https://doi.org/10.1007/978-94-017-8801-4_72., 2016.
[231] Kroupova, H., Machova, J., and Svobodova, Z. Nitrite influence on fish: a review. Veterinarni medicina-praha- 50(11) (2005): 461. https://doi.org/10.17221/5650-VETMED.
[232] Thakur, D.P. and Lin, C.K. Water quality and nutrient budget in closed shrimp (Penaeus monodon) culture systems. Aquacultural engineering 27(3) (2003): 159-176.
[233] Yue, F., Liu, X., Li, J., Zhu, Z., and Wang, Z. Using nitrogen isotopic approach to identify nitrate sources in waters of Tianjin, China. Bull Environ Contam Toxicol 85(6) (2010): 562-7.
[234] Tabayashi, Y. and Koba, K. Heterogeneous Atmospheric Nitrogen Deposition Effects Upon the Nitrate Concentration of Stream Waters in a Forested Mountain Area. Water, Air, & Soil Pollution 216 (2011): 105-115. https://doi.org/10.1007/s11270-010-0519-5.
[235] Mohan Raj, V., Padmavathy, S., and Sivakumar, S. Water quality Parameters and it influences in the Ennore estuary and near Coastal Environment with respect to Industrial and Domestic sewage. Inter. Res. J. of Environ. Sci 2(7) (2013): 20-25.
[236] Adam, S., Pawert, M., Lehmann, R., Roth, B., Müller, E., and Triebskorn, R. Physicochemical and morphological characterization of two small polluted streams in southwest Germany. Journal of Aquatic Ecosystem Stress and Recovery 8(3) (2001): 179-194.
[237] Dari, B., Rogers, C.W., and Walsh, O.S. Understanding factors controlling ammonia volatilization from fertilizer nitrogen applications. https://www.extension.uidaho.edu/publishing/html/BUL926-Understanding-Factors-Controlling-Ammonia-Volatilization-from-Fertilizer-Nitrogen-Applications.aspx?title=Search&category1=Search&category2=NULL (accessed 15 November 2020). 2019.
[238] EPA. Parameters of water quality: interpretation and standards. 2001, Environmental Protection Agency Ireland.
[239] Claude, B.E. and Green, B.W. Coastal water quality monitoring in shrimp farming areas, an example from Honduras. Report prepared under the World Bank, NACA, WWF and FAO Consortium program on shrimp farming and the environment. Work in progress for public discussion. Published by the Consortium 29 (2002).
[240] Sahu, B., Adhikari, S., and Dey, L. Carbon, nitrogen and phosphorus budget in shrimp (Penaeus monodon) culture ponds in eastern India. Aquaculture

International 21 (2012).
[241] Jialu, L. and Qiting, Z. Forms of nitrogen and phosphorus in suspended solids: A case study of Lihu Lake, China. Sustainability 12(12) (2020): 5026. https://doi.org/10.3390/su12125026.
[242] Wasley, D. Phosphorus: Sources, Forms, Impact on Water Quality-A General Overview. Minnesota Pollution Control Agency, Minnesota (2007).
[243] Cavalcante, H., Araújo, F., Noyma, N.P., and Becker, V. Phosphorus fractionation in sediments of tropical semiarid reservoirs. Science of The Total Environment 619-620 (2018): 1022-1029.
[244] Boyd, C.E. and Green, B.W. Coastal water quality monitoring in shrimp farming areas, an example from Honduras. Report prepared under the World Bank, NACA, WWF and FAO Consortium program on shrimp farming and the environment. Work in progress for public discussion. Published by the Consortium 29 (2002).
[245] Kaoud Hussein, A. Article review: heavy metals and pesticides in aquaculture: health problems. European Journal of Academic Essays 2(9) (2015): 15-22.
[246] Katip, A. Bioaccumulation of Trace Metals in Wastewater-Fed Aquaculture: A Case Study in Turkey. Polish Journal of Environmental Studies 28(6) (2019).
[247] Kundu, P. and Cohen, I. Fluid Mechanics, 3rd edition. Academic Press. Elsevier., 2004.
[248] Sahoo, K., Jee, P., Dhal, N., and Das, R. Physico-chemical sediment properties of mangroves of Odisha, India. J Oceanogr Mar Res 5(162) (2017): 2. https://doi.org/10.4172/2572-3103.1000162.
[249] Zhao, D., Cao, X., Huang, R., Zeng, J., and Wu, Q.L. Variation of bacterial communities in water and sediments during the decomposition of Microcystis biomass. PloS one 12(4) (2017): 1-17. https://doi.org/10.1371/journal.pone.0176397.
[250] Burton, E.D., Phillips, I.R., and Hawker, D.W. Reactive sulfide relationships with trace metal extractability in sediments from southern Moreton Bay, Australia. Marine Pollution Bulletin 50(5) (2005): 589-595.
[251] Sidi, N., Aris, A.Z., Talib, S.N., Johan, S., Yusoff, T.S.T.M., and Ismail, M.Z. Influential factors on the cation exchange capacity in sediment of Merambong Shoal, Johor. Procedia Environmental Sciences 30 (2015): 186-189. https://doi.org/10.1016/j.proenv.2015.10.033.
[252] Malvankar, N., King, G., and Lovley, D. Centimeter-long electron transport in marine sediments via conductive minerals. The ISME journal 9 (2014): 527–531. https://doi.org/10.1038/ismej.2014.131.
[253] Ramaswamy, V., Gaye, B., Shirodkar, P.V., Rao, P.S., Chivas, A.R., Wheeler, D., and Thwin, S. Distribution and sources of organic carbon, nitrogen and their isotopic signatures in sediments from the Ayeyarwady (Irrawaddy) continental shelf, northern Andaman Sea. Marine Chemistry 111(3) (2008): 137-150. https://doi.org/10.1016/j.marchem.2008.04.006.
[254] Liu, D., Li, X., Emeis, K.C., Wang, Y., and Richard, P. Distribution and sources of organic matter in surface sediments of Bohai Sea near the Yellow River Estuary, China. Estuarine, Coastal and Shelf Science 165(12) (2015): 128-136. https://doi.org/10.1016/j.ecss.2015.09.007.
[255] Oanh, T.T.K. Characteristics of the sediments and changes in the coastal line in

Ca Mau province, the Vietnamese Mekong Delta. Journal of Earth Sciences 34(1) (2012): 1-9.

[256] Carrasco, M., López-Ramírez, J.A., Benavente, J., López-Aguayo, F., and Sales, D. Assessment of urban and industrial contamination levels in the bay of Cádiz, SW Spain. Marine Pollution Bulletin 46(3) (2003): 335-345. https://doi.org/10.1016/S0025-326X(02)00420-4.

[257] Gu, Y.Y. and Yeung, A. Desorption of cadmium from a natural Shanghai clay using citric acid industrial wastewater. Journal of hazardous materials 191 (2011): 144-9. https://doi.org/10.1016/j.jhazmat.2011.04.054.

[258] Pachana, K., Wattanakornsiri, A., and Nanuam, J. Heavy Metal Transport and Fate in the Environmental Compartments. Naresuan University Science Journal 7 (2010): 1-11.

[259] Equeenuddin, S.M., Tripathy, S., Sahoo, P., and Panigrahi, M. Metal behavior in sediment associated with acid mine drainage stream: role of pH. Journal of Geochemical Exploration 124 (2013): 230-237. https://doi.org/10.1016/j.gexplo.2012.10.010.

[260] Pérez-Esteban, J., Escolástico, C., Moliner, A., and Masaguer, A. Chemical speciation and mobilization of copper and zinc in naturally contaminated mine soils with citric and tartaric acids. Chemosphere 90(2) (2013): 276-283. https://doi.org/10.1016/j.chemosphere.2012.06.065.

[261] Aryal, R., Duong, T.T.T., Lee, B.-K., Hossain, M., Kandel, D., Kamruzzaman, M., Beecham, S., and Chong, M.N. Organic matter composition variability in road sediment and its role in binding heavy metals. Sustainable Environment Research 24 (2014): 81-91.

[262] Baran, A., Mierzwa-Hersztek, M., Gondek, K., Tarnawski, M., Szara, M., Gorczyca, O., and Koniarz, T. The influence of the quantity and quality of sediment organic matter on the potential mobility and toxicity of trace elements in bottom sediment. Environmental Geochemistry and Health 41(6) (2019): 2893-2910. https://doi.org/10.1007/s10653-019-00359-7. .

[263] Baran, A., Mierzwa-Hersztek, M., Gondek, K., Szara, M., and Tarnawski, M. The content and composition of organic matter in bottom sediments of the Rybnik reservoir – preliminary studies. Geology, Geophysics & Environment 44 (2018): 309–317. https://doi.org/10.7494/geol.2018.44.3.309.

[264] Louhi, A., Hammadi, A., and Achouri, M. Determination of some heavy metal pollutants in sediments of the Seybouse River in Annaba, Algeria. Air, Soil and Water Research 5 (2012): 91-101. https://doi.org/10.4137/ASWR.S10081.

[265] Peng, J., Song, Y.-H., Yuan, P., Cui, X.-Y., and Qiu, G. The remediation of heavy metals contaminated sediment. Journal of Hazardous Materials 161 (2009): 633-640. https://doi.org/10.1016/j.jhazmat.2008.04.061.

[266] Gijs, D.L., De Vos, R., Vandecasteele, B., Lesage, E., Tack, F.M., and Verloo, M.G. Effect of salinity on heavy metal mobility and availability in intertidal sediments of the Scheldt estuary. Estuarine, Coastal and Shelf Science 77(4) (2008): 589-602. https://doi.org/10.1016/j.ecss.2007.10.017.

[267] Acosta, J., Jansen, B., Kalbitz, K., Faz, A., and Martínez-Martínez, S. Salinity increases mobility of heavy metals in soils. Chemosphere 85 (2011): 1318-24. https://doi.org/10.1016/j.chemosphere.2011.07.046.

[268] Wong, V.N., Johnston, S.G., Burton, E.D., Bush, R.T., Sullivan, L.A., and

Slavich, P.G. Seawater causes rapid trace metal mobilisation in coastal lowland acid sulfate soils: Implications of sea level rise for water quality. Geoderma 160(2) (2010): 252-263.

[269] Zhao, S., Feng, C., Wang, D., Liu, Y., and Shen, Z. Salinity increases the mobility of Cd, Cu, Mn, and Pb in the sediments of Yangtze Estuary: relative role of sediments' properties and metal speciation. Chemosphere 91(7) (2013): 977-984.

[270] Jiao, Z., Li, H., Song, M., and Wang, L. Ecological risk assessment of heavy metals in water and sediment of the Pearl River Estuary, China. Materials Science and Engineering 394 (2018): 1-13. https://doi.org/10.1088/1757-899X/394/5/052055.

[271] Hacısalihoğlu, S. and Karaer, F. Relationships of Heavy Metals in Water and Surface Sediment with Different Chemical Fractions in Lake Uluabat, Turkey. Polish Journal of Environmental Studies 25(5) (2016): 1937-1946. https://doi.org/10.15244/pjoes/62908.

[272] Tao, Y., Yuan, Z., Wei, M., and Xiaona, H. Characterization of heavy metals in water and sediments in Taihu Lake, China. Environmental monitoring and assessment 184 (2011): 4367-82. https://doi.org/10.1007/s10661-011-2270-9.

[273] Spencer, K.L., Cundy, A.B., and Croudace, I.W. Heavy metal distribution and early-diagenesis in salt marsh sediments from the Medway Estuary, Kent, UK. Estuarine, Coastal and Shelf Science 57(1) (2003): 43-54. https://doi.org/10.1016/S0272-7714(02)00324-4.

[274] Botté, S.E., Freije, R.H., and Marcovecchio, J.E. Distribution of several heavy metals in tidal flats sediments within Bahía Blanca Estuary (Argentina). Water, Air, & Soil Pollution 210(1-4) (2010): 371-388. https://doi.org/10.1007/s11270-009-0260-0.

[275] Rubinos, D., Iglesias, L., Díaz-Fierros, F., and Barral, M.T. Interacting Effect of pH, Phosphate and Time on the Release of Arsenic from Polluted River Sediments (Anllns River, Spain). 17 (2011): 281-306.

[276] Islam, M.D., Raknuzzaman, M., Mamun, A.l.H., M. D;, and Islam, M. Heavy metal pollution in surface water and sediment: A preliminary assessment of an urban river in a developing country. Ecological Indicators 48 (2015): 182-191. https://doi.org/10.1016/j.ecolind.2014.08.016.

[277] Athanasia, D., Kalavrouziotis, I., and Varnavas, S. Geochemical investigations regarding the variability of metal pollution in the Amvrakikos Bay, Greece. Global NEST Journal 21(1) (2018): 7-13. https://doi.org/10.30955/gnj.002733.

[278] Davies, O. and Ugwumba, O. Tidal influence on nutrients status and phytoplankton population of Okpoka Creek, Upper Bonny Estuary, Nigeria. Journal of Marine Biology 2013 (2013): 1-17. http://dx.doi.org/10.1155/2013/684739.

[279] Purnaini, R. and Purwono, S. Tidal influence on water quality of Kapuas Kecil river downstream. 31 (2018): 04006. https://doi.org/10.1051/e3sconf/20183104006.

[280] Fatema, K., Omar, W., and Isa, M. Effects of Tidal Events on the Water Quality in the Merbok Estuary, Kedah, Malaysia. Journal of Environmental Science and Natural Resources 8(2) (2015): 15-19. https://doi.org/10.3329/jesnr.v8i2.26858.

[281] MOST. Saline intrusion in the Vietnamese Mekong Delta: Cause, Impact, and

Response solutions 2016, Ministry of Science and Technology 50.
[282] Rusydi, A.F. Correlation between conductivity and total dissolved solid in various type of water: A review. in IOP Conference Series: Earth and Environmental Science, p. 012019: IOP Publishing, 2018.
[283] Abdullah, H.H., E Rak, A., and Lee, S.W. The impacts of monsoon and dry seasons on physical water quality changes and farmed Asian seabass Lates calcarifer (Bloch, 1790) mortality at Sri Tujuh lagoon, Tumpat, Kelantan, Malaysia.
. AACL Bioflux 11(1) (2018): 167-183. http://www.bioflux.com.ro/docs/2018.167-183.pdf (accessed 20 September 2020).
[284] Be, N., Van, T., Hang, T., and An, N. Saline intrusion impacts on water resources management for agriculture activities in the Long Phu district, Soc Trang
province. Can Tho University, Journal of Science 52 (2017): 104. https://doi.org/10.22144/ctu.jvn.2017.116.
[285] MOARD. Summary report on drought and saline intrusion in the South of Vietnam 2019 - 2020. 2020, Ministry of Agriculture and Rural Development. 15.
[286] DONRE. Center for Meteorology and Hydrology of Bac Lieu Province: The meteorological and hydrological situation in March and September, 2019 in Bac Lieu province. 2019, Department of Natural Resources and Environment. .
[287] Islam, M., Uddin, M.K., Tareq, S.M., Shammi, M., Kamal, A.K.I., Sugano, T., Kurasaki, M., Saito, T., Tanaka, S., and Kuramitz, H. Alteration of water pollution level with the seasonal changes in mean daily discharge in three main rivers around Dhaka City, Bangladesh. Environments 2(3) (2015): 280-294.
[288] Li, J. and Zuo, Q. Forms of nitrogen and phosphorus in suspended solids: A case study of Lihu Lake, China. Sustainability 12(12) (2020): 5026. https://doi.org/10.3390/su12125026.
[289] Moujabber, M.E., Samra, B.B., Darwish, T., and Atallah, T. Comparison of Different Indicators for Groundwater Contamination by Seawater Intrusion on the Lebanese Coast. Water Resources Management 20(2) (2006): 161-180. https://doi.org/10.1007/s11269-006-7376-4.
[290] Sawyer, C.N., McCarty, P.L., and Parkin, G.F. Chemistry for environmental engineering and science - 5th ed. fifth ed ed.: McGraw-Hill., 2003.
[291] Phung, D., Huang, C., Rutherford, S., Dwirahmadi, F., Chu, C., Wang, X., Nguyen, M., Nguyen, N.H., Do, C.M., and Nguyen, T.H. Temporal and spatial assessment of river surface water quality using multivariate statistical techniques: a study in Can Tho City, a Mekong Delta area, Vietnam. Environmental Monitoring and Assessment 187(5) (2015): 229. https://doi.org/10.1007/s10661-015-4474-x.
[292] Bui, T.D., Luong Van, J., and Austin, C.M. Impact of shrimp farm effluent on water quality in coastal areas of the world heritage-listed Ha Long Bay. American Journal of Environmental Sciences 8(2) (2012): 104-116. https://doi.org/10.3844/ajessp.2012.104.116.
[293] Dauda, A.B., Ajadi, A., Tola-Fabunmi, A.S., and Akinwole, A.O. Waste production in aquaculture: Sources, components and managements in different culture systems. Aquaculture and Fisheries 4(3) (2019): 81-88. https://doi.org/10.1016/j.aaf.2018.10.002.

[294] Ebeling, J.M., Timmons, M.B., and Ebeling, J.M. Recirculating aquaculture. Cayuga Aqua Ventures, 2010.
[295] Olusegun, A., Dauda, A., and O.A, O. Haematological Response of Clarias gariepinus Juveniles Rearedin Treated Wastewater after Waste Solids Removal using Alum or Moringa oleifera Seed Powder. International Journal of Aquaculture 6 (2016): 1-8.
[296] Wisha, U. and Ondara, K. Total Suspended Solid (TSS) Distributed by Tidal Currents during Low to High Tide Phase in the Waters of Sayung, Demak: Its Relations to Water Quality Parameters. Journal of Marine and Aquatic Sciences 3 (2017): 154.
[297] Piedrahita, R.H. Reducing the potential environmental impact of tank aquaculture effluents through intensification and recirculation. Aquaculture 226(1) (2003): 35-44. https://doi.org/10.1016/S0044-8486(03)00465-4.
[298] Kawasaki, N., Kushairi, M., Nagao, N., Yusoff, F., Imai, A., and Kohzu, A. Release of nitrogen and phosphorus from aquaculture farms to Selangor River, Malaysia. International Journal of Environmental Science and Development 7(2) (2016): 113. https://doi.org/10.7763/IJESD.2016.V7.751.
[299] Rajwa-Kuligiewicz, A., Bialik, R.J., and Rowiński, P.M. Dissolved oxygen and water temperature dynamics in lowland rivers over various timescales. Journal of Hydrology and Hydromechanics 63(4) (2015): 353-363.
[300] Withers, P.J.A. and Jarvie, H.P. Delivery and cycling of phosphorus in rivers: A review. Science of The Total Environment 400(1) (2008): 379-395.
[301] Biao, X., Zhuhong, D., and Xiaorong, W. Impact of the intensive shrimp farming on the water quality of the adjacent coastal creeks from Eastern China. Marine Pollution Bulletin 48(5) (2004): 543-553.
[302] Ward, B.B. Chapter 5 - Nitrification in Marine Systems. in Capone, D.G., Bronk, D.A., Mulholland, M.R., and Carpenter, E.J. (eds.),Nitrogen in the Marine Environment (Second Edition), pp. 199-261. San Diego: Academic Press, 2008.
[303] Ruiz, Z.I., Halaihel, N., Balcázar, J.L., Ortega, C., Vendrell, D., Pérez, T., Alonso, J.L., and De Blas, I. Effect of fish farming on the water quality of rivers in northeast Spain. Water Science and Technology 60(3) (2009): 663-671. https://doi.org/10.2166/wst.2009.435.
[304] Trai, V.T., Momtaz, S., and Zimmerman, K. Water pollution concerns in shrimp farming in Vietnam: A case study of Can Gio, Ho Chi Minh City. The International Journal of Environmental, Cultural, Economic and Social Sustainability 3(2) (2007): 129-136. https://doi.org/10.18848/1832-2077/CGP/v03i02/54339.
[305] Rönnbäck, P. Shrimp aquaculture: State of the art. Swedish EIA Centre, Swedish University of Agricultural Sciences (SLU), Uppsala, 2001.
[306] Rahman, M.M., Islam, M.A., and Ahmed, K.K.U. Investigation of Improved Extensive Culture System of Shrimp with Special Reference to Soil-water Characteristics in South-West Region of Bangladesh. Asian Journal of Environment & Ecology 2(2) (2017): 1-11. https://doi.org/10.9734/AJEE/2017/32500.
[307] Chow, V.T. Open-Channel Hydraulics. New York: McGraw-Hill Book Company, 1959.

[308] Tan, N.P., and Vo, V.P.Đ.T., and Thanh, Q. The application of a two-dimensional hydraulic model
to simulate the hydraulic
properties and deposition and
erosion patterns in the Dinh
An estuary. (2014).
[309] Veerasamy, R., Rajak, H., Jain, A., Sivadasan, S., Varghese, C.P., and Agrawal, R.K. Validation of QSAR models-strategies and importance. Int. J. Drug Des. Discov 3 (2011): 511-519.
[310] Kasvi, E., Alho, P., Lotsari, E., Wang, Y., Kukko, A., Hyyppä, H., and Hyyppä, J. Two dimensional and three dimensional computational models in hydrodynamic and morphodynamic reconstructions of a river bend: sensitivity and functionality. Hydrological Processes 29 (2015): 1604-1629. https://doi.org/10.1002/hyp.10277.
[311] Mueller, D., Abad, J., García, C., Gartner, J., García, M., and Oberg, K. Errors in acoustic doppler profiler velocity measurements caused by flow disturbance. Journal of Hydraulic Engineering 133 (2007): 1-11. https://doi.org/10.1061/(ASCE)0733-9429(2007)133:12(1411). .
[312] Rennie, C.D. and Church, M. Mapping spatial distributions and uncertainty of water and sediment flux in a large gravel bed river reach using an acoustic doppler current profiler. Journal of Geophysical Research: Earth Surface 115(F3) (2010): 1-27. https://doi.org/10.1029/2009JF001556.
[313] Parsapour-Moghaddam, P. and Rennie, C.D. Calibration of a 3D hydrodynamic meandering river model using fully spatially distributed 3D ADCP velocity data. Journal of Hydraulic Engineering 144(4) (2018): 1-14. https://doi.org/10.1061/(ASCE)HY.1943-7900.0001424. .
[314] Chai, T. and Draxler, R.R. Root mean square error (RMSE) or mean absolute error (MAE)?– Arguments against avoiding RMSE in the literature. Geoscientific Model Development 7 (2014): 1247-1250.
[315] Mueller, D.S., Wagner, C.R., Rehmel, M.S., Oberg, K.A., and Rainville, F. Measuring discharge with acoustic doppler current profilers from a moving boat. in, pp. 1-86.: US Department of the Interior, US Geological Survey Reston, Virginia (EUA), 2009.
[316] Legleiter, C., Harrison, L., and Dunne, T. Effect of point bar development on the local force balance governing flow in a simple, meandering gravel bed river. Journal of Geophysical Research 116 (2011).
[317] Kasvi, E., Laamanen, L., Lotsari, E., and Alho, P. Flow patterns and morphological changes in a sandy meander bend during a flood—spatially and temporally intensive ADCP measurement approach. Water 9(2) (2017): 1-20. https://doi.org/10.3390/w9020106. .
[318] Carpman, N. and Leijon, M. Measurements of tidal current velocities in the Folda Fjord, Norway, with the use of a vessel mounted ADCP. Vol. 8, 2014.
[319] Eke, E.C. Numerical modeling of river migration incorporating erosional and depositional bank processes. University of Illinois at Urbana-Champaign, 2013.
[320] Berhanu, B., Seleshi, Y., Demisse, S.S., and Melesse, A.M. Flow regime classification and hydrological characterization: a case study of Ethiopian rivers. Water 7(6) (2015): 3149-3165. https://doi.org/10.3390/w7063149.

[321] Li, Q., Wei, X., Yang, X., Giles-Hansen, K., Zhang, M., and Liu, W. Topography significantly influencing low flows in snow-dominated watersheds. Hydrology and Earth System Sciences 22(3) (2018): 1947-1956. https://doi.org/10.5194/hess-22-1947-2018.

[322] Bakhtiar Jemily, N.H., Ahmad Sa'ad, F.N., Mat Amin, A.R., Othman, M.F., and Mohd Yusoff, M.Z. Relationship Between Electrical Conductivity and Total Dissolved Solids as Water Quality Parameter in Teluk Lipat by Using Regression Analysis. in Abu Bakar, M.H., Mohamad Sidik, M.S., and Öchsner, A. (eds.),Progress in Engineering Technology: Automotive, Energy Generation, Quality Control and Efficiency, pp. 169-173. Cham: Springer International Publishing, 2019.

[323] Nilsson, C. and Renöfält, B.M. Linking flow regime and water quality in rivers: a challenge to adaptive catchment management. Ecology and Society 13(2) (2008): 21. http://www.ecologyandsociety.org/vol13/iss2/art18/.

[324] Devore, D.L. The Effects of Tidal Forcing on Nutrient Fluxes in the Tidal, Freshwater James River Estuary, VA. (2016).

[325] Rostami, S., He, J., and Hassan, Q.K. Water quality response to river flow regime at three major rivers in Alberta. Water Quality Research Journal 55(1) (2020): 79-92. https://doi.org/10.2166/wqrj.2019.033.

[326] Körner, S., Das, S.K., Veenstra, S., and Vermaat, J.E. The effect of pH variation at the ammonium/ammonia equilibrium in wastewater and its toxicity to Lemna gibba. Aquatic Botany 71(1) (2001): 71-78. https://doi.org/10.1016/S0304-3770(01)00158-9.

[327] Zhou, L. and Boyd, C. Ammonia nitrogen management in aquaculture ponds. Aquaculture Magazine (2015): 1-3. https://www.researchgate.net/publication/284447968.

[328] Mingming, Z., Yao, D., Li, S., Zhang, Y., and Aweya, J. Effects of ammonia on shrimp physiology and immunity: a review. Reviews in Aquaculture 12 (2020): 1-19. https://doi.org/0.1111/raq.12429.

[329] Bowes, M. and House, W. Phosphorus and dissolved silicon dynamics in the River Swale catchment, UK: a mass-balance approach. Hydrological Processes 15(2) (2001): 261-280. https://doi.org/10.1002/hyp.157. .

[330] Merz, S.K. Characterizing the relationship between water quality and water quantity. St Leonards NSW 2065 (2013): 116. https://www.waterquality.gov.au/sites/default/files/documents/characterising.pdf .

[331] Malan, H. and Day, J. Linking discharge, water quality and biotic response in rivers: a literature review. (2002): 1-170. http://www.wrc.org.za/wp-content/uploads/mdocs/956-1-02.pdf. .

[332] House, W.A. Geochemical cycling of phosphorus in rivers. Applied Geochemistry 18(5) (2003): 739-748. https://doi.org/10.1016/S0883-2927(02)00158-0.

[333] Jingsheng, C., Tao, Y., and Ongley, E. Influence of high levels of total suspended solids on measurement of Cod and Bod in the Yellow River, China. Environmental monitoring and assessment 116 (2006): 321-34. https://doi.org/10.1007/s10661-006-7374-2.

[334] Eslamian, S. and Ziaie, R. Eutrophication : The Major Threat to Water Bodies.

2013.

APPENDIX

A. Statistical analysis for seasonal variabilities of physicochemical parameters

Table 1. Tests of normal distribution for seasonal dataset

Parameters	Seasons	Kolmogorov-Smirnov		
		Statistic	df	Sig.
Temp	Dry	.172	75	.000
	Wet	.254	75	.000
pH	Dry	.202	75	.000
	Wet	.173	75	.000
EC	Dry	.125	75	.006
	Wet	.254	75	.000
TDS	Dry	.317	75	.000
	Wet	.252	75	.000
TSS	Dry	.302	75	.000
	Wet	.254	75	.000
Sal	Dry	.129	75	.003
	Wet	.253	75	.000
$N\text{-}NO_2^-$	Dry	.289	75	.000
	Wet	.197	75	.000
$N\text{-}NO_3^-$	Dry	.113	75	.019
	Wet	.162	75	.000
$N\text{-}NH_4^+$	Dry	.115	75	.015
	Wet	.200	75	.000
TN	Dry	.193	75	.000
	Wet	.140	75	.001
$P\text{-}PO_4^{3-}$	Dry	.168	75	.000
	Wet	.263	75	.000
TP	Dry	.100	75	.063
	Wet	.196	75	.000
COD	Dry	.125	75	.005
	Wet	.246	75	.000

DO	Dry	.	75	.
	Wet	.162	75	.000

Table 2. Mann-Whitney test (U test) for seasonal dataset

Parameters	Mann-Whitney U	Wilcoxon W	Z	Asymp. Sig. (2-tailed)
Temp	310.500	3160.500	-9.417	.000
pH	1.500	2851.500	-10.639	.000
EC	.000	2850.000	-10.575	.000
TDS	.000	2850.000	-10.574	.000
TSS	2322.000	5172.000	-1.844	.065
Sal	.000	2850.000	-10.578	.000
$N\text{-}NO_2^-$	124.500	2974.500	-10.248	.000
$N\text{-}NO_3^-$	.000	2850.000	-10.587	.000
$N\text{-}NH_4+$	.000	2850.000	-10.578	.000
TN	.000	2850.000	-10.612	.000
$P\text{-}PO_4^{3-}$	19.500	2869.500	-10.522	.000
TP	.000	2850.000	-10.574	.000
COD	.000	2850.000	-10.630	.000
DO	.000	2850.000	-11.301	.000

B. Statistical analysis for tidal variabilities of physicochemical parameters

Table 1 Test of normal distribution for tidal dataset

Parameters	Tides	Kolmogorov-Smirnov		
		Statistic	df	Sig.
Temp	Ongoing tide	.138	69	.002
	Incoming tide	.219	81	.000
pH	Ongoing tide	.191	69	.000
	Incoming tide	.172	81	.000
EC	Ongoing tide	.351	69	.000
	Incoming tide	.332	81	.000
TDS	Ongoing tide	.281	69	.000
	Incoming tide	.330	81	.000
TSS	Ongoing tide	.294	69	.000
	Incoming tide	.139	81	.001
Sal	Ongoing tide	.330	69	.000
	Incoming tide	.334	81	.000
$N\text{-}NO_2^-$	Ongoing tide	.140	69	.002
	Incoming tide	.218	81	.000
$N\text{-}NO_3^-$	Ongoing tide	.331	69	.000
	Incoming tide	.294	81	.000
$N\text{-}NH_4^+$	Ongoing tide	.177	69	.000
	Incoming tide	.177	81	.000

	Ongoing tide	.198	69	.000
TN	Incoming tide	.118	81	.007
	Ongoing tide	.211	69	.000
$P\text{-}PO_4^{3-}$	Incoming tide	.247	81	.000
	Ongoing tide	.309	69	.000
TP	Incoming tide	.122	81	.005
	Ongoing tide	.151	69	.000
COD	Incoming tide	.174	81	.000
	Ongoing tide	.189	69	.000
DO	Incoming tide	.080	81	.200

Table 2. Mann-Whitney test (U test) for tidal dataset

Parameters	Mann-Whitney U	Wilcoxon W	Z	Asymp. Sig. (2-tailed)
Temp	2040.000	5361.000	-2.849	.004
pH	2559.000	5880.000	-.894	.371
EC	2332.000	5653.000	-1.745	.081
TDS	2136.500	5457.500	-2.482	.013
TSS	2561.000	5882.000	-.881	.379
Sal	2252.000	5573.000	-2.047	.041
$N\text{-}NO_2^-$	1876.500	4291.500	-3.462	.001
$N\text{-}NO_3^-$	2620.000	5035.000	-.658	.510
$N\text{-}NH_4^+$	2169.000	5490.000	-2.360	.018
TN	2196.000	4611.000	-2.264	.024
$P\text{-}PO_4^{3-}$	2117.500	4532.500	-2.563	.010
TP	2407.500	5728.500	-1.460	.144
COD	1891.500	5212.500	-3.425	.001

DO	1610.000	4931.000	-4.467	.000

C. Principal Component Analysis (PCA)

Table 1. KMO and Bartlett's test

Kaiser-Meyer-Olkin Measure of Sampling Adequacy.	**.867**
Bartlett's Test of Sphericity Approx. Chi-Square	1032.633
df	78
Sig.	.000

Table 2. Total Variance Explained

Component	Initial Eigenvalues			Extraction Sums of Squared Loadings			Rotation Sums of Squa Loadings		
	Total	Variance %	Cumulative %	Total	Variance %	Cumulative %	Total	Variance %	Cum
1	6.973	53.638	53.638	6.973	53.638	53.638	6.773	52.099	52
2	2.396	18.434	72.073	2.396	18.434	72.073	2.544	19.566	71
3	1.010	7.768	**79.841**	1.010	7.768	79.841	1.063	8.176	**79**
4	.926	7.122	86.962						
5	.661	5.083	92.046						
6	.481	3.699	95.744						
7	.238	1.829	97.574						
8	.153	1.177	98.750						
9	.070	.542	99.292						
10	.054	.414	99.706						
11	.031	.241	99.947						
12	.006	.049	99.997						
13	.000	.003	100.000						

Table 3. Rotated component matrix

Parameters	Components

	1	2	3
Sal	.988		
EC	.988		
TDS	.982		
pH	.933		
$N\text{-}NO_2^-$	-.909		
$N\text{-}NO_3^-$	-.908		
COD	.795		
Temp	.757		
TSS		.963	
TP		.931	
TN		.573	
DO			.701
$P\text{-}PO_4^{3-}$			-.525

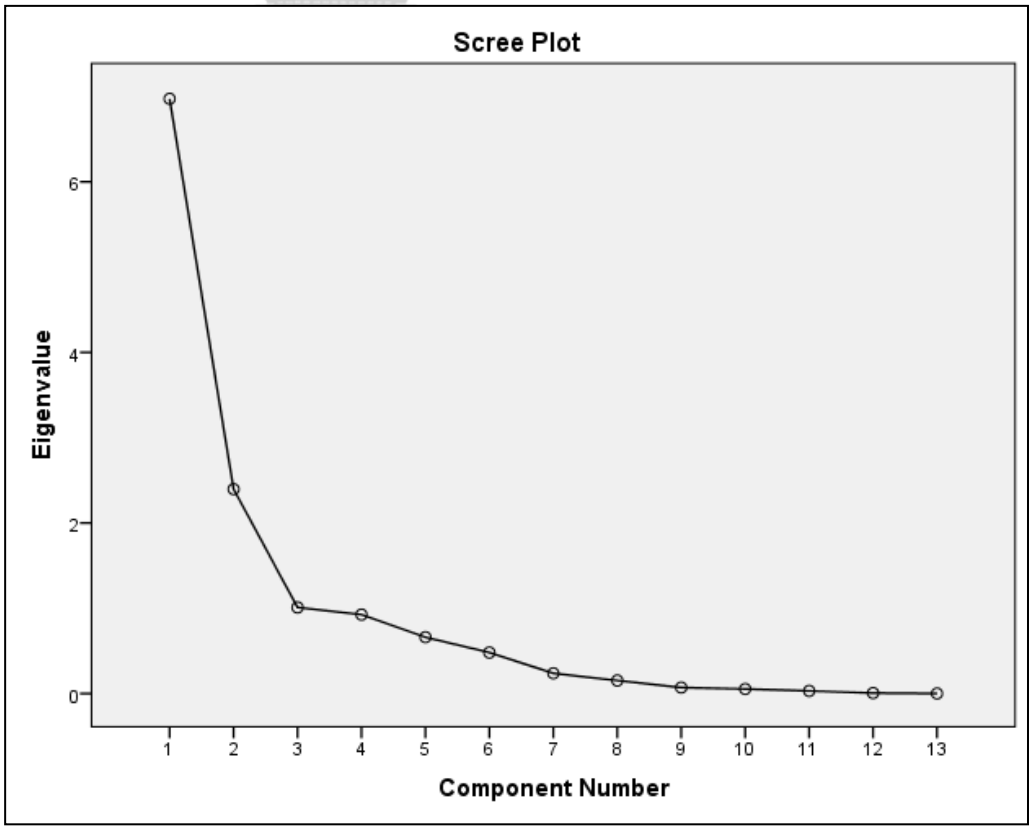

Figure 1. Scree plot indicates eigenvalues and component numbers

D. Logistic regression model analysis

3.1 Data analysis in the dry season

Table 1. Variables in the Equation

Step 1[a]	Parameters	B	S.E.	Wald	df	Sig.	Exp(B)
	EC	10.683	3.181	11.279	1	.001	43596.982
	TSS	.025	.009	7.570	1	.006	1.026
	TP	23.577	12.228	3.718	1	.054	17355618702.117
	$N\text{-}NO_2^-$	471.485	202.440	5.424	1	.020	5.797E+204
	Constant	-403.375	119.606	11.374	1	.001	.000

Table 2. Classification table

			Predicted		
	Observed		Y		Percentage Correct
			0	1	
Step 1	Y	0	43	2	95.6
		1	3	27	90.0
	Overall percentage				93.3

3.2 Data analysis in the wet season

Table 3. Variables in the Equation

Step	Parameters	B	S.E.	Wald	df	Sig.	Exp(B)

1[a]							
	pH	20.419	7.866	6.738	1	.009	737377990.539
	EC	-.730	.564	1.671	1	.019	.482
	$N\text{-}NO_2^-$	130.138	53.136	5.998	1	.014	3.299E+56
	TP	-9.416	3.640	6.692	1	.010	.000
	Constant	-143.561	54.330	6.982	1	.008	.000

Table 3. Classification table

			Predicted		
	Observed		Y		Percentage Correct
			0	1	
Step 1	Y	0	42	3	93.3
		1	2	28	93.3
	Overall percentage				93.3

Table 4. Kruskal-Wallis test for dataset in the dry season in Dong Hai district

	EC	TDS	Sal	TN	$N\text{-}NH_4+$
Kruskal-Wallis H	31.942	14.111	21.369	17.694	29.064
df	2	2	2	2	2
Asump.Sig,	.000	.001	.000	.000	.000

Table 5. Kruskal-Wallis test for dataset in the wet season in Dong Hai district

	Temp	pH	TSS	$N\text{-}NO_2^-$	$N\text{-}NH_4^+$
Kruskal-Wallis H	13.805	11.435	14.623	12.756	5.714
df	1	1	1	1	1
Asump.Sig,	.000	.001	.000	.000	.017

Table 6. Kruskal-Wallis test for dataset in the dry season in Dam Doi district

	EC	TDS	Sal	TN	TP	DO	$N\text{-}NH_4^+$
Kruskal-	31.9	14.1	21.3	17.6	6.1	20.24	29.06

Wallis H	4	1	6	9	6	2	4
df	2	2	2	2	2	2	2
Asump.Sig,	.000	.001	.000	.000	.046	.000	.000

Table 7. Kruskal-Wallis test for dataset in the wet season in Dam Doi district

	Temp	pH	EC	TSS	TDS	Sal	$N\text{-}NO_2^-$	$N\text{-}NH_4^+$	$P\text{-}PO_4^{3-}$	TP	CO
Kruskal-Wallis H	28.49	13.87	24.33	14.98	24.19	25.14	40.36	13.29	9.77	22.37	8.6
df	2	2	2	2	2	2	2	2	2	2	
Asump.Sig,	.000	.001	.000	.001	.000	.000	.000	.001	.008	.000	.01

E. Input data for hydrodynamic model development

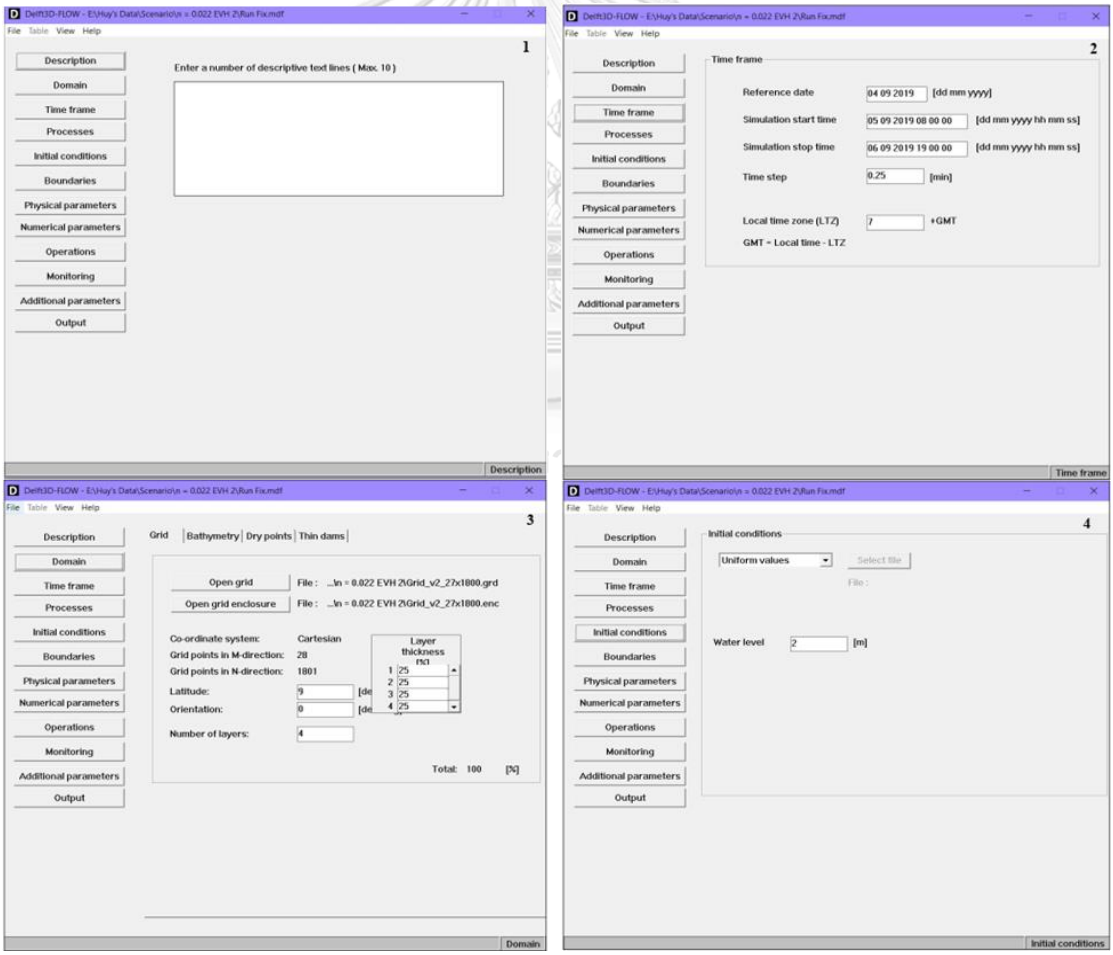

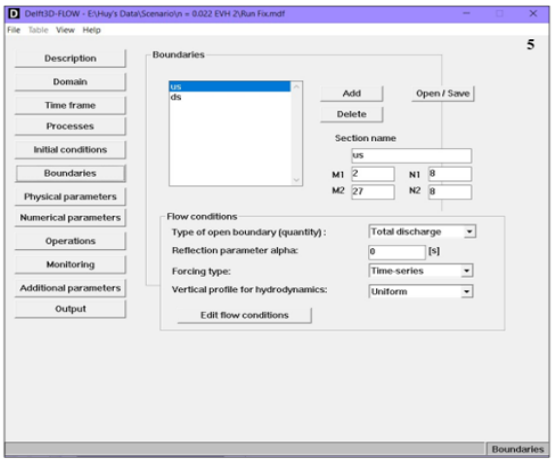

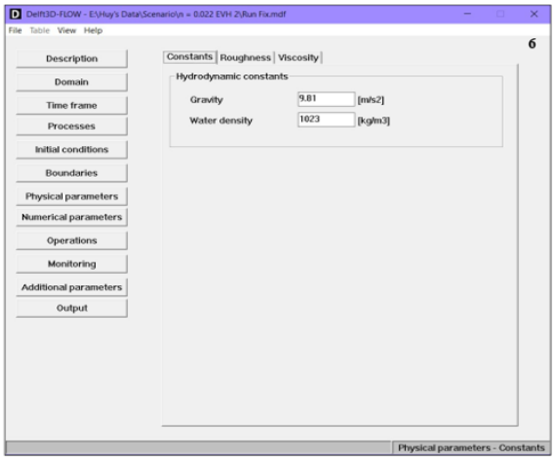

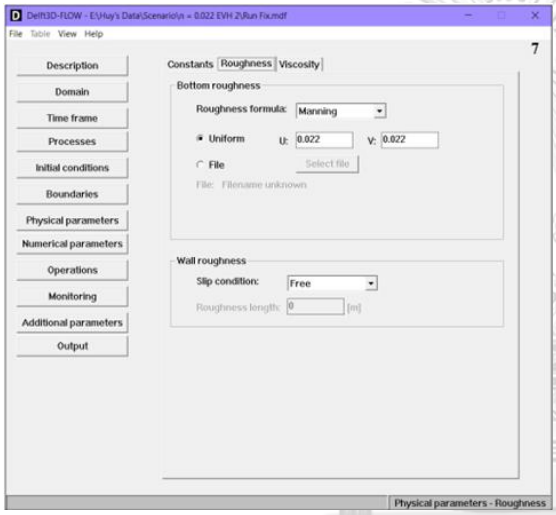

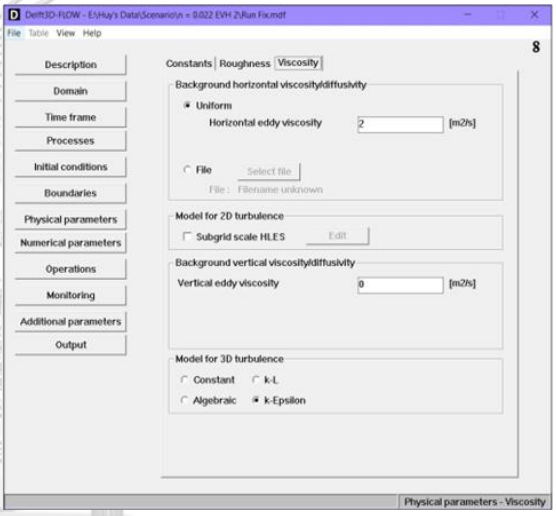

F. Cross-sections obtained by using ADCP

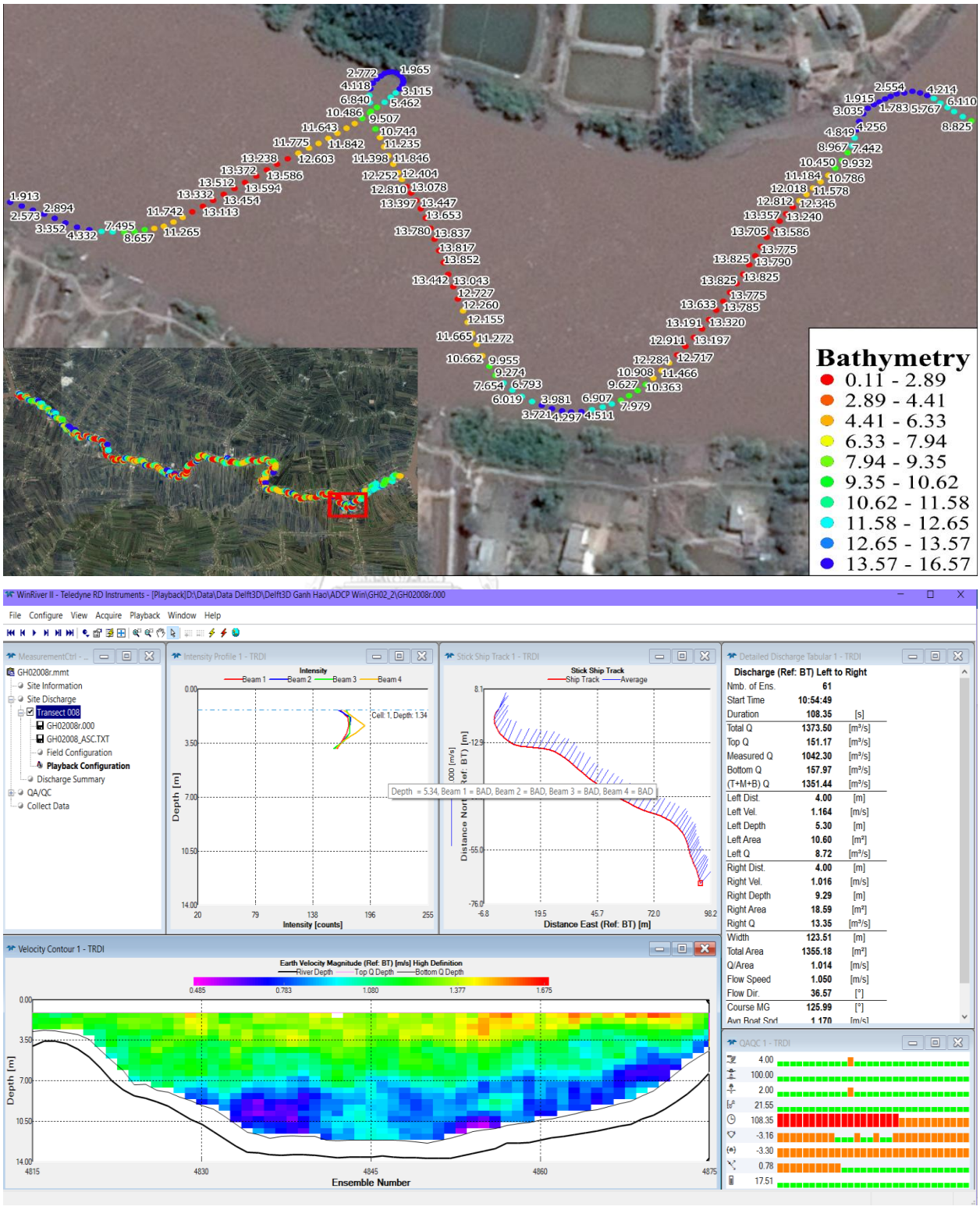

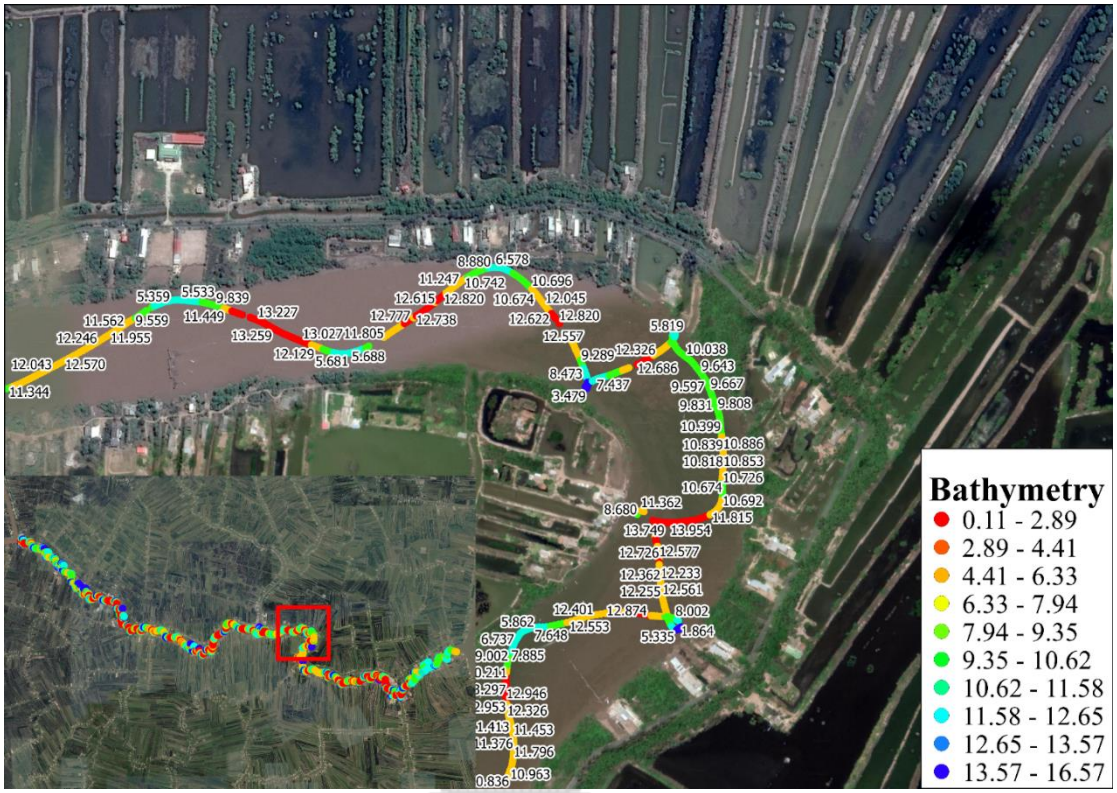

VITA

NAME	Muoi Le Van
DATE OF BIRTH	01-10-1982
PLACE OF BIRTH	Tra Vinh province, Vietnam
INSTITUTIONS ATTENDED	Can Tho university
HOME ADDRESS	Nhi Long Phu commune, Cang Long District, Tra Vinh province
PUBLICATION	Muoi, L.V, Srilert, C., & Van, T. P. (2022). Spatial and temporal variabilities of surface water and sediment pollution at the main tidal-influenced river in Ca Mau Peninsular, Vietnamese Mekong Delta. Journal of Hydrology: Regional Studies, 41, 101082.